CHEMISTRY OF PLASMAS USED IN THE FABRICATION

OF INTEGRATED CIRCUITS.

Michael Simpson

A Thesis submitted for the
Degree of Doctor of Philosophy
at the University of Aston in Birmingham,

October, 1982.

<u>The University of Aston in Birmingham.</u>

<u>Chemistry of Plasmas Used in the Fabrication</u>

<u>of Integrated Circuits.</u>

<u>Summary</u>

Molecular beam mass spectrometry has been used to study the reactive gas plasmas used in semiconductor integrated circuit manufacture. Details of the design parameters, theory of molecular beam sampling and the fabrication of a molecular beam sampling system are given. The system was built, tested and used to sample various reactive gas plasmas during etching and in the absence of a wafer.

Silicon and to a much lesser extent silicon dioxide wafers have been etched in a variety of chlorine containing plasmas such as CCl_4, CCl_4/O_2, CCl_4/Ar and $CFCl_3$. Some other plasmas have also been studied in the absence of a silicon wafer. Polymer formation was found to be a major problem in the present reactor probably due to low gas flow rates. Polymer formation was particularly marked in CCl_4/O_2 plasmas. Aluminium, etched from the r.f. electrodes, was also incorporated into these conductive polymer films.

Preliminary results with this system have shown that molecular beam mass spectrometry can be successfully used to sample these plasmas. The results also show that $CFCl_3$ and CCl_4/Ar plasmas are suitable etchants for silicon.

A detailed survey of the literature on plasma etching and plasma polymer formation is also presented.

Key words:- Etching; Mass Spectrometry; Molecular beam; Plasma; Semiconductor.

Michael Simpson. Submitted for the degree of Ph.D. 1982.

Acknowledgements

CONTENTS

(iv)

List of Tables

List of Figures

(xiv)

(XV)

1 INTRODUCTION

Integrated circuit manufacture is mainly concerned with making transistors and diodes, and to a lesser extent resistors and capacitors, on the surfaces of flat, thin silicon wafers. This is referred to as silicon planar technology.

Silicon wafers, suitable for this manufacturing technique, are produced from large single crystals of silicon which have been drawn or pulled from very high purity molten silicon. These single crystals are further zone refined and thin silicon wafers are sliced from the single crystal along a crystal plane. The wafers are polished and tested for flatness and on these very flat wafers are constructed the various small device features which make up the components of an integrated circuit.

Silicon planar technology involves the successive growth or deposition of films of silicon dioxide, definition with a photoresist pattern, etching and impurity diffusion using the oxide pattern as a diffusion mask. Fig. 1, shows a typical sequence for producing bipolar devices on a silicon substrate. Bipolar devices have both majority and minority charge carriers ie: electrons and "holes" or positive charges and therefore has both p- and n- type silicon semiconductor. A wafer normally has several hundred integrated circuits defined on its surface each with several thousand transistors
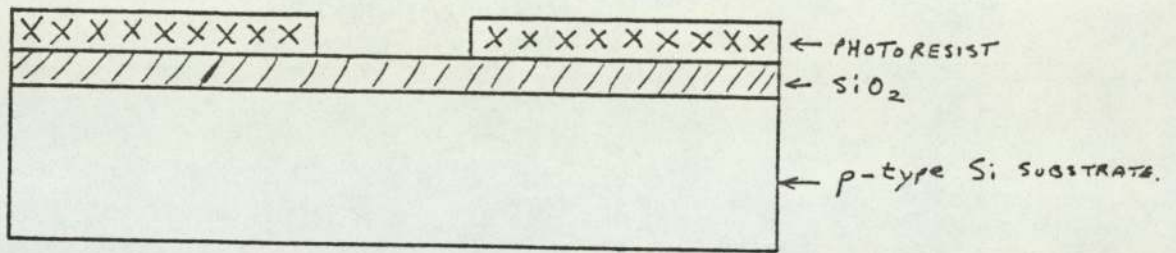
(a) Photoresist pattern
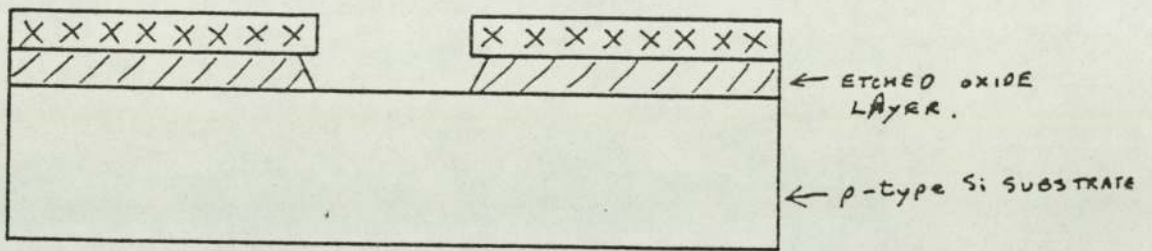
(b) Etched pattern
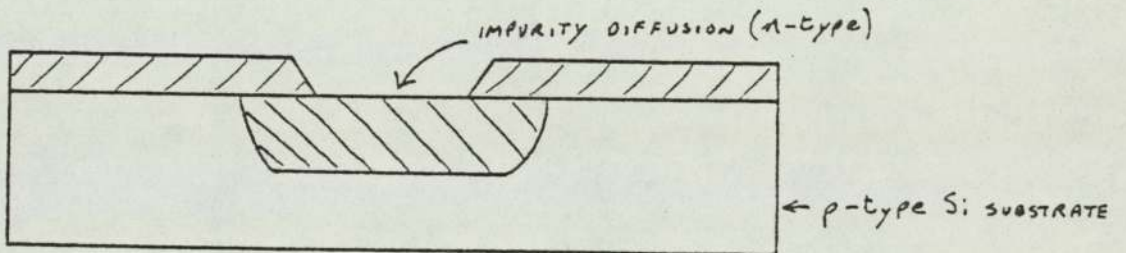
(c) n-type diffusion
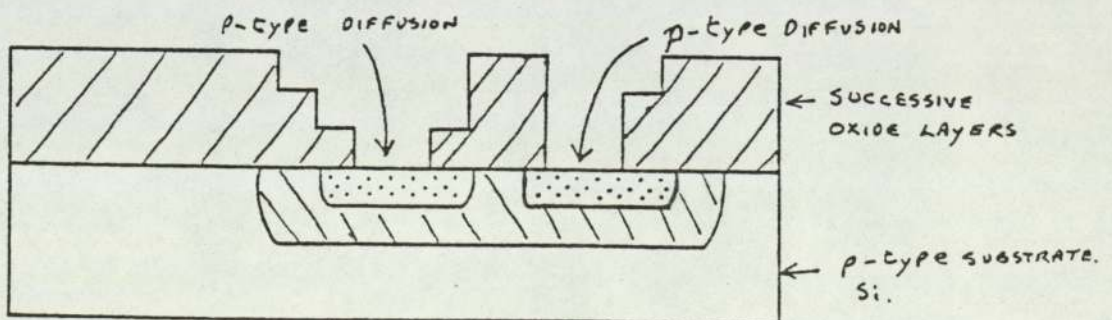
(d) Successive n- and p-type diffusions
produce transistors

Fig.1   I.C. manufacture

similar to that in Fig. 1. Having produced the devices on the silicon wafer a layer of metallization is deposited on the wafer, defined with patterned photoresist and etched to leave a number of metal connecting rails. These metal rails connect up the various transistors and diodes to give different circuit functions. In the case of digital electronics transistors are connected up to give gates which have specific logic functions.

Following metallization a phosphosilicate glass or silicon nitride passivation layer is deposited on the wafer to protect the circuits from moisture and other contamination. Further photoresist patterning and etching is done to open up bonding pads where electrical connections can be made with the metallization layer. The bonding pads are relatively larger areas of metallization near the edge of an integrated circuit to which small wires may be bonded or electric probes connected. Each integrated circuit on the wafer is multiprobe tested to make sure the circuit works correctly and within specification. The wafer is diced up along the crystal planes to give the individual integrated circuits or "chips" of silicon, each chip having a complete integrated circuit etched on its surface.

The integrated circuits are packaged into either ceramic, or cans (hermetically sealed in dry nitrogen) or
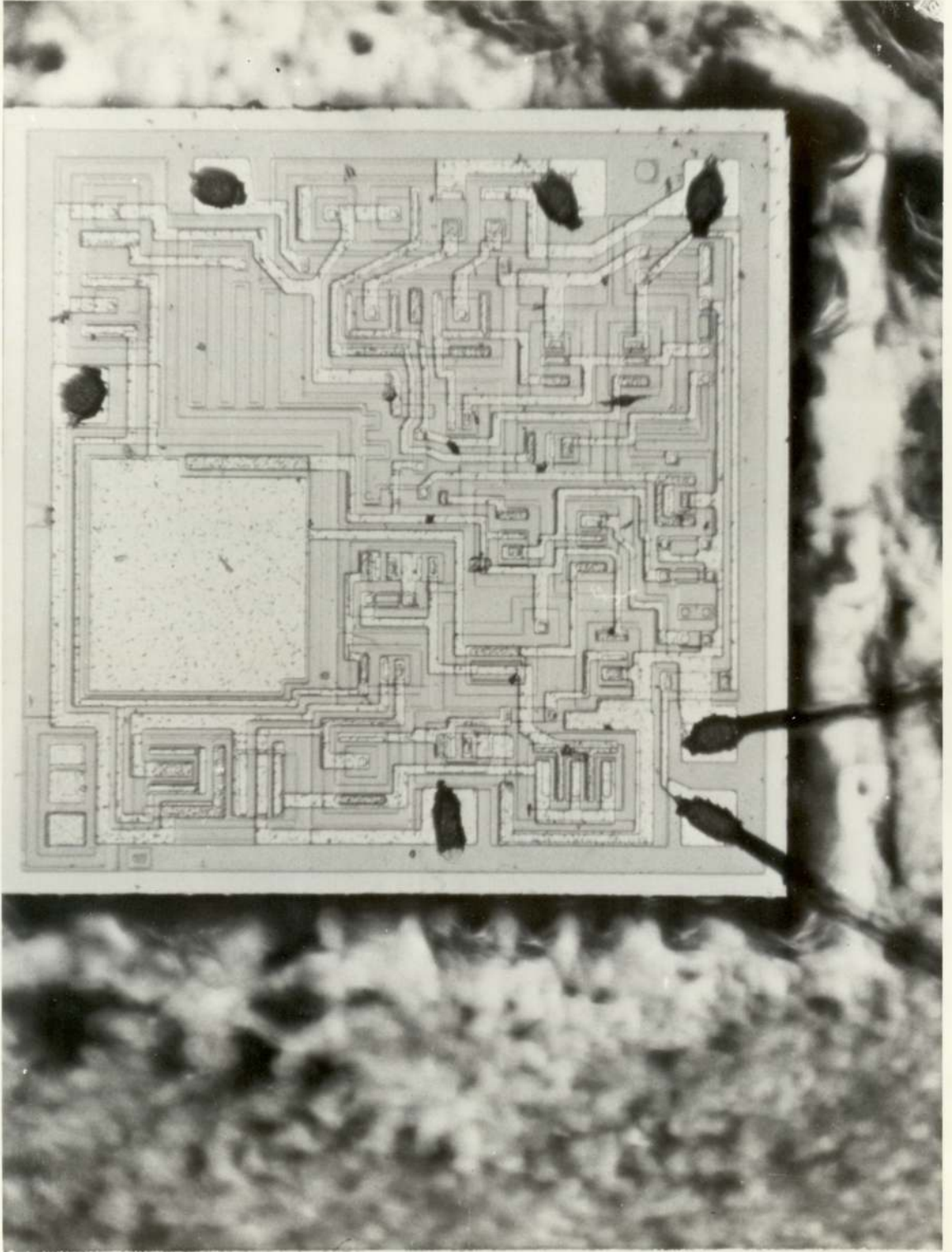
Fig.1(a). Detail of a 741 i.c.(x10).

2(a)
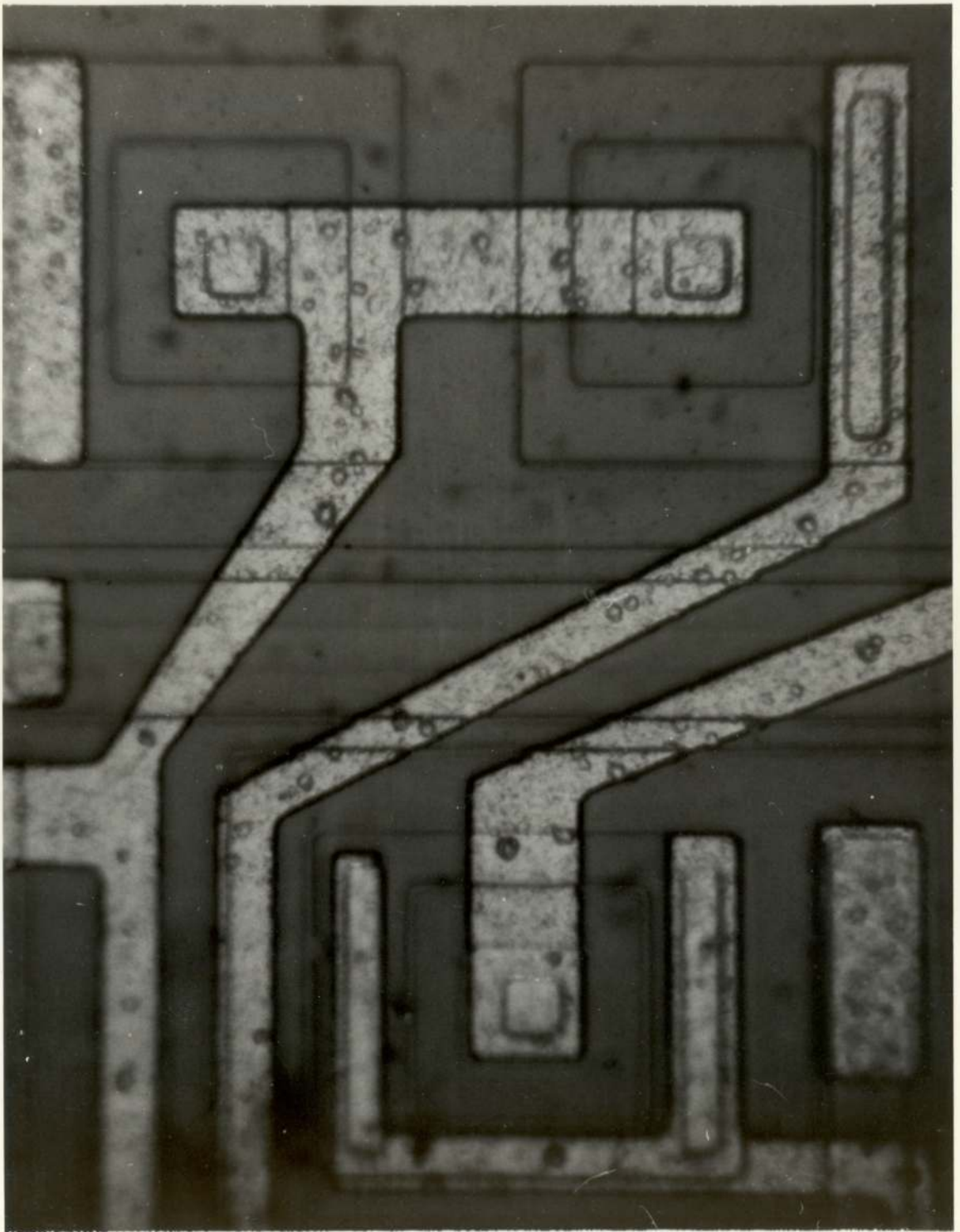
Fig.1(b). Detail of a 741 i.c.(x50).

2(b)

encapsulated in plastic. The integrated circuits are bonded to the package using either a gold-silicon eutectic mixture at 380°C or an epoxy resin. The circuits are wired to the external pins of the device package with ~$2x10^{-3}$ inch thick aluminium or gold wire. Bonding of the thin wire to the bonding pads exposed earlier is done by either thermocompression or ultrasonic bonding or ball bonding. The packages are then sealed and the devices tested. The packaged integrated circuits now look identical to devices available from electronic components suppliers.

The processes used in integrated circuits manufacture are reviewed in more detail elsewhere (1,2,3,4). The process of most importance to this work is etching of the various semiconductor materials and in particular etching of silicon. Etching of semiconductor materials can be done in two ways:

i) with wet chemical etchants and

ii) with dry (plasma) gaseous etchants.

1.1.1. Wet Chemical Etching

The most important manufacturing processes for bipolar transistors are photoresist patterning and oxide etching. The etching of oxide layers involves the use of buffered HF acid baths. For M.O.S. field effect transistors, Fig.2, silicon and aluminium etching is important and requires similar caustic conditions for
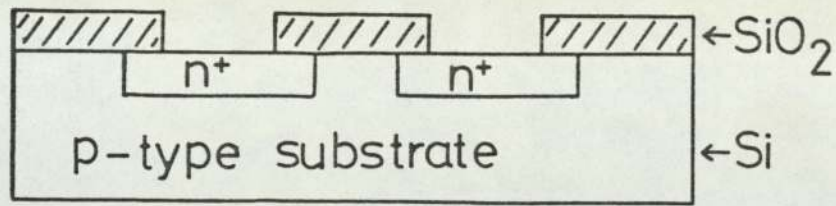
(a) Oxide patterned, etched and heavily n-doped to give n+ diffusions.
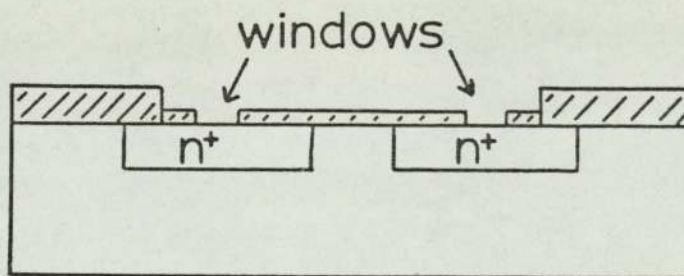
(b) Oxide patterned, etched, 0·1um oxide grown and windows etched.
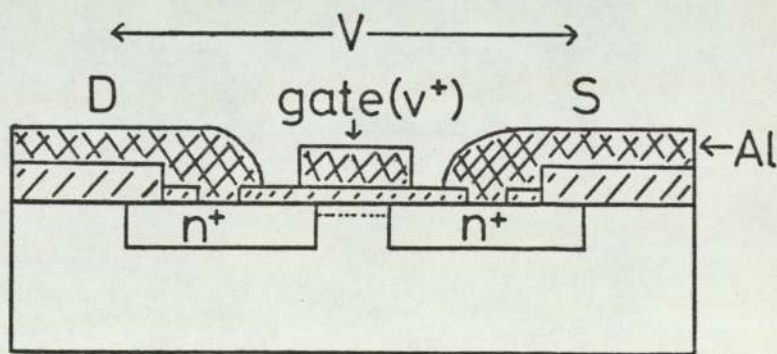
(c) Metalisation deposited and etched.

Fig.2 M.O.S. devices.

etching to take place. Wet chemical etching of semiconductor materials requires high purity reagents which are rapidly used (to avoid cross contamination from one batch of wafers to another) and high purity deionised water for washing between processes. This is both expensive and dangerous. The handling of extremely caustic, corrosive fluids requires care, special protective clothing and fume extraction cupboards. Table: 1, shows the range of wet chemical etchants needed to carry out the production of an integrated circuit and is compared with materials required for dry or plasma etching.

Table: 1 Wet and Dry Chemical Etchants for Semiconductor Materials.

Material	Wet Etchants	Dry (Plasma) Etchants	Ref
SiO_2	Buffered HF	CF_4; CF_4/O_2; CHF_3/Ar; C_2F_6; $CFCl_3$; C_3F_8.	18,5, 112,113
Si	$HF/HNO_3/H_2O$ mixture	CF_4/O_2; CCl_4; Cl_2; CHF_3; $CFCl_3$; SF_6.	18,5, 148
SI_3N_4	Phosphoric acid @170°C	CF_4.	18,5,
Al	Acetic/ orthophos phoric acid @ 55-60°C	CCl_4; Cl_2/Ar.	5,101, 176.
Phospho- silicate glass	HF or NH_4F	CF_4	5,19.
Photo- resist	H_2SO_4/H_2O_2 or HNO_3	Air or O_2	18,
Au	HNO_3/HCl mixture	CCl_2F_2; $C_2Cl_2F_4$.	5,115.
Cr	HCl	Cl_2/O_2 50:50 mixture.	180

It is clear from table: 1, that materials used for wet etching are corrosive and difficult to handle whereas the dry etchants are either gases or are low boiling point liquids with high vapour pressures. Consequently dry (plasma) etchants are easier to handle, can be produced in high purity and are easily obtainable - being used in other applications as refrigerants and solvents.

There are other problems with wet etchants such as:-

(i)   Wetability

The inability of wet chemical etchants to "wet" the
wafer, despite the addition of various surfactants to
reduce surface tension, is a problem where small device
features are concerned. The surface tension of the
liquid tends to bridge over small features defined in the
photoresist causing non-uniformity of etch across the
wafer.

(ii)   Bubble Formation

Bubbles can also bridge over small features causing
non-uniformity and a need for excessive over-etch times
which can produce undercutting in other areas of the
wafer.

(iii)   Photoresist Lift-Off

The photoresist may lift off where etchant solutions
have penetrated underneath the photoresist or where
vigorous agitation has dislodged poorly attached
photoresist.

(iv)   Poor Size Resolution

This is due to a combination of the other problems
which make it impossible to wet etch device features
smaller than a few micrometers in size.

The use of gaseous etchants in plasmas promises to overcome all these problems and allow very small device features to be etched (less than 1um).

1.1.2. Etch Parameters

The parameters to be optimised for any etching process used in the fabrication of integrated circuits are:-

(i) Selectivity

It is necessary to have etchants which are highly selective and therefore have high etch rate ratios for different materials. Etch rate ratios are normally quoted for particular materials on certain substrates eg: SiO_2:Si - silicon dioxide on silicon substrate.

(ii) Photoresist Undercutting

This is undesirable because of the reduction in size of the unetched areas left on the wafer. Under some circumstances photoresist patterns can be made larger to compensate for this pattern size loss but normally photoresist patterns are made the same size as the device features and anisotropic etching is used. Fig:3 shows photoresist undercut during etching.

resist

layer

substrate

(a) Good etch.

substrate
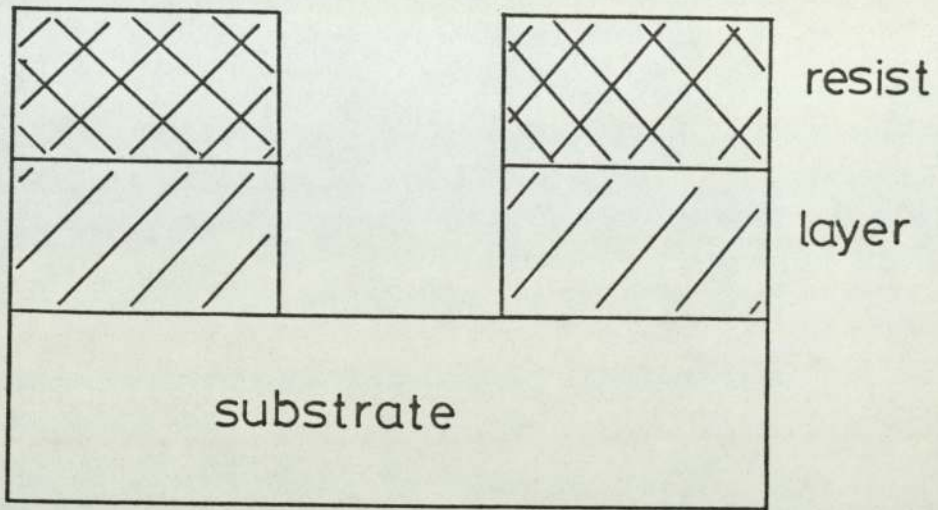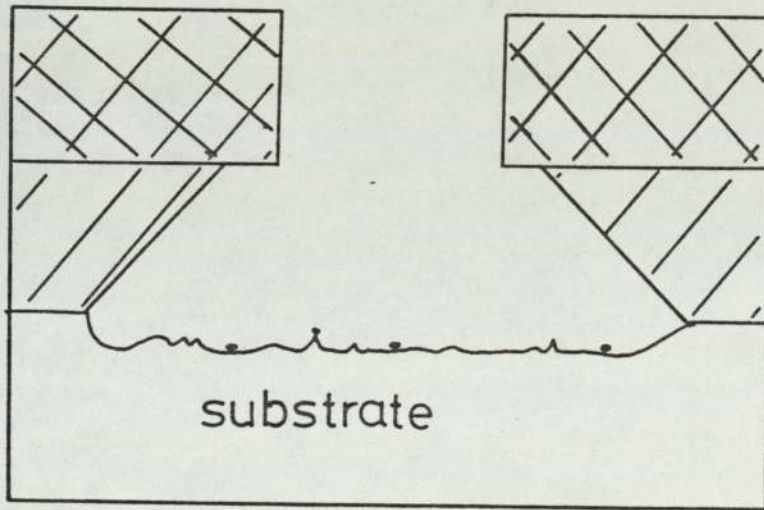
(b) Poor etch

Fig.3 Etch parameters.

7(a)

(iii)   Edge Profiles

Edge profiles of etched features should, ideally, be vertical without photoresist undercutting, and is referred to as anisotropic etching. The degree to which anistropic etching is obtained can be measured by looking at the slope of the edge profiles of etched features.

(iv)   End Points

The end point of an etching process is when a layer of material on a substrate has been completely etched through to the substrate and any further etching will only lead to photoresist undercutting and substrate etching. Highly selective etchants have clearly defined end points, however it is desirable to be able to detect end points and therefore prevent over etching.

(v)   Photoresist Degradation

During etching the photoresist material (usually a cross-linked polymer) should not prematurely degrade, lift off, shrink or be removed in any way otherwise etching will take place in areas where etching is undesirable. Photoresist should be inert in the etching medium or sufficiently resistant to allow normal etching to take place.

(vi)   Surface Texture

The surface revealed by an etching process should ideally be smooth, flat and even. In particular where a polished substrate is revealed by etching the surface should be smooth. Sometimes etched surfaces are rough and uneven because of surface contamination by dust particles.

(vii)   Uniformity

Uniform etching across a wafer is desirable to prevent over-etching and undercutting in some areas and other areas being under etched and not cleared. Non-uniformity can be sometimes observed as "bulleye" effects where the centre of the wafer clears either first or last.

1.1.3. The Plasma Discharge

The plasmas of interest in the etching of semiconductor materials are generally characterised by pressures of 0.1-1.0 torr, mean electron energies of 1 - 10eV and gas temperatures $\sim$300°C. The plasma discharge is usually obtained by exciting the gas with r.f. power at 13.56MHz coupled capacitively or inductively to the gas. Capacitively coupled r.f. power can be via internal electrodes or external electrodes. Unlike some processes (reactive ion etching and sputtering) there is no bias

9

potential applied and the pressure is sufficiently high that negligible sputtering occurs. Plasma etching is strictly a chemical process where the plasma generates reactive species which react chemically with the material being etched to form a volatile compound or species that can be swept away by the gas flow.

The plasma discharge is initiated by free electrons in the gas accelerating in the applied electric field to sufficiently high energies to cause electron-impact ionisation of the gas. This process produces more free electrons which are also accelerated in the applied r.f. electric field and cause further electron impact ionisation. This avalanche effect eventually reaches a steady state equilibrium where the rate of loss of free electrons by recombination is balanced by the rate of production of free electrons by electron impact ionisation. (appendix D).

Electrons, ions (positive and negative) and neutral species (atoms, radicals and molecules) are present in the discharge. However, the plasma remains electrically neutral because of the almost equal numbers of electrons and positive ions, there are generally fewer negative ions present (34). Electronically excited species produce optical emission in the ultra violet and visible regions of the spectrum which is characteristic of the glow discharge gas composition. The most important property of a plasma discharge for etching is the

10

formation of reactive species in the gas phase which can react with any suitable material placed in the plasma and etch it by the formation of volatile etch products.

Fig:4. shows some typical plasmas characterised by their electron energy, density and mean free path, the plasmas of interest to this work are known as glow discharges. The factors affecting the properties of plasmas are as follows:-

(i)   Nature of the gas.
(ii)   excitation power.
(iii)   excitation frequency.
(iv)   gas flow rate.
(v)   pumping speed.
(vi)   pressure.
(vii)   geometrical factors.
(viii) surface effects.

These factors affect gas density, electron density, the energy distribution of electrons, residence times and temperature. Surface effects can arise from interactions with any surface in contact with the plasma such as electrodes, reactor material and the wafers to be etched (21).

The etch rates in a plasma depend, in a complicated way, on the etch gas composition, the rate of generation of etching species and their rate of arrival at the

11
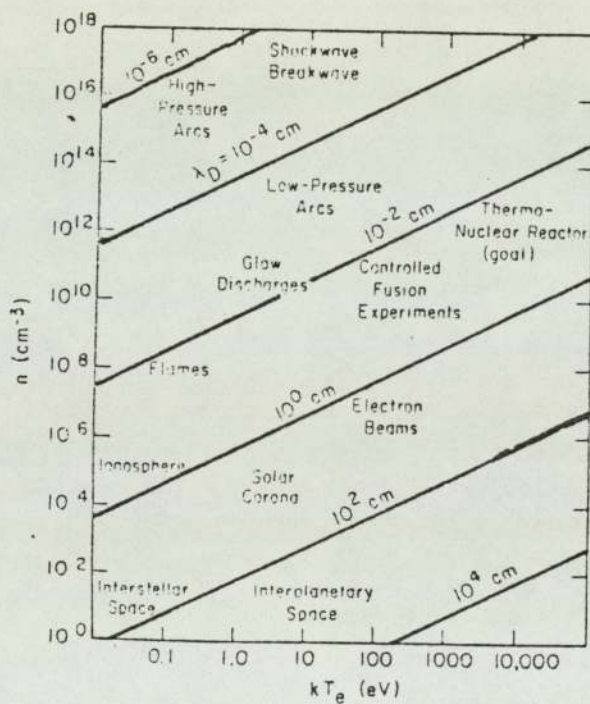
FIGURE 1.1. Typical plasmas characterized by their electron energy and density.

Fig.4   Typical plasmas.

workpiece, the size and spacing of the wafer load, the rates of volatilization and removal of reaction products, the temperature of the material and its composition. It is difficult to generalize about absolute etch rates and compare results from one sytem to another because of these factors. Poulsen (5) has suggested that etch rates depend largely on the reactor design.

The advantages and disadvantages of plasma etching are shown in table:2.

Table:2. Advantages and Disadvantages of Plasma etching.

Advantages	Disadvantages
(i)avoids use of expensive polluting chemicals and solvents,	(i)etching equipment is expensive and compicated,
(ii)fast inexpensive processes,	(ii)etching processes are not well understood.
(iii) simplifies processes and production lines,	
(iv)improves yield because it is clean and requires little wafer handling,	
(v)improves pattern resolution and tolerances,	
(vi)easier automation.	

1.1.4 Early Applications of Plasmas

The use of discharges in molecular oxygen to remove carbon and carbonaceous material from various surfaces and materials was carried out in the sixties (22,23). The discharge produced oxygen atoms which reacted vigorously with these materials producing carbon monoxide as the primary product and later carbon dioxide by reaction with another oxygen atom. This method was used to clean carbonaceous contamination from samples before S.E.M., and later to clean "used" chromium masks and microcircuits (5). In the early seventies oxygen plasmas were used to remove polymeric photoresist materials from wafers.

Plasma cleaning using CF_4 gas for difficult contamination led to plasma etching and later became a standard production process. However, plasma etching was not really understood and several papers appeared observing the effects of various parameter changes such a flow rate, temperature of wafers, gas pressure, and r.f. power (11,15). Many systems were studied with various types of reactor geometry, the two main types of reactor were (a) barrel and (b) diode. However, these were not the only reactor systems to be made, many hybrid varieties based on bell jars, sputter etchers and combinations of barrel and diode reactors were reported (5,6,10,15). Table:3., shows the main differences between barrel and diode type plasma reactors.

13

Table:3. Barrel and Diode Plasma Reactors

Barrel Plasma Reactors	Diode Plasma Reactors
(i)Usually based on long tubular design similar to diffusion furnaces,	(i)Normally are large with two flat internal electrodes on which wafers could be placed,
(ii)external or internal electrodes:- (a)external electrodes could be either plates arranged longitudinally or as bands around the circumference, (b)internal electrodes usually flat plates on which wafers could be placed or wafers held vertically in a quartz rack	(ii)wafers could be placed directly on electrode or on top of insulator such as quartz or P.T.F.E., (iii)gas admitted via a "shower" like top electrode or admitted radially (usually towards the centre),
(iii)tubular r.f. shields or cages sometimes used to limit the discharge region -wafers placed in the regionof no discharge in racks,	(iv)rotating electrodes easily arranged to give uniform exposure to the plasma.
(iv)Plasma could be inductively coupled with barrel reactor inside a large coil,	(v)electrodes could be heated or cooled and r.f. power could be applied to either electrode whilst grounding the other.
(v)internal electrodes could be heated or cooled in some instances,	(vi)electrodes could be d.c. grounded or biased.
(vi)gas flow is usually longitudinal.	(vii)no external electrodes, not inductively coupled and usually free from r.f.shields or cages inside the discharge zone.

Plasma etching became very popular after 1975 and many materials were etched using various gases and gas mixtures (5). However, poor selectivity was encountered and addition of small amounts of other gases to CF_4 was suggested to overcome this problem (112,113). This raised many suggestions for the control of selectivity during etching and many questions about the chemistry of etching in plasmas.

1.2   Plasma Chemistry - Previous Studies

Initially, this project was intended to study the chemistry of fluorine - containing gas plasmas. However, during the course of assembly of the mass spectrometer system many workers were expressing a need for a more selective plasma etching method for polycrystalline silicon than the highly reactive fluorine - containing gas plasmas. Polycrystalline silicon was becoming an important substitute for aluminium in the gate metallization layer in M.O.S. devices and was also finding applications in other areas of integrated ciruit manufacture (111). Additions of other gases such as hydrogen and oxygen to fluorine - containing gas plasmas were reported in an attempt to produce suitable etch rate ratios between silicon and oxide (112). To some extent the selective etching of silicon over oxide was achieved but was insuffient for routine production. Subsequently other gaseous materials were experimented with in order to etch selectively silicon and polycrystalline silicon in the presence of silicon oxide and nitride.

It was known that aluminium had been successfully etched in a carbon tetrachloride plasma (5) and also that the chlorides of silicon were volatile. Layers of chromium and oxide (Cr_2O_3) were being routinely etched on glass substrates in plasmas of 50:50 chlorine and oxygen (5). Interest in chlorinated gas plasmas, particularly CCl_4, was aroused and this appeared to be a fruitful area

16

to explore. There was comparatively little work published on these chlorinated gas plasmas and the mechanism of etching was not understood. Therefore, this work was mainly concerned with etching silicon in carbon tetrachloride gas plasmas. A review of the literature for both the fluorinated and chlorinated gas plasmas used in etching and polymerisation studies is presented.

1.2.1 Fluorine Containing Gas Plasmas

A detailed discussion of the major papers on fluorine containing plasmas is presented and the main conclusions are summarised in section 1.2.8. Table:4 provides a guide to the literature on plasma etching in general.

1.2.2 Selective Etching of Silicon and Silicon Dioxide

Some of the earliest work of Heinecke (112,113) pointed out that etchants such as CF_4 were particularly unfavourable for window etching into SiO_2 films on silicon subtrates because of the relative etch rates of these two materials. The etching of SiO_2 films is particularly important for defining the dopant diffusion mask in bipolar devices and the gate insulation in M.O.S. devices. It is, therefore, important to be able to selectively etch the SiO_2 film without etching the underlying silicon substrate. Heinecke put forward a simple approach to this problem suggesting the suppression of silicon etching as a way of controlling

17

the relative etch rates of silicon dioxide (112). Heinecke suggested additions of H_2 to CF_4 to make the discharge fluorine-deficient (112) and later (113) the addition of oxygen to enhance the fluorine atom concentration in the discharge. Heinecke showed that in fluorine-deficient discharges the etch rate of silicon was lower than in pure CF_4, the SiO_2 etch rate being unaffected. Similarly in CF_4/O_2 discharges the etch rate of silicon was higher than in pure CF_4.

After these early studies by Heinecke many workers (18,19,43,114-128) adopted the use of plasma etching in various forms for both research and routine production of integrated circuits. One use of plasmas was in reactive ion etching (R.I.E.) as described by Schwartz etal (114). The only real difference between this method and the usual plasma etching process was the pressure at which the plasma was maintained. R.I.E. was reported to cover the pressure range 10-140mtorr whereas plasma etching is normally carried out at pressures in the range 0.1-1.5 torr. Anisotropic etching is often reported for R.I.E. and is largely attributed to the incidence of ions, accelerated in the r.f. field, on the wafer. The lower pressure range of the plasma in R.I.E. would allow tnis sort of sputtering effect to take place because the mean free path of species in the gas phase would be longer ($5.7 \times 10^{-3} - 4.0 \times 10^{-4}$m) compared to normal plasma etching ($5.7 \times 10^{-4} - 3.8 \times 10^{-5}$m).

Bondur (18) has reviewed dry process technology
(R.I.E.) pointing out that the use of reactive gas
plasmas has led to etch rates which are 10 times greater
than could be achieved with sputter etching with argon
ions. Bondur has also suggested that CF_4 gas breaks down
to form large amounts of CF_3^+ ions (in agreement with
Heinecke) and these ions may be responsible for etching
in the reactive ion etcher.

1.2.3. <u>Etch Rates and the Influence of Parameters on Selectivity</u>

Schwartz etal (114) have used CF_4 to etch both
silicon and silicon dioxide patterned with AZ1350J
photoresist. The etch rates of SiO_2 and photoresist were
reported to be similar under certain conditions. At
40.68MHz with less than 25% of the quartz (SiO_2) base
plate covered with wafers the etch rate ratios between
SiO_2 and photoresist was 4:1 at best. Etch rate ratios
between Si and SiO_2 varied with the R.I.E. parameters but
the best reported results were 3:1 at 13.56MHz.
Photoresist degradation problems are common in CF_4
plasmas.

The addition of oxygen to CF_4 has been thoroughly
investigated by Jinno (19) etching doped silicate glass
films used as dielectric materials, passivation layers
and diffusion sources. Etching was compared with normal
wet chemical processes. The etching characteristics with

19

gas plasma processes were reported to be less dependent upon the dopant and its concentrations. The results showed a minimum in etch rate for both phosphosilicate glass and arsenosilicate glass films at a Q value of 0.5 where $Q=qO_2/qCF_4$ volume ratio. Above Q=1.0 these silicate glass films showed an increase in etch rate. No explanation was given for this behaviour.

Etch rate ratios of 10:1 for SiO_2 compared to Si were also reported for CHF_3 at 10mtorr and 30mtorr pressures (117). Etch rates were compared, for CHF_3 and CF_4, against argon gas. Etch rates in the reactive gases were generally higher than those in argon. Several effects were reported and were thought to be due to ion bombardment caused by the -300 to -600V d.c. bias which occurred across the electrodes at 13.56MHz.

The effect of mask material and oxygen additions on a CF_4 plasma have been investigated by Schwartz etal (119). The position of the wafer was also investigated at various pressures and r.f. powers (13.56MHz only). The addition of oxygen to a CF_4 plasma was reported to be able to compensate for a fully loaded cathode. Undercutting of the mask was reported in this case.

Silicon and SiO_2 have been etched in CF_4 plasmas with additions of O_2, H_2, N_2, H_2O and C_2F_4 (43). The concepts of flurine-to-carbon ratio (F/C) and oxygen-to-carbon ratio (O/C) were discussed. The etch rate ratio of SiO_2 to Si

20

increased as the F/C ratio was decreased (for instance by addition of C_2F_4 to CF_4 plasmas). The maximum etch rate for Si was shown to be at a point where the plasma gas consisted of 60% CF_4 and 40% O_2. In mixtures of C_2F_4/O_2 the maximum etch rate for Si was shown to be at a 50% mixture of the two gases. For SiO_2 the maximum etch rate was shown to be at $\sim$40% H_2 added to a CF_4 plasma. The silicon at this point did not etch but was reported to have a polymeric material deposited on its surface, hence producing high etch rate ratios for SiO_2 to Si.

Polycrystalline silicon films have been etched in several gas mixtures in plasmas and edge profiles and linewidth losses have been compared (121). C_2F_6/Cl_2 mixtures were reported to be superior for etching very fine features with little or no linewidth losses (no undercutting) compared to the isotropic etches of CF_4/O_2 and 1:1 C_2F_6/CF_3Cl which have linewidth losses of upto twice the thickness of polycrystalline silicon film etched.

Accelerated etch rates for polycrystalline silicon in a $CF_4/5\%O_2$ plasma have been reported where NaOH and KOH residues from positive photoresist developer have been left on the surface of the wafer (122).

Loading and flow rate effects have been investigated and reported by several workers (119,120,143-147) and various models have been proposed to explain these etching effects.

21

Mauer etal (120) have suggested that with increasing area of silicon being etched in a plasma the etch rate falls away asymptotically towards a base level of etching which is produced by physical sputtering alone. With the increase in area of silicon under identical plasma conditions it could be expected that there would be fewer chemically reactive etching species per unit area of silicon available and hence the etch rate would decrease. However, the normal physical sputtering could be expected to continue regardless of area of silicon present in the plasma.

Reactant supply in reactive ion etching has been investigated and related to the total dissociation of CF_4 gas as a function of input power (13.56MHz) and pressure in a diode system (146). A kinetic reaction model was described and compared with experimental results of etch rates of SiO_2 as a function of input power. Mauer and Logan suggested that this model should be able to predict reactant supply over a broader range of pressures with the inclusion of recombination mechanisms.

A simple model has been produced to explain the observed dependence of plasma etch rates on the flow rate of etchant gas (145). Chapman and Minkiewicz suggested that the dependence of etch rate on gas flow rate in the low flow regime was due to inadequate supply of reactant species. However, at high flow rates etch rates were thought to be dependent on the probability that active

species are pumped away before they have a chance to react. Some experimental results were presented showing maxima in both flow rate and pressure curves plotted against etch rate of SiO_2. These etch rate results were obtained with additions of various quantities of oxygen to a CF_4 plasma.

1.2.4. Special Techniques Used to Study Fluorine Containing Plasmas

A substantial amount of work has been reported where special techniques such as emission spectroscopy (78, 128, 136, 77(i)), mass spectrometry (128,130, 132, 133, 35), Auger Spectroscopy (129) and scanning electron microscopy have been applied to the study of plasma etching.

1.2.5 Emission Spectroscopy.

Harshbarger etal (78) were among the first to show that fluorine atoms are present in a discharge of CF_4 by observing the optical emission from excited fluorine atoms. They also showed that emission from fluorine atoms in the CF_4 plasma increased with the addition of oxygen, reaching a maximum at 10-15% of oxygen. The silicon etch rate was reported to reach a maximum at $\sim 8\%$ of oxygen added to the CF_4 plasma. Water vapour was reported to quench, almost completely, the emission from a CF_4/O_2 plasma. The addition of a plain silicon wafer to the $CF_4/8\%O_2$ discharge was reported to reduce

23

considerably the emission from fluorine atoms. They concluded form this that fluorine atoms were the probable etching species for silicon.

Below 20% of added oxygen to CF_4 plasmas, the O atom emission was of low intensity and Harshbarger etal suggested that the O atoms produced in the discharge were consumed in the production of CO, carbon monoxide. The emission intensity of CO also showed a maximum between 10 and 15% of O_2 added to the CF_4 discharge. Above 20% of added oxygen the O atom emission intensity increased rapidly slowing down at higher oxygen partial pressures. It is well known that O atom production proceeds more efficiently in discharges where O_2 is a minority species and this could explain the results presented by Harshbarger etal.

Coburn and Winters have also studied the additions of oxygen to CF_4 and reported a maximum in the fluorine atom emission intensity at $\sim 25\%$ O_2 added to the CF_4 discharge. Silicon etch rates showed a maximum between 15 and 20% of O_2 added to the CF_4 discharge (138).

The emission spectra of CF_4/O_2 plasmas have been studied by Agostino etal (137) during Si and SiO_2 etching as a function of feed gas composition. Additions of small amounts of nitrogen and argon gases were reported to permit the determination of the effect of oxygen additions on the electron densities for a wide range of

electron energies. Relative concentration profiles of F, O, CO and CO_2 were reported to be determined with this technique as a function of feed gas composition. The important role played by fluorine atoms as the active etchant for both Si and SiO_2 was reported to be confirmed. The results of etch rates of Si and SiO_2 and the relative fluorine atom concentration plotted against feed gas composition are in agreement with Harshbarger etal (78). Similarly the CO, CO_2, O and F concentrations plotted against feed gas composition also agree with Harshbarger etal. Furthermore the rapid reduction in CF and CF_2 emission intensities on addition of oxygen to the feed gas also agrees with results presented by Flamm (136). Emission intensities for CO, CO_2 and F atoms reach a maximum between 10 and 20% of added oxygen to a CF_4/O_2 discharge and are almost identical in profile to the results presented by Harshbarger etal.

The emission spectra of CF_3Cl, CF_3Br and C_2F_6 as a function of residence time, oxygen additions, power and pressure have been studied by Flamm (136). Flamm has concluded from this work that the broad continuum spectrum centred at $\sim 614nm$ originates from a common excited species produced by electron impact dissociation of the halocarbon feed gas. Flamm has suggested that this species is an excited state of the CF_3 radical which undergoes a transition to a repulsive state to yield CF_2 and F. This is consistent with the spectral evidence and explains the presence of CF_2 and unsaturated fluorocarbons

25

in these discharges. Although Flamm could not completely exclude the possibility that the continuum was due to an excited state of CF_2. Flamm also pointed out that the reaction:-

$$e + C_2F_6 \longrightarrow C_2F_6^* \longrightarrow CF_4 + CF_2$$
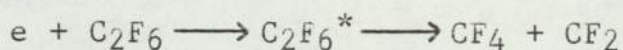
is thermodynamically more favourable than

$$e + C_2F_6 \longrightarrow CF_3 + CF_3$$
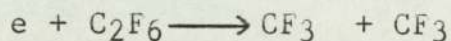
and could in itself account for CF_2 production.

The conversion of CF_4 (in CF_4/O_2 discharges) into stable products (CO, CO_2, COF_2 and SiF_4) and the concentration of free fluorine atoms in the plasma was measured using several techniques (128). Mogab etal reported that the etch rates for Si and SiO_2, concentration of fluorine atoms and the intensity of emission from electronically excited fluorine atoms ($3s^2P - 3p^2P°$ transition at 703.7nm) each exhibit a maximum value as a function of feed gas compostion. These respective maxima occur at distinct oxygen concentrations. The maximum fluorine atom concentration occurred at an oxygen content of $\sim$23%. The maximum silicon etch rate occurred at a concentration of 16.3% O_2 in CF_4 plasma. Absolute concentrations of fluorine atoms were obtained by titration with Cl_2. The maximum CF_4 conversion was reported to be at about the same oxygen content that produces maximum fluorine atom concentration, $\sim$23%O_2. A quantitaive model which takes oxygen adsorption into account was reported to relate the

etch rate to the fluorine atom concentration.

1.2.6 <u>Mass Spectrometry</u>

Mass spectrometry is the principal tool used in the present study. Chapter 2. therefore contains a detailed discussion of the application of mass spectrometry to plasma studies.

The plasma oxidation of CF_4 in a tubular-alumina fast flow reactor has been studied by mass spectrometry (130). These studies were done as a function of reactor pressure (0.15 - 0.6 torr), flow rate (2 - 80 cm^3 min $^{-1}$) and oxygen concentration in the feed gas. Results were reported for discharges investigated both in the presence and abs ence of single crystal silicon.

The only products reported from a CF_4 plasma were F, F_2 and C_2F_6 and in the presence of silicon the products were SiF_4, C_2F_6 and small amounts of atomic fluorine. The products reported from CF_4/O_2 plasmas were F, F_2, COF_2, CO_2 and CO and in the presence of silicon the products were SiF_4, F, F_2, COF_2, CO_2 and CO. The conversion of CF_4 to products was reported to increase monotonically with residence time in the discharge and the oxygen concentration in the feed gas. No direct evidence for CF_3 radicals was reported, their presence being inferred from the product C_2F_6.

27

The insertion of a piece of 304 stainless steel in the CF_4 plasma produced an increase in C_2F_6 and a decrease in F_2 species. Smolinsky and Flamm suggested that the stainless steel reacts with fluorine atoms and might explain why other workers (127) did not detect fluorine species effusing from a stainless steel reactor.

Smolinsky and Flamm reported that both Si and O_2 shifted the product distribution in CF_4 plasmas. Silicon was reported to react with the fluorine atoms to form SiF_4 with concomitant suppression of F_2 and enhancement of C_2F_6 formation. With the addition of oxygen the concentration of fluorine atoms and moleules increased many fold, C_2F_6 vanished and new products of COF_2, CO_2 and CO were formed.

A mechanistic model for fluorocarbon plasmas has been suggested by Truesdale etal (132). In particular the effect of added acetylene on the r.f. discharge chemistry of C_2F_6. Appearance potential studies of the CF_2^+ ion from C_2F_6 gas, plasma and discharges in C_2F_6/C_2H_2 mixtures were reported to show that CF_2 was formed in the discharge in C_2F_6 but only in small amounts. However, the addition of C_2H_2 to the C_2F_6 discharge was reported to markedly enhance the concentration of CF_2 as shown by the persistence of the CF_2^+ ion almost to the published value of 11.7eV.

Difluorocarbene, CF_2 was detected from all plasmas which, under their experimental conditions, etched SiO_2 faster than Si. These included discharges in CHF_3, CHF_3/C_2F_6, C_2F_6/H_2 and CF_4/H_2. In contrast no CF_2 was reported to be detected by this method from plasmas which etched SiO_2 slower than Si. These plasmas included discharges in CF_4 and CF_3Cl. Also Truesdale etal reported that if a SiO_2 wafer was placed in the discharge zone CF_2 was no longer detected from C_2F_6 or C_2F_6/C_2H_2 discharges. This suggested that the presence of low valent CF_x species such as CF_2 may play an active role in etching SiO_2. Although they pointed out that it was not clear if CF_2 was consumed through etching reactions or scavenged from the product stream by products of the etching process. They also suggested that additional work is needed to elucidate the precise role of CF_2, CF_3 and other fluorocarbon radicals in SiO_2 etching.

A novel cryopumped beam mass spectrometer has been described by Visser (133) and discharges in CF_4 with SiO_2 and Al_2O_3 targets have been observed. Visser has compared his data with Coburn's (138). Discharge transients at switch-on and switch-off were observed for fluorine at m/e 19 in a CF_4 gas using various electron energies in the ionisation source of the mass spectrometer. The SiF_3^+ signal was also monitored from discharge ignition whilst etching SiO_2 in a CF_4 plasma. Visser concluded that the etching of silica proceeds inversely to the free fluorine signal intensity. This

confirms that in the initial stage of the discharge the silica surface is protected by a sorbed layer, which must be removed in order to achieve steady state etching conditions.

1.2.7 Other Techniques

The role of chemisorption in plasma etching has been reported by Winters (129) with a wide range of gaseous materials. Winters has shown the sticking probabilities (ie: the probability for dissociative chemisorption plus the probability for non-dissociative chemisorption where $E > 20K$ cal mol^{-1} [$83.7k$ Jmol^{-1}]) for CF_4, CHF_3 and CF_3Cl on polycrystalline Si, SiO_2, Si_3N_4 and Si are less than 10^{-7}. The sticking probabilities for CF_2Cl_2 and CCl_4 are detected on some of the surfaces but are still less than 10^{-6}. Electron collisions with non - dissociating adsorbed molecules ($E < 20k$ cal mol^{-1}) were shown to result in the rapid build up of adsorbed carbon and chlorine which then remained on the surface indefinitely. Winters also reported that CF_x radicals have sticking probabilities between 0.08 and 0.75 on clean silicon.

Similarly CF_3 radicals formed by CF_4 colliding with the electron beam were allowed into contact with the substrate surface and the sticking probability determined as before. Winters concluded that the dissociative chemisorption of stable gases is probably not important

30

in plasma etching while radiation - induced - dissociative chemisorption and chemisorption of CF_x radicals were expected to play an important role in plasma etching.

The reaction of fluorine atoms with SiO_2 has been studied by Flamm etal (131) and the downstream fluorine atom concentration was measured by gas phase titration using Cl_2. Flamm etal concluded that fluorine atoms etch SiO_2 with a probability, $E_f = (0.01626 \pm 0.0015)$ exp $(-0.163eV/kT)$ in the absence of a plasma. They report that this expression is consistent with the rates and activation energies reported for in situ etching of SiO_2 in fluorine atom - containing plasmas at 0.05-0.3 torr. Consequently, the fluorine atom solid reaction alone can account for these previous data. They concluded that ion or electron bombardment may not play an important role in the etching of SiO_2 by fluorine atom-containing plasmas in the few tenths torr pressure range. However, the possibility of enhanced reaction rates due to "higher" energy ion and/or electron bombardment could not be ruled out. Coburn and Winters, however, have reviewed the mechanisms of etching using several techniques (138) and reported that electron and ion bombardment enhanced the etch rates for Si and SiO_2 in CF_4 and CF_4/O_2 discharges.

Furthermore Coburn etal (40) have reported studies of the surface chemistry and etching behaviour of silicon and oxidized silicon bombarded with a CF_3^+ ion beam

(50-4000eV) using Auger electron spectroscopy and a quartz-crystal microbalance fig:5. They concluded that the etch rate of Si due to CF_3^+ ion bombardment can be accounted for by physical sputtering alone. Also the deposition and removal of carbon at the etched surface may be one of the most important phenomena affecting the operation of plasma etching systems.

Coburn etal also suggested that ion bombardment of the etched surface enchances the reaction rate of the neutral etching species which were thought to be most probably fluorine atoms and CF_3 radicals. They showed that carbon deposition will occur when the surface to be etched is subjected to ion bombardment and carbon depositions can be expected in a reactive sputter - etching system when carbon-containing molecular gases such as CF_4, C_2F_6, CCl_4 etc, are used. In addition even when a surface is at ground potential or at a floating potential in a glow discharge, the fact that the plasma potential is usually some 10-50V positive with respect to the most positive major electrode in contact with the plasma causes these surfaces to be subjected to low-energy ion bombardment. Ions with energies in this range can still be dissociated upon impact with a surface and consequently carbon deposition can be expected to occur.

Oxygen in the lattice of oxidized silicon was reported to effectively limit the build up of carbon and
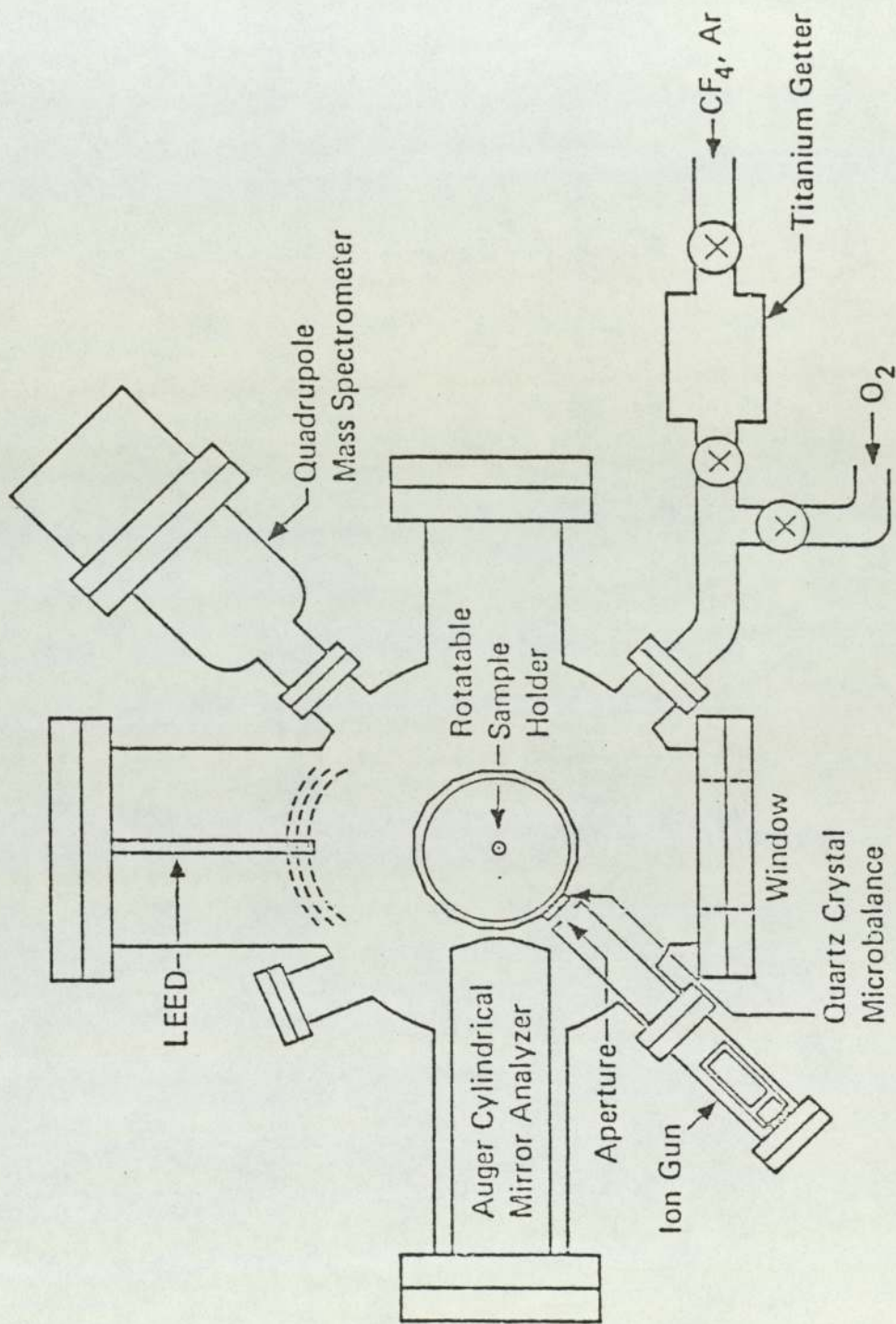
Fig.5. Surface studies (schematic).

can be used as the basis for a mechanism of selective etching. Coburn etal also reported that if a composite surface of Si and SiO_2 is subjected to low-energy CF_3^+ ion bombardment, carbon will accumulate on the silicon surface but not on the SiO_2 surface to any appreciable extent. Therefore the etch rate of Si will be reduced substantially whereas the etch rate of SiO_2 will be unaffected resulting in an increase in the SiO_2/Si etch rate ratio.

Further studies by Coburn and Winters (204) investigated the extent to which gas-surface chemical reactions can be enhanced by energetic radiation (primarily ions and electrons) incident on the surface. In particular they have studied the reactions of Si, SiO_2 and Si_3N_4 with XeF_2, F_2 and Cl_2 where volatile reaction products are formed;fig:5(a). These results showed that ion bombardment is very important in the gas-surface chemistry of plasma etching. Similar ion-enhanced chemistry was reported for F_2 on Si, F_2 on C, Cl_2 on Si and O_2 on C which were reported to behave in a similar way to Cl_2 on Si (their fig:3 in fig:5(a)). The large transient immediately following the introduction of Cl_2 was reported to be due to adsorption of chlorine on Si. The rate of chlorine adsorption overwhelms the etching process for a short period causing the Si sample to gain mass (negative etch rate for $220 < t < 260sec$). The steady state etch rate has been increased by a factor of almost 4 by the introduction of Cl_2. In the absence of the ion

33

FIG. 2. Ion-assisted gas-surface chemistry using Ar$^+$ and XeF$_2$ on silicon (volatile reaction product). Ar$^+$ energy = 450 eV, Ar$^+$ current = 0 ($t < 200$ sec), Ar$^+$ current = 2.5 μA ($t > 200$ sec), XeF$_2$ flow = 2×10^{15} mol/sec ($t < 660$ sec), and XeF$_2$ flow = 0 ($t > 660$ sec). (The Ar$^+$ current density and the XeF$_2$ flux are not uniform over the Si surface. The effective area for the Ar$^+$ current and the XeF$_2$ flux are estimated at 0.1 and 0.3 cm^2, respectively.)
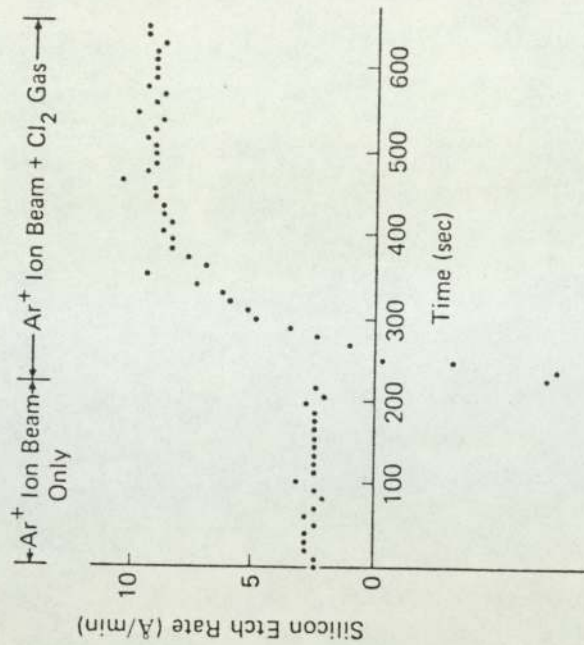
FIG. 3. Ion-assisted gas-surface chemistry using Ar$^+$ and Cl$_2$ on silicon (volatile reaction product). Ar$^+$ energy = 450 eV, Ar$^+$ current = 1.0 μA, Cl$_2$ flow = 0 ($t < 220$ sec), and Cl$_2$ flow = 7×10^{15} mol/sec ($t > 220$ sec).
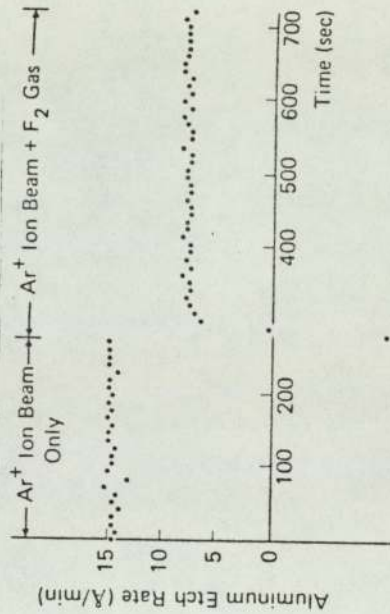
FIG. 4. Ion-assisted gas-surface chemistry using Ar$^+$ and F$_2$ on aluminum (involatile reaction product). Ar$^+$ energy = 450 eV, Ar$^+$ current = 3.0 μA, F$_2$ flow = 0 ($t < 270$ sec), and F$_2$ flow = 2×10^{15} mol/sec ($t > 270$ sec).

FIG. 1. Schematic diagram of the apparatus used to study ion-assisted gas-surface chemistry. The gas injection tube is 1.6 mm inside diameter and is about 3 mm from the quartz crystal microbalance. The gas flow is determined from the rate of pressure increase in the reservoir when the shut-off valve is closed.

Fig.5(a)

33(a)

FIG. 7. The SiF_4 pressure as a silicon surface is rotated into a beam of XeF_2 molecules with and without Ar^+ ion bombardment. The SiF_4 pressure was determined mass spectrometrically. The ratios of the pressure increases (top curve to bottom curve), indicate the magnitude of ion-assisted etching. The experiments were performed in a standard UHV system of the type often used for surface experiments. The experimental arrangement was similar to that described in Fig. 1.

FIG. 6. Electron-assisted gas-surface chemistry using 1500-eV electrons and XeF_2 on SiO_2. $P(total) = 6 \times 10^{-4}$ Torr with most of the ambient gas being xenon. Neither exposure to XeF_2 nor an electron beam produces etching by itself. Simultaneous exposure produces an etch rate of ~ 200 Å/min.

FIG. 5. Electron-assisted gas-surface chemistry using 1500-eV electrons and XeF_2 on Si_3N_4. $P(total) = 6 \times 10^{-4}$ Torr with most of the ambient gas being xenon. Neither exposure to XeF_2 nor an electron beam produces etching by itself. Simultaneous exposure produces an etch rate of ~ 600 Å/min.

Fig.5(b)

33(b)

beam the etch rate was reported to be zero since Cl_2 alone does not etch Si at a detectable rate ($<0.1\overset{\circ}{A}min^{-1}$) under these conditions ($\sim 7.5 \times 10^{-6}$ torr to 7.5×10^{-4}torr).

Coburn and Winters also used F_2 on Al (their fig:4, in fig:5(a).) to show the effects of an involatile product, AlF_3. When the F_2 is injected onto the Al surface during Ar^+ ion bombardment the sputter-etch rate decreased by a factor of 2. A similar result was reported using O_2 on Si.

The effects of electron assisted gas-surface chemistry were also shown by Coburn and Winters (their figs: 5 and 6 in fig; 5(b)) using 1500eV electrons and XeF_2 on Si_3N_4 and SiO_2. It was reported that XeF_2 does not chemically attack SiO_2, Si_3N_4 or SiC in the absence of radiation and nor does electron radiation by itself produce etching. However, with electron bombardment in the presence of XeF_2, all these materials were reported to be etched at appreciable rates and etching occurred only in the region of the sample which was subjected to the electron bombardment.

1.2.8. Summary of Fluorine Containing Plasmas

Fluorine containing gases, particularly CF_4, can etch both Si and SiO_2. However, additions of O_2,H_2,C_2H_2 or the use of P.T.F.E. or carbon platforms can considerably

34

modify the etching characteristics of the plasma.

The mechanisms of etching in CF_4 plasmas rely on an ion-assisted process for SiO_2 and a free radical process for Si although neither mechanism is fully understood. The role of carbon in both suppressing Si etching and enhancing SiO_2 etching is still not clear. Although almost certainly F atoms etch both Si and SiO_2 and CF_x^+ ions etch SiO_2 whereas carbon accumulates on Si preventing etching.

Selectivity is still rather poor for Si and SiO_2 despite the large amount of work done in this area. One reason for this is that F atoms are produced in all the fluorcarbon gases even in the presence of scavengers like H_2 and C_2H_2. However, etch rates have improved with the understanding of loading, flow rate and temperature effects.

Chemisorption of stable gases is probably not important in plasma etching. However, chemisorption of CF_x radicals formed by the discharge in the gas phase plays an important role in plasma etching and may be enhanced by radiation from the plasma. It has been shown that etching behaviour depends to some extent upon the incidence of energetic radiation (mainly ions and electrons) on the surface in the presence of etchant molecules. This has led to the use of d.c. biasing, reactive ion etchers and ion sources in the hope of obtaining anisotropic etching and enhanced etch rates.

1.3 Chlorine Containing Gas Plasmas

As can be seen from table:4 there is considerably more work available on the etching of films of aluminium and its oxide in chlorine containing plasmas than there is on etching silicon. The literature available on aluminium etching will not be reviewed here but there are nevertheless some papers which are of special interest (101,176,77(ix),141(vi) and 198).

1.3.1 Silicon Etching

Silicon and polycrystalline silicon have been etched in a variety of chlorine containing plasmas (12,117,109, 121,177). Chlorine, Cl_2 plasmas have been reported to produce highly anistropic etching of silicon (12). However, after etching in chlorine the etched surfaces were reported to have a black appearance which was initially thought to be due to deposition of a material of unknown composition. Auger analysis revealed the presence of silicon only. This effect could be reliably reproduced if the silicon wafer was first briefly subjected to a CHF_3 plasma. Etching was reported to be carried out for up to an hour in Cl_2 at $0.5Wcm^{-2}$. S.E.M. examination showed that the etched surface consisted of very closely spaced silicon "bristles" with diameters between 100 and 200nm with spacing of the same order. These silicon bristles were reported to be between 1 and 2um in length. Such a surface is an ideal absorber for

solar thermal applications. Reflectivities of the surface in the visible up to the band gap of silicon were reported to be less than 0.1% and began to rise at 1.2um and reaching 70% at 1.5um. Shorter etch times of 20 minutes in Cl_2 produced reflectivities as low as 0.2%.

Anisotropic plasma etching has also been reported by Mogab and Levinstein using some mixtures of fluorinated and chlorinated hydrocarbons or partially chlorinated fluorocarbons (177). This work suggested that the etching species for silicon was chlorine atoms. The effect of doping on etch rates was also reported. Selective plasma etching of phosphorus and arsenic doped polycrystalline silicon relative to SiO_2 was reported for mixtures of C_2F_6 and Cl_2 in a parallel plate reactor, the primary etching product was $SiCl_4$. A Differential in etch rate between, n-, p- type or undoped polycrystalline silicon was observed and thought to be related to the need for electron transfer to adsorbed chlorine at the silicon surface in order for chemisorption to take place. This mechanism has also been suggested by Schwartz and Schaible (77(xi)) to explain some of the unusual temperature and pressure effects they have observed.

Schwartz and Schaible (109) have used both CCl_4/Ar and Cl_2/Ar plasmas to etch silicon using masks of SiO_2, Al_2O_3 and MgO. They have studied etch rates as a function of r.f. power, freqency, reactant concentration, flow rate

and pressure. The addition of CCl_4 to Cl_2/Ar plasmas or heat sinking the wafers to the water cooled electrode reduced lateral etching. Surface effects similar to those found by Lehman and Widmer were reported and they were not consistently reproducible. A "polymer" like film near the CCl_4 inlet on the silicon wafer was also noted. In Cl_2 plasmas they reported that the silicon surface sometimes blackened and it was not uniform in intensity but most pronounced near the chlorine gas inlet. Auger analysis was reported to show silicon and a high oxygen content. The surface was easily damaged and almost wiped clean with a swab.

Schwartz and Schaible also reported a separate phenomenon independent of background water or batch size giving rise to rough surfaces similar to Lehman and Widmer. Groove formation near the unetched features was reported and thought to be due to sputtering by CCl^+_3 ions. The groove diminished in size with increasing pressure, i.e: shorter mean free path of species. Both etch rate and groove formation were reported to be insensitive to substitution of helium for argon and they suggested that Cl^+_2 and CCl^+_3 ions were the predominant sputtering species at 10mtorr pressure. Unfortunately Schwartz and Schaible did not give the etch rates for silicon in these plasmas.

The effect of frequency on chlorinated gas plasmas has been studied by some workers (77 (xii), 178

38

178, 141(viii)). The difference in the chemical composition of the discharge in CCl_4 at low and high frequency r.f. power has been studied by Bruce (77(xii)) using a mass spectrometer sampling gas via a pinhole in the base plate of a stainless steel reactor chamber. The range of frequencies used was 20kHz to 27.5MHz and both aluminium and silicon etch rates were observed as a function of frequency. Mass spectral measurements were made of both neutral and charged species representative of gas striking the wafer as a function of frequency. Etch rates for silicon were reported to be ~1500Å min^{-1} at best and for aluminium ~2000Å min^{-1}.

Bruce noted that in pure CCl_4 the stainless steel electrodes became coated with a polymer film which had an increasing deposition rate with increasing frequency. The increase in abundance of C_2Cl_2 at higher frequencies suggested that C_2Cl_2 was a polymer precursor. The etch rate of silicon at higher frequencies was reported to be lower and was suggested to be due to either polymer formation on the surface or lower ion energies at the silicon surface. The higher etch rate of aluminium could not be explained at the higher frequencies but Cl_2^+ ions were more abundant at higher frequencies and these may have been a predominant factor in aluminium etching.

Discharges in Cl_2 gas etching silicon at r.f. frequencies from 15kHz to 27MHz with the same sampling system as previously described (77(xii))have been

39

investigated by Bruce and Reinberg (178). Electrical characteristics and ion energies were also investigated under indentical conditions as a function of excitation frequency. As the excitation frequency was increased the silicon etch rate was reported to decrease and also the ion energy decreased. The operating voltage amplitude was shown to have a maximum which corresponded to the maximum etch rate for silicon at 0.5MHz. Silicon etching was anisotropic at both high and low frequencies and Bruce and Reinberg concluded that the etching process appeared to be a "bombardment" induced process with negligible chemical contribution.

Similarly the effects of frequency on voltage-current characteristics, emission spectra, etching and the energy distribution of ions across the sheath of chlorine plasmas at 0.3 torr have been observed by Flamm etal (141(viii)). They reported that with increasing frequency an increase in the potential across the sheath region and an increase in the energies of ions bombarding the electrodes was observed. Helium and argon additions were made to determine relative chlorine species concentrations from their excited state emission intensities. Various reactors were used in this study ranging from 2cm to 20cm internal diameter. In one reactor, ions could be extracted through pinholes into a differentially pumped high vacuum chamber. Retarding grids and an in-line mass spectrometer were used to detect ions and measure their energies. Dye laser

fluorescence and optical emission were also used on separate reactors.

Emission spectra and mass spectral analysis of ions extracted from the sheath region showed shifts in the ratio of Cl_2^+ to Cl^+ signals as excitation frequency is lowered. Flamm etal reported anisotropic etching of silicon at low frequencies and isotropic etching at higher frequencies. This was explained by an increase in ion bombardment energies at the lower frequencies despite having earlier shown that the sheath region potential increases and therefore the energy of ions bombarding the surface increased with increasing frequency.

1.3.2. Carbon Tetrachloride - Other studies

Several other studies related to carbon tetrachloride gas plasmas have been made (182,187,56,170,49).

The ionisation potentials of both CCl_3 and CF_3 radicals and the bond dissociation energies in several chloro-fluoro-methanes have been measured by mass spectrometry (56).

The effect of wavelength on the gas-phase photolysis of carbon tetrachloride has been observed by Davis etal (182). They showed that there was a clear trend towards increasing molecular fragmentation with increasing photon energy. A detailed mechanism was described based upon

41

scavenging by bromine and oxygen added to the carbon tetrachloride and analysis of the product yield by gas chromatography. Davis etal pointed out that it has been known for many years that phosgene is formed when CCl_3 radicals are generated in the presence of oxygen. Steacie (185) gives a discussion of possible mechanisms involved.

The gas-phase radiolysis and fast flow microwave discharge studies of CF_4-CCl_4 mixtures have also been reported (184,170). The reaction of fluorine atoms with CCl_4 using molecular beam analysis has been studied by Kolb and Kaufman (49).

Table: 4 Guide to the Literature on Plasma Etching

Materials (s) Etched	Gas(es)	Comments	Reference
Various	Various	Review paper by Poulsen, R.G.	5
Various	Various	Etching Sympsium 1976 Reinburg A.R. Review.	15
Various	Ar, CF_4, CHF_3	Profile Control; comparison of sputtering and Plasmas.	117
Si, SiO_2	SF_6/N_2; CHF_3; Cl_2	Rough surface on Si with Cl_2 plasma.	12
Various	Ar/O_2	Introductory paper on dry etching techs.	7
Various	------	Review of Vacuum processes.	9
Si, SiO_2	Ar/F_2; XeF_2; CF_4/O_2; CHF_3.	Plasma Etching-A Discussion of Mechanisms.	11
Various	Various		14
Si, SiO_2, Si_3N_4, AZ1350J	$CF_4, CF_4/O_2$; CCl_2F_2; others	Dry process technology (R.I.E).	18
Silicate glass	CF_4	Doped silicate glass films.	19
SiO_2, Si_3N_4	CF_4; C_2F_6; C_3F_8	End point determination.	26
Various	CF_4; BCl_3; others	End point determination and gas analysis.	27
Cu	O_2/Ar; Ne	Glow discharge mass spectrometry.	33
Si	CF_3^+	Ion surface interactions.	40
Si, SiO_2	CF_4/H_2; various others	Etching and Polymerization studies.	43
SiO_2, Si	CF_4; C_3F_8; CHF_3	Heinecke − bell jar system.	112
SiO_2, Si	CF_4/O_2	Heinecke − bell jar system.	113
SiO_2, Si, AZ 1350 J	CF_4	Reactive ion etching; Photoresist degradation. 40.68 MHz and 13.56 MHz	114
SiO_2	Dry HF	Dryox process; 150 − 190°C; 0.1 −30 torr.	115,116
$Si; SiO_2$	CF_4; CF_4/C_2H_2	Used teflon and carbon substrate or mixed C_2H_2.	118,123
$Si; SiO_2$	CF_4	Mask material effects, pressure and power	119,120

Table: 4 Guide to the Literature on Plasma Etching   contd.

Materials (s) Etched	Gas(es)	Comments	Reference
Poly Si	C_2F_6/Cl_2; CF_4/O_2; C_2F_6/CF_3Cl	Polycrystalline silicon etched, compared linewidth losses.	121
Poly Si	$CF_4/5\%O_2$	NaOH and KOH residues, accelerated etch	122
SiO_2;Si PMMA.AZB50B	CF_4/H_2; CF_4	Reactive on etching.	124
Si;SiO_2;Si_3N_4;AZ1350J	CF_4	Diode system parameters, power, pressure loading effect.	125
Poly Si	CF_4	Phosphorus doped Polycrystalline Si	126
Si, SiO_2	CF_4	"Pseudo - black box" approach.	127
Si, SiO_2	CF_4/O_2	Effect of oxygen additions.	128
Poly Si, Si, Si_3N_4, SiO_2	CF_4, CF_3H; CF_3Cl; CF_2Cl_2;CCl_4	Determined sticking probabilities for these gases on various materials.No etching done.	129
Si; Stainless steel	CF_4/O_2	Plasma oxidation of CF_4 studied. Addition of Stainless Steel to discharge increased C_2F_6.	130
SiO_2	F atoms	Flow Tube and mass spectrometer.	131
SiO_2, Si	C_2F_6/C_2H_2	Also CHF_3/C_2F_6; C_2F_6/H_2 and CF_4/H_2.	132
SiO_2, Al_2O_3	CF_4	Cryopumped Mass Spectrometer.	133
Si_3N_4	CF_4/O_2	Emission spec. shows F Atoms.	78
Si, SiO_2,	CF_4/O_2	Emission spec.	137
---	CF_3CFCl_3; Cl; CF_3Br; C_2F_6	Emission spec.	136
Si	He/F_2;CF_4/O_2; SF_6/O_2;CF_3Cl/O_2; SiF_4/O_2.	Emission Spec. luminescence on downsteam Si surface.	77(i)

Materials (s) Etched	Gas(es)	Comments	Reference
Si, SiO_2	CF_4/O_2;F_2	Review; effect of O_2 additions.	138
---	$SiBr_4$	Emission from SiBr.	142
Si	CF_4/O_2	Loading, temperature effects end point det.	143
GaAs.	CCl_4; CCl_2F_2; CF_4.	Using 90 Mole% Ar diluent.	141(i)
Si	CF_4	Loading effect; model.	120
SiO_2	CF_4	Reactant supply; loading effect.	146
SiO_2	CF_4/O_2	Flow rate effects; model.	145
Si, SiO_2	$CF4/O_2$	Flow rate effects.	147
Si	SF6	Selective etch for Si.	148
Si, SiO_2	$SF6/O_2$	Composition studies at 27MHz;45W ltorr (Si: SiO_2; 40:1)	149
---	SF_6/O_2;SF_6	Kinetic and spectroscopic analysis.	141(ii)
Si;SiO_2;Si_3N_4	SF_6; C_3F_8; C_2F_6	Saddle- field sources; also Ar,CF_4 gases.	150
SiO_2; Si	SiF_4;C_2F_6	Ion beam;angular depence of sputtering yield.	77(ii)
Si	SiF_4; CF_4	Correlation of emission spectra suggest main etch product SiF_2. Also CF_4/O_2	77(iii)
SiO_2;Si_3N_4	SiF_4/O_2;	compared. Poly Si;Si also compared. Compared to CF_4/O_2;investigated role of	77(iv)
Si	CF_4/CO_2	CO_2 in plasma. also NF_3/Ar;Photoresist	77(vi)
Si;AZ1350H	NF_3;NF3/O_2	etched; ratio Si: Resist, 3.5:1.	77(v)
Si	F_2/N_2 or O_2	Oxygen quenches Fluorine emission.	141(iii)
Si;SiO_2;Si_3N_4	XeF_2;F_2	Ion Surface, gas surface radiation induced etching.	204
Si;SiO_2	$CBrF_3$	Also poly Si and Mo etched relative to SiO_2.	152

Materials (s) Etched	Gas(es)	Comments	Reference
Si; SiO_2	$CBrF_3$	Polymerization, n-doped Si etches faster than Si. Bromine monolayer under Polymer.	153
Si; Resist	CF_4/NO	NO is preferable to O_2 in improving selectivity.	141(iv)
Ti-Pd-Av	$CBrF_3$; $CClF_3$	$CBrF_3$-He-O_2 mixtures; $CClF_3$-He optimum 63% $CBrF_3$, 25% He and 12%O_2. Emission Spectrocopy of plasmas.	154
$LiNbO_3$;Cr	CHF_3;CF_4;Ar	Photoresist Az1350J; reactive ion beam etching.	156
Al;Al/4% Cu; Al/4% Cu/Si	CCl_4;Cl_2;Br_2; HCl; HBr,	Reactive ion etching of aluminium and alloys.	174
Al_2O_3;Si	Ar/Cl_2;BCl_3 Ar/CCl4	High rates of etch ; R.I.E. ; MgO mask.	175
Al;Al_2O_3	CCl_4;CCl_4/O_2	Effluent compostion monitored; various electrodes.	101
Al;Al_2O_3	BCl_3; CCl_3;	Compared etching; high reflected powers for CCl_4 plasmas.	176
Al;Si;SiO_2	CCl_4; BCl_3	Others PCl_3;BBr_3;BCl_3;BBr_3 etc: CCl_4 residues.	77(vii)
Al; Poly Si	CCl_4;CF_4	4 cycle process-CF_4 descumming and oxide removal.	77(viii)
Al	CCl_4;	Influence of humidity on etch reproducibility.	77(ix)
Al	CCl_4	CF_4 photoresist pretreatment, photoresist also etches.	141(v)
Al	CCl_4	Polymer formation; Quartz microbalance used.	141(vi)
Si;Poly Si	C_2F_6/Cl_2; C_2F_6/CF_3Cl; Ar/Cl_2	Effect of doping on Si etch rate. Interesting discussion and review.	177
Si; Special Structure.	CCl_4/Ae or He Cl_2/Ar	N^+ layer laterally etched; CCl_4/Cl_2 does not latterally etch N^+ layer. Rough surfaces after etching.	109
Si	Ar/Cl_2	Small percentages of Cl_2 in Argon modelled around diode etcher. Flow rate and loading.	77(xi)

Table: 4 Guide to the Literature on Plasma Etching   contd.

Materials (s) Etched	Gas(es)	Comments	Reference
Si; Al	CCl_4	Frequency effects;mass Spectra;polymer and $AlCl_3$.Effect of power at different frequencies.	77(xii)
Al; Al-2% Si	CCl_4;	Double beam and point detector Broad band CCl and OH emission obscured atomic Al.	77(xiii)
Si;	Cl_2	Anisotropic etching at low and high frequencies;maximum etch rate @ 0.5Mhz.	178
Si;In P; GaAs	Cl_2	Emission intensity of $Cl;Cl^+$ and Cl_2^+ against frequency and etch rates for Si vs frequency.	141(vii)
Cr implanted with Sb^+, As^+	CCl_4/Air	Also Ar^+ ion implanted films used. Etch rates unaffected by Ar^+ but reduced by As^+ and Sb^+.	179
$Cr;Cr_2O_3$	CCl_4 + Additions; Cl_2 + additions.	Varied ratio of added gases; He; Ar; O_2; N_2+O_2. W, Fe and Cu impurities accumulate on the wafer surface.	180
Au;Pt; others	$CClF_3$;	Gold or Platinum redeposits on Photoresist	115
Au; others	$C_2Cl_2F_4$	Review	5
Ta;Cr	Various	Review	9
GaAs	Various	Sixteen different reagents investigated.	181
Si;Poly Si;Al	$CCl_4;SiCl_4$	Aluminium etched in $SiCl_4$ compared to CCl_4. CCl_4 leaves a film of polymer.	198
GaAs;GaSb; In $P;Si_3$- N_4 and oxides	H_2	Emission-U.V. of Hydrogen plasmas.Power and pressure effects; etch rates Si 250-500 $A°$ min^{-1}. 30:1 etch rate ratio for $Si:SiO_2$.	199
Poly Si	$NF_3;CCl_4$	Etch rates measured as a function of wafer area and power density.	209
Al	$SiCl_4$	Anisotropic etchant; sputter etched.	210
$SiO_2;Si$	CHF_3	Pressure-to-flow rate ratio P/F investigated; 500-2500W;5-45 Sccm and pressures 45-99m torr.	211

Table: 4 Guide to the Literature on Plasma Etching   contd.

Materials (s) Etched	Gas(es)	Comments	Reference
Si;	Cl_2	Profile control with d.c. bias.	212
SiO_2;Si	CF_4;C_2F_6; C_3F_8	Selective for oxide over Si in ion beam etching.	213
SiO_2	CF_4	Kaufman ion source and current probe; reactive ion etching.	214
Poly Si;SiO_2	CF_4/H_2	Computer controlled reactive ion etching.	205
Poly Si	CCl_4/O_2	Emission spec and etch rates 0-60% O_2.	206
Mo;Si;SiO_2	CCl_4/O_2	Mass spec and etch rates 0-100% O_2.	232
Poly Si	F_2	S.I.M.S studies on F_2 adsorbed layers on Poly Si.	207
Al;SiO_2;Si	C_4F_8;$SiCl_4$	R.I.E. microwave electron cyclotron resonance discharge ion source.	233

1.4   Polymer Formation

Polymer formation in both fluorine and chlorine containing plasmas is dealt with in this section under separate headings. Table:5 is a guide to the literature on Polymer formation in plasmas used in plasma etching.

1.4.1   Fluorine Containing Plasmas

Recently work on plasma polymerization has become more widespread (188-196, 102, 153, 129, 138). Plasma polymerization of fluorine-containing gases in the etching process is an intolerable nuisance during semiconductor integrated ciruit manufacture. Layers of polymer obscure the silicon surface preventing etching and hence produce inferior devices. Many workers have attempted to identify and understand the particular plasma conditions in which plasma polymerization takes place.

Coburn and Winters (138) have tried to identify the boundary between polymerizing and etching conditions by considering the fluorine-to-carbon (F/C) ratio of the chemically reactive species and the bias applied to a surface in the discharge. The F/C ratio can be varied by using fluorine deficient gases or their mixtures with other fluorine containing gases or modified by the addition of oxygen, hydrogen, or C_2H_2 which result in fluorine or carbon being converted into relatively

43

unreactive species which cannot participate in etching or polymerizing chemistry. For example Coburn and Winters give the F/C ratio of the active species generated by dissociation of CF_4 as 4.

Coburn and Winters suggest that as an etching fluorocarbon plasma is made more and more fluorine deficient, a point will be reached where polymerization starts to dominate over etching. The position on the F/C axis where this occurs is, they suggest, dependant on many of the parameters of the plasma system. On this basis they point out that polymerization will occur on Si more readily than on SiO_2. Coburn and Winters also give some interesting discussions of the possible mechanisms of polymerization and etching in fluorine containing plasmas.

Similarly Coburn and Kay (43) have examined the behaviour of a variety of gases and gas mixtures and have concluded that low F/C ratios are likely to give rise to polymerization more readily than gases with higher F/C ratios. However, they point out that some polymerizing gases can be made to etch silicon when bombarded with energetic ions.

Coburn and Kay have also discussed the idea of the oxygen-to-carbon (O/C) ratio for several oxygen containing gases and have reported that gases with O/C ratios of 1 give rise to fast etch rates for silicon.

They have concluded that unsaturated monomers inevitably
lead to polymerization upon exposure to a glow discharge
but can be converted to etching discharges by the
addition of oxygen.

Flamm etal (153) have reported that etching and film
formation in CF_3Br plasmas exhibit a number of unusual
phenomena. Under certain conditions both Si and SiO_2 can
be concurrently etched, while in other circumstances only
SiO_2 is etched and Si is coated with a uniform,
crosslinked fluorocarbon film. The fluorocarbon polymer
was reported to overlay a monolayer of bromine at the
silicon interface, but negligible bromine is incorporated
into the fluorocarbon film. In order to account for this
they suggested that CF_xBr incident on the surface may
dissociatively chemisorb by the thermodynamically
favourable reaction:-

$$CF_xBr + Si \text{ (surf)} \longrightarrow CF_x + Br-Si \text{ (surf)}.$$
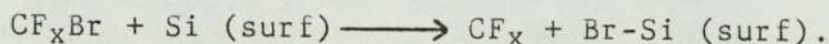
and if the flux of unsaturated radicals is not sufficient
to terminate $(CF_x)n$ at short chain lengths an involatile
polymeric film can form. Several other mechanisms were
suggested and Rutherford backscattering was used to
elucidate the nature of the polymer film deposited on the
Si surface.

Truesdale and coworkers (132) have reported large
quantities of polymeric material with composition $(CF)n$
formed in the discharge zone of a C_2F_6/C_2H_2 plasma. They
have also used a chemical model for fluorocarbon plasmas

to explain the formation of polymeric material in the discharge.

Kay etal (189) have presented mass spectrometric studies, sampling neutral and ionic species, of both polymerizing and etching fluorocarbons in glow-discharges. Polymer deposition rates were studied for $C_2F_4, C_2F_6, C_2F_6/10\%$ H_2 and C_2F_5H as a function of flow rate. They reported that the intensity of highly unsaturated species is a reliable indicator of the deposition rate of polymer film as determined by a quartz crystal microbalance. In addition, they report that the carbon-to-fluorine ratio of these species in a C_2F_4 discharge is close to one and this was approximately the carbon-to-fluorine ratio of polymer films deposited in the discharge region. The nature and amount of polymer reported deposited adjacent to the r.f. electrode (where the surface was at a large negative potential) differed markedly from the nature and amount of polymer deposited on floating or grounded surfaces. In the case of unsaturated monomers the depostion rate was reported to be substantially greater near the r.f. electrode.

Kay etal reported that the intensity of C_2F_2 species in the mass spectrometer correlated with the polymer deposition rate suggesting that these species are involved in the polymerization process.

Vasile and Smolinsky (38) have studied the chemistry of the r.f. discharge of C_2F_4 by mass spectrometry. They

reported that the C_2F_4 discharge chemistry is dominated by the production of neutral gas phase species and polymeric deposits on the electrodes and wall of the discharge vessel. Ionic species observed in the discharge were reported to be characteristic of electron impact ionization of C_2F_4 and the neutral products were reported to be C_2F_6, C_3F_6, C_3F_8, and C_4F_8. In contrast to discharges in hydrocarbons they report that ion-molecule reactions are not a dominant feature of the C_2F_4 discharge. Appearance potential measurements were reported to give direct evidence of the effusion of CF_2 radicals from the discharge but not for CF or CF_3 radicals.

Before making their mass spectrometric observations Vasile and Smolinsky coated all the inside surfaces of the reactor with a plasma-polymerized tetrafluoroethylene film to avoid any possible complications in the observed spectra due to the interaction of the glass walls with fluorine containing species. Vasile and Smolinsky also report that the literature on the photolysis of C_2F_4 can explain the presence of all the C_3 and C_4 molecules found in the discharge.

Kay and Dilks (102) have presented a critical review of plasma polymerization of fluorocarbons in an r.f. capacitively coupled diode system. The formation of metal containing fluoropolymers by simultaneous plasma etching

47

and polymerization in the same system was discussed in detail. The polymer deposition rate, at the grounded electrode, was reported to be strongly dependent on the excitation electrode material as well as the F/C stoichiometry of the injected fluorocarbon. The metal content of the films could be varied by addition of oxygen and hydrogen to the plasma. E.S.C.A. spectra of the films formed with Cu,Mo and Ge cathodes in C_3F_8 plasmas at 20W and 15mtorr were presented. Consideration of the signal intensities allowed Kay and Dilks to estimate the quantity of metal incorporated into the films, 19% molybdenum and 14% copper. Germanium was only incorporated into the polymer film at high r.f. power levels (100W) and the metal was then homogeneously dispersed throughout the film.

Further work by Kay etal (191) has explored the effects of adding H_2 or O_2 on the metal containing fluoro-polymer films produced by simultaneous plasma etching and polymerization. They reported that the likely precursors to plasma polymerization have been identified for the C_2F_4/O_2 and C_3F_8/O_2 systems studied. The primary precursors to polymerization of films incorporating molybdenum were reported to be of the general form $(CF_2)n$, n= 1,2,3,4 and their relative concentrations were dependant upon the oxygen partial pressure.

The fluorine and metal content of the polymer was reported to be decreased when hydrogen was added to the plasma. Kay etal concluded that the use of additive gases provides a convenient method to continuously vary the metal content of the films formed by simultaneous plasma etching and polymerization.

1.4.2. Chlorine Containing Plasmas

Several workers have reported the deposition of polymer-like films on wafers, electrodes, walls and surfaces near the gas inlet in chlorine containing gas plasmas and particularly in carbon tetrachloride plasmas.

Tokunaga and Hess (101,176) reported that stainless steel electrodes were particularly susceptible to polymer formation when using a CCl_4 plasma at 0.75 torr (100Pa). They investigated the films produced using Auger electron spectroscopy and reported that the films were mainly C-Cl polymer films. By collecting the effluent gases from the discharge in CCl_4 and analysing them by gas chromatography they were able to show that the C_2Cl_4 in the effluent increased by a factor of 10 compared to the same conditions with aluminium electrodes. Tokunaga etal suggested that C_2Cl_4 was a polymer precursor and also pointed out that iron and nickel are both Fischer-Tropsch catalysts and are used to generate long chain hydrocarbons (C_5-C_{30}) from CO and H_2. Such a mechanism could be operative on stainless steel electrodes when

chlorocarbon species are present thereby generating polymer-type films.

Bruce (77(xii)) has reported that the deposition rate of polymer from a CCl_4 discharge increases with increasing r.f. frequency. From mass spectral measurements Bruce has suggested that C_2Cl_2 was a polymer precursor, the abundance of C_2Cl_2 increases with increasing r.f. frequency.

Curtis and Brunner (141(vii)) have used an oscillating quartz microbalance coated with aluminium films to study the initial stages of etching of aluminium in CCl_4 plasmas. They found that the delay time between plasma ignition and the onset of etching depended upon reactor cleanliness. During this induction period they reported a polymeric film was first deposited on the aluminium and then removed again as etching began. Induction periods of upto 24 minutes were reported before aluminium etching began, this was confirmed by the appearance of the optical emission band at 216.4 nm due to AlCl after 24 minutes. Auger analysis clearly showed that the weight increase during the induction period was caused by the deposition of a polymeric material which contained about 50% carbon. These results also showed that even during etching it is possible that polymeric material is being deposited on the aluminium surface.

In a thoroughly clean reactor etching was reported to begin almost at once with an initially lower etch rate which could in part have been due to oxide removal. The etch rate in this case stabilized at 2700Åmin^{-1} which was similar to the etch rate (2100Åmin^{-1}) obtained after the 24 minute induction period.

Curtis and Brunner also reported that r.f. (13.56MHz) powers below 0.2Wcm^{-2} caused the quartz crystal to continuously increase in weight linearly for periods upto 1.75 hours with no sign of etching taking place. The use of higher powers of 1.5Wcm^{-2} resulted in very short induction periods of about 1 minute and weight increases of less than 100Å equivalent aluminium thickness (the microbalance was reported to be calibrated in Å of aluminium). By varying the r.f. power during a run an increase or decrease in the sample weight could be obtained. These results indicated that a power density of 0.3Wcm^{-2} was somewhere near to a critical value for their apparatus. This was supported by their report that induction periods at this power level were of variable length.

Table:5 Guide to the literature on Polymer formation in Plasmas

Gas(es)	Comments	Reference
Various	Conference abstracts and papers on Plasma Polymerization and deposition.	188
CF_4/O_2	Auger electron spectroscopy.	138
Various	Defined region of changover from etching to polymer.	43
$CBrF_3$	Bromine monolayer then fluorocarbon polymer film.	153
Various	Sticking Probabilities of gases and effect of ions.	129
C_2F_6/C_2H_2	Polymeric material $(CF)_n$; model of discharge.	132
C_2F_4;others	Low electron energy mass spectra. Polymer deposition versus flow rate.	189
C_3F_8; others	Metal Containing polymers; Cu;Mo;Ge;E.S.C.A.	102
Propylene	Polymer deposited on both glass and Aluiminium.	190
CF_4/H_2 or O_2	Metal containing fluoropolymer films; E.S.C.A.	191
T.F.E.	P.T.F.E. and Carbon deposition; Review.	6
Ethylene	@ 60Hz; 10kHz; 13.56MHz. Polymer deposited on Electrodes.	192
C_3F_8	Metal containing fluoropolymers; $(CF_2)_n$, n=1,2,3,4,5.	193
Background gas	SiC formation on Si with Ar^+ ion etching; Auger.	194
C_2F_4;C_3F_6;C_4F_8	Emmission spectra suggest CF_2 radicals responsible.	195
Various	Symposium or "Plasma Polymerization"	196
CCl_4;CCl_4/O_2 BCl_3; CCl_4	Polymer formation on stainless steel electrodes worse than aluminium electrodes. Effluent monitored.	101/176
CCl_4/Ar	Rough surfaces and Polymer.	109
Various	C_2F_6; C_2Cl_4; CBr_2Cl_2; $CHCl_3$; PH_3; CHF_3 all Polymerize trying to etch GaAs.	181
Benzene	Microwave and radiofrequency plasmas comparative study.	144
Organic vapours	Double probes in glow-discharge polymerization studies.	96

2. TECHNIQUES FOR STUDING PLASMAS

The techniques for studying plasmas can be divided into direct and indirect techniques. The direct techniques sample material directly from the plasma unchanged and indirect techniques depend upon some effect of the plasma, such as optical emission or electrical properties, which is related in some way to the composition of the plasma.

2.1   Mass Spectrometry - General Discussion

Mass spectrometry is, in principle, the most useful analytical technique available for directly sampling the species present in a plasma discharge. The mass spectrometer may be attached to a plasma discharge system in different ways: e.g.

a) downstream mass spectrometry of effluent gases from a discharge;

b) directly sampling from the plasma (i)ions - both positive and negative; and (ii)neutral species - molecules, atoms and radicals.

The first method (a) is an indirect method which can be used for process control and end point determinations.

2.1.1   Appearance Potentials

Although mass spectrometry allows unambiguous

52

indentification of ions (within the limit of finite m/e resolution), identification of the neutral parent of each ion requires considerable care. Atoms and free radicals are usually identified by the method of appearance - potential discrimination. That is the formation of ions with energy lower than that needed to produce the atomic or free radical ion by any fragmentation process. For example, if the products of the discharge:-

$$A_2 \xrightarrow{\text{r.f. discharge}} \overset{\bullet}{A} + \overset{\bullet}{A} \; (+A_2) \tag{1}$$
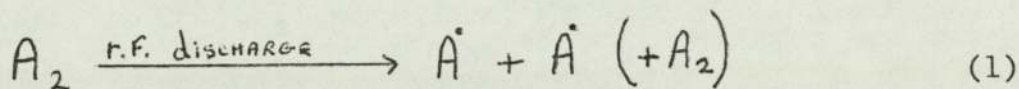
are sampled into a mass spectrometer ion source, then the ion current observed at m/e A, where A represents the molecular weight of species A, will consist of contributions from both the atom, A and the molecule, A_2. The possible electron impact processes in the ion source are:-

(i)   Ionisation
$$\overset{\bullet}{A} + e \longrightarrow A^+ + 2e \; ; \; E_1 > I\,(\overset{\bullet}{A}) \tag{2}$$
$$A_2 + e \longrightarrow A_2^+ + 2e \; ; \; E_2 > I\,(A_2) \tag{3}$$
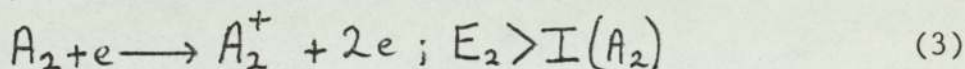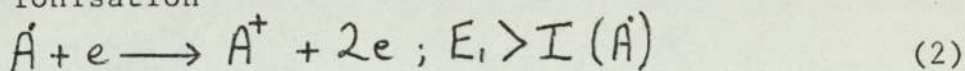
(ii)   Dissociative ionisation
$$A_2 + e \longrightarrow A^+ + \overset{\bullet}{A} + 2e \; ; \; E_3 > I(A) + D(A-A) \tag{4}$$
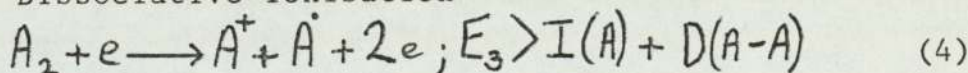
(iii)   Ion - pair production
$$A_2 + e \longrightarrow A^+ + A^- + e \; ; \; E_4 > I\,(A) + D(A-A) - EA(A) \tag{5}$$
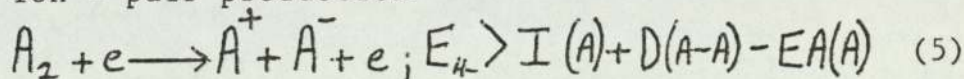
where

EA(A) = electron affinity of A

I(A) = ionisation potential of atom A

D(A-A)= bond dissociation energy of A-A

E_x = electron energy.

If the electron energy is set lower than E_3 or E_4, but greater than E_1, then the only contribution to the ion current at m/e A should be from A atoms. Process (3) does not contribute at all to the ion current at m/e A. Similar considerations are made for the detection of radicals.

As the bond dissociation energy of the molecule increases, it becomes easier to differentiate between the two contributing ion currents to m/e A. Foner (57) has shown a theoretical appearance potential plot of ion current, for A^+ from A, and A^+ from A_2 by dissociative ionisation, as a function of electron energy. (Foner's Fig.3. p393). The ion current, or log ion current, plots are linear and parallel at low electron energy, within a few electron volts of the appearance potential of A^+ and separated by D(A-A) the bond dissociation energy.

As the energy of thermally produced electrons is not monochromatic but has a Boltzmann distribution the ionisation plots do not intersect the electron energy axis at the ionisation potential but tail off asymptotically. Therefore to obtain the appearance or ionisation potential of a species A, it is necessary to refer to a standard (Ar, Kr etc.) and use one of the normal techniques such as semilog matching (71) or extrapolated voltage difference (70). These methods are reviewed elsewhere (57,69).

2.1.2   Downstream Mass Spectrometry

In this method the mass spectrometer is connected some way downstream from the plasma reactor onto the vacuum pumping system. Hence, any material sampled by the mass spectrometer is recombined effluent gases from the plasma reactor which have undergone many wall collisions and are therefore the final reaction products from the discharge. (24,25).

Flamm (24) has pointed out that analysis of products downstream from a fluorocarbon plasma is difficult at the high ionisation energies ($\simeq$ 70eV) normally used in mass spectrometry. This is due to fragmentation of the gas molecules caused by the energetic electrons in the mass spectrometer ion source. These fragment ions are not uniquely characteristic of the parent molecules. Hence, Flamm has shown that low energy electrons of 18-25eV (usually 20eV) range will yield large parent ion peaks relative to secondary fragments for a variety of halocarbons. This is a well known phenomenon but involves reduced sensitivity at low electron energies due to a decrease in the ionisation cross-sections with a decrease in electron energy.

Suggestions for overcoming sensitivity problems include higher emission currents, higher potentials on electron photomultipliers, slower mass scan rates (higher integration time) and longer amplifier time constants.

The usual method is to increase potentials on the photomultiplier to obtain sufficient gain in sensitivity.

Effluent gases can be sampled using leak valves, capillary tubes or small orifices which have small "dead volumes" to give better response times. It is important to be able to maintain the normal working pressure of the mass spectrometer (10^{-6} torr) under operating conditions in the reactor ($\simeq 0.5$ torr). This can usually be achieved and some systems are capable of sampling from atmospheric pressures.

Even with low-energy electron-impact ionisation Flamm observed that some fragments seen in the mass spectrum were not assignable to a particular parent molecule. In addition, chlorinated species adsorbed on the stainless steel surfaces and gave an interfering background spectrum.

Downstream mass spectrometry can be used as a process controller giving end point indications in some etching processes (25).

2.1.3   Direct Sampling from the Plasma

Both neutrals and ionic species are normally sampled from the plasma into the mass spectrometer ion source via some form of beam system. Many methods have been used but the main difference between sampling ions and neutral

56

species is that ions require an electrostatic focussing lens system whereas neutrals are only collimated by several apertures into the mass spectrometer.

A beam of species from the plasma can be formed by consecutive orifices, slits, crossed slits and nozzles. In the case of neutral species tnese apertures are kept as close together as possible to reduce wall losses and give large concentrations of species in the beam. In the case of ions a lens system is normally placed between the apertures to focus ions onto the second orifice for collimation into the mass spectrometer.

(a) Ions

Ions are thought to be important in anistropic etching. Positive ions have consequently been studied by several workers (29-32). Few workers have considered negative ions in etching plasma discharges. However, some work has been done on the production of negative - ion - rich plasmas as possible sources of negative ion beams (34,37).

Sampling ions from plasmas is usually via an orifice into an ion lens system. Energy analysers have been used by Coburn and Kay (32) to observe the energies of ions under various conditions in the plasma. The effects of r.f. power modulation and confining the plasma with biased electrodes have been studied. In these studies the plasma was sampled through an orifice in the

substrate electrode of a diode glow-discharge sputtering system. This allowed direct sampling of ions incident on the substrate electrode into the quadrupole mass filter. Coburn and Kay were also able to determine the plasma potential with their system.

Other workers have sampled ionic species from the bulk plasma and from fast flow tubes (28-31). Vasile and Smolinsky (31) have sampled both ions and neutral species from discharges in tetrafluoroethylene and methane. When sampling neutrals the ion focussing lenses were used to prevent all ions from the discharge reaching the mass filter. This was done by grounding some lenses and applying + 200V to the first lens. They obtained electron impact ionisation spectra at 20eV with and without a discharge present in the reactor.

(b) Neutral Species

Atoms, molecules and free radicals are normally sampled as a molecular beam formed by a differentially pumped nozzle beam system. The nozzles are usually small orifices or pinholes mounted in such a way as to produce a direct molecular beam into the mass spectrometer ion source. This type of system has been used to sample species from discharges, flow tubes, shock waves and flames (44-64).

Ideally, atoms and radicals should not undergo any collisions with the walls or other gas molecules during transit from the reaction zone to the point of ionisation in the mass spectrometer ion source. The species sampled should be a representative sample of the plasma or reaction mixture. In general it has been found sufficient to use several small differentially pumped, planar orifices to collimate the molecular beam (63). However, with this method there is some probability that some effusing molecules which have undergone collisions with the walls of the collimating chambers can reach the mass spectrometer. Background gases from the molecular beam can reach the mass spectrometer after many wall collisions in the mass spectrometer chamber. The use of modulated molecular beams using a beam chopper may overcome this in some circumstances by correcting the intensity of the spectrum obtained for any contribution from the background gases. A disadvantage of beam choppers is that the distance between the mass spectrometer and the reaction chamber is longer and therefore the molecular beam more diffuse than the molecular beam normally sampled from an unmodulated beam system.

The size of the orifice or aperture from the reactor depends upon the pressure of the reactants being sampled. In general the orifice diameter, D, must be less than the mean free path, λ, for pure molecular flow but can be operated at higher pressures (57) with a

maximum at $D/\lambda \simeq 70$.

Supersonic molecular beams can be generated using nozzles and skimmers. The reaction mixture or plasma expands out of the first sampling cone at supersonic velocities in the forward direction. The skimmer then selects the central portion of this beam which is allowed to pass into the ion source of the mass spectrometer. Because of the high degree of collimation and supersonic velocity of the beam, collisions between species in the gas phase and the wall are insignificant. This type of sampling is referred to as "collision free". Supersonic beams increase the sensitivity but produce problems of unrepsentative sampling and formation of shock waves in front and behind the nozzle and skimmers. This is particularly marked at high mach numbers (>5); (60,74).

2.1.4 Molecular Beam Sampling of Neutral Species

For the efficient transfer of reactive species of the plasma discharge to the mass spectrometer ion source, there must be a minimum of gas phase and wall collisions. Foner (57) has shown a three stage molecular beam system and assumed molecular flow conditions everywhere in the sampling system, Fig.6. The molecular densities (molecules cm^{-3}) p_1, p_2 and p_3 in the three sections of the apparatus due to the incoming gas and p_B,

60
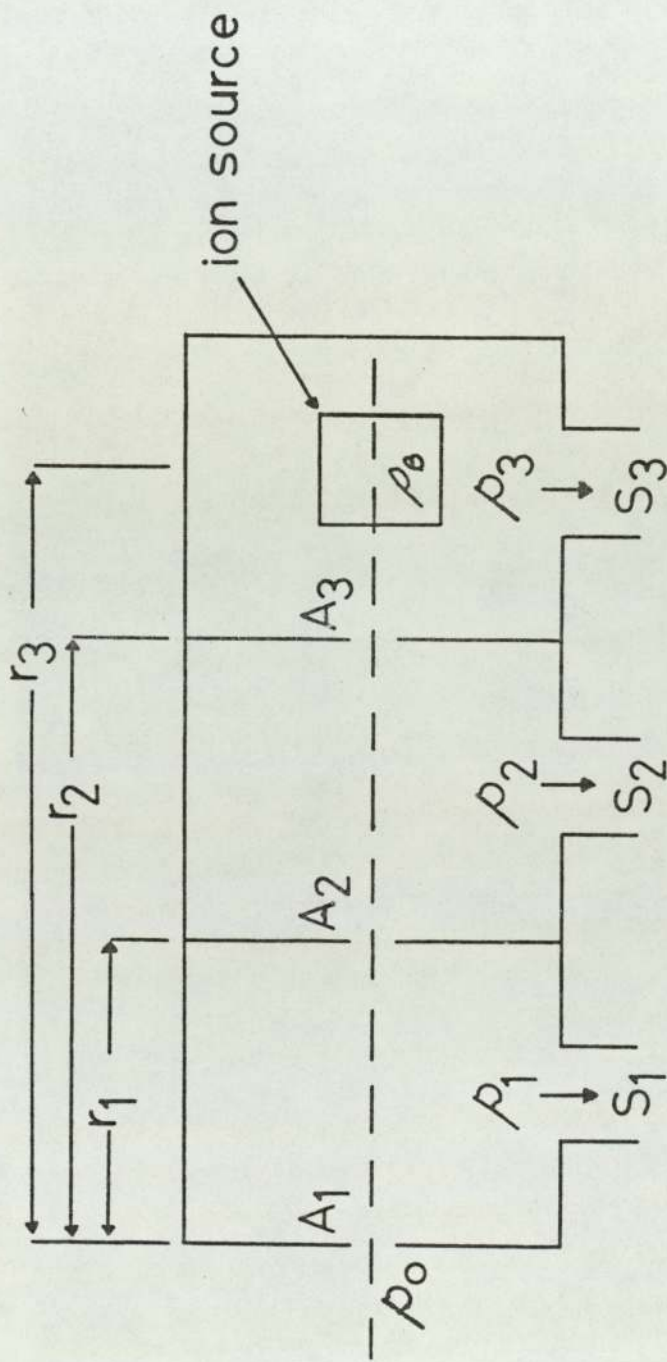
Three stage molecular beam sampling system indicating design parameters.

Fig.6 3-Stage system.

the beam density in the ion source were, with a few minor
approximations, expressed in terms of the denisity p_0 on
the hign-pressure side of the first orifice as:-

$$\rho_1 = \frac{\rho_0 A_1 \bar{v}}{4 S_1} \qquad\qquad \text{eqn} \quad (1)$$

$$\rho_2 = \frac{\rho_0 A_1 A_2 \bar{v}}{4 S_2} \left(\frac{\bar{v}}{4 S_1} + \frac{1}{\pi r_1^2} \right) \qquad\qquad \text{eqn} \quad (2)$$

$$\rho_3 = \frac{\rho_c A_1 A_3 \bar{v}}{4 S_3} \left[\frac{A_2 \bar{v}}{4 S_2} \left(\frac{\bar{v}}{4 S_1} + \frac{1}{\pi r_1^2} \right) + \frac{1}{\pi r_2^2} \right] \qquad \text{equ} \quad (3)$$

$$\rho_B = \frac{\rho_0 A_1}{4 \pi r_3^2} \quad (3-\text{stage system}) \qquad\qquad \text{eqn} \quad (4)$$

$$\rho_B = \frac{\rho_0 A_1}{4 \pi r_2^2} \quad (2-\text{stage system}) \qquad\qquad \text{eqn} \quad (5)$$

where $\bar{v}$ is the molecular velocity of the gas in cm s^{-1}

A is the area of the pinhole in cm^2

S is the pumping speed in cm^3 s^{-1}

p is the gas density in molecules cm^{-3}

According to Watson (54) the beam density for a two
stage
^system is given in equation (5) and p_2 can be rewritten
as :-

$$\rho_2 = \frac{\rho_1 A_2 \bar{v}}{4 S_2} + \frac{\rho_c A_1}{4 \pi r_2^2} \cdot \frac{A_2 \bar{v}}{S_2} \qquad\qquad \text{eqn} \quad (6)$$

and similarly p3 can be expressed as:-

$$\rho_3 = \rho_2 \frac{A_3 \bar{V}}{4 S_3} + \frac{\rho_0 A_1}{4 \pi r_2^2} \cdot \frac{A_3 \bar{V}}{S_3}$$ 　　　eqn (7)

Equation (6) is obtained by substituting for p_0 from equation (1) in the first part of the expanded equation (2) and equation (7) is obtained by substituting P_2 into equation (3) using the expanded equation (2) for P_2.

The beam density p_B is due to species which have suffered no wall collisions, whereas the background P_3 (P2 for a two-stage system) is from species which have effused from the first stages and have undergone many wall collisions. In order to sample species directly the parameter which must be maximised is P_B/P_3 (P_B/P_2 for a two-stage system) i.e.: the beam density relative to the effusive background. This is the effective signal-to-noise ratio for the sampling system. The ratio of beam density to background density for a three-stage system is:-

$$\frac{\rho_B}{\rho_3} = \frac{S_3 \bar{V}}{\pi A_3 \bar{V} r_3^2} \left[\frac{A_2 \bar{V}}{4 S_2} \left(\frac{\bar{V}}{4 S_1} + \frac{1}{\pi r_1^2} \right) + \frac{1}{\pi r_2^2} \right]^{-1}$$ 　eqn (8)

and for a two-stage system is:-

$$\frac{\rho_B}{\rho_2} = \frac{S_2}{\pi A_2 r_2^2 \bar{V}} \left[\frac{\bar{V}}{4 S_1} + \frac{1}{\pi r_1^2} \right]^{-1}$$ 　　　eqn (9)

Watson has discussed the beam-to-background ratios for his particular system and has also shown that a three-stage system has a much lower effusive background gas density in the mass spectrometer than a two-stage system.

62

2.1.5. <u>A Simple Method for a Two-Stage Beam System</u>

This method was first presented by Fite (65) for beam density and background pressure calculations for a two stage modulated beam mass spectrometer.

In the two-stage system fig:7. gas flows effusively from the source into the first of two differentially pumped vacuum chambers. The pressure in the first chamber is maintained sufficiently low so that molecules from the source will cross the chamber without suffering gas phase collisions. A portion of the direct stream of gas from the source passes through an aperture in a partition separating the two chambers and forming a collimated molecular beam that crosses the second chamber. The total gas flow from the source is given by the effusive flow expression for an orifice as:-

$$Ns= \frac{n_s c A_s}{4} \qquad \text{eqn (1)}$$

where N_s = gas flow through the aperture in molecules s^{-1}

n_s = gas number density in molecules cm^{-3}

A_s = area of the source aperture in cm^2

c = mean thermal velocity in cm s^{-1}

Equation (1), while applying strictly only in the case of effusive flow from sources working at extremely low pressure, is a reliable approximation for sources working at pressures upto several tens of torr.

63

Fig.7 Two stage system.
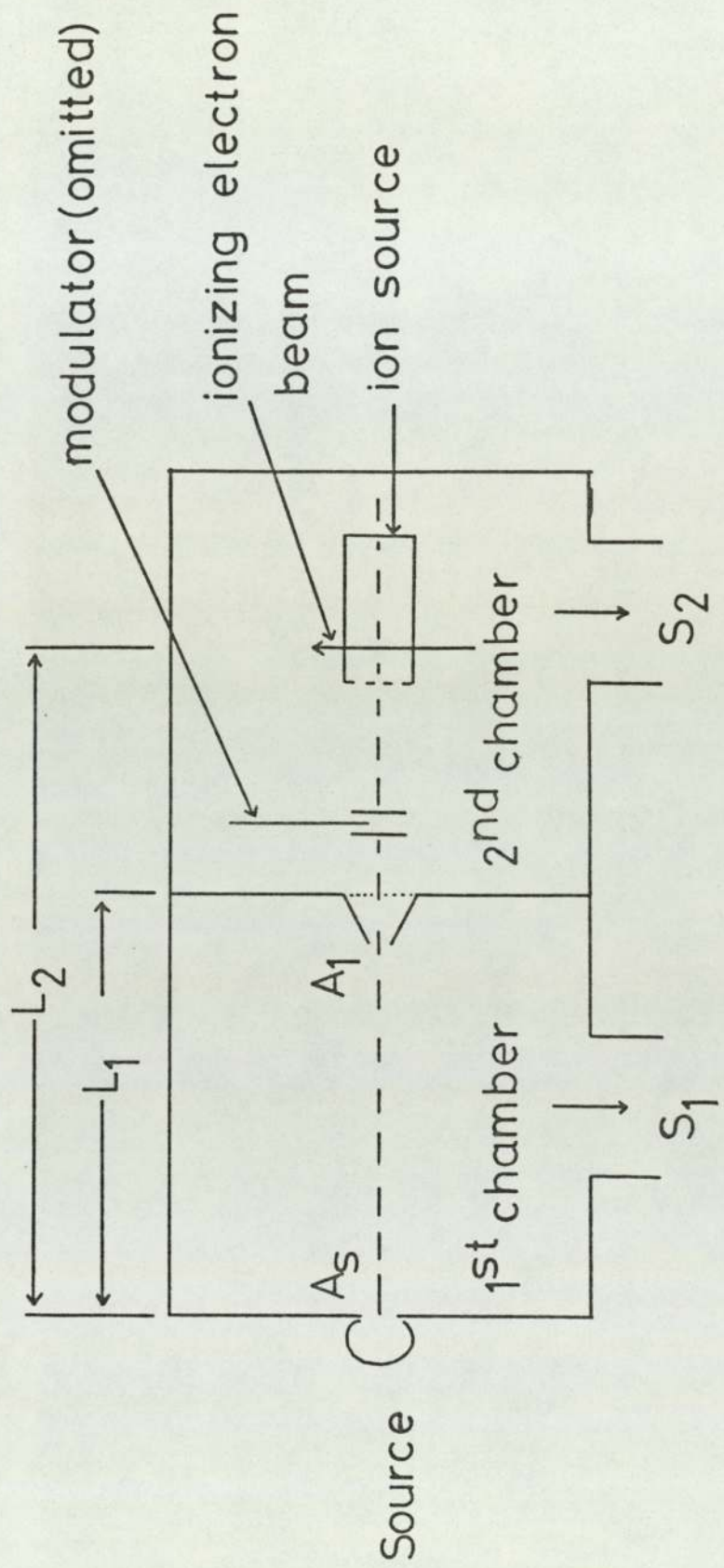
Two stage molecular beam sampling system.

63(a)

The gas flow Ns has to be removed by the pump evacuating the first chamber, neglecting losses into the second chamber, by conservation of mass:-

$$Ns = n_1 S_1 \qquad \text{eqn (2)}$$

where n_1 = gas number density in the first chamber

S_1 = pumping speed of the first chamber pump system.
Combining equations (1) and (2) gives:-

$$n_s A_s = \frac{4 n_1 S_1}{c} \qquad \text{eqn (3)}$$

It is necessary to keep n_1 sufficiently small so that a molecule from the source will cross the first chamber with a low probability of colliding with another molecule in the gas phase. That is, the mean free path, λ, must be very much greater than L, the distance between the apertures. In general this condition is met if $n_1 \leqslant 4 \times 10^{12}$ molecules cm^{-3}, corresponding to a pressure in the first chamber of 10^{-4} torr. (Appendix C).

Gas flow in the beam between the chambers can be considered:-

$$n_b = \frac{n_s A_s}{4 \pi L^2} \qquad \text{eqn (4)}$$

where n_b = number density in the beam in molecules cm^{-3}

L = the distance in the cm from the source aperture.

The "current", I_b in a beam of cross sectional area $A(cm^2)$ is related to the beam number density, n_b by

64

$$I_b = n_b \, c \, A \qquad\qquad \text{eqn (5)}$$

Combining equations (4) and (5) gives:-

$$I_b = \frac{n_s \, A_s \, c \, A}{4\pi \, L^2} \qquad\qquad \text{eqn (6)}$$

which relates the beam current in molecules s^{-1} and cross sectional area A to the number density in the source. The total current entering the second chamber can be found by applying equation (6) to the beam passing through the aperture of area A_1 located between the vacuum chambers i.e: by setting $A = A_1$ and $L = L_1$ giving:-

$$I_b = \frac{n_s \, A_s \, c \, A_1}{4\pi \, L_1^2} \qquad\qquad \text{eqn (7)}$$

The beam-to-background ratio may now be obtained. It is of interest to consider the ion current arising from the beam on passing through the ion source of the mass spectrometer, compared to background signals originating from molecules from all other sources. The number density, n_b, in the beam at the position of an ion source located a distance L_2 from the beam source is given from equation (4) and is:-

$$n_b = \frac{n_s \, A_s}{4\pi \, L_2^2} \qquad\qquad \text{eqn (8)}$$

Background gas densities arise from two sources. Firstly the beam terminates in the second chamber by striking the wall, and molecules in the beam become background gas in the second chamber until they are pumped away. The number density increase, n_2, can be calculated from tne current in the beam, I_b, from:-

$$I_b = n_2 S_2 \qquad\qquad \text{eqn (9)}$$

where S_2 = the pumping speed of the second chamber pump system. Therefore, from equations (7) and (9) we obtain:-

$$n_2 = \frac{I_b}{S_2} = \frac{n_s A_s c A_1}{4\pi L_1^2 S_2} \qquad\qquad \text{eqn (10)}$$

The second source of background gas in the second chamber arises from the general gas flow between the first chamber, operating at a number density of $n_1 = 4 \times 10^{12}$ molecules cm^{-3}, and the second chamber through the aperture separating the two chambers. Using equation (1) and assuming effusive flow gives:-

$$N_2 = \frac{n_1 c A_1}{4} \qquad\qquad \text{eqn (11)}$$

where N_2 = flow through the aperture or effusion rate in molecules s^{-1} and applying equation (9) gives, (putting $I_D = N_2$ in equation (9)):-

$$n_2' = \frac{n_1 c A_1}{4 S_2} \qquad\qquad \text{eqn (12)}$$

where n'_2 is the value for the second source of background gas in the second chamber in molecules cm^{-3}.

Fite has claimed that this contribution to the background gas density in the second chamber is an order of magnitude less than the contribution due the termination of the beam in the second chamber and to a good approximation can be neglected under certain geometrical conditions. Comparing equations (8) and (10) gives:-

$$\frac{n_b}{n_2} = \frac{L_1^2 \, S_2}{L_2^2 \, c \, A_1} \qquad\qquad \text{eqn (13)}$$

where n_b/n_2 is the beam-to-background ratio. Fite has quoted values for $n_b/n_2 \simeq 15$, below this value the mass spectrometer is sampling large background gas densities and few reactive species.

However, Fite is optimistic in assuming that n'_2 is much less than n_2 and usually n'_2 and n_2 have comparable values. Therefore:-

$$n_2''(\text{tot}) = n'_2 + n_2 = \frac{n_1 \, c \, A_1}{4 \, S_2} + \frac{n_s \, A_s \, c \, A_1}{4 \, \pi \, L_1^2 \, S_2} \qquad \text{eqn (14)}$$

where n_2'' (TOT) is the total background gas density in the second chamber, is more reasonable and should be used to calculate beam-to-background ratios in equation (13) instead of n_2.

2.2   Emmission Spectroscopy

Molecules may undergo inelastic collisions with electrons in a plasma which leave the molecule in one of many excited states. Electronically excited states give rise to optical emission, which is characteristic of the species, when relaxing back to the normal ground state electronic structure. By studying the emission spectra from plasmas the various electronically excited species present in the discharge can be identified.

67

2.2.1 Excitation

Electronically excited states can be formed directly by electron impact. When the corresponding radiative transition is allowed the excitation cross-section rises to a broad maximum and slowly decreases at higher energies, whereas for forbidden radiative transitions the cross-section is often sharply peaked at the corresponding energy and falls off rapidly at higher energies. Peak cross-sections are often in the 10^{-17} to 10^{-18} cm^2 molecule range.

Appreciable vibrational excitation can also occur in plasmas and effective vibrational temperatures may be established which are between Te, the electron temparature and Tg, the gas temperature. Electron impact excitation of vibrational energy is a highly specific process and depends upon the existance of virtual negative ion states which decay into vibrationally excited ground-state molecules. Vibration-translation collisional energy exchanges are inefficient for strongly bound homonuclear diatomic molecules allowing high T_{viB} to be established. The high vibrational temparature T_{viB}, of N_2 in plasmas and glow discharges is likely to be responsible for much of its electronic excitation. This is explained if T_{viB} approaches Te the internal equilibration of vibrational states will produce appreciable concentrations of molecules with 5-8eV of vibrational energy and electionically excited molecules

by the reverse process of the very fast quenching reactions of $A^3\Sigma$ state of N_2 by N-atoms (76).

Emission spectra of atoms or free radicals cannot give quantitative measurement of concentrations of ground states because the number of electronically excited states is not directly related to the number of ground state species. The relative number of ground state and excited species depends upon the plasma conditions and is not easily determined. However, in plasmas where electron energies are high enough to cause excitation, spectra may not only constitute reliable evidence for the presence of radicals and atoms but can also be used for determining relative concentrations of ground state species. The main problem with emission spectroscopy is that information is only obtained about species which are in electronically excited states and emit radiation at suitable wavelengths (23,78-81)

2.2.2   Gas Rotational Temperatures

Porter and Harshbarger (79) have shown that molecular gas temperatures in an r.f. discharge of nitrogen gas can be determined using the unresolved rotational structure of the emission spectrum. Rotational excitation energies are small, and the collisional exchange of translation and rotational energy is so rapid that rotational states are unlikely to be substantially out of kinetic temperature equilibrium. For this reason gas rotational

69

temperatures are approximately the same as the gas temperature in the discharge.

Porter and Harshbarger calculated the gas rotational temperature of nitrogen gas with substantial error limits but nevertheless were able to show that the gas was hot. Reported activation energies of the order of 0.5 - 2.5eV should therefore, be interpreted with consideration that the gas phase reactants are hot and their temperature depends upon the discharge parameters.

2.3   Other Techniques

2.3.1. Absorption Spectrometry

Optical absorption with continuum sources has been used in flash photolysis experiments and to some extent in discharge flow systems. Kinetic studies have been done for ClO, BrO, NCl_2 and N_3 radicals. However, many molecular radicals have low absorption cross-sections and require long path lengths with multiple traversals across flow tubes. Alignment problems and spatial resolution, and therefore time resolution in kinetic studies, along the flow tube become unacceptable after 10 traversals in the ultraviolet region (64).

The continuum source of radiation is not suitable for most non-metallic atoms which absorb in the vacuum ultraviolet. Resonance line sources have greatly improved the sensitivity of optical absorption, by the close matching between the source line profile and the absorption line profile. Provision may be made for

70

compensating for any emitted radiation from the atoms at the same frequency as that being used. This can be done by modulating the radiation (with a chopper or modulating power supply) from the source and using a phase sensitive detector amplifying the output of the photomultiplier at the modulation frequency. Radiation emitted from the excited states does not produce a signal under these conditions and only an absorption signal is observed.

Atomic resonance radiation can be produced by a microwave discharge in a trace of the parent molecule mixed with inert gas. Lamps powered by electrodeless discharges are less intense than those produced by arc-glow discharge but give few excited ions. Their ease of operation and low continuum emission are advantages in kinetic studies with resonance absorption. Resonance absorption has mainly involved atoms but can in principle be applied to monitoring molecular radicals. However, the low line strengths for resonance absorption by most molecules, and the difficulty in finding convenient light sources, except for a few cases such as OH, CN and NH, have caused problems. Tuneable dye lasers in the vacuum ultraviolet are likely to help in providing new sources of resonance radiation.

2.3.2 Langmuir Probes

Small electric probes can be placed in stationary or flowing discharges. These probes are normally small

metallic electrodes immersed in a plasma and generally connected across a potential source to a reference electrode. The current flowing to a probe is measured as a function of applied potential difference. The resulting relation between the probe current and the probe voltage is called the "characteristic". From this characteristic the electron temperature, electron density, plasma density (+ve ion density) and plasma floating potential can be derived in principle for simple, well-behaved plasmas. Characteristics of special probe arrangements may give additional information on oscillations, flow, drift and diffusion processes in the plasma. Probe measurments can be made over about seven orders of magnitude of pressure from 10^{-5} torr to 10^2 torr, and more than eight orders of magnitude in charge carrier concentration above 10^6 cm^{-3}.

However, probe measurements are subject to many serious restrictions. Compared to many other diagnostic techniques probes are distinguished by the possibility of direct local measurement of plasma parameters. This advantage is connected to their main problems and restrictions. The insertion of a probe into a plasma under investigation involves disturbing the plasma with a new "wall" in addition to the existing boundaries. In the probe environment, the plasma parameters may deviate seriously from those in the absence of the probe. Another problem is that a probe can only be used for simple systems with any reliability. This means that

ideal conditions for probes are in non-reactive, monoatomic gases with high mobility. The use of probes in reactive plasmas can lead to the formation of insulating polymer layers deposited on tne probe or alternatively the probe and holder may be etched (84-89).

Altnough probes were used for investigation of gas discnarges at the turn of the century, it was not until the early twenties when Langmuir and co-workers made probes a useful means of plasma diagnostics. To perform probe measurements in low pressure discharges using simple theory, some conditions or restrictions must apply:-

(a) electron and ion densities must be equal,

(b) the probe radius must be smaller than the mean free path of electrons and ions,

(c) electron temperature must be greater than ion temperature (non-isothermal plasmas),

(d) probe radius must be greater than the Debye length,

(e) tnere must be a maxwellian velocity distribution of electrons.

The use of double probe techniques has allowed investigation of plasmas in which a reference potential in the form of an electrode is absent or where space potential is not defined. For example high frequency discharges, afterglows and tne upper atmosphere (31,90).

Measurements can be made of other electric properties
and potentials of a system. For instance wall and probe
potentials, specimen support potentials, induced d.c. bias
on electrodes and the effects of grounded mesh shields can
be measured (91-96).

2.3.3   Electron Spin Resonance

Many chemical species contain an odd number of
electrons with the consequence that the effects of
electron spin are not cancelled out by the pairing of
electrons. These species are paramagnetic. Examples
include organic free radicals, some transition-metal ions,
and the molecules NO_2 and NO. Some species have two
unpaired electrons and are paramagnetic even though they
have an even number of electrons. These are triplet
states; for example O_2 molecules have triplet states as
their ground state, and many organic molecules may be
excited into the triplet state by irradiation. For
organic free radicals there is normally only one unpaired
electron which has only two electron spin energy levels.
The unpaired electron may be excited into the upper energy
level by absorption of radiation of a suitable frequency
while a magnetic field is applied. The frequency of
radiation normally used is in the microwave region. The
signal intensity observed is proportional to the
population of the upper and lower states, the upper states
are less populated than the lower states. It is possible
to detect as little as 10-11 mole of paramagnetic species,

making electron spin resonance a very sensitive analytical technique.

The use of electron spin resonance for the detection of atoms and radicals in the gas phase has been reviewed by Westernberg (97) and more recently by Clynne and Nip (64). Fast flow tubes have been used with an electron spin resonance cavity downstream from the reaction zone. Absolute concentrations of species may be calculated if a calibration gas has been used under identical cavity conditions. Absolute concentrations of several transient species can be followed in the same experiment and has been useful in kinetic studies of reactions with complex stoichiometries (64, 98-100).

However, the use of gas phase electron spin resonance in the study of plasmas is largely limited by the fact that the resonance cavity is positioned downstream from the discharge. Under these circumstances only long lived species will be detected after undergoing many wall collisions. The electron spin spectra obtained in this way may not show any of the reactive species which are present in the discharge but only secondary products from recombination or fragmentation.

2.4   Associated Techniques

In this section other useful techniques will be briefly discussed which give complementary information to the analytical techniques discussed earlier. These

techniques are mainly related to wafer etching and surface analysis.

2.4.1   Effluent Collection

This technique can be used to determine the final products of a plasma discharge. It is only useful for volatile products which can be condensed on a suitable cold trap. Tokunaga and Hess (101) have used this technique to look at effluent gas compositions from carbon tetrachloride plasmas etching aluminium. The effects of various electrode material were studied and the effluent gases, analysed by gas chromatography, were found to vary substantially with different electrode materials.

Effluents can also be analysed by infrared absorption spectrophotometry using gas cells with sodium chloride windows.

2.4.2   Scanning Electron Microscopy

Scanning electron microscopy can be used to observe the highly magnified etched surfaces of the silicon wafers. Surface morphology and etch profiles can be observed by arranging for the sample to be rotated in the electron beam so that the beam strikes the surface at suitable angles. At moderate angles of 42° surface roughness and other features like stacks, lumps or debris

76

can be easily seen. At higher angles 85° undercutting, edge profiles and etch depths can be seen. The scanning electron microscope with its high magnification allows surface details to be observed which cannot be seen in any other way.

2.4.3   Optical Microscopy

The use of an interference microscope allows measurements of etch depths (and etch rates and ratios) of features etched on the wafer surface. This non-destructive technique is useful for obtaining etch rate information quickly. Refractive index measurments can also be made on thin films, for instance oxide on silicon.

2.4.4   Talystep and Alphastep

These techniques can also provide information about etch depths and therefore etch rates. These instruments use a tiny counterbalanced stylus which is dragged across the etched wafer. The stylus follows the contours on the surface of the wafer and records the small changes in height on the chart. These techniques are less accurate than other methods but provide quick checks for etch rates.

2.4.5 Surface Techniques

Surface techniques are useful for analysing residues or "polymers" deposited on the surfaces of the etched wafer from various processes. These techniques include Auger, E.S.C.A, S.I.M.S. and electron probe microanalysis. The scanning electron microscope can also be used in conjunction with the Kevex X-ray analyser. The latter three methods (S.I.M.S., E.P.M.A. and X-ray analysis) provide information about the types of material present on the surface e.g: Carbon, silicon, aluminium, chlorine etc. However, they do not give any information about the structure of any material on the surface. Auger, E.S.C.A. (and Photoelectron spectroscopy) give much more information about the presence of different bonds. It is, therefore, possible to analyse the surface material and deduce some kind of structure for the material. This is of particular interest where films have been deposited on wafers and electrodes from plasmas (102, 103).

3.   APPARATUS AND EXPERIMENTAL PROCEDURE

A system for sampling reactive gas plasmas into a mass spectrometer has been designed and built at the University of Aston in Birmingham in the department of Chemistry. (see fig. 8). The system consists of a number of high vacuum chambers connected together via a pinhole or molecular beam interface with differential pumping. The mass spectrometer is contained in a high vacuum chamber and receives a continuous flow of material from the plasma reactor via the molecular beam interface. The plasma reactor has two internal electrodes across which an r.f. field is applied to various gases entering from the gas control system. The plasma reactor also has a glass vacuum line, with traps, to exhaust gases and provide sufficient background vacuum. A capacitance manometer (BARATRON gauge) is connected to the reactor and can be used in conjunction with the gas controller to maintain constant pressure control in the reactor; Fig. 9.

3.1.1   The Vacuum System

The mass spectrometer chamber consists of a large (16 hour) liquid nitrogen trap, a water cooled Edwards type EO4 (4 inch) polyphenyl ether oil diffusion pump backed by an Edwards ED200 two-stage rotary pump. There is also an alumina foreline trap between the rotary pump and the diffusion pump.

79
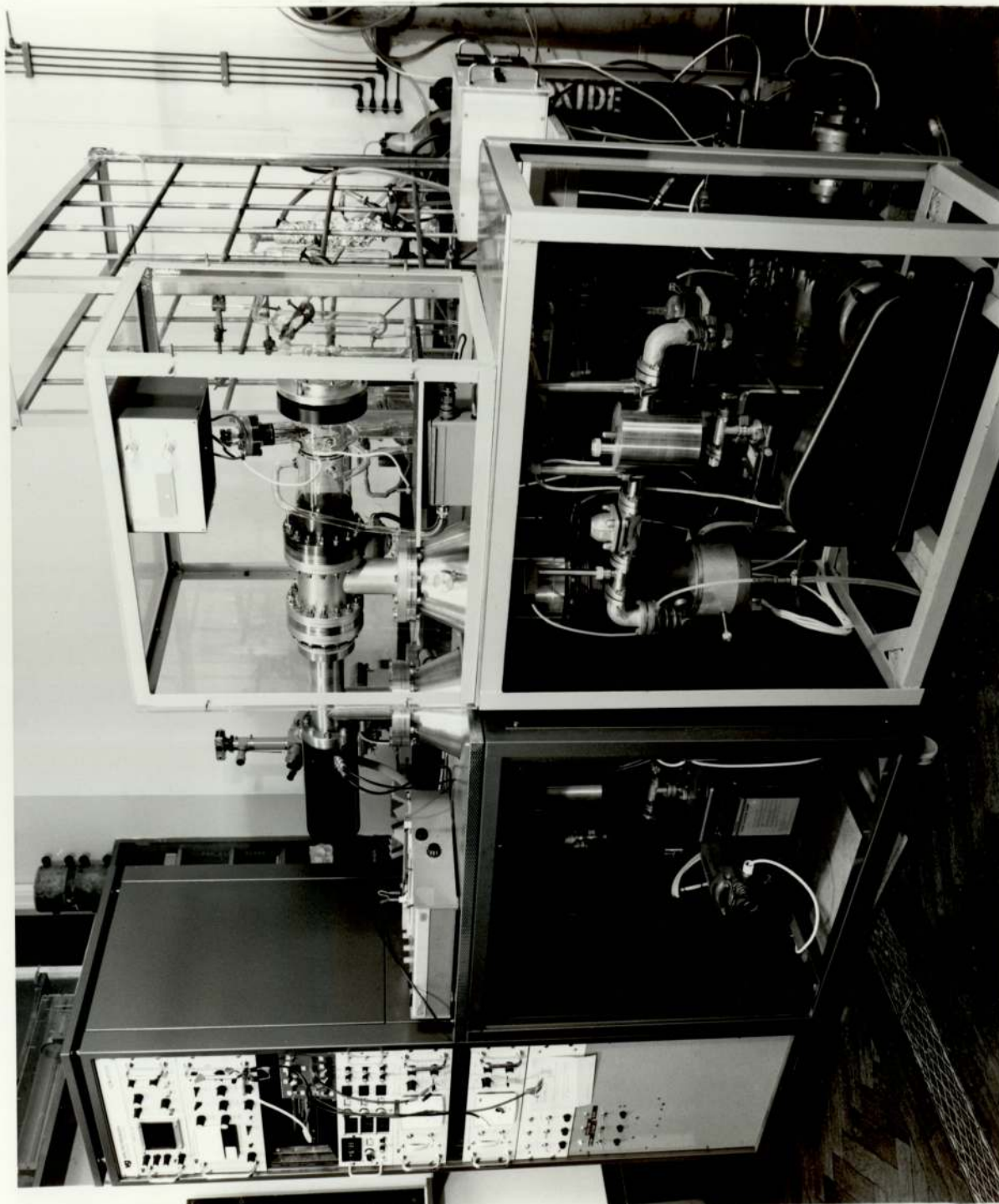
FiG 8

79(a)

PLASMA REACTOR (schematic)

(with molecular beam sampling to quadrupole mass spectrometer, and control system for reactor pressure and gas flow rates)
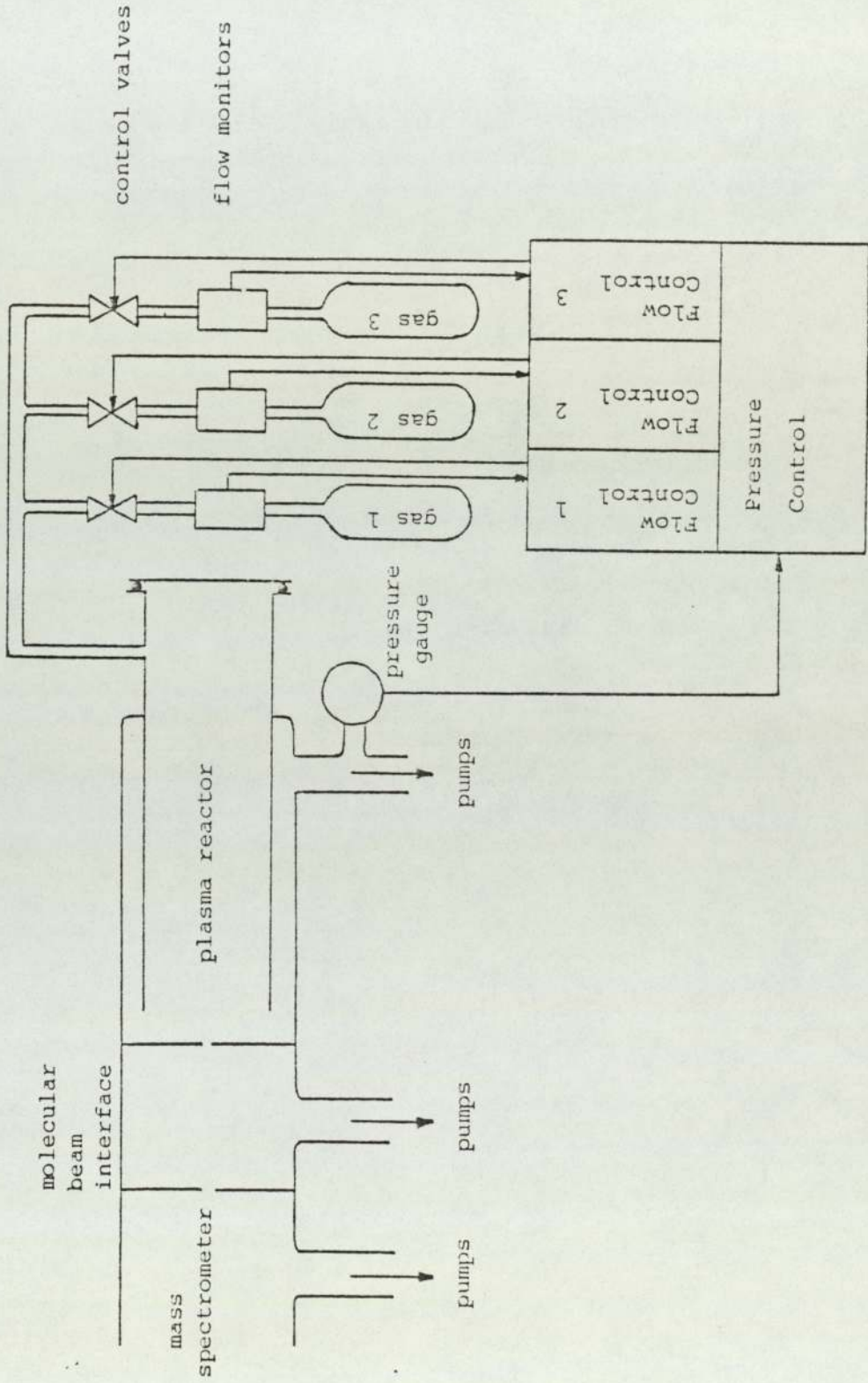
Fig.9 Plasma reactor (schematic).

79(b)

The intermediate or pinhole interface chamber was almost identical to the mass spectrometer chamber except that an Edwards ES200 single stage rotary pump was used as the backing pump. The pinholes were mounted as an assembly ontop of the liquid nitrogen trap. (See section 3.1.4). Where possible copper gaskets or gold seals were used for the high vacuum chambers, however the pinholes were mounted using viton 'O' rings which limited baking of the system to $\sim 150°C$.

In operation, this system typically reached pressures of $1x10^{-8}$ torr in the mass spectrometer and $1x10^{-7}$ torr in the intermediate or interface chamber with a plasma reactor pressure $< 10^{-3}$ torr.

3.1.2   Gas Handling and Pressure Measurement

Normally standard B.O.C. or Air Products gas cylinders were used with pressure metering valve heads. The cylinders were connected to the gas handling system by flexible $1/4$ inch nylon and stainless steel tubing. It was possible to evacuate this tubing using a rotary pump and a ball valve connected to a T-piece connector. Where possible Swagelok gas fittings have been used and an attempt has been made to standardize on this type of fitting.

The gas handling was performed by three separate linear mass flowmeters (Tylon type) and automatic control

valves. The valves were controlled by the M.K.S. type 254 Gas controller which also senses and controls a pressure measuring capacitance manometer (110). The controller could be set to maintain flow ratios between the three inlet gases and control the overall pressure in the reactor. The instrument displayed both pressure in torr and flow rates in standard cubic centimeters per minute (sccm) on digital display units. The instrument operated as a feedback system when switched to AUTO and controlled the flows via the ratio controls to maintain a set pressure. When switched to MANUAL the flow rates of gas were controlled and the pressure determined by the pump speed.

The system had a 20sccm flow meter and valve and a 50sccm flow meter and valve. There was also a special 10sccm capillary flow device with a differential pressure Baratron across the constriction to measure the pressure drop and hence the flow rate for low flow rates.

Pressure measurements on the other chambers were made with Pirani gauges and ion gauges which were standard V.G. components supplied with Pirani - ion gauge controllers. Two controllers and two of each gauge were used, one for the mass spectrometer chamber and one for the intermediate chamber.

3.1.3   The Plasma Reactor and Glass Vacuum Line

The plasma reactor Figs. 10 and 11, consists of two large diameter concentric glass tubes joined near the gas inlet and outlet. Gas entering the reactor flowed down the longer central tube into a region of discharge between two parallel aluminium plate electrodes 4.5cm apart. These electrodes were supported on glass rods fused to the inside of the glass central tube. The gas and any reactive species formed in the discharge region then flowed over the first flat pinhole mounted on the inside of the top hat assembly (see section 3.1.4) and down the outer annulus to the outlet where it was pumped away into the glass vacuum line.

The first flat pinhole was 1.5cm from the end of the central glass tube and the two electrodes, which were pushed to the end of the tube. The electrodes dimensions were:-

Top electrode 4.6cm wide by 12.6cm long and 3mm in thickness,

Bottom electrode 5.9cm wide by 12.6cm long and 3mm in thickness.

The electrodes were arranged longitudinally down the central tube and were prevented from being accidentally shorted to the pinhole by small glass stops on the ends of the glass rod supports. Connections were made to the electrodes with 16s.w.g. stainless steel wire to studs in

FIG 10

82(a)

gas inlet

pressure gauge

electrodes

mass spectro--meter

f.c.38

vacuum line electrical and pumps feed-through

pumps
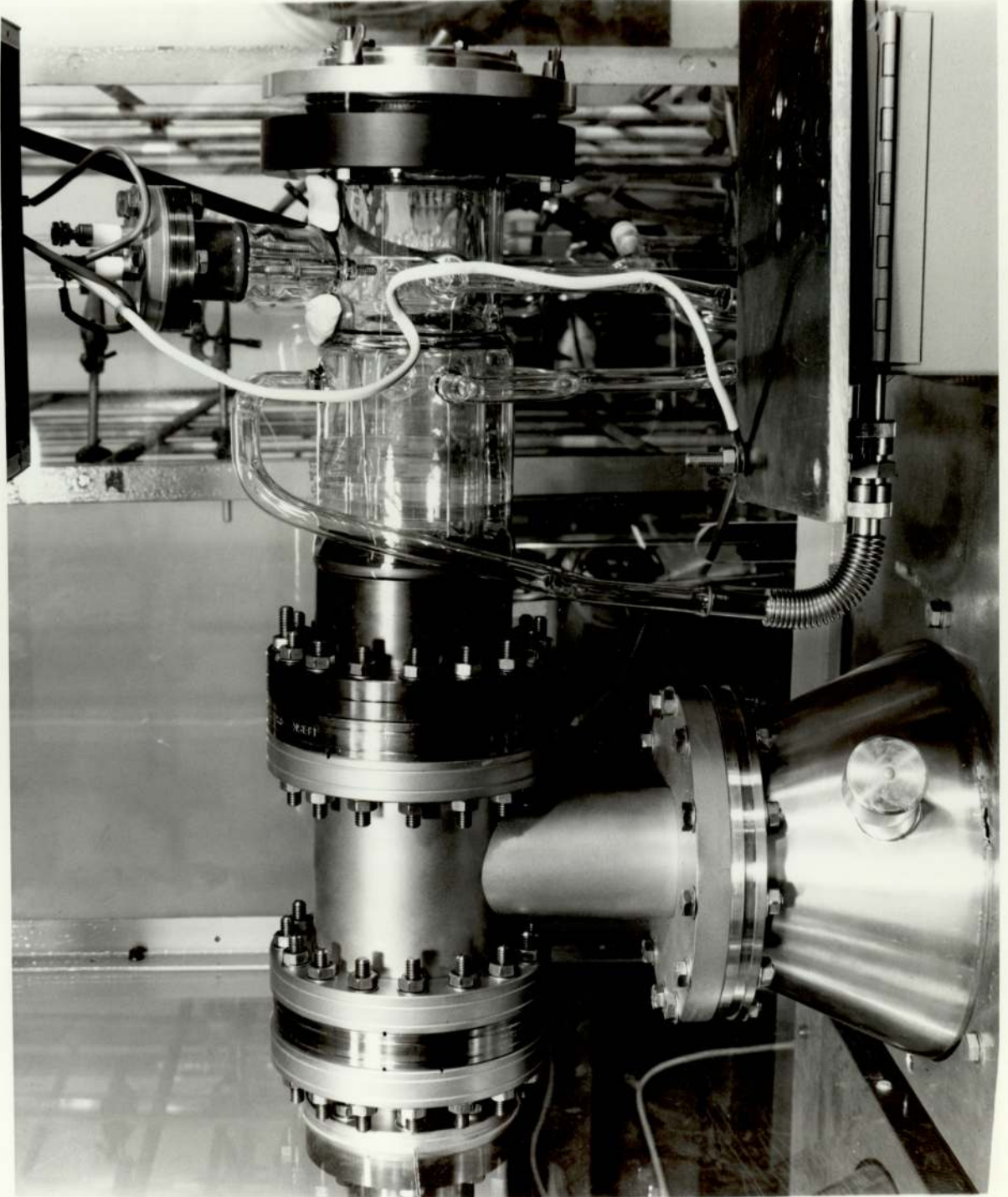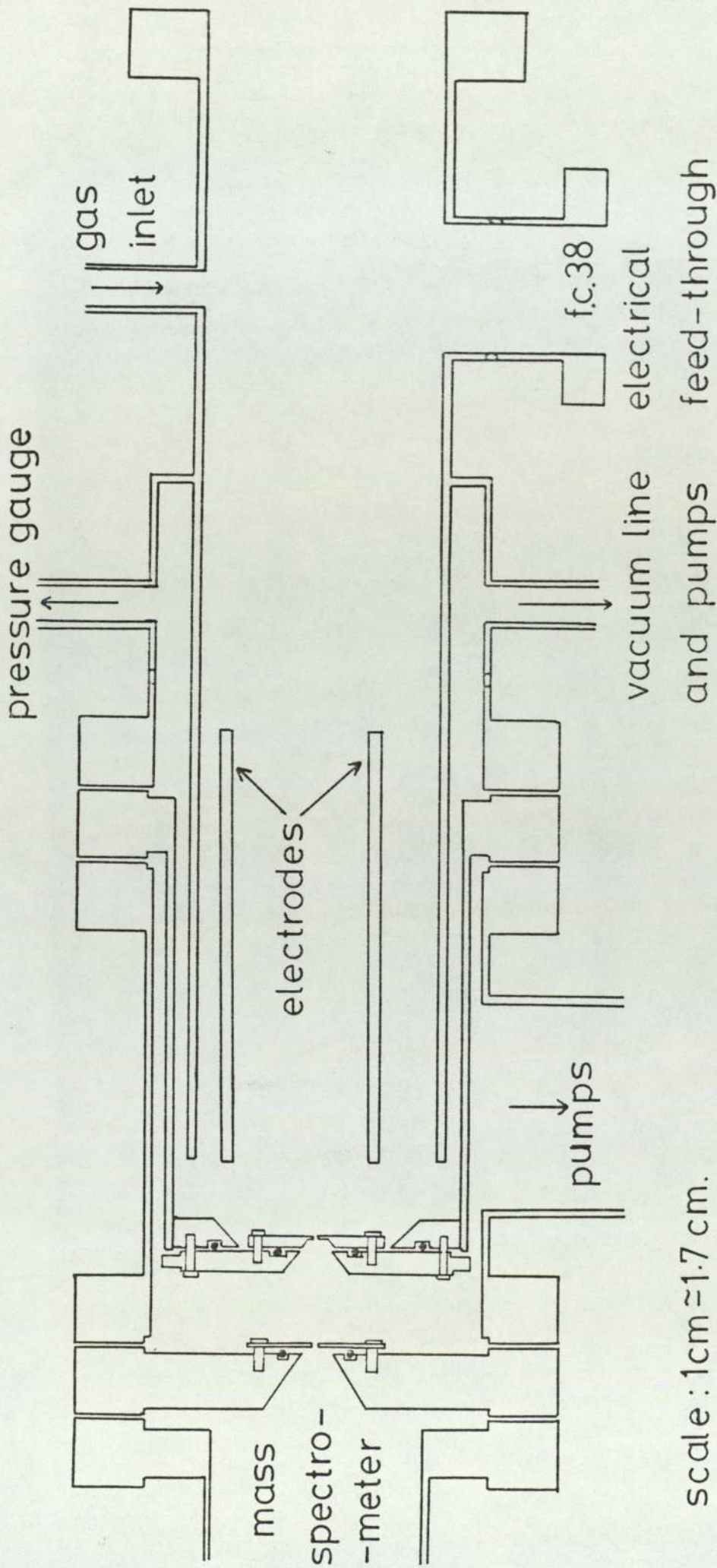
scale : 1cm ≃ 1.7 cm.

Fig.11 Plasma reactor (detail).

82(b)

the electrodes from an electrical feedthrough glass blown into the reactor near the door. The lower electrode was normally grounded and the top electrode was connected to the 13.56MHz r.f. supply which was capable of delivering $\sim$150W of r.f. power.

The glass reactor was built on an FC100 flange with a glass to metal seal. The electrical feedthrough was an FC34 rotatable flange with glass-to-metal seal. Both of these flanges were sealed with copper gaskets.

The reactor door was made from aluminium plate and is demountable using a viton 'O' ring sealed onto a Q.V.F. glass flange. A tufnol collar was made to fit the fibre compression ring on the Q.V.F. flange and the door was secured in position with three pieces of studding in the tufnol collar, washers and wing nuts. The viton 'O' ring was seated in a groove in the aluminium door and compressed onto the ground glass flange. The seal was leak tested with helium using the mass spectrometer and no leak was detected.

The aluminium door also has a quartz glass window made from a standard 7.5cm optical flat and sealed in place with a viton 'O' ring. This provides a 4cm diameter window for viewing the plasma and using the optical emission spectrophotometer.

The reactor was also connected by glass-to-metal seals to the Baratron capacitance manometer and by two flexible bellows type glass-to-metal seals to the gas control equipment and the glass vacuum pumping line.

The volume of the plasma reactor was estimated to be about 3.0 litres. This was found by using Boyles' Law in a convenient form, i.e:

$$P_1 V_1 = P_2 V_2 \qquad\qquad (1)$$

where P_1 and P_2 are pressures (in mm Hg) and V_1 and V_2 are volumes at the respective pressures (in cm^3). The pressures were measured on the mercury manometer on the glass vacuum line. A known calibrated volume was available and this was attached to the glass vacuum line using the B10 quickfit socket. This volume was used to calibrate the volume of the main glass vacuum line and this was used to obtain the volume of the reactor. This was done by rearranging the above equation and substituting for the two pressure measurements. The calculation of the reactor volume was subject to some error due to the pumping of some gas through the pinhole. The manometer mercury levels were falling during the readings and a slightly lower pressure was recorded than would have been the case in a static measurement. This meant that volume calculations gave larger values for the reactor volume than it really was.

84

From the volume of the reactor, gas flow rate, pressure and residence times of gas can be calculated:-

$$T = \frac{V}{F} = \frac{V P_2}{P_1 F_1} \qquad (2)$$

where T is the residence time, V is the reactor volume, F is the flow rate, P_1 is the gas pressure at the flow meter (760 torr), F_1 is the flow rate at pressure P_1 and P_2 is the reactor pressure.

F, in the first part of equation (2), is calculated from the gas flow rate at atmospheric pressure, measured by the flow meters, by using a similar equation to equation (1) and substituting F_1 and F_2 for V_1 and V_2.

Table: 6 Residence times

F @ 760torr (sccm)	Pressure, P, in reactor (torr)	F @ P torr (sccm)	$T_{reactor}$ (sec)	T_{plasma} (sec)
1.0	0.1	7600	24.0	3.8
40.0	1.0	30400	6.0	0.9

The reactor volume was 3.0 litres and the plasma volume was approximately $500 cm^3$ ie: the volume of the inner tube containing the electrodes. $T_{reactor}$ and T_{plasma} are the residence times of the gas in the reactor and plasma discharge volumes respectively. F @ 760 torr

and F @ P torr are the flow rates of gas at atmospheric (inlet) pressure and the corresponding reactor pressure.

The glass vacuum line consisted of two mercury diffusion pumps, two backing rotary pumps, two demountable vacuum traps, a "Vacustat" type McLeod gauge and a mercury manometer. An air inlet valve and a B10 cone and greased tap were also provided. Young's greaseless taps were used where possible. The demountable traps were normally cooled in liquid nitrogen and any condensed material was disposed of in a fume cupboard by allowing the trap to warm up overnight.

3.1.4   The Molecular Beam Interface

This is a differentially pumped molecular beam sampling system and is based on several previous designs (54, 57-60, 65, 73, 74). In general it has been usual to produce nozzles for sampling species from flames, flow tubes, shock waves and plasmas. The use of nozzles overcomes difficulties of "dead" spaces or boundary layers of gas molecules near the orifice at higher pressures ie: where the mean free path, λ is less than D, the diameter of the orifice. Foner and Hudson have shown that maximum beam intensity occurs at a pressure where $D/\lambda \simeq 70$. This shows that the attainable beam intensity was about 1000 times higher than for pure molecular flow through the orifice (104). However, due to difficulties in making nozzles reliably in easily handled materials it was

86

decided to make flat stainless steel pinholes initially. Two flat pinholes were simply made by drilling out and carefully skimming down two discs of stainless steel. The important criteria for these pinholes was to approximate them to an orifice where $l/a \longrightarrow 0$, and where l is the length of the tube and a, the radius of the tube. Therefore the thickness of stainless steel near the pinholes had to be as small as possible but within reasonable engineering limits.

a)   The First Pinhole

This pinhole, which samples species directly from the plasma reactor, was constructed from a 3mm thick, 3.3cm diameter disc of stainless steel plate. The pinhole dimensions are shown in Fig:12. The pinhole has been carefully angled at the rear to try to minimise the number of collisions between molecules flowing through it. This pinhole was mounted on the inside of the "top hat" using 4BA stainless steel bolts and a viton 'O' ring seal Figs. 13-16. The "top hat" consists of an FC100 flange with a piece of 9cm diameter stainless steel tube welded to it and a collar welded inside the top of the stainless steel tube. This "top hat" arrangement was found to be approximately 1mm out of true when placed in a lathe chuck and rotated. This problem was overcome by positioning the top plate of the "top hat" slightly to one side so that the pinhole became more centrally placed. There was also some movement available for positioning the pinhole plate
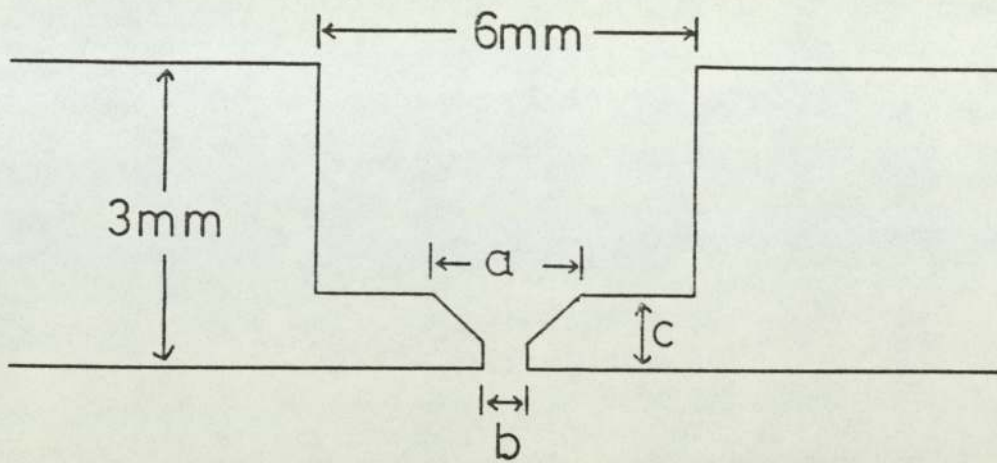
Flat pinhole

(a) 1.40 ± 0.02mm

(b) 1.00 ± 0.02mm

(c) 0.572 ± 0.001mm

Top hat pinhole

(a) 1.08 ± 0.02mm

(b) 0.51 ± 0.02mm

(c) 0.508 ± 0.001mm

(a) and (b) were measured using a
travelling microscope.

(c) was measured using a micrometer.

Fig.12 Pinhole dimensions.

FIG 13
87(b)
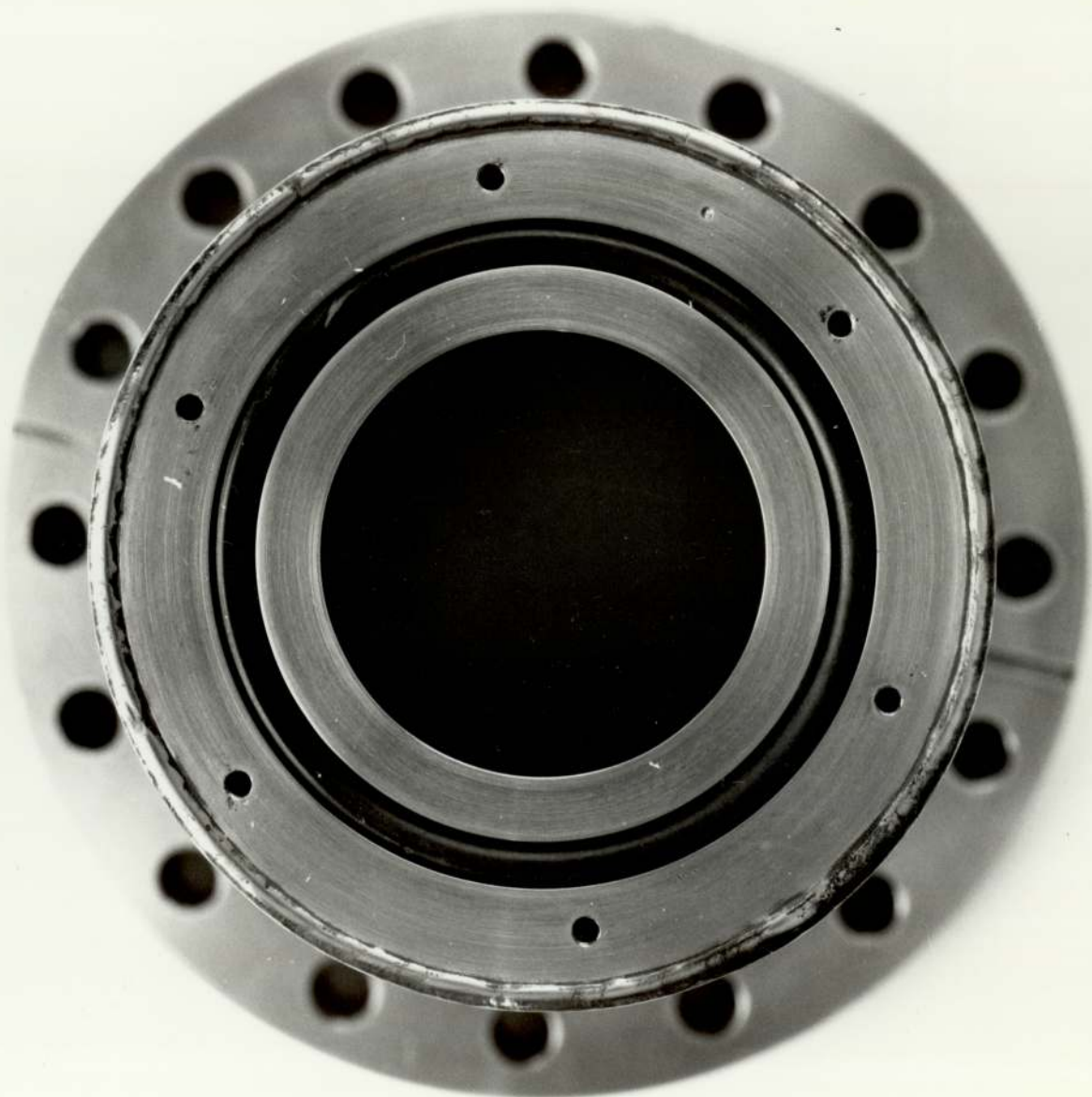
FIG 14
87(c)

FIG 15

87(d)

FIG 16
87(e)

on to the top plate. The bolt holes were all blind tapped into the stainless steel to prevent unwanted leaks from the separate chambers.

b)   The Second Pinhole

This pinhole plate was made in exactly the same way as the first pinhole but was mounted on a flat stainless steel FC100 blank flange Figs. 17 and 18. On the 'front' side a viton 'O' ring sealed the pinhole to the flange secured with blind tapped 4BA stainless steel bolts. The reverse side of the flange was tapered away from the pinhole to minimise molecular collisions with the metal surfaces, Fig: 18. The thicknesses of the skimmed-down sections of both pinholes were measured using a micrometer and a 0.762cm slug. (see fig. 12).

c)   Pinhole Alignment and Performance

The pinholes were aligned using a photographic method. Fig: 19. This method used a diffuse light source shone down the pinhole assembly onto a piece of photographic paper positioned on the FC 64 flange on the mass spectrometer housing. The paper was developed and fixed in the usual way. A travelling microscope was then used to find the position of the dark spot on the paper due to light passing through the pinhole assembly. The best positioning obtainable with the limited movement of the stainless steel pinhole discs was calculated to be
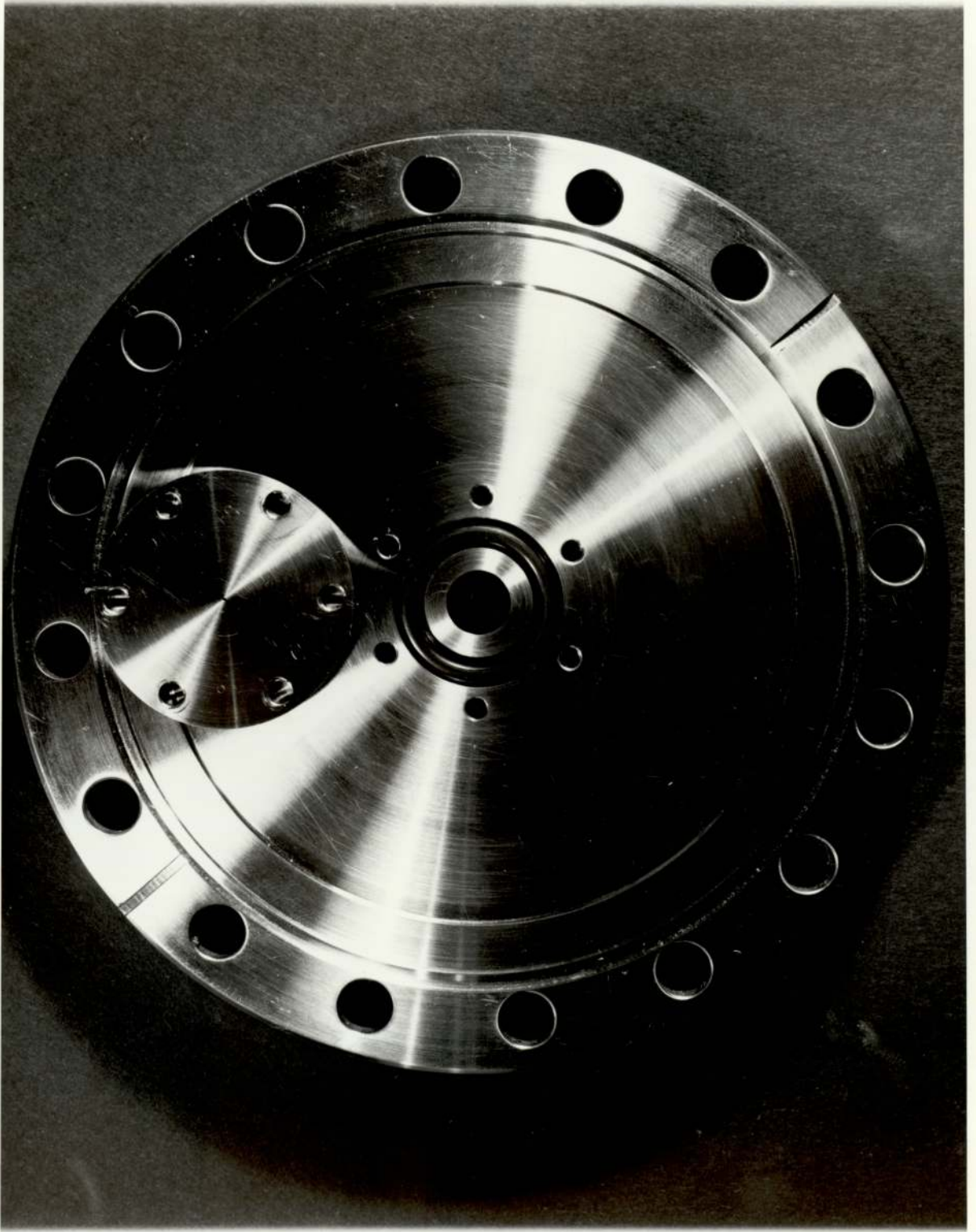
FIG 17

88(a)
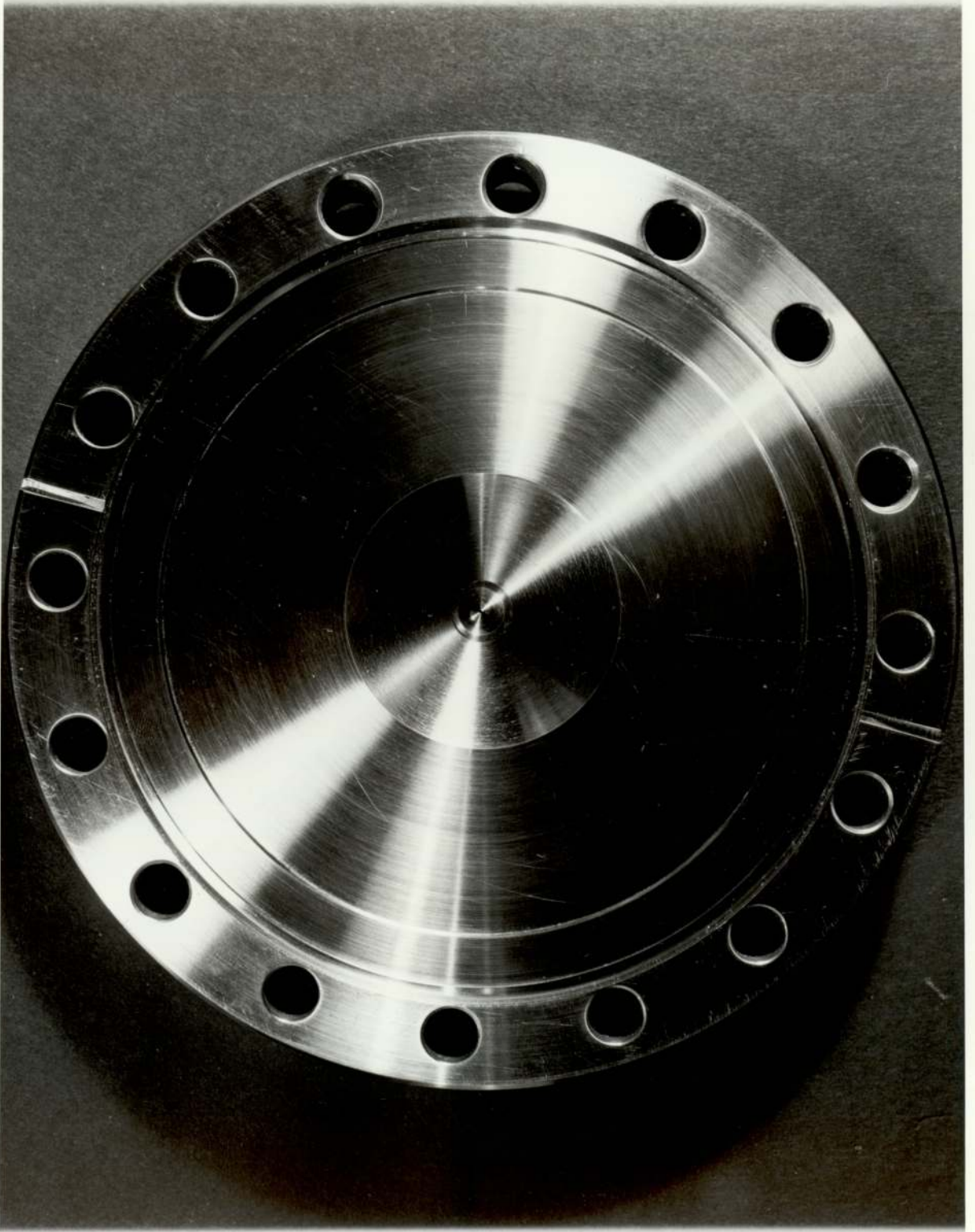
FIG 18
88(b)
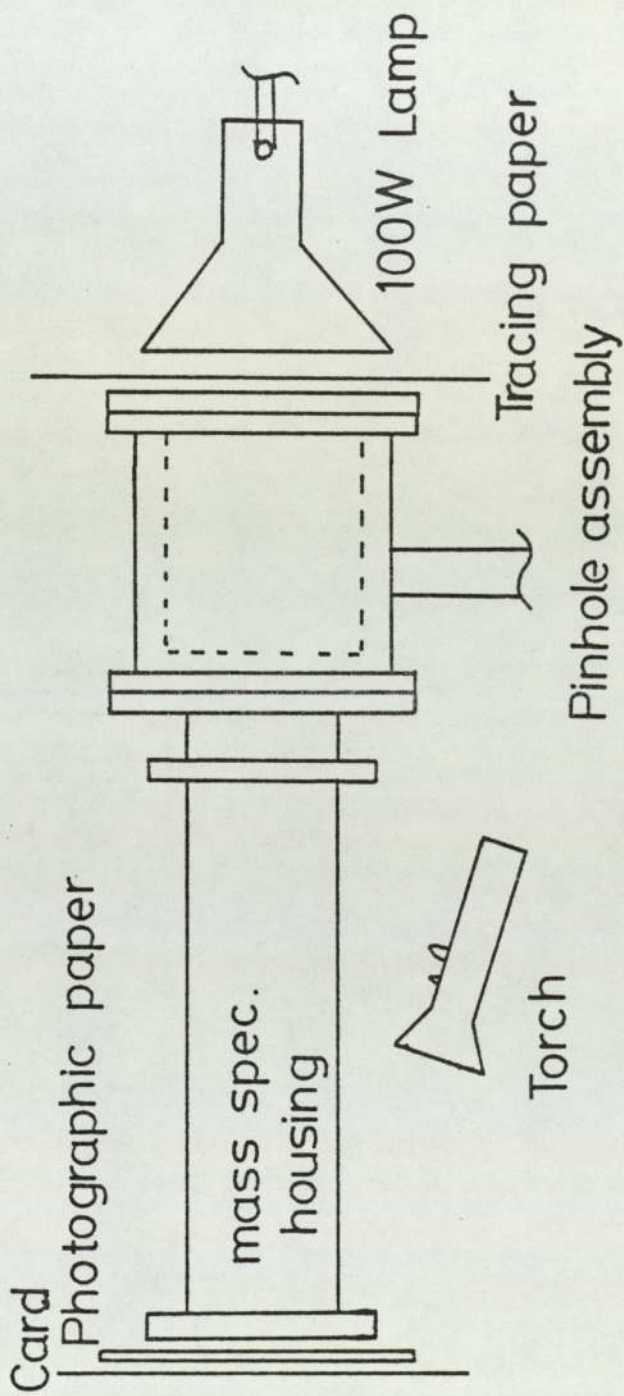
Fig.19. Photographic pinhole alignment

0.5mm off centre at the mass spectrometer source. This was acceptable because the mass spectrometer source inlet was 5mm in diameter and has a wide acceptance angle of 60°.

The pinhole sizes were experimented with initially but the final system employed pinholes of 0.5mm and 1mm in diameter for the first and second pinholes respectively. This system was finally aligned and tested with argon gas and performance curves were obtained with the reactor sealed off at a suitably high pressure. The pump speed of the system was obtained by observing the rate of change of pressure with time in the sealed off reactor (Appendix C). A plot of ln (P_O/P) against time produced an almost linear curve Fig:20. The deviation from the expected linear plot may be explained by the wide pressure range taken, 5torr to 0.05 torr, affecting the performance of the pinhole. At the higher pressures effusive flow conditions may be enhanced by viscous flow through the orifice and at lower pressures effusive flow maybe more predominant. A polynominal was fitted to the original Pressure against time plot using a computer programme.

Table:7. Pinhole effusion rate

Reactor Pressure (torr)	Time (secs)	ln (Po/P)
5.00	0	0.000
4.00	27	0.223
3.00	63	0.511
2.00	117	0.916
1.50	159	1.204
1.20	191	1.427
1.00	220	1.609
0.90	237	1.715
0.80	259	1.832
0.70	279	1.966
0.60	306	2.120
0.50	338	2.303
0.40	379	2.525
0.30	434	2.813
0.25	470	2.996
0.20	516	3.219
0.15	576	3.507
0.10	666	3.912
0.09	690	4.017
0.08	717	4.135
0.07	749	4.269
0.06	786	4.423
0.05	832	4.605
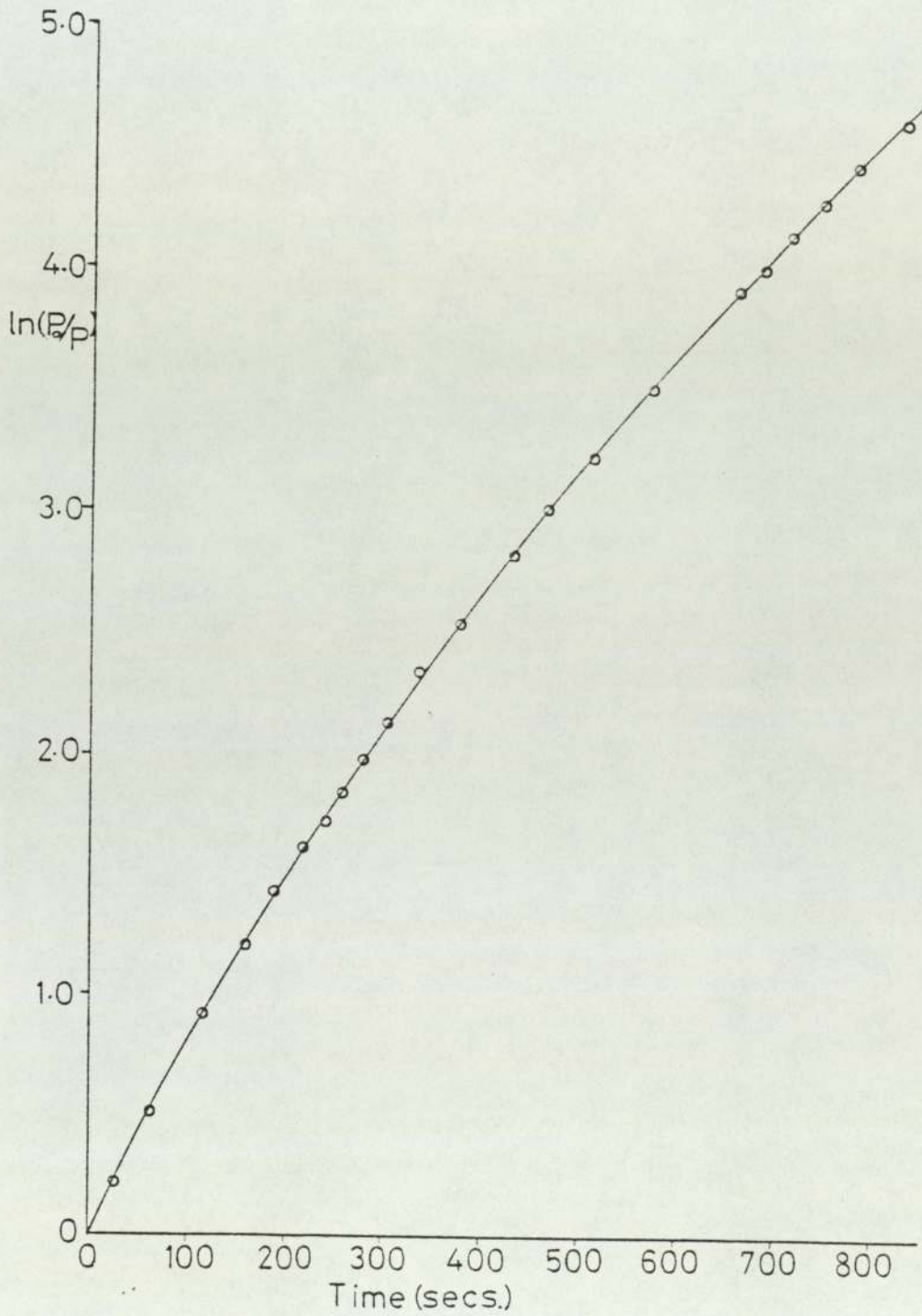
Fig.20. Effusion rate.

90(a)

3.1.5   The Detection System - Mass Spectrometer

The mass spectrometer was a V.G. QX2001 quadrupole mass filter with a single filament source. The mass filter was linear in mass up to 200 a.m.u. and had a facility for low-electron-energy studies. A special attenuator interface was made to provide an output to an X - Y plotter. (Appendix B).

When using the low-electron-energy facility it was found necessary to use emission currents of about 0.2mA. This reduced the possibility of burning the filament out and also reduced the flicker of signal current due to current limiting of the filament current. However, below 10eV the current limit for the filament operated and gave an oscillating signal current. This was due to two ciruits in the controller trying to maintain normal operating conditions in the mass spectrometer source. The emission current control circuit was trying to maintain the emission current at the set value and the filament current limit was preventing overloading of the filament by cutting off the filament current above a certain value ($\simeq 4_{AMPS}$). At higher emission currents the current limit operated at higher electron energies and interfered with appearance potential measurements.

The filament in the mass spectrometer was replaced three times during the course of this work. It was found that if care was taken to position the filament the intensity of the spectrum was affected from one filament

to the next to within ~5%. This was not surprising as the emission current was controlled by the mass spectrometer controller in a feedback system and was independent of filament quality up to the point where the current limit operated or the filament failed. Therefore there was no apparent ageing effect on any of the spectra. However, when a filament was removed and examined it showed signs of degradation presumably due to attack by the reactive species from the plasma. The filaments used were standard tungsten filaments as supplied by Vacuum Generators.

3.1.6 Emission Spectroscopy System

A facility for emission spectroscopy was constructed with a quartz (initially pyrex) barrel reactor with a 50mm optically flat quartz window. The vacuum system consisted of a mercury diffusion pump, a single stage backing rotary pump, a mercury manometer and a "Vacustat" type Mc leod gauge. Two glass traps, one of which was demountable, were on the downstream side of the reactor and also a B10 cone and tap was provided to allow the vacuum line to be used for handling materials and extracting effluent gases for analysis. Gaseous materials were metered into the system via needle valves, ball valves and rotameter flow meters Fig:21.

The spectroscopic equipment, Fig:22, consisted of an optical bench with two quartz lenses and a beam chopper;

92

ball valves

needle valves

flowmeters

gas A   gas B   gas C   gas D   gas E

to reactor and pumps
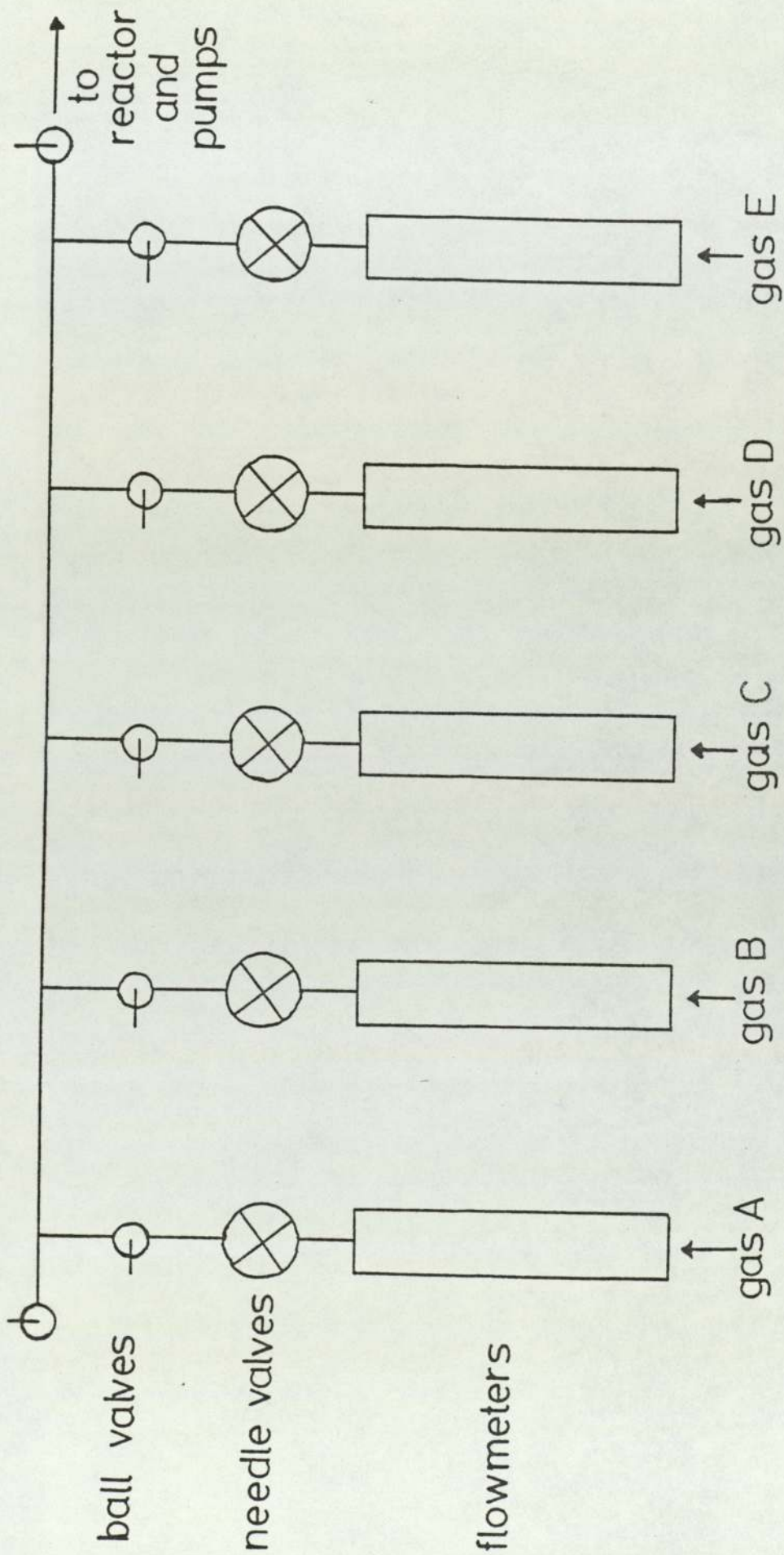
Fig:21.   Gas control panel

92(a)
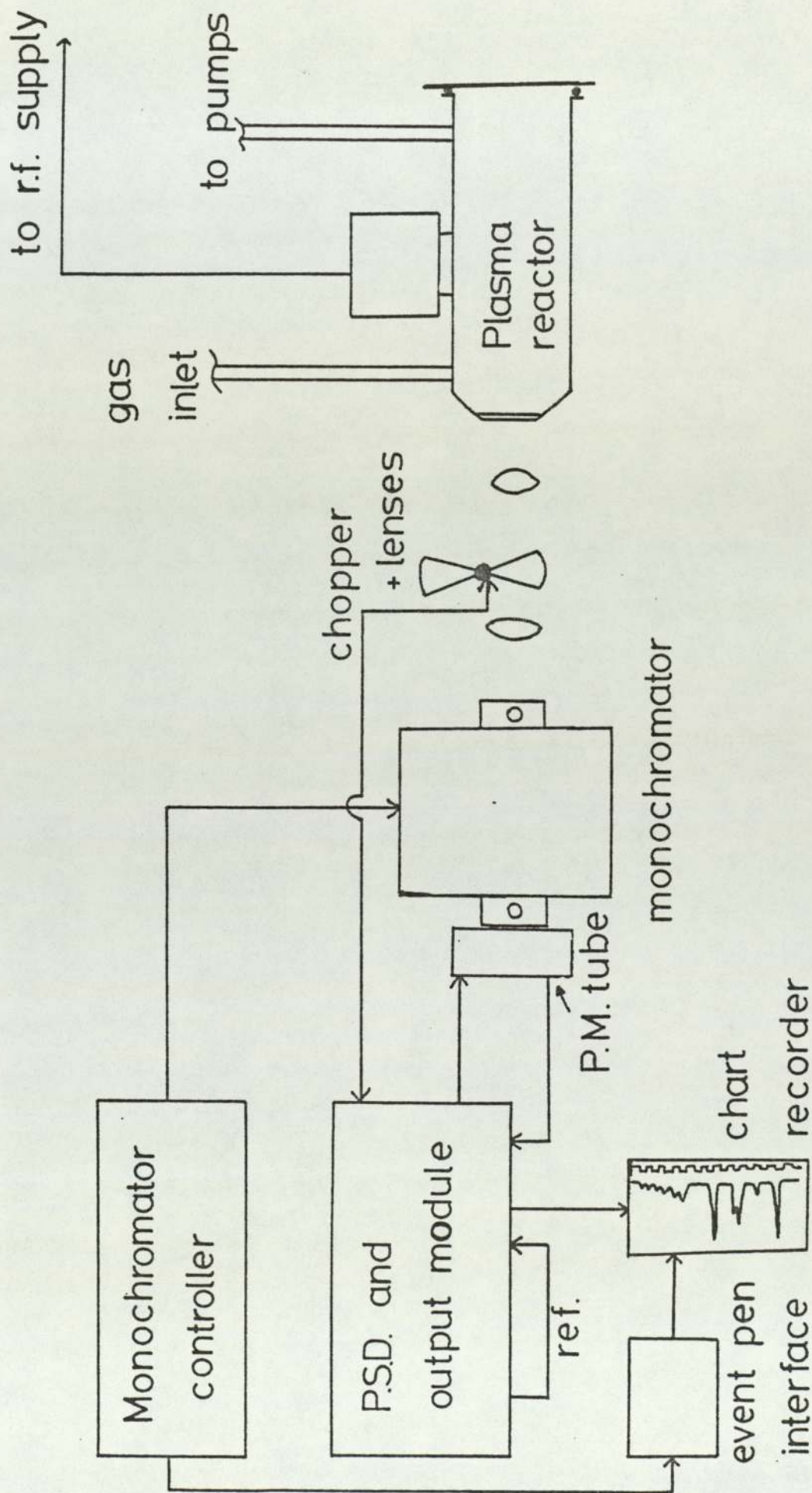
Fig.22. Emission spec. schematic

to r.f. supply

to pumps

gas inlet

Plasma reactor

chopper + lenses

monochromator

P.M. tube

Monochromator controller

P.S.D. and output module

ref.

chart recorder

event pen interface

92(b)

a holographic grating monochromator with variable inlet and outlet slit widths; a monochromator controller and a lock-in phase sensitive amplifier. A EMI extended S5 type photomultiplier was attached to the outlet slit on the monochromator and supplied with a variable high voltage supply from the phase sensitive detector (P.S.D.) and output module.

The spectroscopic equipment was supplied by Bentham Instruments and the resolution was claimed to be 1A° under ideal conditions. The sodium d-lines could easily be distinguished. The equipment required a small event marker pen interface in order to drive the Bryans Southern 28000 chart recorder, (Appendix A).

3.2.   Experimental Procedures
3.2.1   Mass Spectrometry

Mass spectra of various gaseous reactants were obtained at a pressure of 0.10 torr in the plasma reactor with electron energies of 70eV and 20eV. Gaseous reactants were admitted into the reactor via the automatic valves and flow meters on the gas controller system. However, special arrangements for the solid C_2Cl_6 were made. These included subliming the solid in the vacuum line to remove impurities. For this purpose a small flask ($300cm^3$) was attached to the B10 socket and the C_2Cl_6 was repeatedly sublimed and the line evacuated. The C_2Cl_6 was admitted into the reactor by

steady evaporation whilst heating the flask and a steady pressure of vapour maintained. This was only possible because the C_2Cl_6 has a high vapour pressure at room temperatures.

All the other materials used were highly volatile and could be admitted into the reactor in the normal way through the flow meters.

The appearance potential or ionisation potential of a species was determined by measuring the ion current at the m/e value of the species as a function of electron energy. Argon gas was used as the reference material. The intensity of the fragment species and argon were adjusted to be equal at 50eV and a plot of ion current against electron energy was obtained, using the Bryans 21000 series X-Y plotter and interface, for both the species and the argon. A voltage scale was recorded using a Philips digital voltmeter and the pulse marker on the interface unit (see appendix B). The voltage readings obtained were not absolute values and the voltage scale was calibrated against the argon which has an accurately known ionisation potential.

As the energy of thermally produced electrons is not monochromatic but has a Boltzmann distribution the ionisation potential plots do not intersect the electron energy axis at the ionisation potential but tail off asymptotically. Therefore, to obtain the appearance or

ionisation potential of a species it is necessary to refer to a standard such as argon (or Kryton, etc) and use one of the usual techniques for calculating, matching or extrapolating the ionisation potential curves. The techni ques available are semilog matching (71); critical slope (72); extrapolated voltage difference (70); or vanishing current, all of which have been discussed by several workers (57,69). Another method recommended by Lossing et al (71) which involves a 1% level semilog matching of the plots has also been used.

Mass spectra were obtained from various plasmas with a (type 100) plain silicon wafer placed on the bottom grounded electrode. The species in the plasma could be monitored singly by setting the mass spectrometer on a particular m/e value. The intensity of the particular peak could be monitored with additions of various other gases or changes in parameters such as pressure or r.f. power.

3.2.2   Silicon Wafer Etching

(a)   Opening the Reactor

Due to the pinhole molecular beam sampling system being designed to operate to pressures of 0.1 to 1 torr in the reactor, opening the reactor to air produced a considerable pressure rise in the intermediate region and the mass spectrometer. The intermediate region diffusion pump has to be switched off and helium gas was vented

95

into the reactor via the air inlet valve on the glass vacuum line.

The reactor door could be removed once the reactor achieved atmospheric pressure with the vented helium gas and wafers could be placed into or removed from the reactor.

(b)   Wafer Preparation

Prior to placing plain wafers into the reactor cleaning with suitable solvents (acetone, carbon tetrachloride) was necessary to remove any contamination from the surface of the wafer.

Wafer preparation prior to etching in the plasma reactor involved a plasma "cleaning" stage for plain wafers only. Initially plain wafer "cleaning" was done in an oxygen plasma at 0.25 torr. However, after some preliminary results a 50:50 mixture of argon and oxygen at 0.10torr was shown to remove hydrocarbon residues faster and etching could be started after only 10 minutes "cleaning".

Experiments in which this "cleaning" pre-treatment was omitted resulted in either no etching or there was a long induction period before etching occurred. In some cases a film was deposited on the wafer without any etching taking place.

(c)   Photoresist Patterning

The photoresist used was AZ1350J (a positive resist) and was patterned in the following way:-

i)   ten drops of 10% H.M.D.S. (hexadimethylsilazane) in carbon tetrachloride were spun onto the clean 2 inch wafers at a voltage setting of 80 on the spinner for 15 seconds;

ii)   30 seconds were allowed for the solvent to evaporate;

iii) 13 drops of photoresist were placed in the centre of the wafers and spun for 30 seconds at voltage setting 80;

iv)   the wafers were baked at 90°C for 5 minutes;

v)   the mask aligner (Cobilt type mask aligner) with 20 units (45 seconds) onthe exposure timer, was used to expose the wafers through an N10 ALB mask to a U.V. light source;

vi)   the pattern was developed in a 50:50 solution of water and Shipley M312 amine alkaline developer at 20°C $\pm$ 1° for40 seconds;

vii) tne wafers were washed thoroughly in running deionised water and baked for 10 minutes at 90°c.

(d)   Etching

The patterned silicon wafers were etched for 15 minutes in various plasmas at either 0.1 torr or 0.15 torr and at various r.f. powers.

(e)   Photoresist Stripping

After etching the photoresist was stripped in situ using an oxygen plasma at 0.25 torr pressure and with 100W of r.f. power for 20 minutes. It has been found that photoresist removal rates are high at this higher pressure and flow rate, (105-108). In some instances the mass spectrometer was used to monitor the stripping of the photoresist.

3.2.3. Infrared Spectrophotometry
a)   Gas Phase

Samples of some effluent gases trapped on the liquid nitrogen trap were taken by allowing the trap to warm up and allowing the gases to evaporate and expand into a previously evacuated infrared gas cell. The cell had sodium chloride windows and could be placed in the beam of a transmission infrared spectrophotometer.

(b)   Thin solid Films

Some weak infrared spectra were obtained using a special total internal reflectance (T.I.R.) attachment with a crystal of thallium iodide. The samples of wafer were placed against the crystal mounted in a stainless steel holder. The mirrors were aligned and the reflectance attachment placed in the beam of a Perkin-Elmer 457 infrared grating spectrophotometer where

the mirrors were finally set for maximum signal strength from the transmitted infrared radiation.

3.2.4   Scanning Electron Microscopy

Samples of etched semiconductor materials of about $1cm^2$ were prepared by scoring the backs of the wafers with a diamond scriber and breaking the wafer over a ruler. The samples cut from the wafer in this way were mounted onto standard sample holders with double sided adhesive tape.

A layer of gold was deposited onto the samples to increase the conductivity and prevent charging of the surface during examination in the electron beam. The gold was deposited in a bell jar vacuum system using a gold electrode 1cm above the samples with a d.c. discharge in argon at 200mtorr for 3 minutes.

The samples were examined under a Stereoscan electron microscope and photographs were obtained at 42° and 85° angles.

3.3   Chemical Preparation

3.3.1. Solids

Only C_2Cl_6 required purification in the vacuum line by repeated sublimation under vacuum in a flask attached

to the B10 socket. The C_2Cl_6 was easily sublimed using a hot air blower and leaving some surfaces at room temperature on which the C_2Cl_6 crystallized, this removed any air trapped in the sample.

3.3.2 Liquids

A study by gas chromatography of the available grades of carbon tetrachloride showed that "Spec. Pure" grade material has some impurities, mainly $CHCl_3$, of 0.5 molar%. Analar grade carbon tetrachloride, after drying over anhydrous sodium sulphate overnight, was shown to have 0.08 molar% impurity of $CHCl_3$ and was therefore used in the mass spectrometric work. The C_2Cl_4 was also dried and analysed similarly and no impurities were detected.

The $CFCl_3$ was taken to be as specified on a new bottle (99.9% pure) but was dried in the same way with anhydrous sodium sulphate. No attempt was made to analyse the $SiCl_4$ due to its very reactive nature.

All the liquids were degased before use using the rough vacuum line and liquid nitrogen to repeatedly freeze and thaw the liquids under vacuum.

3.3.3   Gases

All bottled gases were analysed using the mass spectrometer and one bottle of argon which was almost empty showed water background higher than normal and was exchanged. The use of molecular sieve drying tubes in the inlet lines was explored but appeared to make no difference to water background in the mass spectrometer. All the other bottled gases were used as supplied by B.O.C.

4. RESULTS

4.1 Background Conditions in the Mass Spectrometer.

Background pressures of $\sim 1 \times 10^{-8}$ torr and 1×10^{-7} torr were routinely obtained in the mass spectrometer and intermediate region respectively after pumping down and baking the system for 8 hours at $\sim 120°C$. Baking the system was very important for the removal of adsorbed water vapour and hydrocarbon material from the rotary and oil diffusion pumps.

After the system had been in use for some time and had been exposed to carbon tetrachloride plasmas the background spectra showed high levels of chlorine and hydrogen chloride. Baking the system for upto 8 hours reduced the levels of these background gases but did not restore the original background levels prior to exposure to carbon tetrachloride plasmas.

The glass plasma reactor became coated with brown and white deposits after exposure to a few discharges in carbon tetrachloride. These deposits were thought to be mainly C_2Cl_6 and were expected to contribute to the background spectra even when the system had been thoroughly baked. Unfortunately the plasma reactor could not be reliably baked at $\sim 120°$ like the rest of the system. When this was attempted the quartz glass window in the aluminium door shattered resulting in immediate

shut-down of the apparatus. Further attempts at baking the glass plasma reactor were abandoned in view of the possibility of damage to the numerous glass-to-metal and glass-to-glass seals in the reactor. Also the inner tube of the glass reactor, where the electrodes were mounted, would not have been raised to a sufficiently high temperature by heating the reactor externally.

Plasma cleaning was investigated as an alternative to simply baking the reactor because the discharge region was the least accessible and yet required some means of reducing the background contribution from adsorbed gases in this region. A discharge in 0.25torr of oxygen at 100W(F) and a flow rate of 4.58sccm for 30 minutes reduced the hydrocarbon background to very low levels. However, background water vapour was unaffected and chlorine and HCl were reduced slightly. A discharge in a 50% mixture of argon and oxygen at the same pressure and power for 10 minutes reduced the entire background levels considerably and was found to be the best mixture. Prolonged treatment with this plasma upto 60 minutes showed little improve ment after 10 minutes and in some cases the background spectra began to show increases in intensity. This was probably due to heating of the reactor by the plasma causing further desorption of adsorbed gases.

The baratron capacitance pressure gauge attached to the reactor showed some unusual features during this

103

work. After initially zeroing the gauge in a clean high vacuum with full liquid nitrogen traps, background pressure readings were taken as a matter of course throughout these experiments. These readings showed that after a few discharges in carbon tetrachloride the system showed some reluctance to pump down below 0.03torr and residual pressures of ~0.01torr were obtained even after pumping the system down overnight or over-weekends. Also filling the liquid nitrogen traps on the intermediate and mass spectrometer chambers resulted in rapid reductions in the reactor pressure even when the liquid nitrogen traps were quite full (more than half full).

These residual pressures in the reactor were consistent with the slow desorption of some species from the reactor walls. The species involved are probably HCl and chlorine which show increases in the background mass spectra after discharges in CCl_4 and other chlorine containing gases. As noted by Flamm (24) chlorine has a strong affinity for stainless steel and has been difficult to pump away and instead slowly desorbs over long periods of time.

4.2   Carbon Tetracnloride Plasmas.

4.2.1   Appearance Potentials

The reliable measurement of appearance potentials allows the detection of atoms and radicals to be made from the discharge. The measurement of appearance potentials was made using the electronic interface (Appendix B) and the x-y plotter. The interface also allowed the wider range curves in fig:23, to be produced using the low electron facility on the mass spectrometer.

Appearance potential curves were recorded over the wide range from 70eV to 10eV for the fragments normally observed from CCl_4 gas at 0.1torr pressure, 100X gain and with 1.75kV supplied to the photomultiplier. The filament emmission current was reduced (from 0.5mA normally) to 0.2mA for this work to avoid over-driving the tungsten filament at the low electron energies. All the conditions for the wide range curves were the same and the CCl_3^+ ion was used to initially set-up the gain and the electronic interface.

The appearance potentials of CCl_3^+, CCl_2^+ and CCl^+ ions were determined seperately from curves taken over much shorter ranges (10-25eV) using argon gas as the standard. The appearance potentials were obtained from semi-log plots (using the 1% method described by Lossing etal (71)) and compared with the extrapolated voltage

105
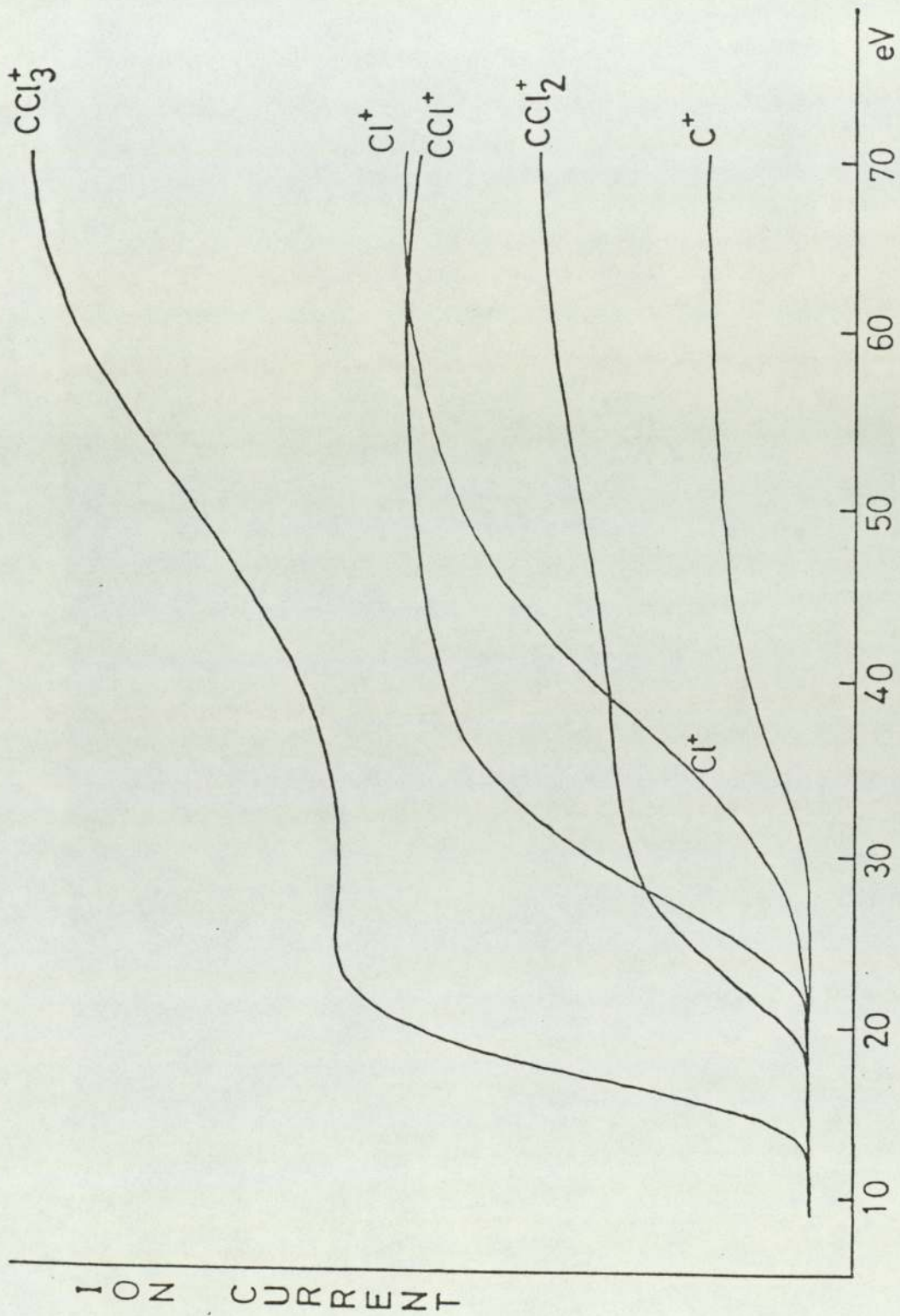
Fig.23 Ion currents for CCl_4 fragments (10–70eV)

difference method. The results are compared with the National Bureau of Standards reference tables (139) in table 8.

TABLE: 8.   Appearance potentials for CCl_4 fragment ions.

ION	MASS	National Bureau of Standards. (eV)	Semi log Plot 1% method (eV)	Extrapolated voltage difference (eV)
CCl_3^+	117	$11.9 \pm 0.1/11.65 \pm 0.1$	11.8 ± 0.2	12.0 ± 0.3
CCl_2^+	82	$16.1 \pm 0.1/16.5 \pm 0.2$	16.6 ± 0.2	16.4 ± 0.3
CCl^+	47	$19.4 \pm 0.1/19.35 \pm 0.05$	19.0 ± 0.2	20.1 ± 0.3
Cl^+	35	16.1 ± 0.2	------	------

It was not possible to determine the appearance potential for Cl^+ ions from the CCl_4 gas because of excessive noise on the appearance potential curve obtained on the x-y plotter. The mass spectrometer gain was increased to 1000 (maximum) and the photomultiplier supplied with 1.9kV in order to obtain a measurable ion current for Cl^+ ions. This resulted in excessive noise which could not be eliminated with the mass spectrometer controls.

Appearance potentials for fragments from the plasma were unobtainable because of radio-frequency interference. The electron energy calibration was unstable and could be offset by ± 0.4eV by r.f. interference even when using low r.f. powers (~ 40W). Screening the chart recorder, x-y plotter and plasma reactor with earthed gauze and aluminium sheet failed to

reduce the r.f. interference. Changing the sockets in which the apparatus was plugged and checking for good earth connections failed to reduce the r.f. interference. At high r.f. powers the baseline of the oscilloscope was also affected during normal mass spectrometric work at 70eV. The mass spectrometer could be used down to $\sim$20eV before the noise level became excessive. The baseline fluctuations and noise level were sensitive to the tuning of the r.f. matching network.

Despite several attempts at screening the r.f. discharge and trying to reduce the noise electronically it was not possible to obtain appearance potentials for the species in the discharge. It was also not possible to show that atoms or radicals were being produced and sampled into the mass spectrometer. It was necessary to use indirect approaches in the interpretation of the mass spectra in order to make some deductions concerning the involvement of atoms and free radicals.

4.2.2 Carbon Tetrachloride Plasmas

The results presented in table:9 and plotted to the same scale (for 70eV results) in fig:24 show marked differences between carbon tetrachloride gas and plasma. The results show that $C_2Cl_x^+$ and $C_3Cl_x^+$ ions are present in the mass spectrometer which are undoubtedly due to gas phase recombination of CCl_x radicals. The $C_2Cl_5^+$ and some of the $C_2Cl_4^+$ ion intensties are due to C_2Cl_6 formed

107

TABLE 9 CCl_4 Gas and Plasma[*] @ 70eV and 20eV

ION	MASS	CCl_4 GAS @ 70eV INT(mm)	CCl_4 PLASMA @ 70eV INT(mm)	CCl_4 GAS @ 20eV INT(mm)	CCl_4 PLASMA @ 20eV INT(mm)
C^+	12	137	53	----	----
H_2O^+	18	70	138	35	56
C_2^+	24	20	27	----	----
$N_2^+;CO^+$	28	17	24	5	5
Cl^+	35	505	352	5	10
HCl^+	36	50	205	65	100
CO_2^+	44	---	17	---	3
CCl^+	47	525	243	5	3
C_2Cl^+	59	20	70	----	2
$AlCl^+$	62	---	---	---	---
$COCl^+$	63	---	7	---	---
Cl_2^+	70	10	289	---	63
CCl_2^+	82	370	135	33	13
$C_2Cl_2^+$	94	---	132	---	27
$AlCl_2^+$	97	---	4	---	---
$C_3Cl_2^+$	106	---	5	---	---
CCl_3^+	117	1065	354	589	371
$C_2Cl_3^+$	129	---	65	---	21
$C_3Cl_3^+$	141	---	4	---	---
$C_2Cl_4^+$	164	---	55	---	23
$C_2Cl_5^+$	199	---	20	---	17

[*]Plasma conditions for table: 9, were:-

0.10 torr; 50W(F), ~ 10W(R); Flow rates 1.11sccm r.f. off
and 0.91sccm r.f. on. Gain: X30.
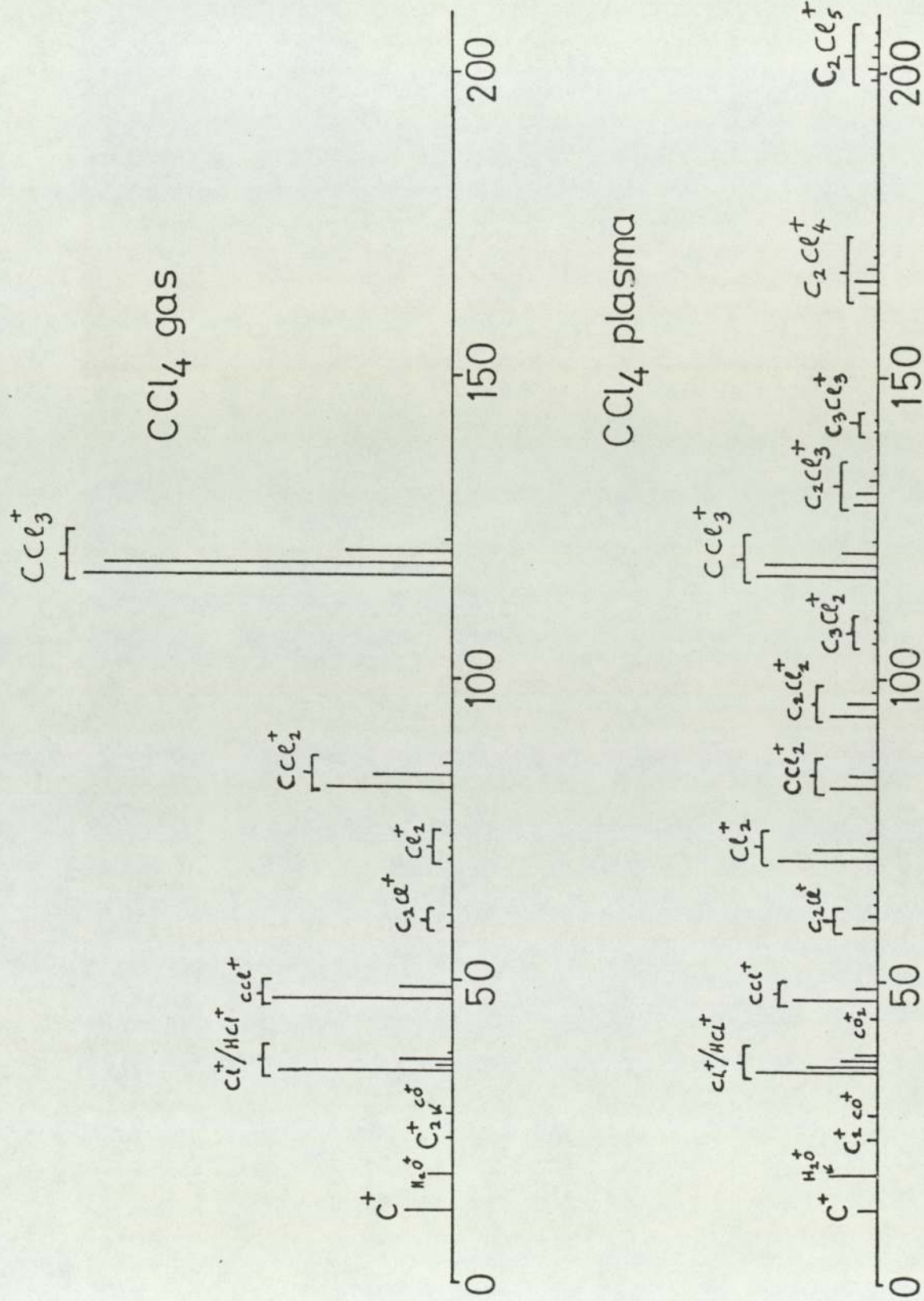
Fig.24. CCl₄ gas and plasma (70eV).

TABLE 10 C_2Cl_6 Gas and Plasma* @ 70eV and 20eV

ION	MASS	C_2Cl_6 GAS @ 70eV INT(mm)	C_2Cl_6 PLASMA @ 70eV INT(mm)	C_2Cl_6 GAS @ 20eV INT(mm)	C_2Cl_6 PLASMA @ 20eV INT(mm)
C	12	45	21	1	---
H_2O	18	29	8	2	---
C_2	24	50	4	---	1
$N_2^+;CO^+$	28	8	162	---	36
Cl^+	35	301	143	2	8
HCl^+	36	119	200	14	156
CO_2^+	44	5	2	---	---
CCl^+	47	351	45	---	---
C_2Cl^+	59	149	7	---	1
Cl_2^+	70	20	110	2	48
CCl_2^+	82	202	17	1	2
$C_2Cl_2^+$	94	263	11	2	2
CCl_3^+	117	638	42	127	28
$C_2Cl_3^+$	129	75	4	3	---
$C_2Cl_4^+$	164	110	3	12	1
$C_2Cl_5^+$	199	91	2	34	---

*Plasma conditions for table: 10, were:-

0.10 torr; C_2Cl_6 gas maintained by heating glass bulb containing C_2Cl_6

cystals on the vacuum line.

50W(F) $\sim$ 8W(R) @ 13.56MHz.

Note: the plasma results were not for a flowing plasma as is usual because of
method of introduction of gas.

TABLE II C_2Cl_4 Gas and Plasma* @ 70 and 20eV

ION	MASS	C_2Cl_4 GAS @ 70eV INT(mm)	C_2Cl_4 PLASMA @ 70eV INT(mm)	C_2Cl_4 GAS @ 20eV INT(mm)	C_2Cl_4 PLASMA @ 20eV INT(mm)
C^+	12	72	110	2	---
H_2O^+	18	31	50	1	---
C_2^+	24	89	60	---	1
$N_2^+;CO^+$	28	9	870	---	21
Cl^+	35	254	950	2	6
HCl^+	36	53	1170	4	103
CO_2^+	44	3	10	---	---
CCl^+	47	360	350	---	2
C_2Cl^+	59	198	190	---	2
Cl_2^+	70	9	965	1	37
CCl_2^+	82	90	125	2	2
$C_2Cl_2^+$	94	297	325	13	10
CCl_3^+	117	5	390	1	28
$C_2Cl_3^+$	129	352	150	56	7
$C_2Cl_4^+$	164	281	110	58	8
$C_2Cl_5^+$	199	---	10	---	1

*Plasma conditions for table: II, were:-

0.10 torr; C_2Cl_4 gas;   50W(F) ∼ 8W(R) @ 13.56MHz.

Flow rates: 0.68sccm (r.f. off)
              0.46sccm (r.f. on)
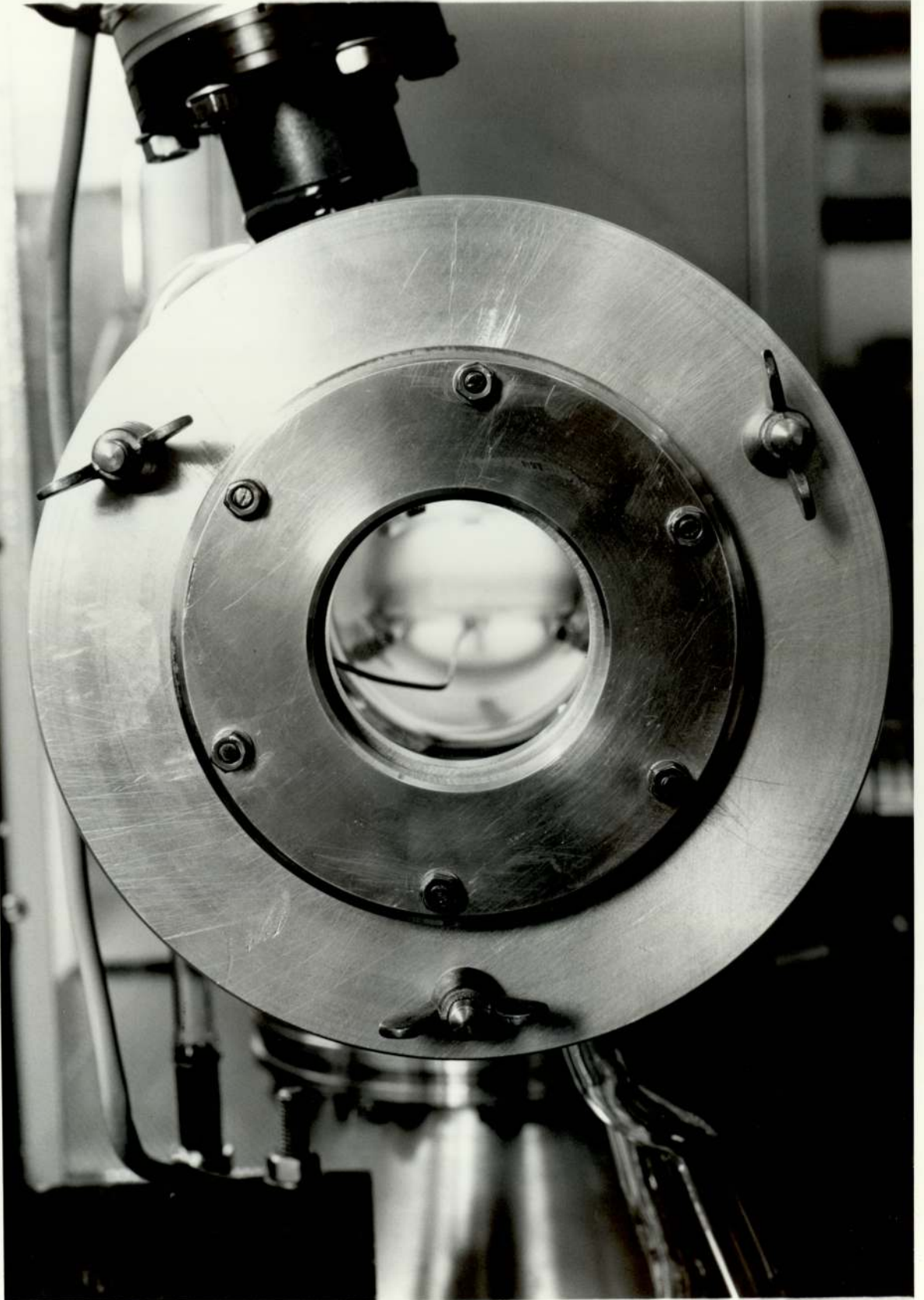
FIG 25
110(a)

in the discharge and fragmenting in the mass spectrometer ion source. Some of the $C_2Cl_4^+$ ion intensity is expected to be due to C_2Cl_4 formed in the discharge.

The amounts of C_2Cl_6 and C_2Cl_4 formed in the discharge in CCl_4 were determined by obtaining mass spectra of these two materials both from the gas and discharge. The mass spectra of C_2Cl_6 and C_2Cl_4 gas and plasma are shown in tables:10 and 11. From these tables the amount of C_2Cl_6 in the CCl_4 plasma was estimated to be $\sim 17\%$ and the amount of C_2Cl_4 in the CCl_4 plasma is estimated to be $\sim 11\%$. The contribution from C_3Cl_x species to $C_2Cl_4^+$ or $C_2Cl_5^+$ ion intensities was ignored because they were very small and no ions could be detected for $C_3Cl_x^+$ ions above $C_3Cl_3^+$ at 141 a.m.u.

A typical discharge in CCl_4 gas at $\sim 100W(F)$ is shown in the photograph, fig:25, taken through the quartz glass window. The discharge at this power is a bright blue-white colour.

4.2.3 Effect of Power on CCl₄ Plasmas

The effect of r.f. power on the ion currents for species in the CCl_4 plasma are shown in table:12, and for CCl_3^+, CCl_2^+ and Cl_2^+ ions in fig:26. There are clearly two regions of discharge which can also be observed from the characteristic emission from the plasma. At low powers ($<50W(F)$) the discharge has a dull turquoise

111

TABLE 12   Effect of r.f. power on CCl_4 plasmas[*] @ 70eV.

ION	MASS	CCl_4 GAS 70eV INT(mm)	CCl_4 Plasmas (intensities (mm))		
			40W(F)	50W(F)	100W(F)
C^+	12	159	117	90	78
H_2O^+	18	54	66	66	72
C_2^+	24	---	12	21	18
$N_2^+; CO^+$	28	21	78	105	186
Cl^+	35	630	648	594	558
HCl^+	36	162	486	549	672
CO_2^+	44	---	12	9	12
CCl^+	47	576	480	363	276
C_2Cl^+	59	30	54	60	48
$COCl^+$	63	---	12	18	18
Cl_2^+	70	21	243	420	429
CCl_2^+	82	375	324	222	162
$C_2Cl_2^+$	94	---	75	114	108
$AlCl_2^+$	97	---	---	4	5
CCl_3^+	117	1053	876	588	414
$C_2Cl_3^+$	129	---	36	57	42
$C_3Cl_3^+$	141	---	9	12	8
$C_2Cl_4^+$	164	---	28	44	25
$C_2Cl_5^+$	199	---	11	7	2
Flow rates (sccm)		0.87	0.71	0.65	0.59

[*]Plasma conditions were:-

0.10 torr CCl_4 gas; 40W(F) ∿ 6W(R);   50W(F) ∿ 8W(R)

100W(F) ∿ 20W(R)
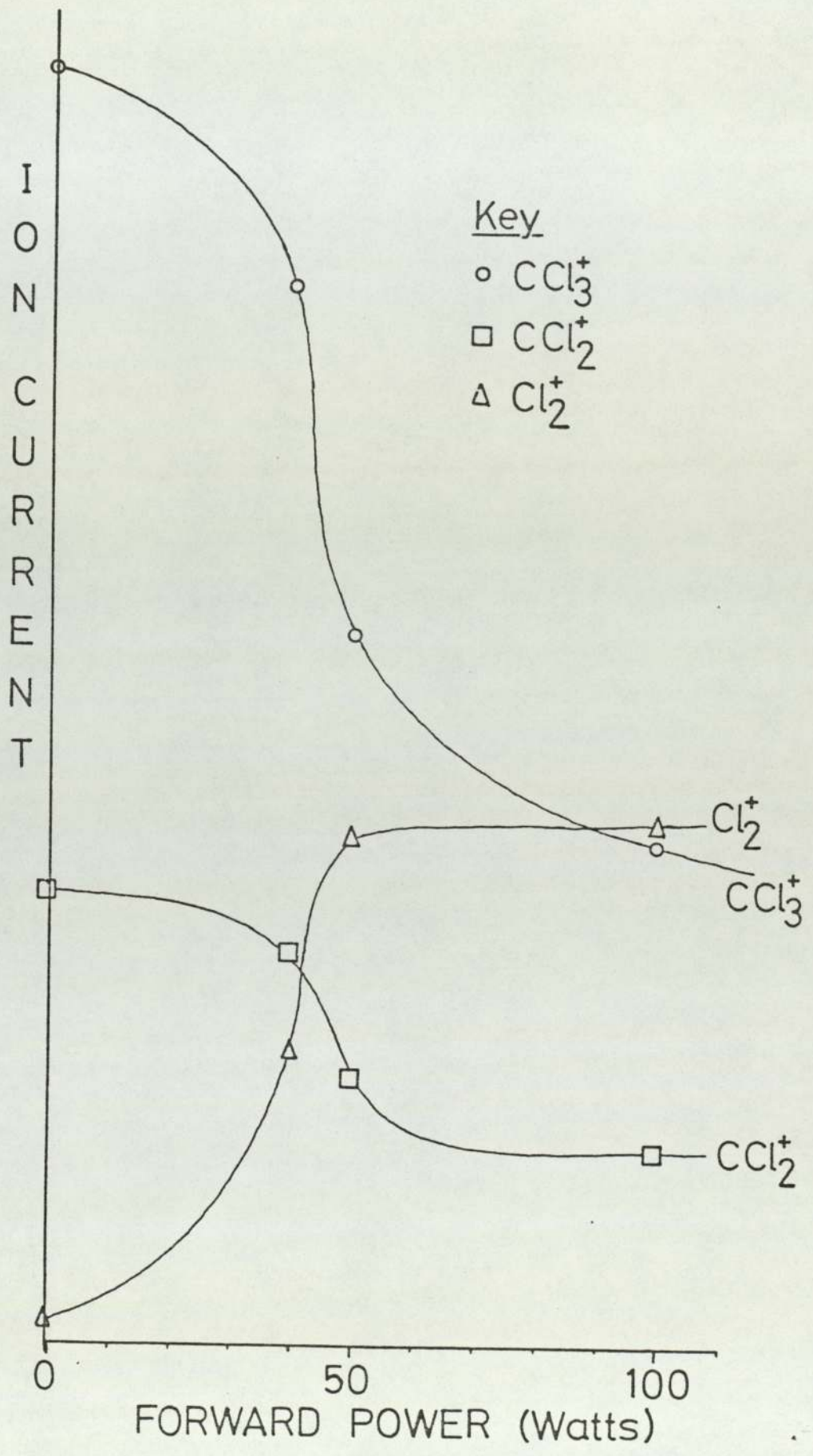
Fig.26. Effect of power.

112(a)

colour and is confined between the electrodes. At higher powers ($>50W(F)$) the discharge is a very bright white-blue colour and the discharge extends above and below the electrodes. There is also a region of abrupt change-over between these two types of discharge.

The CCl_4 plasma gives high reflected powers of between 15 and 30% of the forward powers applied to the discharge. In general the greater the applied r.f. power the larger the proportion of the power is reflected. However, it was not always possible to tune the reflected power to the same value for plasmas at the same pressure. The additions of other gases such as O_2, Ar or H_2 to the CCl_4 discharge reduced the reflected power from these plasmas.

4.2.4   The Effect of Additives on CCl_4 Plasmas.

The effect of additions of O_2, N_2O, H_2 and Ar to CCl_4 plasmas are shown in tables: 13-20 and figs:27-30. The addition of oxygen to CCl_4 plasma monitoring $C_2Cl_4^+$ and $C_2Cl_3^+$ ions from C_2Cl_x species in the plasma have also been studied and the results are shown in tables: 15-17, and figs:27 and 28.

TABLE 13 CCl_4/O_2 Gases and Plasma[*] at 70eV and 20eV.

ION	MASS	70eV $CCl_4/23\%$ O_2·GAS	70eV $CCl_4/23\%$ O_2·Plasma	70eV $CCl_4/50\%$ O_2·GAS	70eV $CCl_4/50\%$ O_2·Plasma	20eV $CCl_4/50\%$ O_2·GAS	20eV $CCl_4/50\%$ O_2·Plasma
C^+	12	84	53	70	36	---	---
O^+	16	33	15	75	20	---	12
H_2O^+	18	84	105	5	27	---	---
C_2^+	24	---	6	1	1	---	---
CO^+	28	45	387	65	667	28	228
O_2^+	32	246	16	615	28	291	13
Cl^+	35	330	244	260	185	6	43
HCl^+	36	135	319	20	356	12	216
CO_2^+	44	15	30	1	25	1	10
CCl^+	47	318	135	273	19	3	16
C_2Cl^+	59	18	18	19	1	---	---
$AlCl^+$	62	---	1	---	1	---	1
$COCl^+$	63	---	7	---	14	---	4
Cl_2^+	70	12	213	16	229	1	170
CCl_2^+	82	219	90	200	18	---	36
$C_2Cl_2^+$	94	---	37	---	10	---	23
$AlCl_2^+$	97	---	5	---	2	---	10
$COCl_2^+$	98	---	4	---	2	---	5
CCl_3^+	117	588	210	598	187	331	196
$C_2Cl_3^+$	129	---	10	---	9	---	11
$C_3Cl_3^+$	141	---	1	---	---	---	---
$C_2Cl_4^+$	164	---	6	---	11	---	11
$C_2Cl_5^+$	199	---	1	---	4	---	4

[*]Plasma conditions for table: 13 were:-

Pressure: 0.10 torr total.

Flow rates:- 23% O_2; 0.16sccm O_2, 0.57sccm CCl_4 (r.f off)

0.13sccm O_2, 0.42sccm CCl_4 (r.f on)

50% O_2; 0.52sccm O_2, 0.52sccm CCl_4 (r.f off)

; 0.48sccm O_2, 0.48sccm CCl_4 (r.f on)

Power: 13.56MHz; 100W(F), ~3W(R). Gain: 30.

N.B. reflected power is lower because of the high oxygen content of the plasma.

Table 14: Addition of Oxygen to CCl$_4$ Plasmas*

Flow Rates (sccm)		Total Flow Rate (sccm)	Plasma Gas Composition		CCl$_3^+$ at 117amu (mm)	CCl$_2^+$ at 82amu (mm)	CCl$^+$ at 47amu (mm)	Cl$_2^+$ at 70amu (mm)	CO$^+$ at 28amu (mm)	HCl$^+$ at 36amu (mm)	Cl$^+$ at 35amu (mm)
CCl$_4$	O$_2$		%CCl$_4$ (mm)	%O$_2$ (mm)							
0.52	--	0.52	100	---	586	213	360	366	113	513	600
0.50	0.12	0.62	81	19	420	160	260	326	553	566	506
0.51	0.12	0.62	81	19	440	167	266	306	546	532	512
0.50	0.13	0.63	80	20	460	160	260	280	540	513	526
0.49	0.15	0.64	77	23	406	153	253	266	560	500	480
0.47	0.16	0.63	75	25	340	127	213	346	666	600	480
0.49	0.18	0.67	73	27	380	140	233	266	613	526	466
0.46	0.20	0.66	70	30	286	113	153	340	752	620	453
0.44	0.20	0.64	69	31	373	133	220	313	666	513	466
0.43	0.23	0.66	65	35	253	100	167	353	812	606	440
0.43	0.26	0.69	62	38	233	87	147	360	852	612	432
0.41	0.29	0.70	60	40	213	80	140	380	900	660	426
0.39	0.34	0.73	53	47	180	67	113	400	941	680	413

*Plasma conditions for table:14 were:-

Pressure: 0.10 torr total.

Power: 13.56MHz; 50W(F), ~8W(R).

. Flow rate: 0.71sccm CCl$_4$ gas with r.f. off.

Electron energy: 70eV; Gain: 30.

115

Oxygen additions to CCl₄ plasma.

Key.
o CCl_3^+
△ CCl^+
□ CO^+

CCl_3^+↗

CCl^+↗

CO^+↖

% Oxygen added
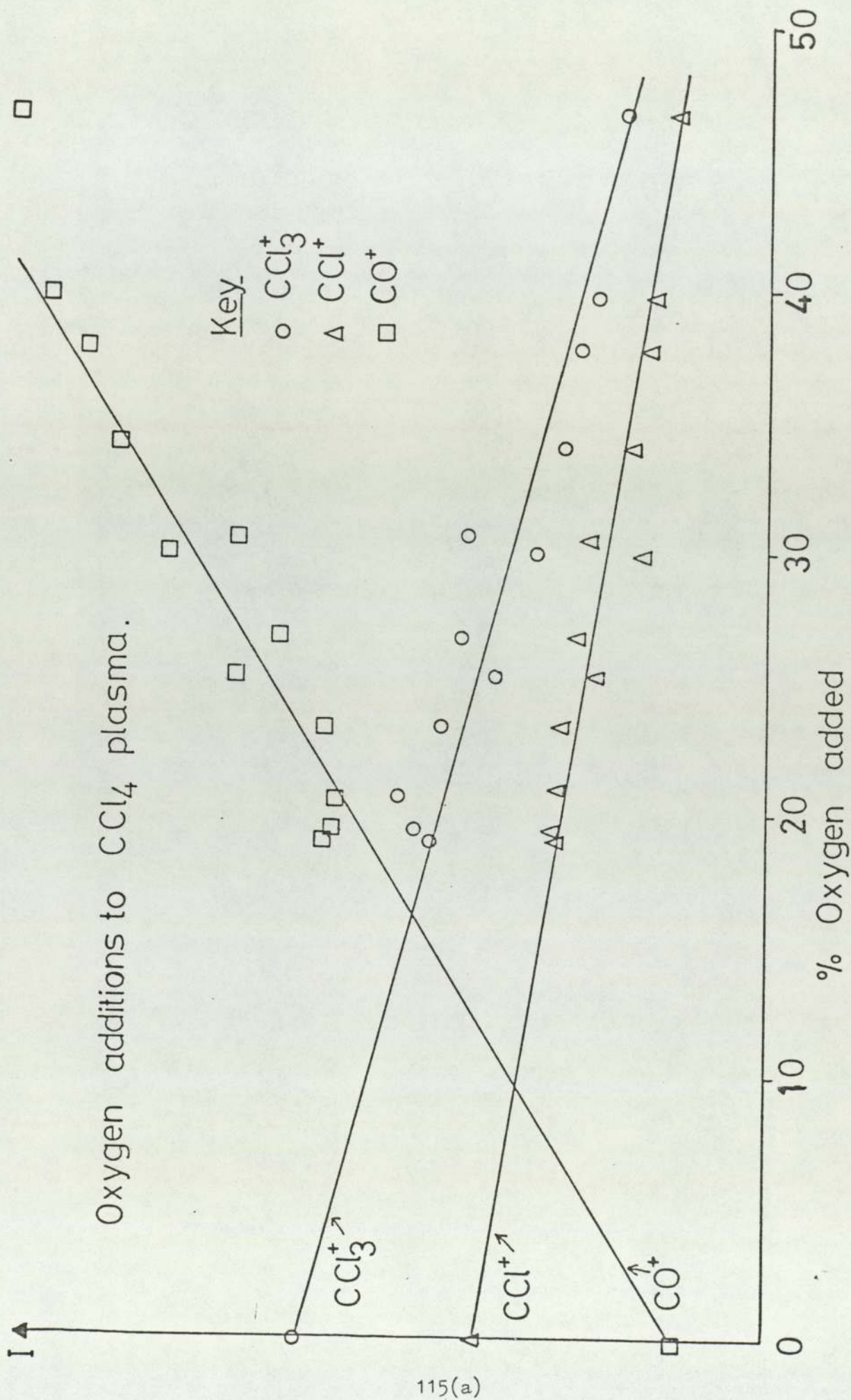
Fig.27. Addition of oxygen to CCl₄ plasma.

115(a)

Fig.28. Addition of oxygen to CCl_4 plasma.

Key-
o Cl_2^+
△ Cl^+
□ CCl_2^+

% Oxygen added

Cl^+

Cl_2^+

CCl_2^+

115(b)
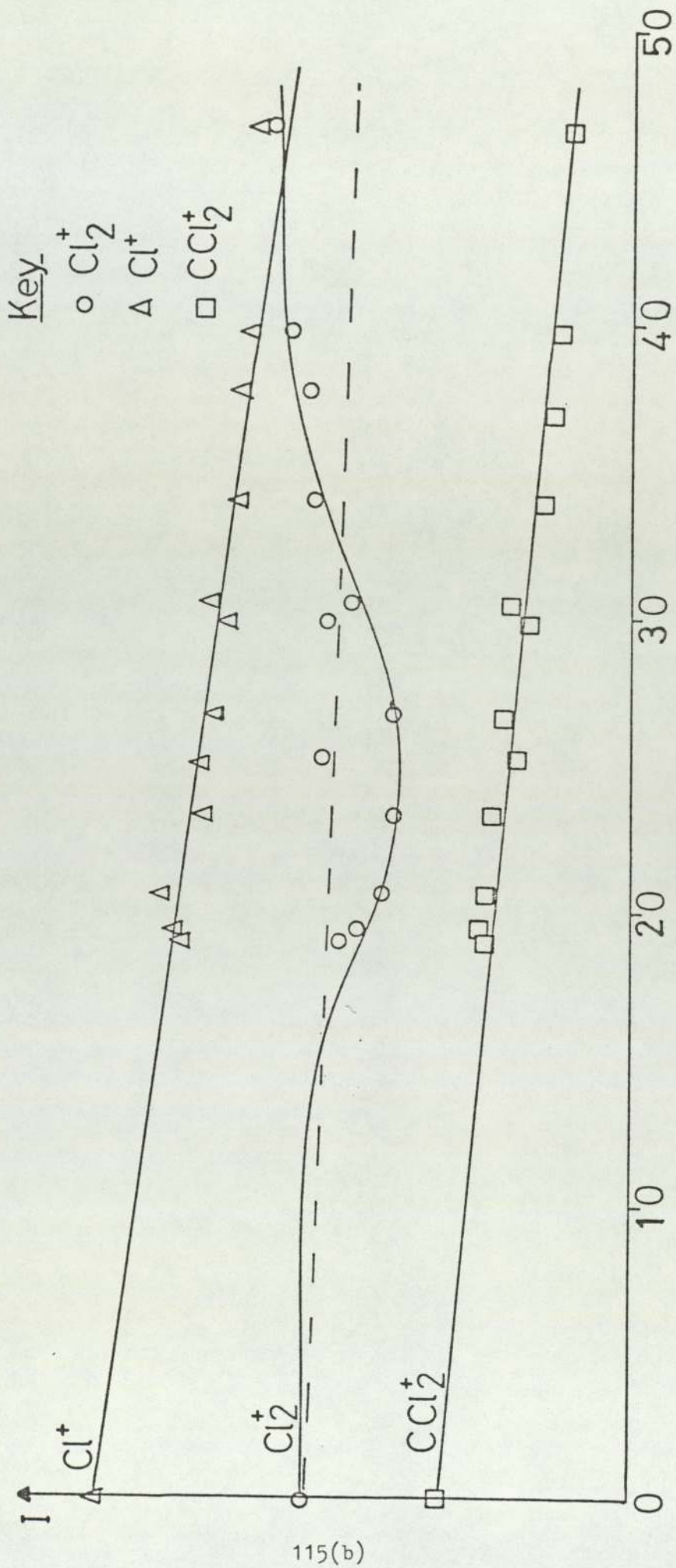
Table: 15   Addition of Oxygen to CCl_4 Plasmas[*] Monitoring $C_2Cl_3^+$ ions at 129 amu and 50W.

Flow Rates(sccm)		Total Flow	Plasma Composition		$C_2Cl_3^+$ ion intensity (mm)
CCl_4	O_2	Rate (sccm)	%CCl_4	%O_2	X100 GAIN
0.72	---	0.72	100	---	85
0.40	0.01	0.41	97	3	41
0.41	0.02	0.43	96	4	38
0.40	0.02	0.42	95	5	35
0.36	0.04	0.40	90	10	29
0.35	0.04	0.39	89	11	25
0.32	0.05	0.37	87	13	23
0.32	0.06	0.38	85	15	21
0.31	0.06	0.37	84	16	19
0.29	0.07	0.36	81	19	16
0.28	0.08	0.36	78	22	14

[*]Plasma conditions for table: 15, were:-

Pressure: 0.10 torr total.

Power: 50W(F), $\sim$7W(R)

Flow rate: 0.88sccm r.f. off.

Electron energy: 70eV; Gain: 100

Table: 16   Addition of Oxygen to CCl_4 Plasmas* Monitoring $C_2Cl_3^+$ ions at 129 amu and 100W.

Flow Rates(sccm)		Total Flow	Plasma Composition		$C_2Cl_3^+$ion intensity (mm)
CCl_4	O_2	Rate (sccm)	$\%CCl_4$	$\%O_2$	X100 GAIN
0.63	---	0.63	100	---	42
0.50	0.01	0.51	98	2	26
0.50	0.02	0.52	96	4	26
0.48	0.03	0.51	94	6	22
0.48	0.05	0.53	91	9	19
0.47	0.05	0.52	90	10	24
0.47	0.08	0.55	86	14	18
0.48	0.10	0.58	83	17	16
0.47	0.11	0.58	81	19	16
0.46	0.13	0.59	78	22	15
0.45	0.15	0.60	75	25	15

*Plasma conditions for table: 16, were:-

Pressure: 0.10 torr total.

Power: 13.56MHz; 100W(F),$\sim$20W(R)

Flow Rate of CCl_4 with r.f. off was 0.82 sccm.

Electron energy: 70eV; Gain: 100

Addition of oxygen to CCl_4 plasma at 0.10 torr monitoring $C_2Cl_3^+$ ions.

Power: □ – 50W(F),~7W(R); o – 100W(F),~20W(R).

100W,

50W?

% Oxygen added
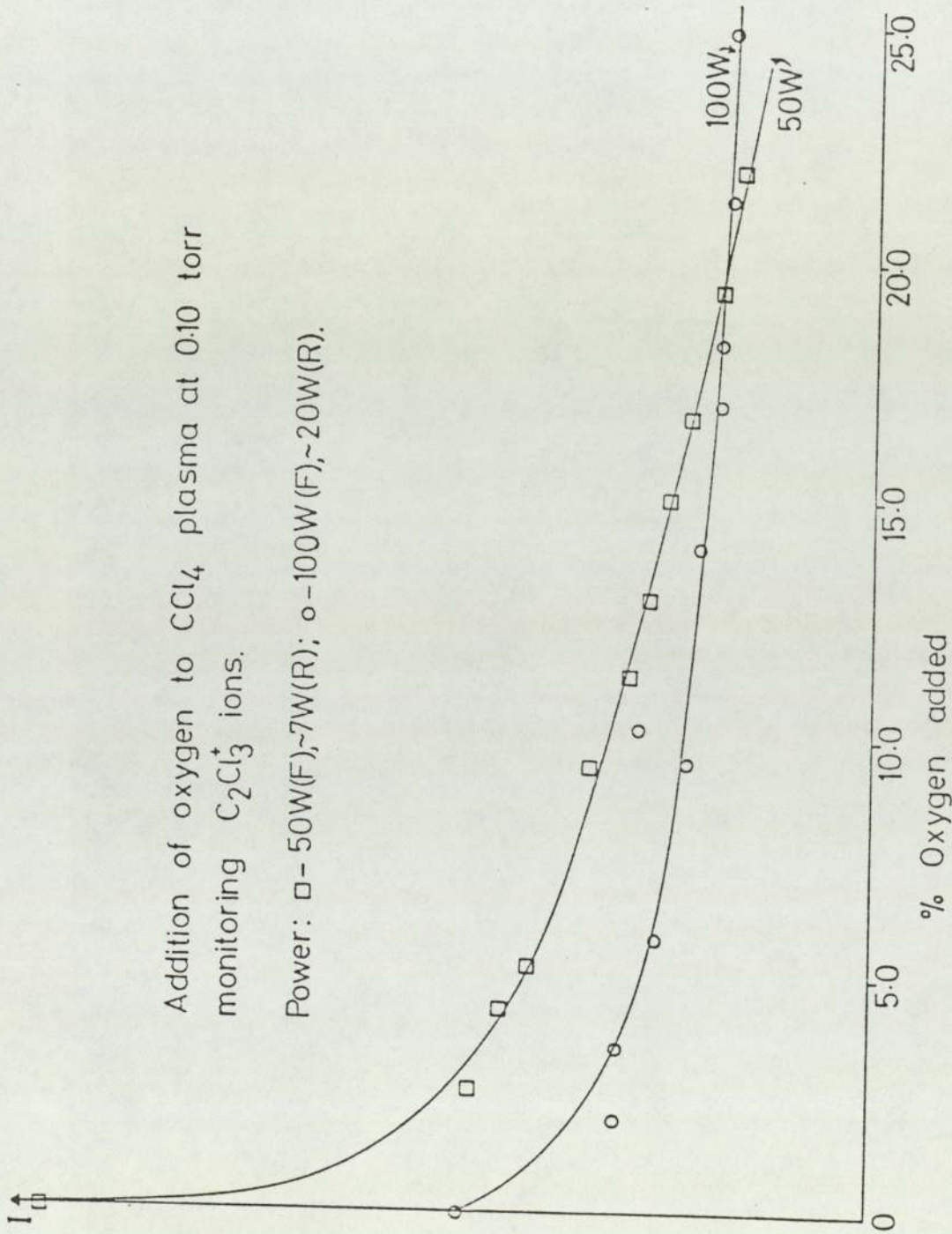
Fig.29. $C_2Cl_3^+$ monitoring.

117(a)

Table: 17   Addition of Oxygen to CCl_4 Plasmas[*] Monitoring $C_2Cl_4^+$ ions at 166 amu and 50W.

Flow Rates(sccm)		Total Flow	Plasma Composition		$C_2Cl_4^+$ ion intensity (mm)
CCl_4	O_2	Rate (sccm)	%CCl_4	%O_2	X100 GAIN
0.66	---	---	100	---	81
0.57	0.02	0.59	97	3	40
0.56	0.03	0.59	95	5	42
0.55	0.03	0.58	94	6	44
0.52	0.04	0.56	93	7	47
0.47	0.05	0.52	90	10	45
0.53	0.08	0.61	87	13	36
0.52	0.10	0.62	84	16	35
0.33	0.07	0.40	83	17	29
0.50	0.13	0.63	79	21	34
0.48	0.15	0.64	75	25	33

[*]Plasma conditions for table: 17, were:-

Pressure: 0.10 torr total.

Power: 13.56MHz; 50W(F), $\sim$ 7W(R)

Flow Rate of CCl_4 with r.f. off was 0.82 sccm.

Electron energy: 70eV; Gain: 100

Addition of oxygen to CCl_4 plasma monitoring $C_2Cl_4^+$ ions.

Power: 50W(F), ~7W(R).   Pressure: 0·10 torr.

% Oxygen added
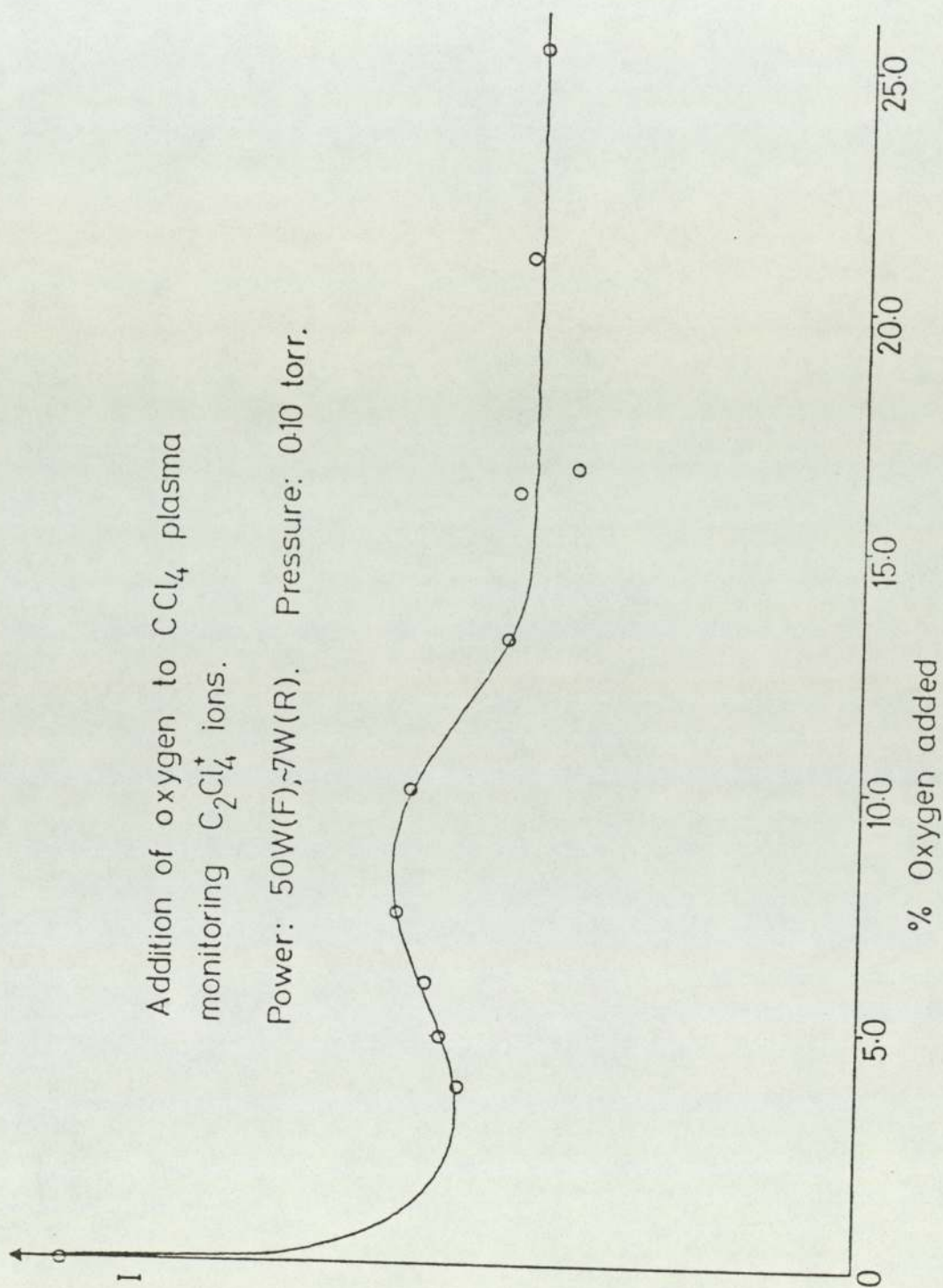
Fig. 30. $C_2Cl_4^+$ monitoring.

118(a)

Table:18   Additions of N_2O to CCl_4 Plasmas[*] @ 70eV and 50W.

ION	MASS	100% CCl4 GAS (mm)	100% CCl_4 Plasma(mm)	33% N_2O in CCl_4 GAS	33% N_2O in CCl_4 Plasma	30% N_2O in CCl_4 Plasma	23% N_2O in CCl_4 Plasma
C^+	12	138	90	120	52	48	48
N^+	14	---	---	54	52	66	66
O^+	16	---	---	24	23	39	24
H_2O^+	18	21	66	24	52	60	60
Al^+	27	---	---	---	14	9	6
$N_2^+;CO^+$	28	27	105	93	882	1134	1140
NO^+	30	---	---	156	14	15	12
O_2^+	32	---	---	3	3	3	3
Cl^+	35	588	594	477	345	315	315
HCl^+	36	96	549	111	447	588	588
$CO_2^+;N_2O^+$	44	24	9	498	95	108	108
CCl^+	47	516	363	468	16	12	12
C_2Cl^+	59	24	60	21	95	33	31
$AlCl^+$	62	---	---	---	4	12	11
$COCl^+$	63	---	18	---	8	15	12
Cl_2^+	70	15	420	12	486	498	528
CCl_2^+	82	345	222	285	5	9	9
$C_2Cl_2^+$	94	---	114	---	10	1	---
$COCl_2^+$	98	---	---	---	4	---	---
$AlCl_2^+$	97	---	4	---	2	---	---
CCl_3^+	117	1014	588	825	24	9	9
$C_2Cl_3^+$	129	---	57	---	1	1	1
$C_3Cl_3^+$	141	---	12	---	---	---	1
$C_2Cl_4^+$	164	---	44	---	---	1	1
$C_2Cl_5^+$	199	---	7	---	---	---	---

[*]Plasma Conditions for table: 18, were:-

Pressure: 0.10 torr total.

Flow rates:

100% CCl_4 : 0.79sccm (r.f. off)

100% CCl_4 : 0.65sccm (r.f. on)

 33% N_2O/CCl_4 : 0.54sccm CCl_4; 0.28sccm N_2O r.f. off

 33% N_2O/CCl_4 : 0.22sccm CCl_4; 0.11sccm N_2O r.f. on

 30% $N_2O/CCl4$: 0.21sccm CCl_4; 0.06sccm N_2O r.f. on

 23% N_2O/CCl_4 : 0.15sccm CCl_4; 0.04sccm N_2O r.f. on

Power: 13.56MHz; 50W(F),$\sim$8W(R).

Electron energy: 70eV; Gain 30.

Table:19   Addition of Hydrogen to CCl_4 Plasmas*

ION	MASS	100% CCl_4 GAS (mm)	100% CCl_4 PLASMA (mm)	15% H_2 85% CCl_4 GAS (mm)	15% H_2 85% CCl_4 PLASMA (mm)	14% H_2 86% CCl_4 PLASMA (mm)	24% H_2 76% CCl_4 PLASMA (mm)	30% H_2 70% CCl_4 PLASMA (mm)
H^+	1	---	---	27	140	165	214	259
C^+	12	157	---	144	72	56	52	49
H_2O^+	18	22	66	24	30	34	34	37
C_2^+	24	---	---	---	17	19	11	15
N_2^+;CO^+	28	37	24	34	45	37	34	37
Cl^+	35	671	352	573	585	664	604	607
HCl^+	36	157	205	180	1114	1335	1432	1477
CCl^+	47	562	243	480	237	289	210	199
C_2Cl^+	59	15	70	12	44	45	35	37
$AlCl^+$	62	---	---	---	5	4	7	7
$COCl^+$	63	---	7	---	7	7	4	7
Cl_2^+	70	4	289	4	257	289	247	248
CCl_2^+	82	352	135	30	125	127	112	139
$C_2Cl_2^+$	94	---	130	---	110	116	109	109
CCl_3^+	117	1000	550	852	320	356	300	262
$C_2Cl_3^+$	129	---	65	---	38	39	36	34
$C_3Cl_3^+$	141	---	4	---	4	---	---	4
$C_2Cl_4^+$	164	---	54	---	40	26	22	22
$C_2Cl_5^+$	199	---	8	---	3	---	3	---

*Plasma Conditions for table:19, were:-

Pressure: 0.10 torr total
Power: 13.56MHz; 50W(F) ≈ 8W(R)
Flow rates:-
100% CCl_4 : 0.75sccm (r.f. off); 0.65sccm (r.f. on)
 15% H_2/CCl_4 : 0.64sccm CCl_4; 0.11sccm H_2 (r.f. off)
 15% H_2/CCl_4 : 0.68sccm CCl_4; 0.12sccm H_2 (r.f. on)
 14% H_2/CCl_4 : 0.70sccm CCl_4; 0.12sccm H_2 (r.f. on)
 24% H_2/CCl_4 : 0.65sccm CCl_4; 0.21sccm H_2 (r.f. on)
 30% H_2/CCl_4 : 0.61sccm CCl_4; 0.26sccm H_2 (r.f. on)

Electron energy: 70eV; Gain: 30.

Table:20. Addtion of Argon to CCl_4 Plasma* at 70eV and 150W.

ION	MASS (amu)	100% CCl_4 Gas (mm)	100% CCl_4 Plasma (mm)	50% Ar in CCl_4 gas(mm)	50% Ar in CCl_4 Plasma (mm)
C^+	12	120	60	80	36
H_2O^+	18	45	70	75	85
C_2^+	24	---	10	10	8
Al^+	27	---	---	---	8
$N_2^+;CO^+$	28	12	115	15	65
Cl^+	35	450	315	320	198
HCl^+	36	75	410	130	309
Ar^+	40	---	---	585	570
CO_2^+	44	5	10	15	15
CCl^+	47	465	220	315	129
C_2Cl^+	59	25	40	20	21
$AlCl^+$	62	---	---	---	2
$COCl^+$	63	---	---	---	3
Cl_2^+	70	15	190	12	151
CCl_2^+	82	335	125	235	80
$C_2Cl_2^+$	94	---	80	---	48
$C_3Cl_2^+$	106	---	---	---	2
CCl_3^+	117	900	335	650	214
$C_2Cl_3^+$	129	---	25	---	9
$C_3Cl_3^+$	141	---	---	---	2
$C_2Cl_4^+$	164	---	20	---	6
$C_2Cl_5^+$	199	---	10	---	---

*Plasma Conditions for table: 20, were:-

Pressure : 0.10 torr total
Power: : 13.56MHz; 150W(F), ~40W(R)
Flow rates:-
100% CCl_4 : 0.72sccm (r.f. off)
100% CCl_4 : 0.64sccm (r.f. on)
 50% CCl_4/Ar : 0.44sccm CCl_4; 0.44sccm Ar (r.f. off)
 50% CCl_4/Ar : 0.44sccm CCl_4; 0.44sccm Ar (r.f. on)

Electron energy:- 70eV; Gain 30.

4.3   Other Gases

SiCl$_4$ and CFCl$_3$ gases and plasmas were sampled into the mass spectrometer and the results are shown in tables: 21 and 22. The addition of oxygen to CFCl$_3$ plasmas was also briefly investigated and the results are presented in table:23.

Table:21. $SiCl_4$ Gas and Plasma[*] at 70 and 20eV

ION	MASS	$SiCl_4$ Gas @ 70eV, (mm)	$SiCl_4$ Plasma @ 70eV, (mm)	$SiCl_4$ Gas @ 20eV, (mm)	$SiCl_4$ Plasma @ 20eV, (mm)
C^+	12	2	1	---	---
H_2O^+	18	6	12	---	1
$N_2^+; Si^+$	28	171	194	1	2
SiH_4^+	32	12	18	---	---
Cl^+	35	298	348	5	1
HCl^+	36	61	131	---	20
CO_2^+	44	1	2	---	---
$SiCl^+$	63	363	489	---	---
Cl_2^+	70	9	21	---	3
$SiCl_2^+$	98	86	88	---	1
$SiCl_3^+$	133	451	654	140	116
$SiCl_4^+$	168	202	204	59	47

[*]Plasma conditions were:-

0.10 torr $SiCl_4$ gas;   50W(F), ∼8W(R);   13.56MHz

Flow Rates: 0.93 sccm (r.f. off)

0.79 sccm (r.f. on)

Table:22. $CFCl_3$ Gas and Plasma[*] at 70 and 20eV.

ION	MASS	$CFCl_3$ Gas @ 70eV, int (mm)	$CFCl_3$ Plasma @ 70eV, int (mm)	$CFCl_3$ Gas @ 20eV, int (mm)	$CFCl_3$ Plasma @ 20eV, int (mm)
C^+	12	61	23	---	---
H_2O^+	18	11	14	---	1
F^+	19	18	11	---	---
C_2^+	24	---	8	---	---
$N_2^+;CO^+$	28	7	61	---	3
CF^+	31	175	92	1	---
Cl^+	35	283	275	1	10
HCl^+	36	47	186	6	24
C_2F^+	43	1	3	---	---
CO_2^+	44	1	4	---	---
CCl^+	47	160	88	---	1
CF_2^+	50	18	28	---	1
C_3F^+	55	---	3	---	---
C_2Cl^+	59	1	12	---	---
$CFCl^+$	66	178	32	2	1
CF_3^+	69	---	66	---	---
Cl_2^+	70	13	443	1	80
C_2FCl^+	78	---	12	---	1
CCl_2^+	82	42	34	---	1
CF_2Cl^+	85	2	109	---	14
C_3FCl^+	90	---	2	---	---
$C_2Cl_2^+$	94	---	25	---	2
$CFCl_2^+$	101	769	168	207	33
$C_3F_2Cl^+$	109	---	2	---	---

Table:22. $CFCl_3$ Gas and Plasma* at 70 and 20eV.   contd.

ION	MASS	$CFCl_3$ Gas @ 70eV, int (mm)	$CFCl_3$ Plasma @ 70eV, int (mm)	$CFCl_3$ Gas @ 20eV, int (mm)	$CFCl_3$ Plasma @ 20eV, int (mm)
$C_2FCl_2^+$	113	---	7	---	--1
CCl_3^+	117	13	60	2	14
$C_2Cl_3^+$	129	---	8	---	1
$C_2F_2Cl_3^+$	132	---	4	---	1
$C_2F_4Cl^+$	135	---	6	---	1
$C_2FCl_3^+$	148	---	6	---	2
$C_2F_3Cl_2^+$	151	---	6	---	2
$C_2Cl_4^+$	164	---	5	---	2
$C_2F_2Cl_3^+$	167	---	4	---	2
$C_3F_2Cl_3^+$	179	---	---	---	1
$C_2FCl_4^+$	183	---	2	---	2

*Plasma conditions for table:22, were:-

0.10 torr $CFCl_3$ gas; 50W(F) $\approx$ 8W(R) @ 13.56MHz.

Flow rates:-   0.74sccm (r.f. off)

                0.61sccm (r.f. on)

Table:23. Addition of Oxygen to $CFCl_3$ Plasmas[*] at 50W and 20eV

ION	MASS	$CFCl_3$ 70eV GAS	$CFCl_3$ 20eV GAS	$CFCl_3$ 20eV PLASMA	$CFCl_3$ 11% O_2 PLASMA 20eV	$CFCl_3$ 16% O_2 PLASMA 20eV	$CFCl_3$ 19% O_2 PLASMA 20eV	$CFCl_3$ 25% O_2 PLASMA 20eV	$CFCl_3$ 29% O_2 PLASMA 20eV	$CFCl_3$ 35% O_2 PLASMA 20eV
C^+	12	90	1	1	---	---	---	---	---	---
H_2O^+	18	15	1	1	---	---	---	---	---	---
F^+	19	---	1	1	---	---	---	---	---	---
$CO^+;N_2^+$	28	---	---	2	9	13	16	17	17	17
CF^+	31	237	1	1	---	1	---	---	---	---
O_2^+	32	---	---	---	1	1	1	1	1	1
Cl^+	35	377	1	9	9	9	9	9	10	9
HCl^+	36	47	6	12	13	14	15	15	15	14
CO_2^+	44	---	---	---	1	1	1	1	1	1
CCl^+	47	210	---	1	1	2	2	2	2	1
CF_2^+	50	15	---	1	1	1	1	1	1	1
$CFCl^+$	66	210	2	1	1	1	1	1	1	1
CF_3^+	69	---	---	6	6	6	6	7	6	6
Cl_2^+	70	8	1	52	64	68	71	71	73	71
CCl_2^+	82	40	---	1	1	1	1	1	1	1
CF_2Cl^+	85	---	---	13	10	9	9	8	7	5
$C_2Cl_2^+$	94	---	---	1	1	1	1	1	1	---
$CFCl_2^+$	101	747	215	29	17	16	15	12	11	7
CCl_3^+	117	8	3	13	10	9	9	6	5	4
$C_2Cl_3^+$	129	---	---	1	1	1	1	---	---	---
$C_2FCl_3^+$	148	---	---	1	1	1	1	---	---	---

Table:23.   Addition of Oxygen to $CFCl_3$ Plasmas* at 50W and 20eV   contd.

ION	MASS	CFCl₃ 70eV GAS	CFCl₃ 20eV GAS	CFCl₃ 20eV PLASMA	CFCl₃ 11% O₂ PLASMA 20eV	CFCl₃ 16% O₂ PLASMA 20eV	CFCl₃ 19% O₂ PLASMA 20eV	CFCl₃ 25% O₂ PLASMA 20eV	CFCl₃ 29% O₂ PLASMA 20eV	CFCl₃ 35% O₂ PLASMA 20eV
$C_2F_3Cl_2^+$	151	---	---	2	1	1	1	---	---	---
$C_2Cl_4^+$	164	---	---	2	1	1	1	1	---	---
$C_2F_2Cl_3^+$	167	---	---	1	1	1	---	---	---	---
$C_2FCl_4^+$	183	---	---	1	1	1	1	1	---	---
$C_2Cl_5^+$	199	---	---	1	---	---	---	---	---	---

*Plasma Conditions for Table:23 were:-

Pressure: 0.10 torr total

Power: 50W(F), $\approx$ 8W(R) @ 13.56MHz

Flow Rates:-

100% $CFCl_3$ r.f. off : 1.20 sccm

100% $CFCl_3$ r.f. on : 0.90 sccm

11% O_2 in $CFCl_3$ r.f. on : 0.80 sccm $CFCl_3$; 0.10 sccm O_2

16% O_2 in $CFCl_3$ r.f. on : 0.73 sccm $CFCl_3$; 0.14 sccm O_2

19% O_2 in $CFCl_3$ r.f. on : 0.68 sccm $CFCl_3$; 0.16 sccm O_2

25% O_2 in $CFCl_3$ r.f. on : 0.59 sccm $CFCl_3$; 0.20 sccm O_2

29% O_2 in $CFCl_3$ r.f. on : 0.54 sccm $CFCl_3$; 0.22 sccm O_2

35% O_2 in $CFCl_3$ r.f. on : 0.43 sccm $CFCl_3$; 0.23 sccm O_2

Electron energies: 70eV and 20eV; Gain: 30.

4.4   Etching and Etch Rates

Several conventional etching experiments were carried out using CCl_4, $CFCl_3$ and $SiCl_4$ plasmas on photoresist patterned wafers of silicon and silicon with $4000\mathring{A}$ of SiO_2 deposited on the surface. Table:24, shows the etch rate results for various plasmas of CCl_4 and $CFCl_3$. These results were obtained by etching the patterned wafers for 15 minutes in the reactor used for the mass spectrometric work.

The etch rate for 0.15torr CCl_4 plasma on silicon at 100W(F) had to be obtained from S.E.M. photographs. The usual method involving the optical microscope and interference fringes was unsuitable because the profiles of the etched features were sloping and the etched surfaces were extremely rough fig:31. Figures 32-34, show details of silicon features etched in 0.15torr $CFCl_3$ plasma. These scanning electron microscope photographs were obtained from a Jeol type S.E.M.

Table: 24.   Etch Rates

Material	Etchant	Power (Watts) (F)	(R)	Pressure (torr)	Flow rate (sccm)	Etch rate ($\overset{o}{A}\,min^{-1}$)	After Etch resistance (Ω)
Si	CCl_4	50	8	0.10	0.78	126	6
Si	CCl_4	50	8	0.15	1.20	117	20
Si	$CFCl_3$	50	8	0.10	0.54	95	12
Si	$CFCl_3$	50	8	0.15	1.49	217	8
SiO_2	$CFCl_3$	50	8	0.10	0.70	43	∞
Si	$CFCl_3$	100	20	0.15	1.66	398	10
Si	CCl_4	100	20	0.15	1.18	1000[*]	10

[*]Measured from the S.E.M. photograph.

129

Fig.31. Si etched in CCl_4 plasma.
129(a)
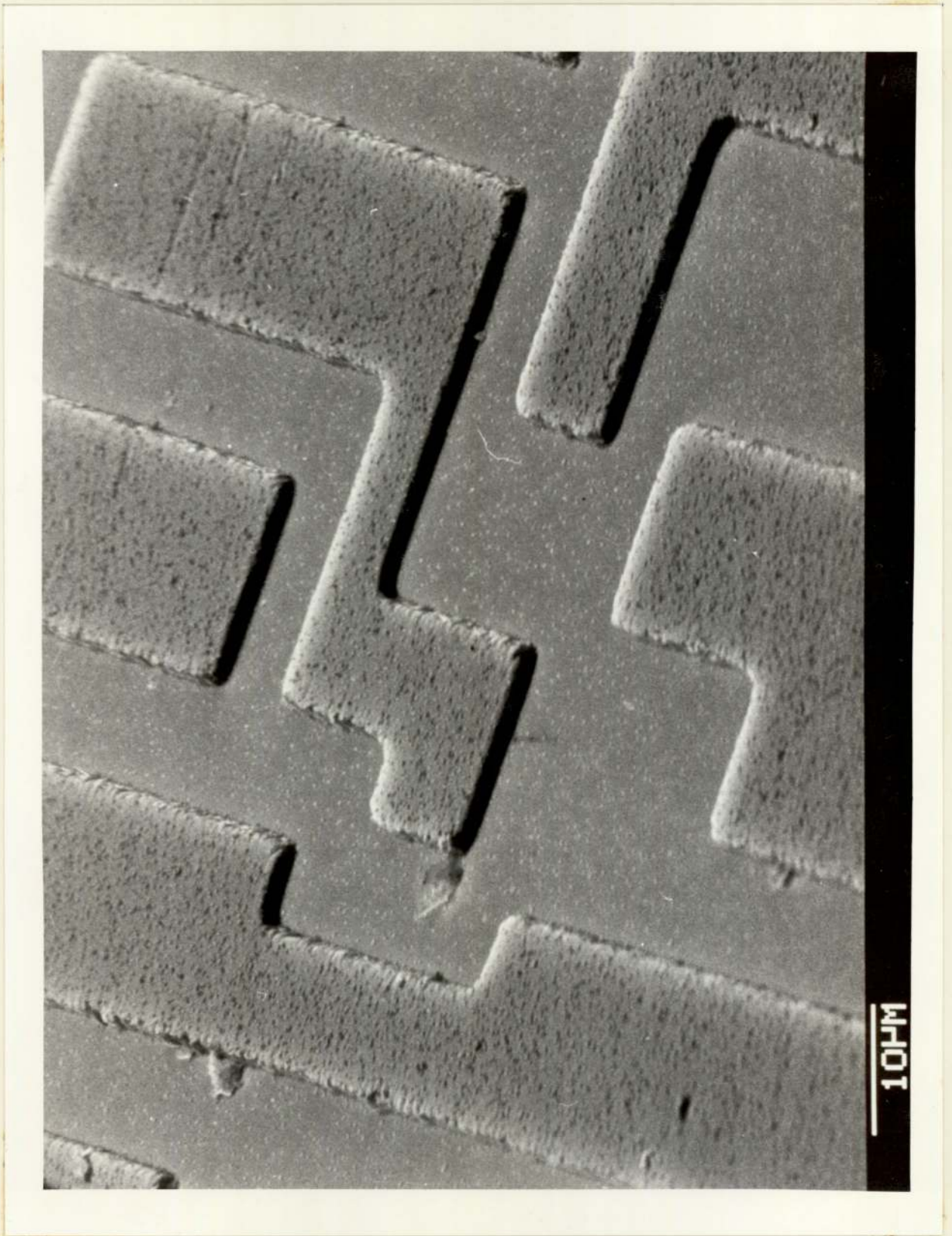
Fig.32. Si etched in CFCl₃ plasma.
129(b)
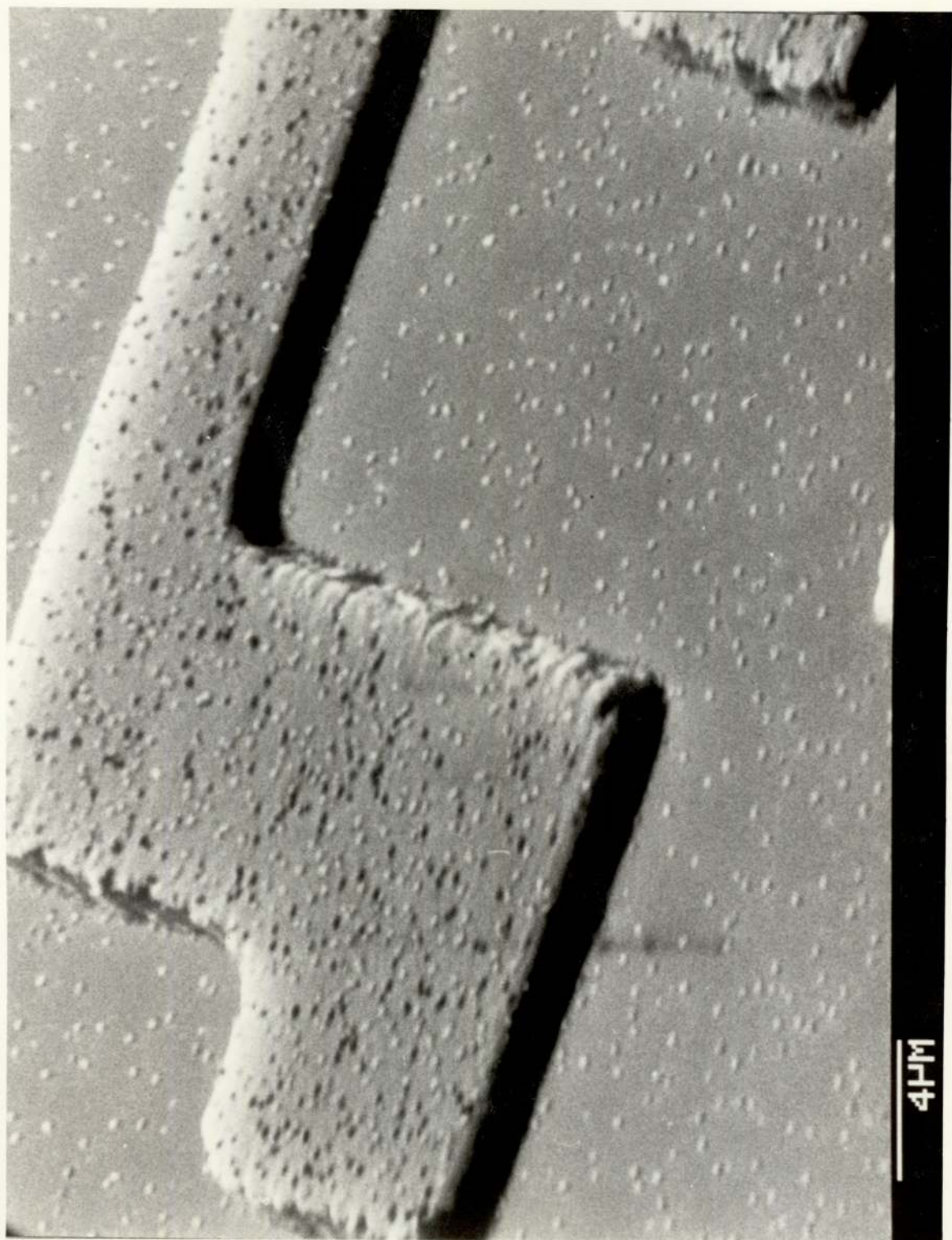
Fig.33. Si etched in CFCl₃ plasma.

129(c)
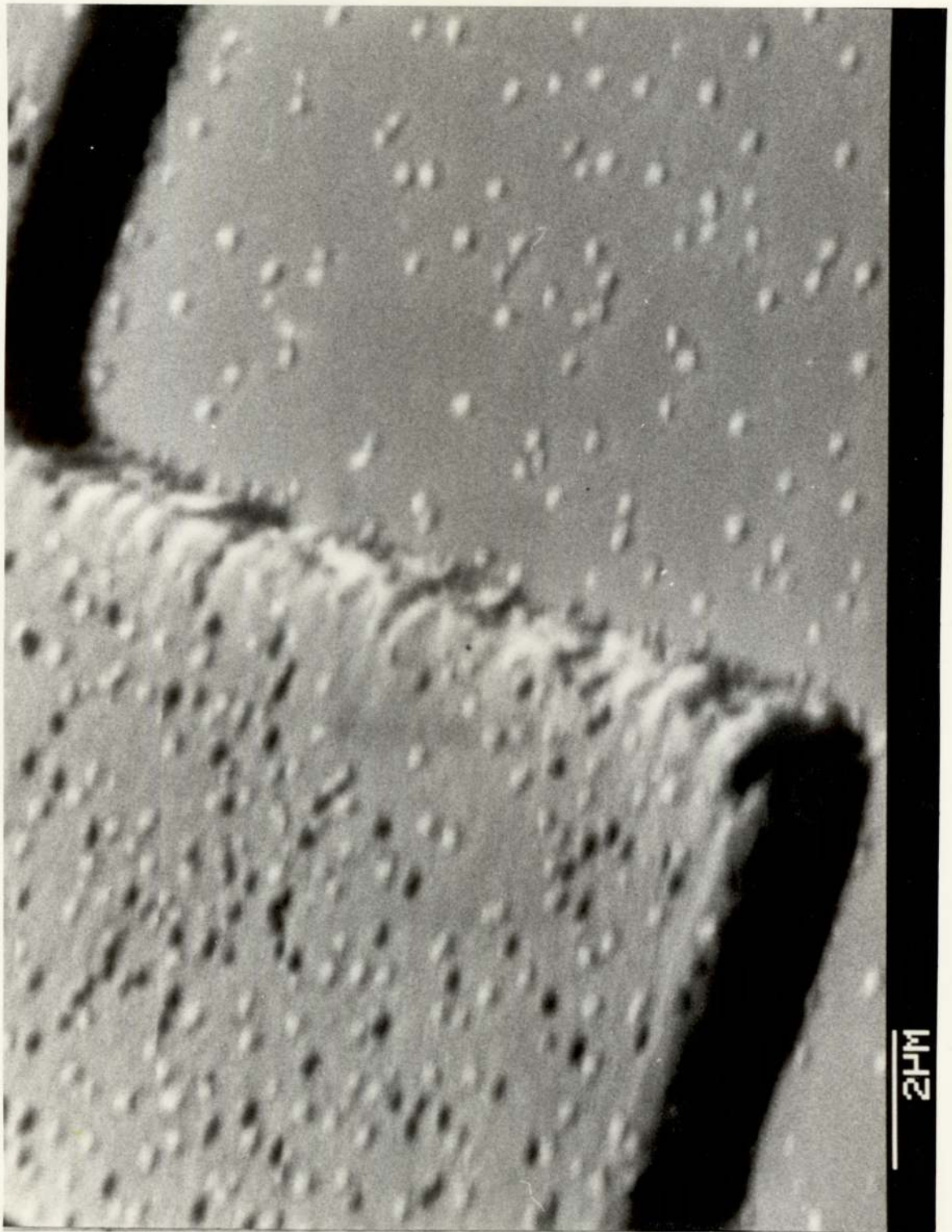
Fig.34. Si etched in CFCl$_3$ plasma.

129(d)

4.5   Silicon Etching in CCl$_4$ Plasmas

The results of sampling plasmas etching plain silicon wafers at 50W and 100W of r.f. power are shown in tables: 25 and 26. The plasma ignition transients for Cl$_2^+$, SiCl$_4^+$, SiCl$_3^+$, CCl$_3^+$, C$_2$Cl$_4^+$ and C$_2$Cl$_3^+$ ions are shown in figs: 35-41. These transients were observed to see if any of the ions showed similar transients or could in any way be correlated with the SiCl$_3^+$ and SiCl$_4^+$ ion transients.

The plasma conditions for Figs: 39-41, were:

Pressure: 0.10 torr CCl$_4$ gas

Power: 50W(F), ~8W(R) @ 13.56MHz.

Electron energy: 70eV; Gain: 30.

Flow rates:-

Fig: 39;   0.82sccm CCl$_4$ (r.f. off) ⎱   CCl$_3^+$
     0.64sccm CCl$_4$ (r.f. on) ⎰

Fig: 40;   0.82sccm CCl$_4$ (r.f. off) ⎱   C$_2$Cl$_4^+$
     0.66sccm CCl$_4$ (r.f. on) ⎰

Fig: 41;   0.88sccm CCl$_4$ (r.f. off) ⎱   C$_2$Cl$_3^+$
     0.73sccm CCl$_4$ (r.f. on) ⎰

Table:25.   Etching Silicon in CCl$_4$ Plasmas* at 50W and 100W.

ION	MASS	CCl$_4$ GAS 70eV(mm)	CCl$_4$ PLASMA 70eV(mm)50W	CCl$_4$ PLASMA on Si at 50W; 70eV (mm)	CCl$_4$ PLASMA on Si at 100W; 70eV (mm)
C$^+$	12	120	90	69	62
H$_2$O$^+$	18	75	66	85	88
C$_2^+$	24	---	21	16	14
CO;$^+$Si$^+$	28	25	105	75	55
Cl$^+$	35	470	594	369	360
HCl$^+$	36	100	550	360	348
CO$_2^+$	44	10	9	18	19
CCl$^+$	47	480	363	270	258
C$_2$Cl$^+$	59	30	60	50	46
AlCl$^+$	62	---	---	2	4
SiCl$^+$	63	---	---	20	21
Cl$_2^+$	70	15	420	192	204
CCl$_2^+$	82	360	222	186	170
C$_2$Cl$_2^+$ ⎫	94;96;	---	114	100; 69;	96; 62;
SiCl$_2^+$ ⎭	98;100;102	---	---	19; 3; 1	15; 5; 2
C$_3$Cl$_2^+$	106	---	3	3	5
CCl$_3^+$	117	1000	588	513	469
C$_2$Cl$_3^+$ ⎫	129; 131;	---	57	45; 43;	35; 33;
SiCl$_3^+$ ⎭	133;135;137	---	---	47; 30; 11	46; 35; 12
C$_3$Cl$_3^+$	141	---	12	3	5
C$_2$Cl$_4^+$ ⎫	164; 166	---	44	33; 41;	24; 30;
SiCl$_4^+$ ⎭	168;170;172	---	---	29; 35; 15	22; 29; 14
C$_2$Cl$_5^+$	199	---	7	3	2

The plasma conditons for table:25, were:-

Pressure: 0.10 torr CCl$_4$; Gain: 30; Electron Energy: 70eV

Power: 50W(F), ∿ 8W(R) and 100W(F), ∿ 20W(R)

Flow rates: r.f. off: 1.10sccm CCl$_4$ gas
r.f. on (no silicon present) 1.00sccm CCl$_4$ gas.
r.f. on (with silicon) 1.04sccm CCl$_4$ @ 50W(F)
r.f. on (with silicon) 1.05sccm CCl$_4$ @ 100W(F)

N.B. Brackets show overlap of C$_2$Cl$_x^+$ and SiCl$_x^+$ ions.

Table:26.   Etching Silicon in CCl_4 Plasmas* at 100W.

ION	MASS	CCl_4 GAS 70eV (mm)	CCl_4 PLASMA 70eV (mm)	CCl_4 PLASMA on Si 70eV (mm)	CCl_4 PLASMA on Si 20eV (mm)
C^+	12	110	78	57	---
H_2O^+	18	40	72	59	54
C_2^+	24	---	18	15	---
$CO;^+Si^+$	28	30	186	295	48
Cl^+	35	410	558	355	45
HCl^+	36	90	672	550	429
CO_2^+	44	10	12	20	8
CCl^+	47	430	276	191	36
C_2Cl^+	59	32	48	40	6
$AlCl^+$	62	---	18	4	---
$SiCl^+$	63	---	---	52	11
Cl_2^+	70	15	429	150	158
CCl_2^+	82	309	162	115	57
$C_2Cl_2^+$⎫	94;96;	---	108	89; 57;	51; 33;
$SiCl_2^+$⎭	98;100;102	---	---	19; 8; 2	11; 5; 1
$C_3Cl_2^+$	106	---	2	4	---
CCl_3^+	117	960	414	300	372
$C_2Cl_3^+$⎫	129; 131;	---	42	29; 28;	17; 15;
$SiCl_3^+$⎭	133;135;137	---	---	106; 96; 32	62; 54; 18
$C_3Cl_3^+$	141	---	8	5	2
$C_2Cl_4^+$⎫	164; 166	---	33	22; 27;	15; 20;
$SiCl_4^+$⎭	168;170;172	---	---	40; 38; 17	27; 26; 10
$C_2Cl_5^+$	199	---	4	2	2

Plasma conditions of table: 26, were:-

Pressure: 0.10 torr

Power: 100W(F), $\sim$20W(R)

Flow rates: 1.16 sccm CCl_4 r.f. off.
                0.78 sccm CCl_4 r.f. on.

Electron energy: 70eV and 20eV; Gain 30.

SiCl$_3^+$ switch-on transient monitoring in 0.10 torr CCl$_4$ plasma.

R.f. power: 13.56 MHz; 50W(F), ~8W(R).

Flow rate: 0.86 sccm(r.f. off)
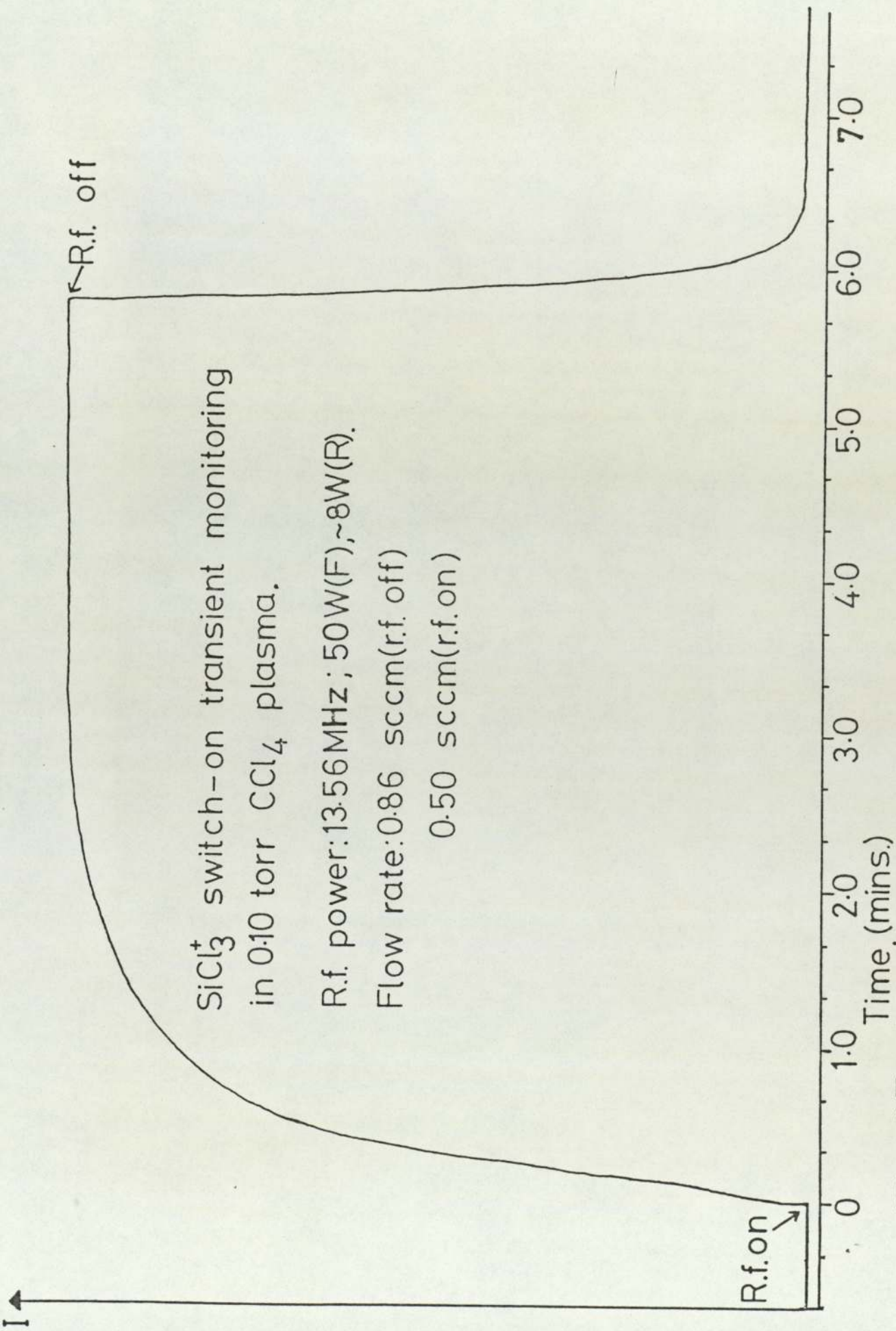
0.50 sccm(r.f. on)

Fig.35. SiCl$_3^+$ transient monitoring.
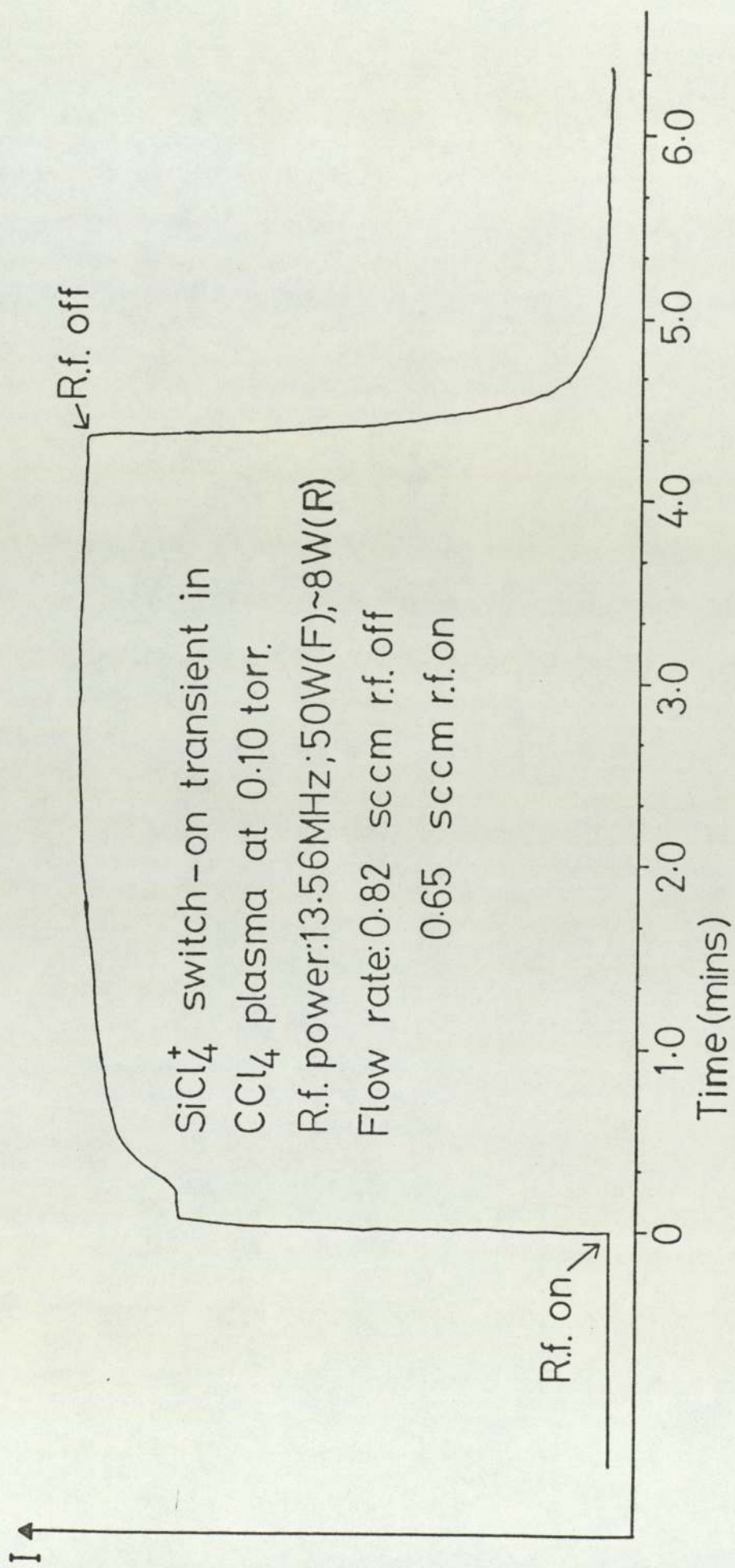
Fig.36. SiCl₄⁺ transient monitoring.

SiCl$_4^+$ switch-on transient in
CCl$_4$ plasma at 0.10 torr.
R.f. power:13.56MHz;50W(F),~8W(R)
Flow rate:0.82 sccm r.f. off
0.65 sccm r.f. on

R.f. off

R.f. on

I

Time (mins)

0   1.0   2.0   3.0   4.0   5.0   6.0

'Dirty wafer' effect monitoring $SiCl_4^+$ in CCl_4 plasma at 0.10 torr.

R.f. power: 13.56 MHz; 50W(F), ~8W(R).

Flow rate: 0.86 sccm (r.f. off)
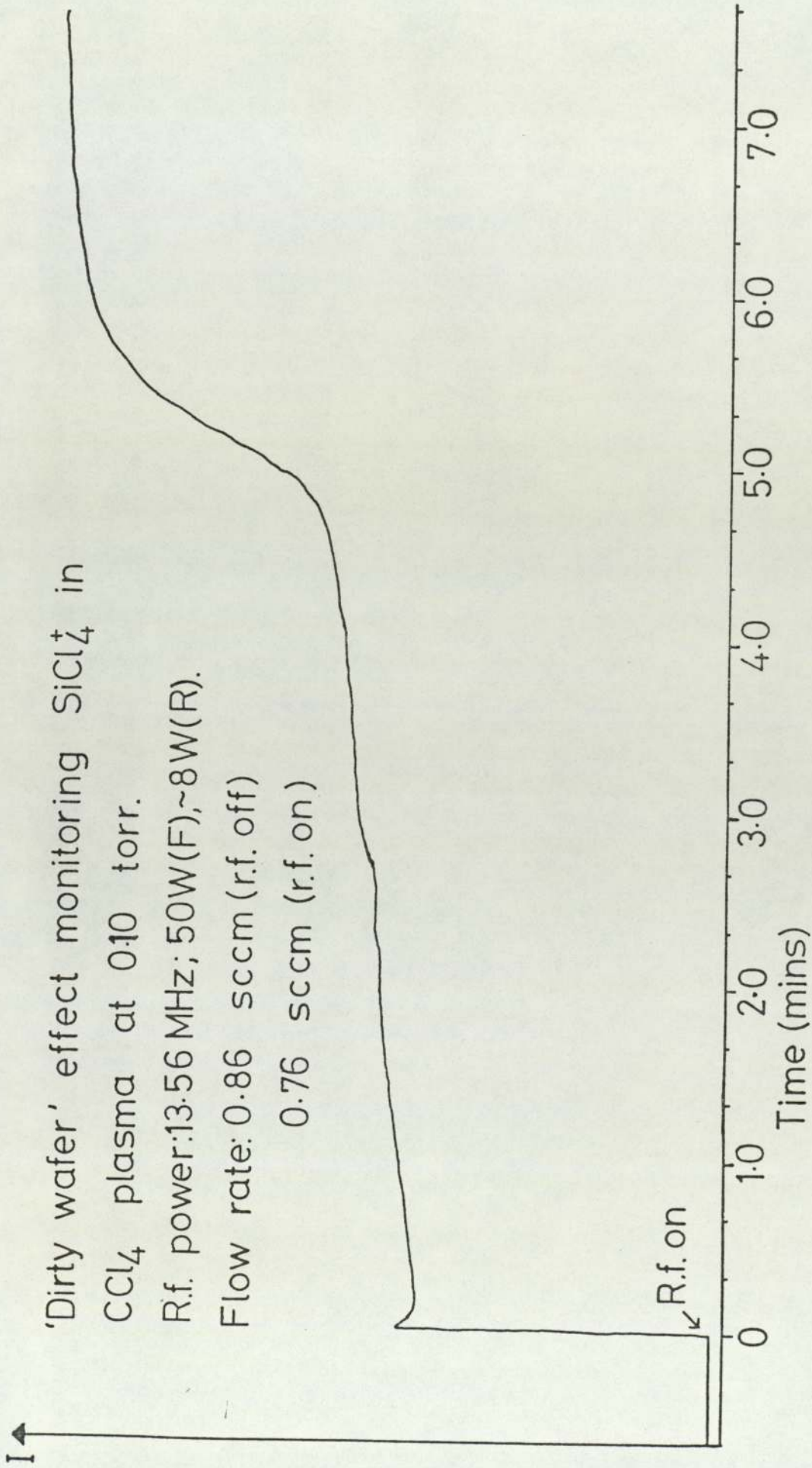
0.76 sccm (r.f. on)

Fig. 37. $SiCl_4^+$ monitoring.

132(c)

Cl_2^+ switch–on transient in 0.10 torr CCl_4 plasma.

Power:13.56 MHz; 50W(F),~8W(R).

Flow rate:0.82 sccm r.f. off; 0.68 sccm r.f. on
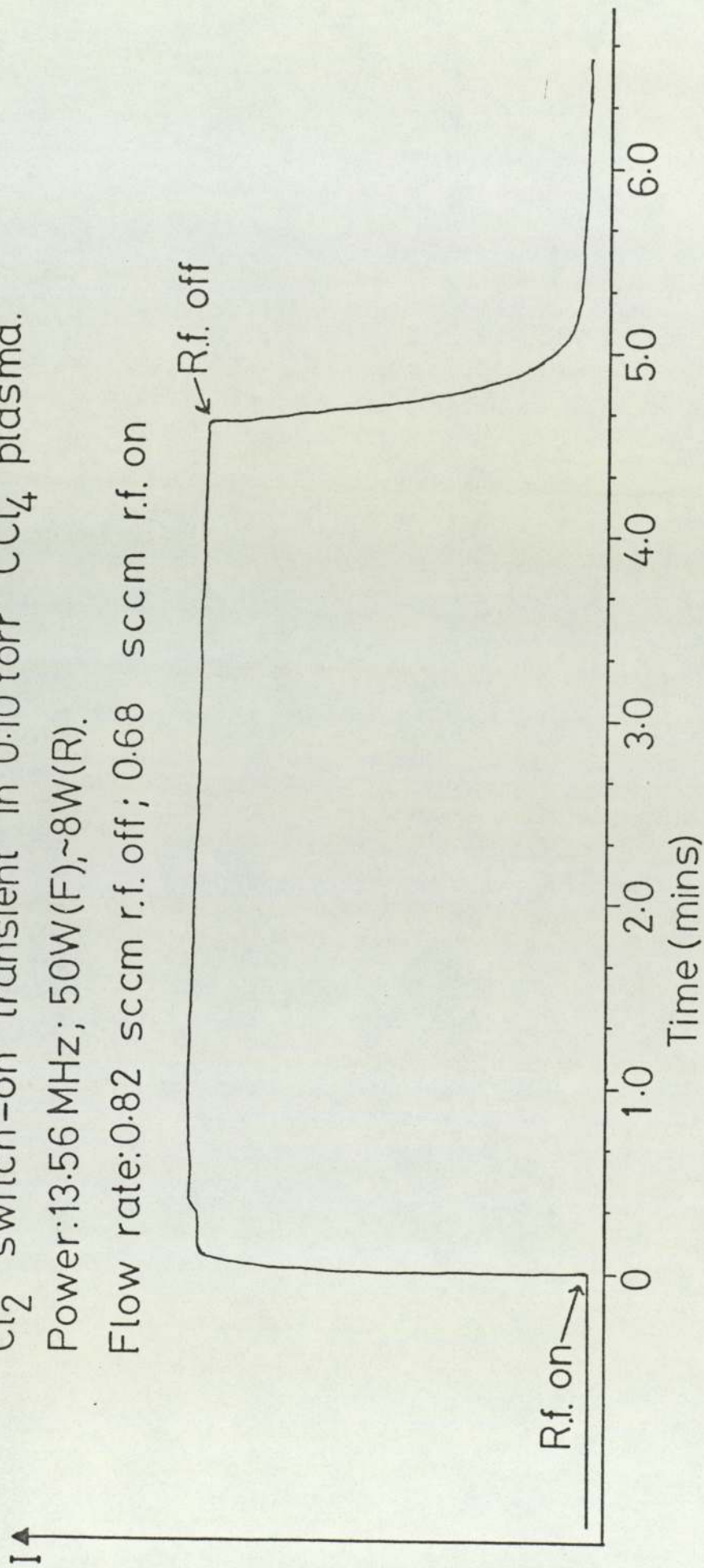
Fig.38. Cl_2^+ transient monitoring.

132(d)
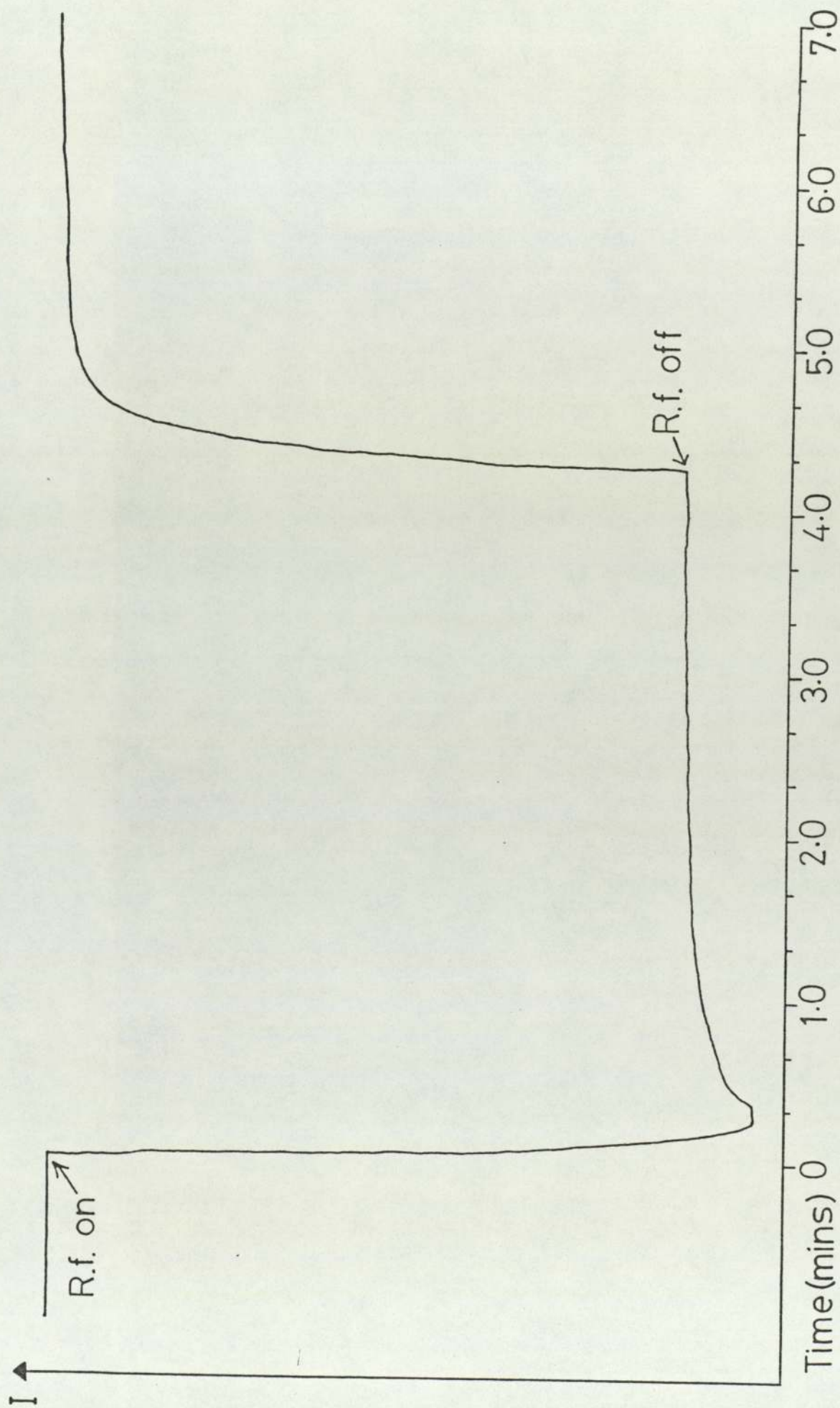
Fig.39. CCl_3^+ transient monitoring.

132(e)
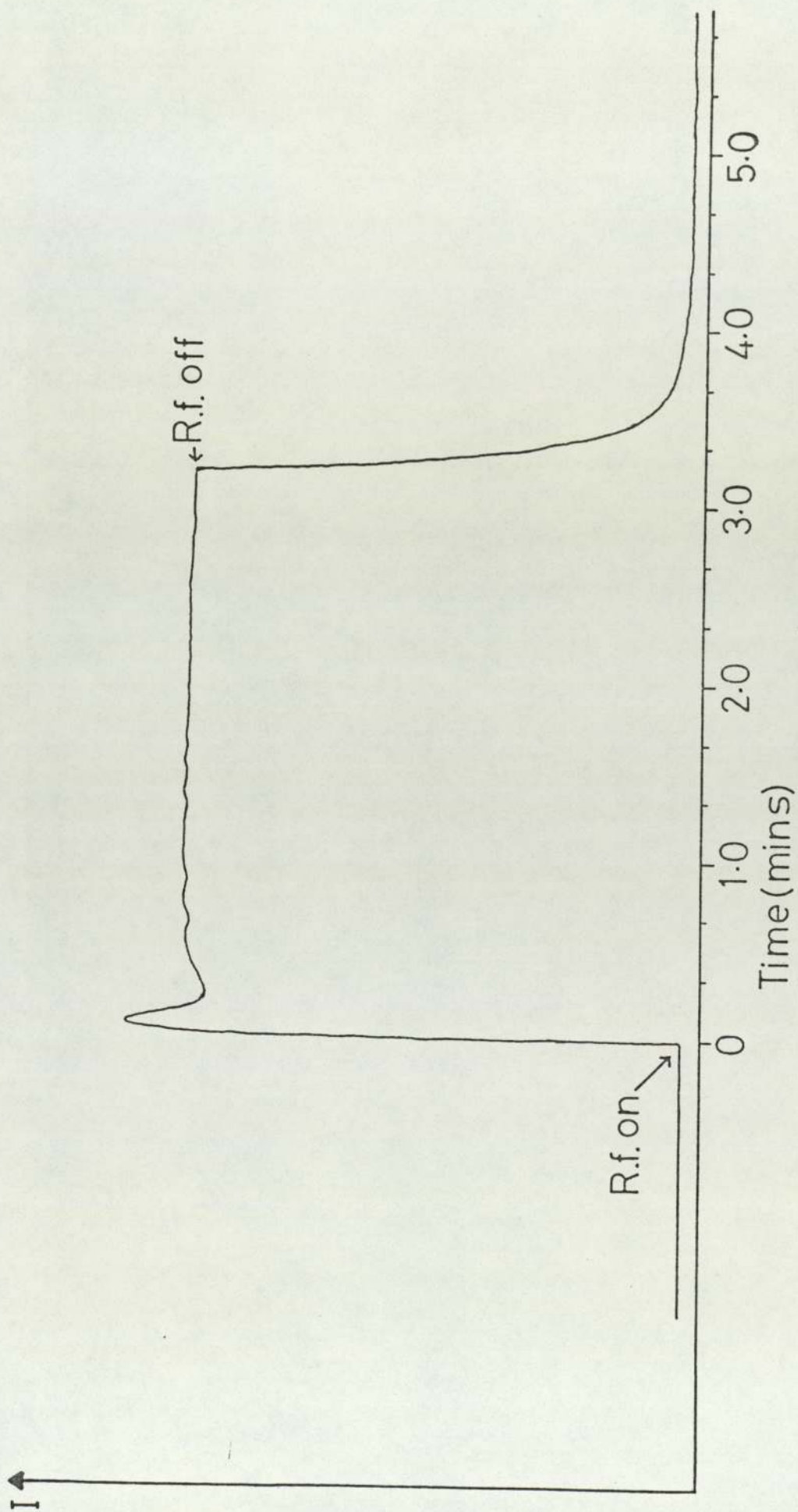
Fig.40. $C_2Cl_4^+$ transient monitoring.

132(f)
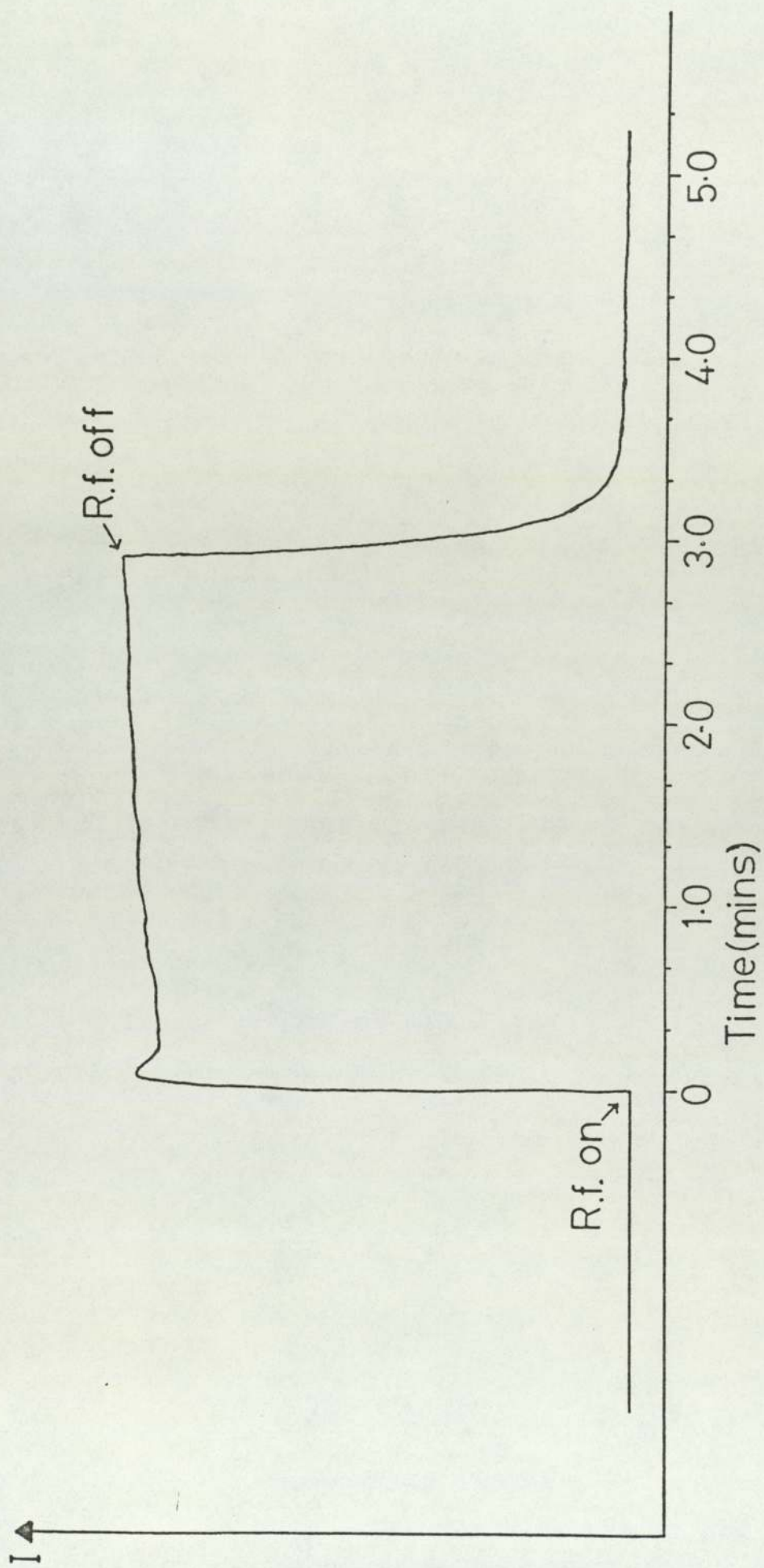
Fig. 41. $C_2Cl_3^+$ transient monitoring.

132(g)

4.5.1   Silicon Etching in CCl$_4$ - O$_2$ Plasmas

The results of addition of oxygen to CCl$_4$ plasmas at 0.10 and 0.15 torr etching silicon monitoring SiCl$_3^+$ ions are shown in tables: 27 and 28, and fig: 42. Some transients were also monitored by switching off the oxygen supply at 0.10torr fig: 43, and 0.15torr fig: 44. The difference between 0.15torr CCl$_4$ plasmas and 0.10torr CCl$_4$ plasmas is also shown in Fig: 44.

4.5.2   Silicon Etching in CCl$_4$ - Ar Plasmas

The results of addtion of argon to CCl$_4$ plasmas at 0.10torr etching silicon and monitoring SiCl$_3^+$ and SiCl$_4^+$ ions are shown in tables: 29 and 30, and Fig: 45. The argon switch-off transients were monitored using the SiCl$_3^+$ ion intensity, as before, and are shown in figs: 46 and 47.

Table: 27.   Monitoring $SiCl_3^+$ in $CCl_4 - O_2$ plasmas* at 0.10 torr.

FLOW RATES (sccm)		TOTAL FLOW	Plasma Composition		$SiCl_3^+$ intensity at
CCl_4	O_2	Rate (sccm)	% CCl_4	% O_2	70eV; 30 GAIN
0.50	---	0.50	100	---	63
0.40	0.02	0.42	95	5	60
0.39	0.02	0.42	93	7	57
0.37	0.03	0.40	92	8	55
0.34	0.06	0.40	85	15	48
0.33	0.07	0.40	82	18	45
0.32	0.09	0.41	78	22	38
0.32	0.10	0.42	76	24	36
0.31	0.12	0.43	72	28	33
0.30	0.13	0.43	70	30	29
0.27	0.14	0.41	66	34	20
0.26	0.15	0.41	63	37	16

*Plasma conditions for table: 27, were:-

Pressure: 0.10 torr total

Power: 50W(F), ∼ 8W(R) @ 13.56MHz

Flow rate: 0.86 sccm 100% CCl_4 gas (r.f. off)

0.50 sccm 100% CCl_4 gas (r.f. on)

Electron energy: 70eV;   Gain: 100;   Mass: 135 ($SiCl_3^+$)

Table: 28.　Monitoring $SiCl_3^+$ in $CCl_4 - O_2$ plasmas* at 0.15 torr.

FLOW RATES (sccm)		TOTAL FLOW	Plasma Composition		$SiCl_3^+$ intensity at
CCl_4	O_2	Rate (sccm)	% CCl_4	% O_2	70eV; 30 GAIN
#1.57	---	1.57	100	---	2
#1.13	0.12	1.25	90	10	15
#1.11	0.23	1.34	83	17	26
1.07	0.26	1.33	80	20	38
1.01	0.29	1.30	78	22	43
0.97	0.30	1.27	76	24	46
0.91	0.32	1.23	74	26	46
0.84	0.34	1.18	71	29	44
0.75	0.38	1.13	66	34	42
0.68	0.41	1.09	62	38	38
0.62	0.44	1.06	58	42	32
0.56	0.45	1.01	55	45	23

*Plasma conditions for table: 28, were:-

Pressure:　0.15 torr total pressure.

#Power:　50W(F), $\sim$ 11W(R)　others 50W(F), $\sim$ 8W(R)

Flow rate:　1.80 sccm CCl_4 (100%) gas (r.f. off)

　　　　　　1.57 sccm CCl_4 (100%) gas (r.f. on)

Electron energy: 70eV;　Gain: 100;　Mass: 135 ($SiCl_3^+$)

Key.
o 0.10 torr
□ 0.15 torr

0.15 torr

0.10 torr
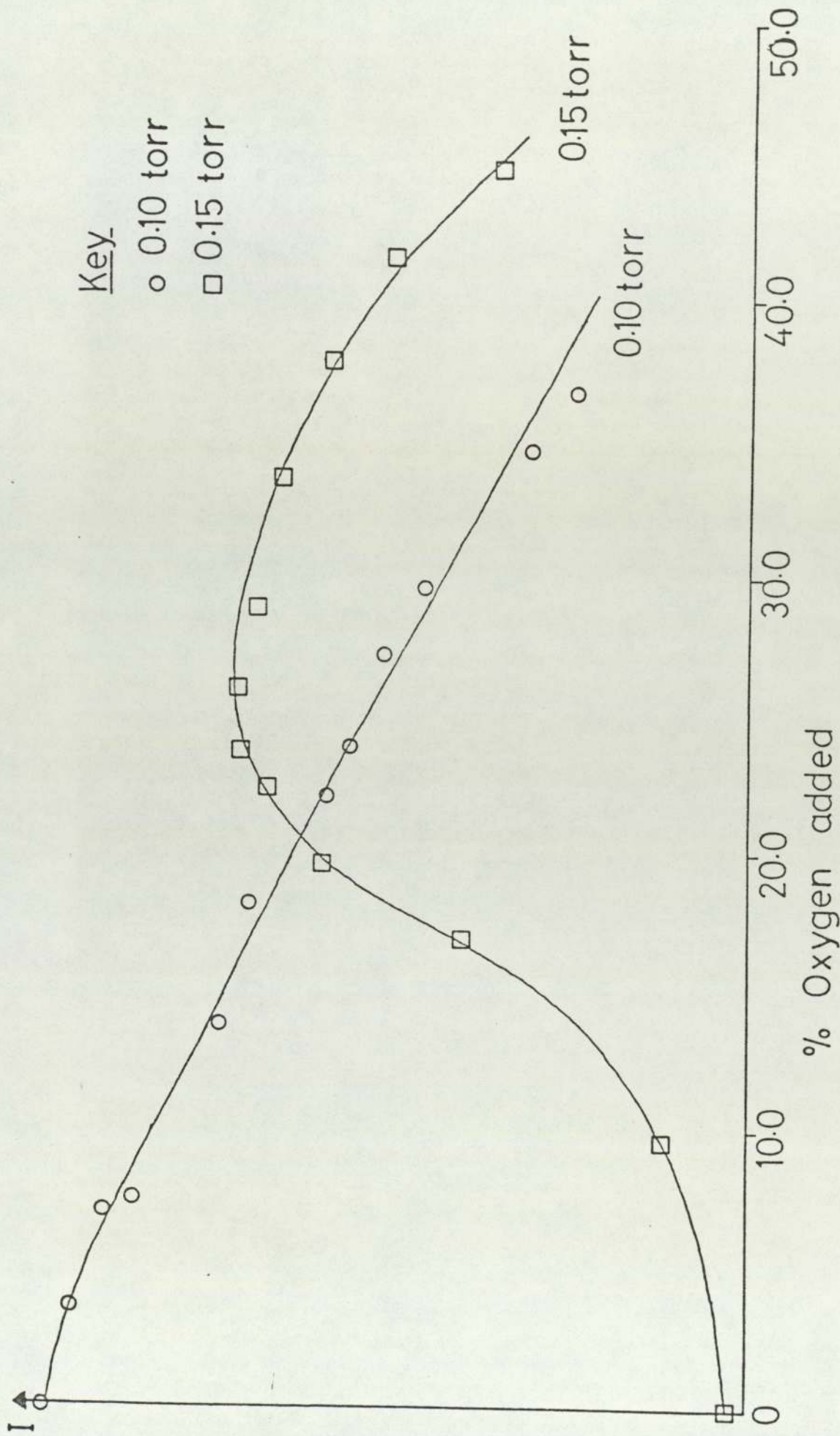
% Oxygen added

Fig.42. SiCl$_3^+$ monitoring-oxygen additions.

I

135(a)

$SiCl_3^+$ monitoring in 0.10 torr CCl_4/O_2 and CCl_4 plasmas. O_2 switched off.

O_2 off

36.6% O_2

Time(mins)
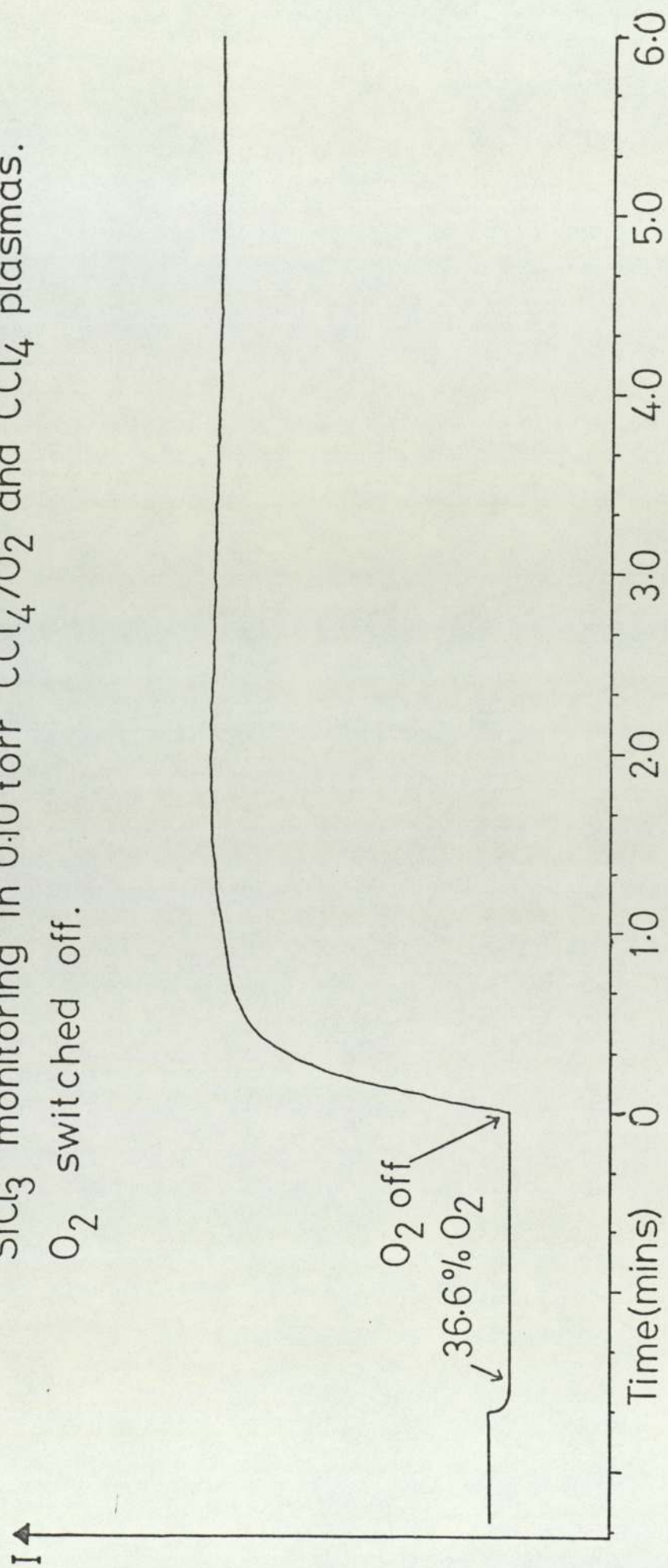
Fig.43. $SiCl_3^+ - O_2$ switch-off transient(0.10 torr).

I

135(b)

SiCl$_3^+$ monitoring in CCl$_4$/O$_2$ and CCl$_4$ plasmas

A – O$_2$ off in 0.15 torr CCl$_4$/O$_2$ plasma

B– 0.15 torr CCl$_4$ to 0.10 torr CCl$_4$ plasmas.
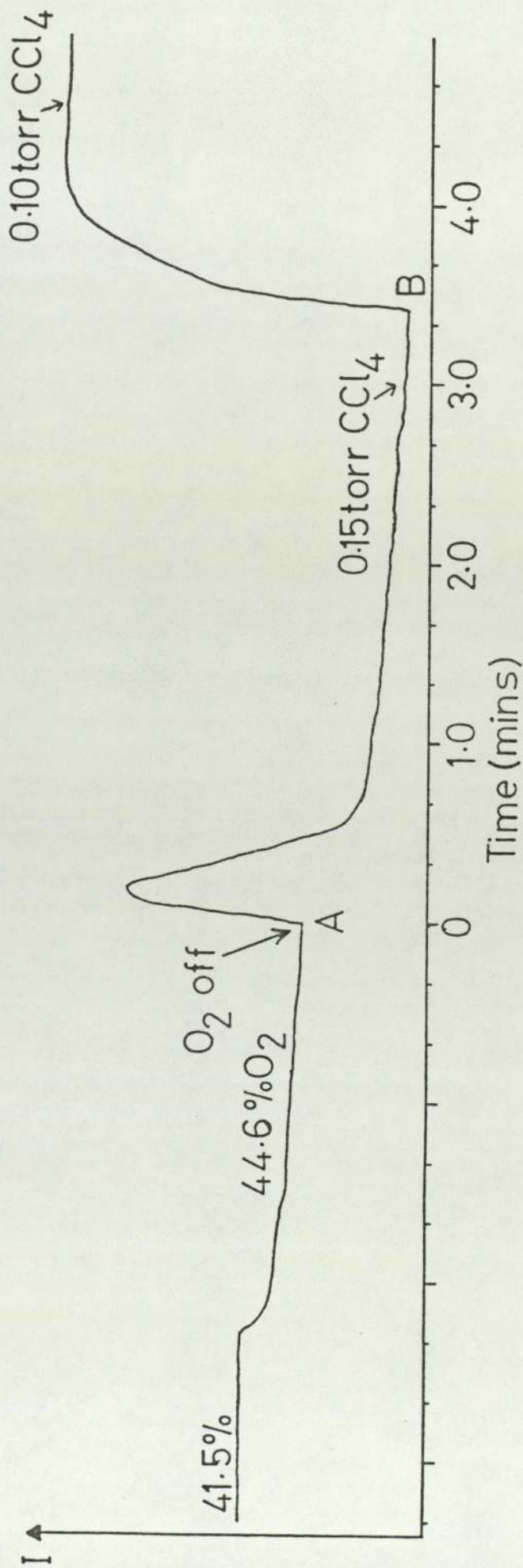
Fig. 44. SiCl$_3^+$–O$_2$ switch–off transient.

135(c)

Table: 29. Addition of Argon to CCl_4 Plasma[*] Monitoring $SiCl_3^+$ ions.

FLOW RATES (sccm)		TOTAL FLOW	Plasma Composition		$SiCl_3^+$ Intensity at
CCl_4	Ar	Rate (sccm)	% CCl_4	% Ar	70eV; 100 GAIN
0.86	---	0.86	100	---	124
0.73	0.06	0.79	92	8	124
0.71	0.08	0.79	90	10	126
0.68	0.09	0.77	88	12	128
0.69	0.10	0.79	87	13	129
0.68	0.11	0.79	86	14	131
0.65	0.13	0.78	83	17	132
0.63	0.15	0.78	81	19	133
0.62	0.17	0.79	78	22	133
0.60	0.19	0.79	76	24	132
0.58	0.20	0.78	74	26	131
0.57	0.22	0.79	72	28	133
0.56	0.23	0.79	71	29	133
0.53	0.24	0.77	69	31	131
0.52	0.26	0.78	67	33	132
0.49	0.26	0.75	66	34	134
0.50	0.28	0.78	64	36	132
0.48	0.29	0.77	62	38	133
0.46	0.30	0.76	61	39	132
0.45	0.30	0.75	60	40	131
0.44	0.31	0.75	59	41	130
0.42	0.33	0.75	56	44	129
0.40	0.34	0.74	54	46	126

Table: 29. Addition of Argon to CCl_4 Plasma[*] Monitoring $SiCl_3^+$ ions. contd.

FLOW RATES (sccm)		TOTAL FLOW	Plasma Composition		$SiCl_3^+$ Intensity at
CCl_4	Ar	Rate (sccm)	% CCl_4	% Ar	70eV; 100 GAIN
0.39	0.36	0.75	52	48	125
0.38	0.38	0.76	50	50	124
0.36	0.39	0.75	48	52	122
0.35	0.41	0.76	46	54	119
0.34	0.41	0.75	45	55	119
0.33	0.43	0.76	43	57	117
0.31	0.43	0.74	42	58	115
0.29	0.46	0.75	39	61	111
0.28	0.47	0.75	37	63	105
0.26	0.48	0.74	35	65	99

Plasma conditions fo table:29, were:-

Pressure: 0.10 torr total.

Power: 50W(F), ∿ 8W(R)   @ 13.56MHz.

Flow Rate: 1.01sccm CCl_4 (100%) gas (r.f. off)
           0.86sccm CCl_4 (100%) gas (r.f. on)

Electron energy: 70eV; Gain: 100; Mass: 135 a.m.u.

Table: 30. Addition of Argon to CCl_4 Plasma* Monitoring $SiCl_4^+$ ions.

FLOW RATES (sccm)		TOTAL FLOW	Plasma Composition		$SiCl_4^+$ intensity at
CCl_4	Ar	Rate (sccm)	% CCl_4	% Ar	70eV; 100 GAIN (mm)
0.92	---	0.92	---	---	110
0.77	0.06	0.83	93	7	103
0.73	0.10	0.83	88	12	102
0.71	0.12	0.83	86	14	100
0.70	0.14	0.84	83	17	98
0.67	0.16	0.83	81	19	96
0.66	0.18	0.84	79	21	94
0.65	0.19	0.84	77	23	92
0.63	0.21	0.84	75	25	90
0.62	0.22	0.84	74	26	89
0.61	0.23	0.84	73	27	87
0.59	0.24	0.83	71	29	86
0.57	0.25	0.82	70	30	84
0.56	0.28	0.84	67	33	79
0.54	0.30	0.84	64	36	77

Plasma conditions for table: 30, were:-

Pressure: 0.10 torr total.

Power: 50W(F), $\sim$ 8W(R) @ 13.56MHz

Flow rate: 1.01sccm 100% CCl_4 gas (r.f. off)

0.92sccm 100% CCl_4 gas (r.f. on)

Electron energy: 70eV; Gain: 100; Mass: 172 ($SiCl_4^+$)

Monitoring $SiCl_3^+$ and $SiCl_4^+$ in CCl_4/Ar plasmas.

o – $SiCl_3^+$
□ – $SiCl_4^+$
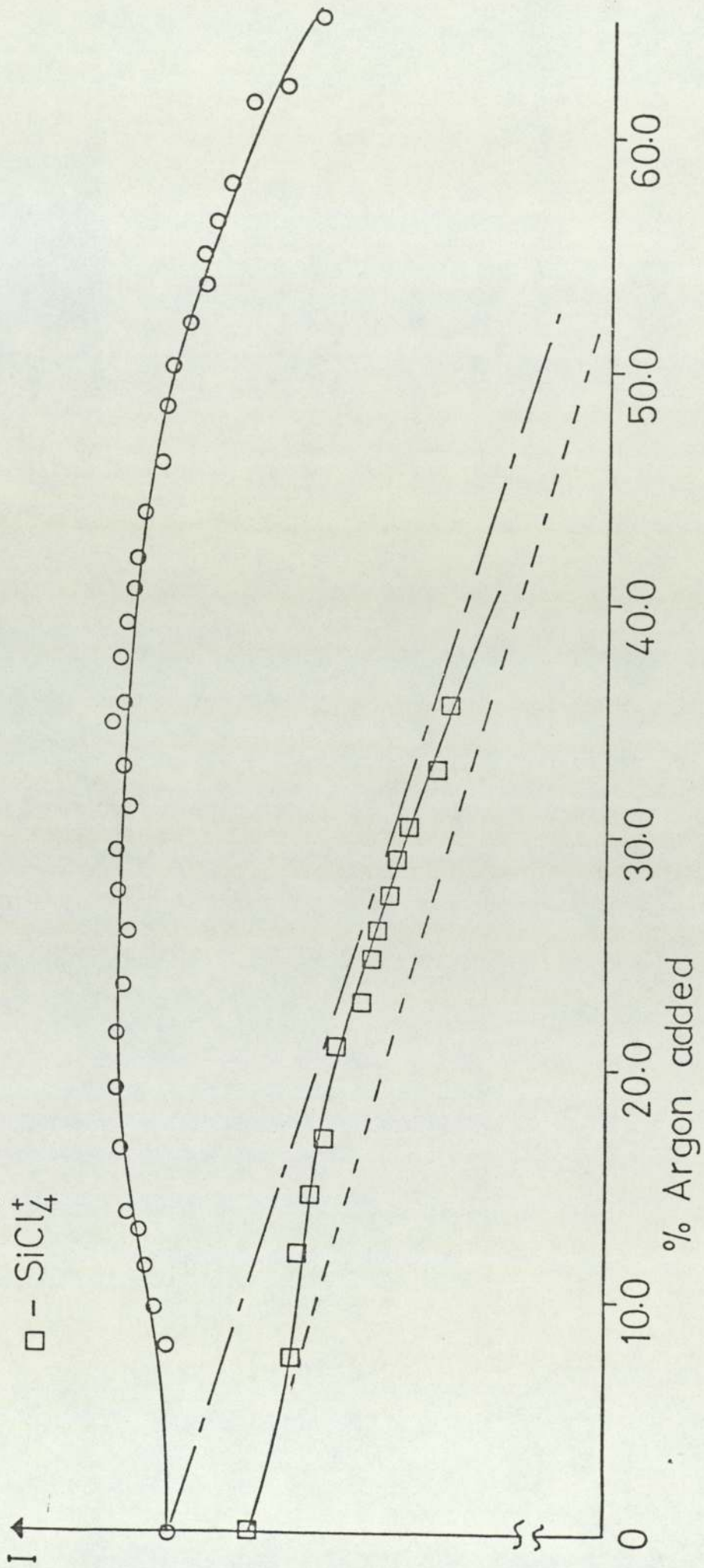
% Argon added

Fig. 45. Argon additions to CCl_4 plasmas.

138(a)

SiCl$_3^+$ monitoring in CCl$_4$/Ar plasmas at 0.10 torr.
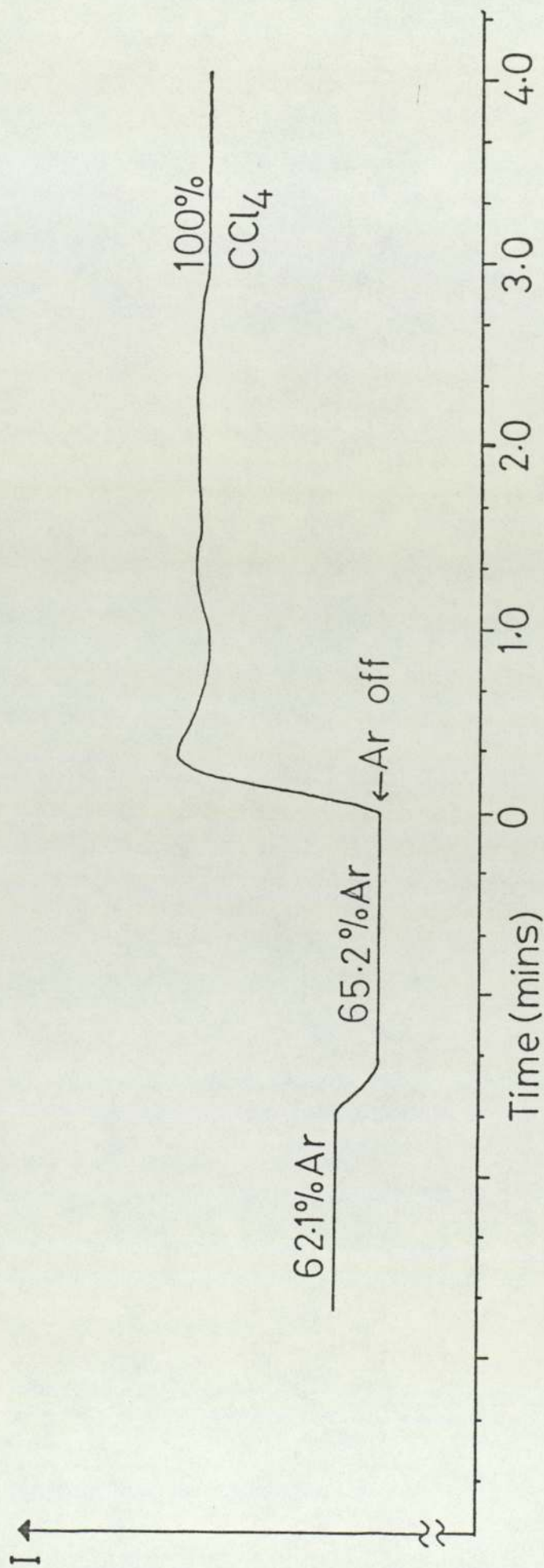
Fig.46. Argon switch-off transient.

138(b)
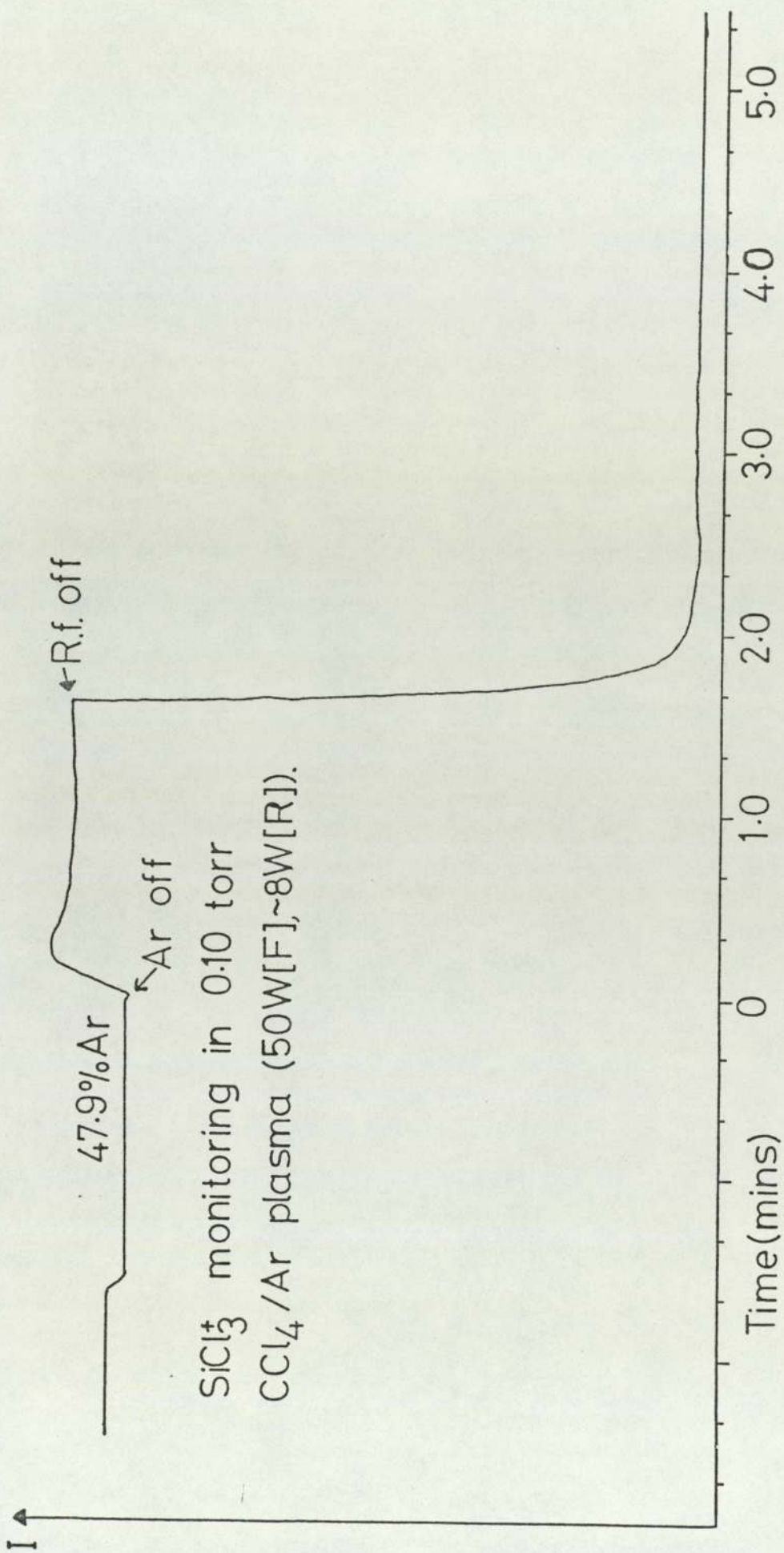
Fig. 47. Argon switch-off transient.

47.9%Ar

←R.f.off

←Ar off

$SiCl_3^+$ monitoring in 0.10 torr
CCl_4/Ar plasma (50W[F],~8W[R]).

I

Time(mins)

0   1.0   2.0   3.0   4.0   5.0

138(c)

4.6   Silicon Etching in CFCl₃ Plasmas

The mass spectrometric results of etching plain silicon wafers in 0.10torr CFCl₃ plasmas are shown in table: 31. The overlap of silicon containing masses and the normal fragments of CFCl₃ plasma was observed.

ION	MASS	$CFCl_3$ Plasma @ 70eV 50W(F)	$CFCl_3$ on Si; Plasma @ 70eV 50W(F)	$CFCl_3$ on Si; Plasma @ 20eV 50W(F)	$CFCl_3$ on Si; Plasma 70eV; 100W(F)	$CFCl_3$ on Si; Plasma 20ev; 100W(F)
C^+	12	23	32	---	28	---
H_2O^+	18	14	52	---	88	---
F^+	19	11	6	31	8	28
HF^+	20	---	3	---	5	---
C_2^+	24	8	7	---	8	---
$CO;^+Si^+$	28	61	68	13	109	17
CF^+	31	92	112	2	86	2
Cl^+	35	275	275	40	280	38
HCl^+	36	186	300	240	300	250
C_2F^+	43	4	5	---	6	---
$SiF^+;CCl^+$	47; 49	88; 25	103; 30	2; ---	91; 27	1; ---
CF_2^+	50	28	35	4	35	4
C_3F^+	55	4	4	---	5	---
C_2Cl^+	59	12	13	---	15	---
$AlCl^+$	62	---	4	---	3	---
$SiF_2^+;CFCl^+$	66; 68	33; 13	48; 13	2; 1	8; 5	--
CF_3^+	69	66	81	28	89	30
Cl_2^+	70	443	327	311	481	292
C_2FCl^+	78	13	15	4	16	3
$SiFCl^+;CCl_2^+$	82; 84; 86	34; 20; 4	36; 21; 3	5; 3; 2	30	4; 2; 1
$SiF_3^+;CF_2Cl^+$	85; 87	109; 40	138; 41	58; 17	148; 37	49; 18

Table: 31. $CFCl_3$ Plasmas[*] Etching Silicon.   contd.

ION	MASS	$CFCl_3$ Plasma @ 70eV 50W(F)	$CFCl_3$ on Si; Plasma @ 70eV 50W(F)	$CFCl_3$ on Si; Plasma @ 20eV 50W(F)	$CFCl_3$ on Si; Plasma 70eV; 100W(F)	$CFCl_3$ on Si; Plasma 20ev; 100W(F)
C_3FCl^+	90	2	3	---	3	---
$C_2Cl_2^+$	94	25	26	15	34	20
$SiF_2Cl;^+CFCl_2^+$	101;103;105	168;86;18	193;120;20	128;78;8	140;87;14	98;54;8
$C_3F_2Cl^+$	109	2	4	---	4	---
$C_2FCl_2^+$	113	8	8	4	10	3
$SiFCl_2;^+CCl_3^+$	117;119;121	60;46;15	65;58;8	45;40;13	61;55;17	74;59;17
$C_2Cl_3^+$	129	8	8	5	9	3
$C_2F_2Cl_2^+$	132	4	5	4	6	3
$C_2F_4Cl^+$	135	6	7	5	9	4
$C_2FCl_3^+$	148	7	9	8	10	8
$C_2F_3Cl_2^+$	151	7	9	5	7	4
$C_2Cl_4^+$	164	5	3	6	4	5
$C_2F_2Cl_3^+$	167	4	8	5	8	4
$C_3F_2Cl_3^+$	179	---	1	2	2	1
$C_2FCl_4^+$	183	2	5	5	4	5

[*]Plasma conditions for table: 31; were:-

Pressure: 0.10 torr $CFCl_3$ gas

Flow rates: 1.10 sccm $CFCl_3$ (r.f. off)
0.90 sccm $CFCl_3$ (r.f. on); 50W(F) $\sim$ 8W(R)
0.89 sccm $CFCl_3$ (r.f. on); 100W(F) $\sim$ 20W(R)

Gain: 30; Electron energy:- 70eV and 20eV.

4.7   <u>Silicon Etching in SiCl$_4$ Plasmas.</u>

Initially these etching results looked promising and a pattern was left on the photoresist patterned wafer after etching and the usual oxygen plasma photoresist stripping. The "etch rate" could not be determined in the usual way with the optical microscope because the surfaces (which were thought to have been etched) were too rough and gave poor reflections. On closer examination of these wafers it was noticed that the pattern could be easily scratched off revealing the polished wafer beneath. The material removed in this way was red in colour and was without doubt the original photoresist pattern which had somehow escaped the oxygen plasma stripping.

At first this was thought to be due to insufficient stripping times, although 15 minutes was sufficient for other patterned wafers exposed to CCl$_4$ plasmas. The exposure time to oxygen plasma was increased without success. The photoresist surface had a dark blackish appearence similar to etched silicon. Examination of a sample with the S.E.M. showed the photoresist was corrugated and lifted up from the wafer in places where previously it had been a smooth pattern of photoresist figs: 48 and 49. Removal of large areas of this pattern showed the clean polished silicon beneath with no visible shadow effects or rough surfaces suggesting the wafer had not been etched at all in the SiCl$_4$ plasma.
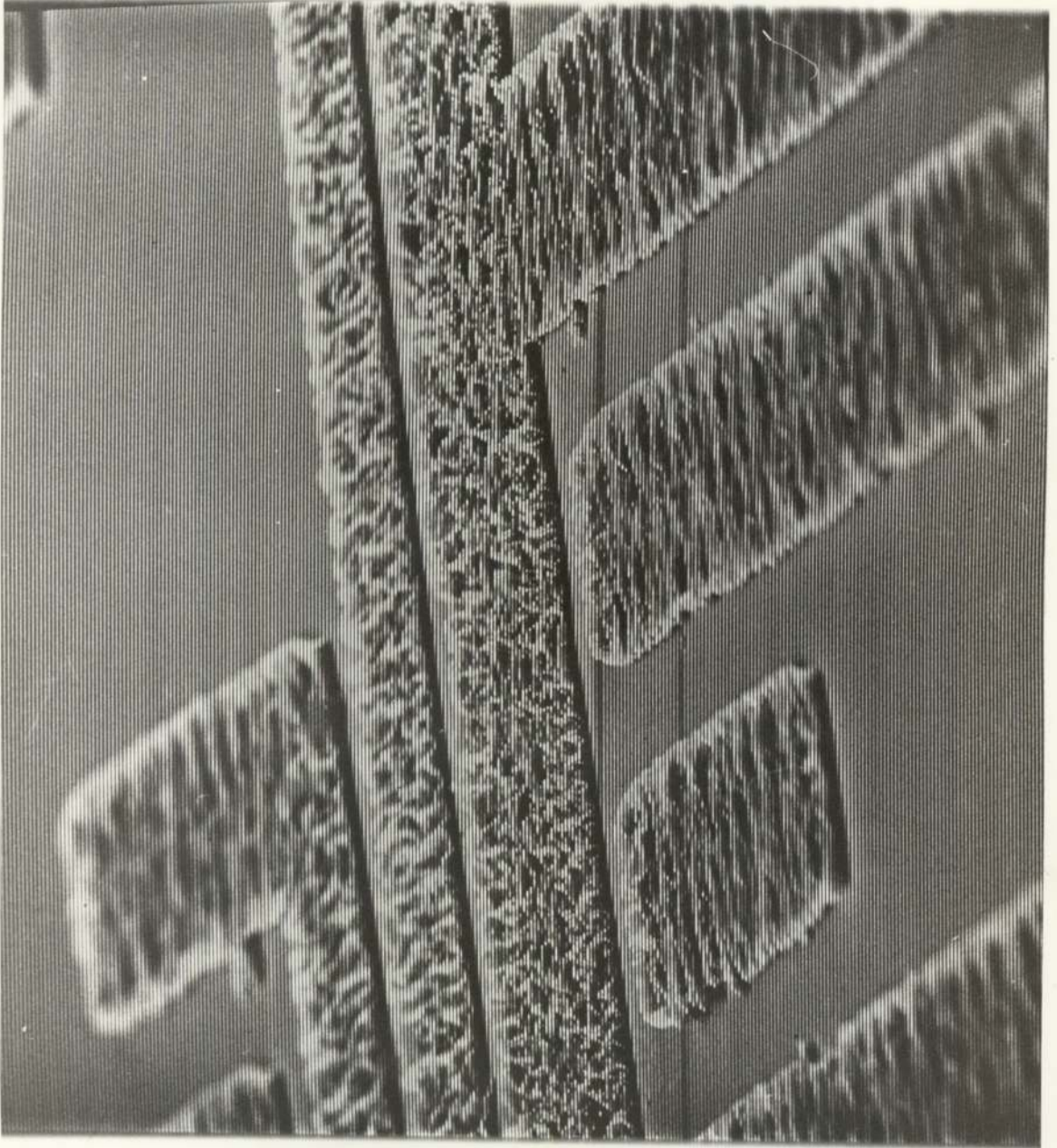
Fig.48. SiCl$_4$ plasma treated resist.

142(a)

(x5k)

Fig.49. SiCl$_4$ plasma treated resist.

142(b)

Fig: 48, is x1k magnification and fig:49, is x5k magnification. These pnotographs were obtained from a Stereoscan scanning electron microscope, later photographs were obtained using a Jeol type scanning electron microscope.

4.8   Polymer Formation and Structure

'Polymer' films were repeatedly deposited from the CCl$_4$ and CFCl$_3$ plasmas onto silicon wafers and interfered with the etching experiments. The films were found to be conductive giving resistances of 10-20Ω across a 2" silicon wafer. Even etched wafers showed some conductivity (see section 4.4). The films deposited from CCl$_4$ plasma onto the silicon were generally black and showed striations in the direction of the gas flow across the wafer. The films from CFCl$_3$ plasmas were greyish in colour and showed similar striations across the wafer.

Reflectance infrared spectra of these films were poor and showed only C-Cl and C-F bands. The bands were broad and very weak. The silicon wafers are transparent to infrared radiation and it was therefore possible to obtain some weak transmission spectra. The reverse side of the silicon wafers was not highly polished and a great deal of radiation was lost by scattering. However, placing the rough side of the wafer near the detector slit minimised these losses. Only very small broad absorption bands at 1100-1200 cm^{-1} and 700-800cm^{-1} were observed. These were thought to be due to C-F and C-Cl bonds respectively.

Auger, X.P.S. and S.E.M. (with Kevex X-ray fluorescence facilities) were more successful. Fig: 50

Fig.50. X.P.S. of film on silicon (CCl_4/O_2 plasma)
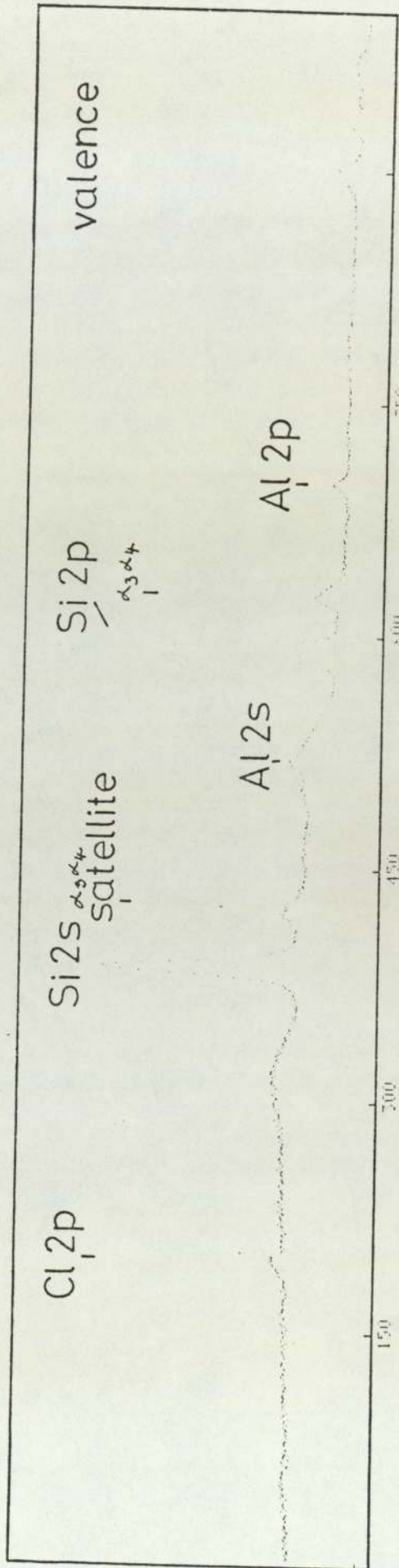
each channel 0.25 eV

(150; 50s sweeps)

Cl 2p

Si 2s $_{\alpha_3\alpha_4}$
satellite

Si 2p
$_{\alpha_3\alpha_4}$

valence

Al 2s

Al 2p

File B:ASTON2 Channels 1 - 1006
Detail CCl4/Si search for minor elements

shows a wide range X.p.s. scan for minor elements on a film produced from CCl_4-O_2 plasma on silicon. The surface stoichiometry of this sample (assuming it to be a homogeneous solid) was roughly Si_{100} Al_6 Cl_2 C_{200} O not determined but >100. All the silicon within the sampling depth (50-100Å) being in an oxidised form (presumably SiO_2). The carbon on this sample does not appear to be graphitic (c.F. ref.217 and fig: 51) because the Cls peak was shown to be symmetrical and there was no sign of the graphite plasmon (217).

The films from $CFCl_3$ and CCl_4 plasmas were shown to be almost identical. The spectra for CCl_4/O_2 plasma fig: 52, was typical of these films.

Auger analysis of films deposited from CCl_4/O_2 plasmas onto silicon showed C,O,Cl, Al and Si figs: 53 (a)-(f). The amount of aluminium on the surface was about 36% compared to the aluminium sample holder signal. These spectra also suggested that the polymer film was ~ 1000Å thick and that the composition of the film changes with the thickness of the film.

Work on CCl_4-O_2 plasmas 'etching' silicon showed that the $SiCl_3^+$ ion intensity would, on certain occasions, suddenly fall at a particular oxygen content of the plasma. The results of this work are shown in tables: 32 and 33, and fig: 54.
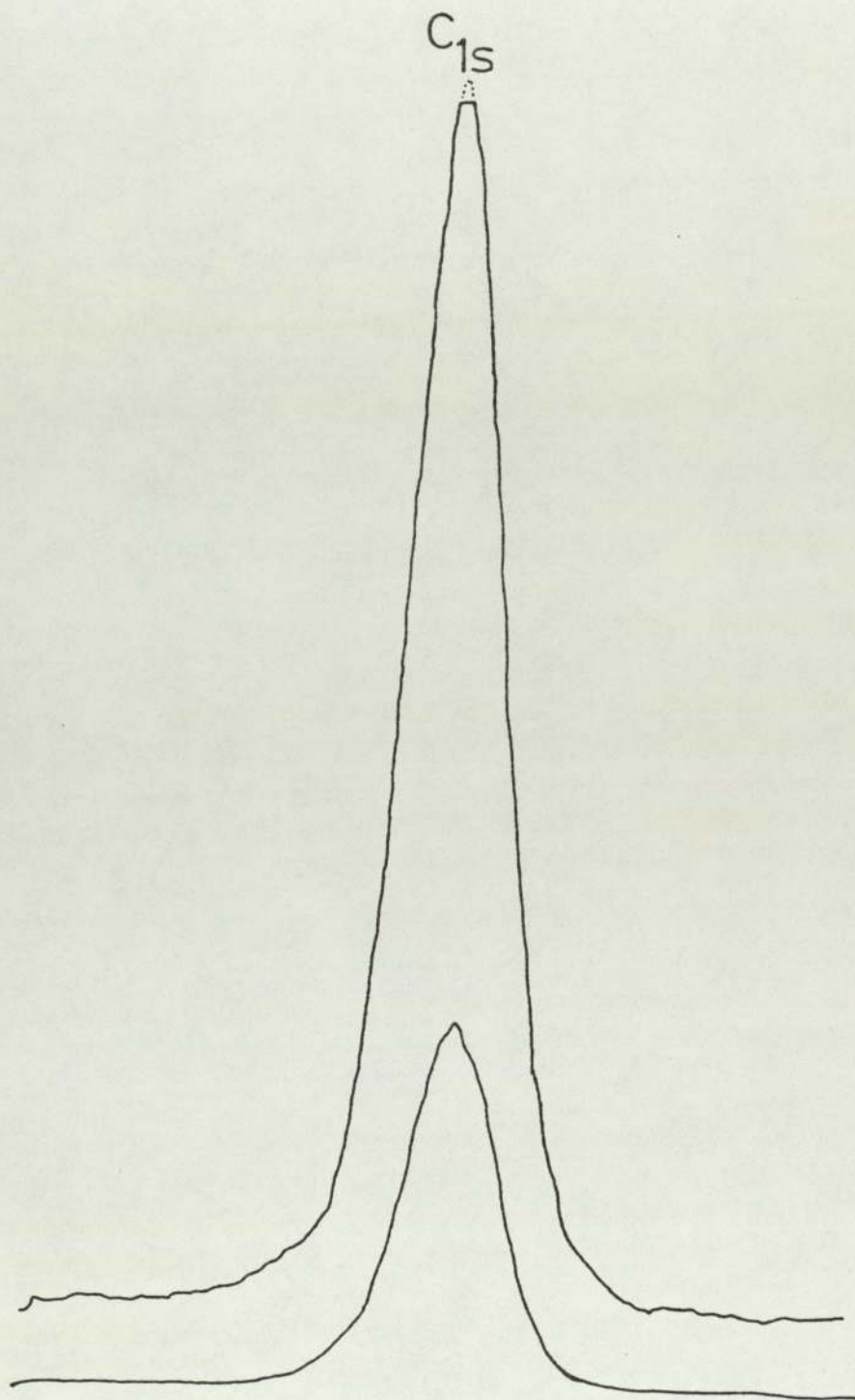
Fig.51. C1s X.p.s. detail(CCl_4/O_2)
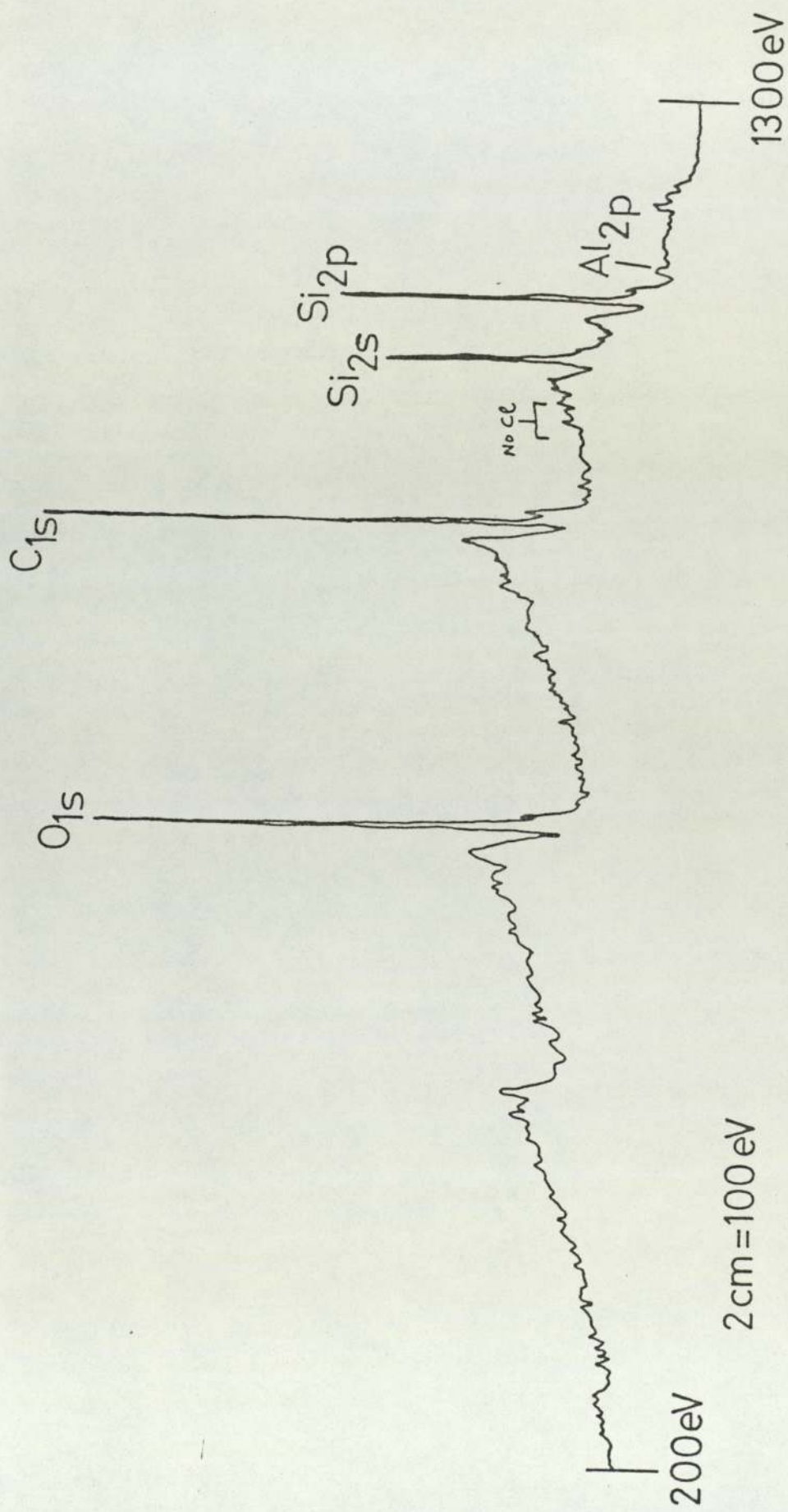
Fig.52. X.p.s. of 'polymer'(CCl_4/O_2 plasma).
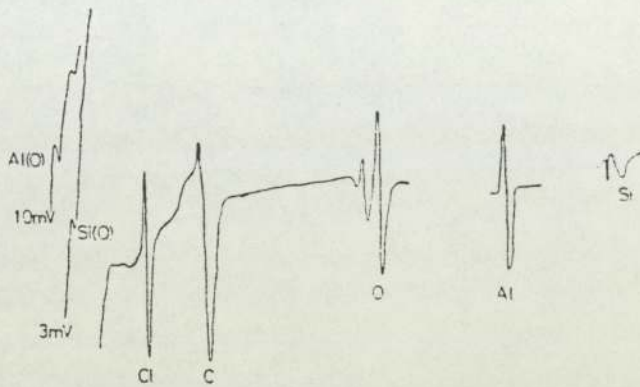
Fig.(a). 'Polymer' on silicon (as received).
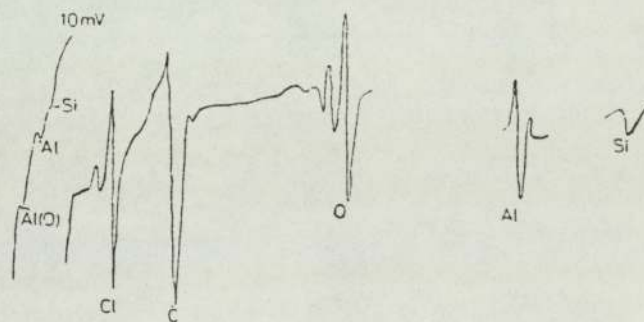
Fig.(b). 'Polymer' (Ar⁺ clean 5kV, 30uA, 2min ≈70Å)
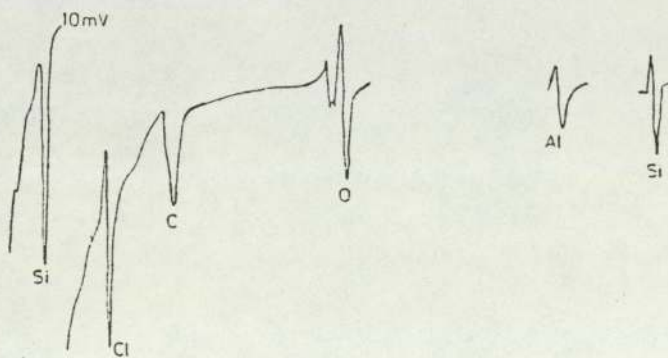
Fig.(c). 'Polymer' (Ar⁺, 5kV, 30uA, 10min ≈350Å)

Fig.53. A.e.s. of film (CCl_4/O_2).

145(c)
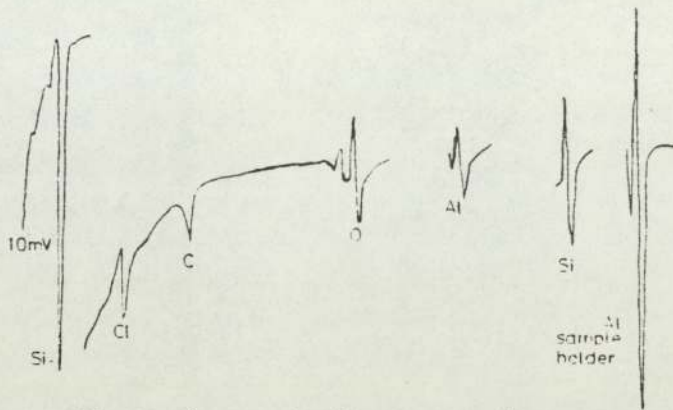
Fig.(d). 'Polymer' (Ar, 18 min, ≈630Å)
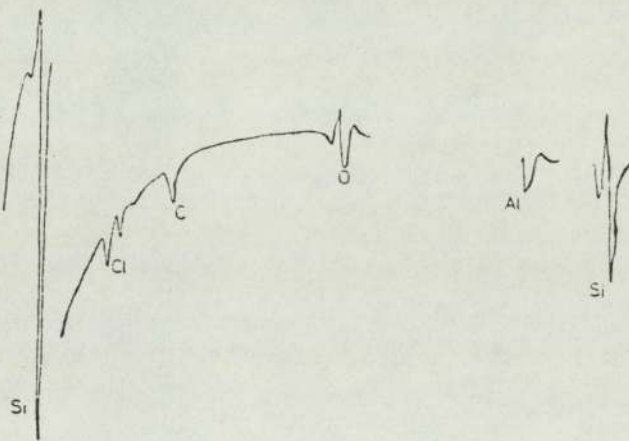
Fig.(e). 'Polymer' (Ar, 28 min, ≈980Å)
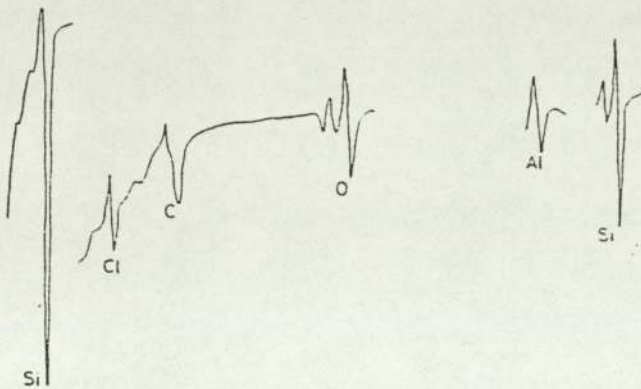
Fig.(f). 'Polymer' (glancing angle)

Fig.53. A.e.s. of film (CCl_4/O_2).

The S.E.M. photographs figs: 55-56 show the very rough surfaces of the films deposited by CCl_4-O_2 plasmas on silicon. The unusual "spikes" of material were shown to contain aluminium using the Kevex X-ray facility on the S.E.M. fig:57.

The Polymer would not deposit on a glass slide placed in the discharge. A very thin oily yellow film was produced which could not be analysed in detail. The film did not appear to be the same as the material deposited on the silicon wafers.

Table:32.   "Polymer" formation in CCl_4-O_2 Plasma[*] at 0.10 torr.

Flow Rates(sccm)		Total Flow rate(sccm)	Plasma Composition		$SiCl_3^+$ ion intensity (mm) at 135 amu	$\dfrac{I_{O_2/CCl_4}}{I_{CCl_4}}$
CCl_4	O_2		% CCl_4	% O_2		
0.94	---	0.94	100	---	176	1.00
0.68	0.07	0.75	91	9	168	0.95
0.65	0.09	0.74	88	12	160	0.91
0.63	0.10	0.73	86	14	159	0.90
0.62	0.11	0.73	85	15	157	0.89
0.61	0.12	0.73	84	16	156	0.87
0.60	0.13	0.73	83	17	152	0.86
0.58	0.13	0.71	82	18	144	0.82
0.58	0.14	0.72	81	19	146	0.83
0.57	0.15	0.72	80	20	141	0.80
0.57	0.16	0.73	78	22	130	0.74
0.55	0.18	0.73	76	24	107	0.61
0.53	0.19	0.72	74	26	49	0.28
0.49	0.23	0.72	68	32	16	0.09
0.46	0.25	0.71	65	35	9	0.05

[*]Plasma conditions for table: 32, were:-

Pressure: 0.10 torr total pressure.

Power: 50W(F), ∿ 8W(R); @ 13.56MHz.

Flow rate: 1.14sccm CCl_4 (100%) r.f. off

Electron energy: 70eV; Gain 100; Mass: 135 a.m.u.

Table:33.   "Polymer" formation in CCl_4-O_2 Plasma[*] at 0.10 torr.

Flow Rates(sccm)		Total Flow rate(sccm)	Plasma Composition		$SiCl_3^+$ ion intensity (mm) 100 Gain	$\dfrac{I_{CCl_4/O_2}}{I_{CCl_4}}$
CCl_4	O_2		% CCl_4	% O_2		
0.88	---	0.88	100	---	175	1.00
0.60	0.07	0.67	90	10	167	0.95
0.60	0.09	0.69	87	13	155	0.88
0.63	0.10	0.73	86	14	149	0.85
0.64	0.11	0.75	85	15	137	0.78
0.65	0.12	0.77	84	16	122	0.70
0.63	0.13	0.76	83	17	92	0.53
0.63	0.14	0.77	82	18	60	0.34

[*]Plasma conditions for tbale: 33, were:-

Pressure: 0.10 torr total pressure.

Power: 50W(F), ∿8W(R); 13.56MHz.

Flow rate: 1.05sccm CCl_4 (100%) (r.f. off)

Electron energy: 70eV; Gain: 100; Mass: 135.

SiCl$_3^+$ monitoring in 0.10 torr CCl$_4$/O$_2$ plasma.
Typical errors: ±,H.

I_{O_2}/I_{ca_*}

1.0

0.5

0

10.0   20.0   30.0   40.0

% O$_2$ added
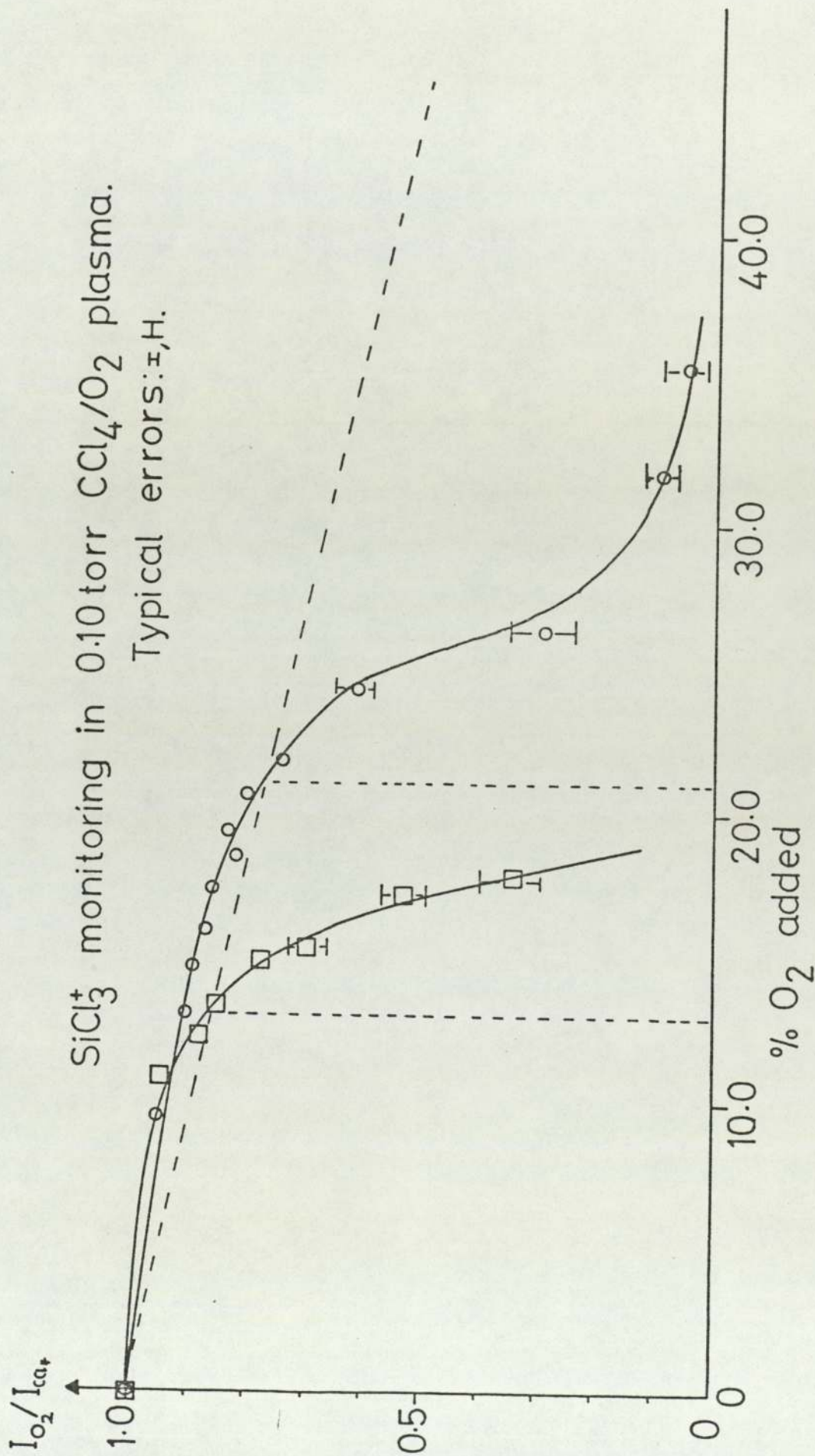
Fig.54. 'Polymer' formation in CCl$_4$/O$_2$ plasma.
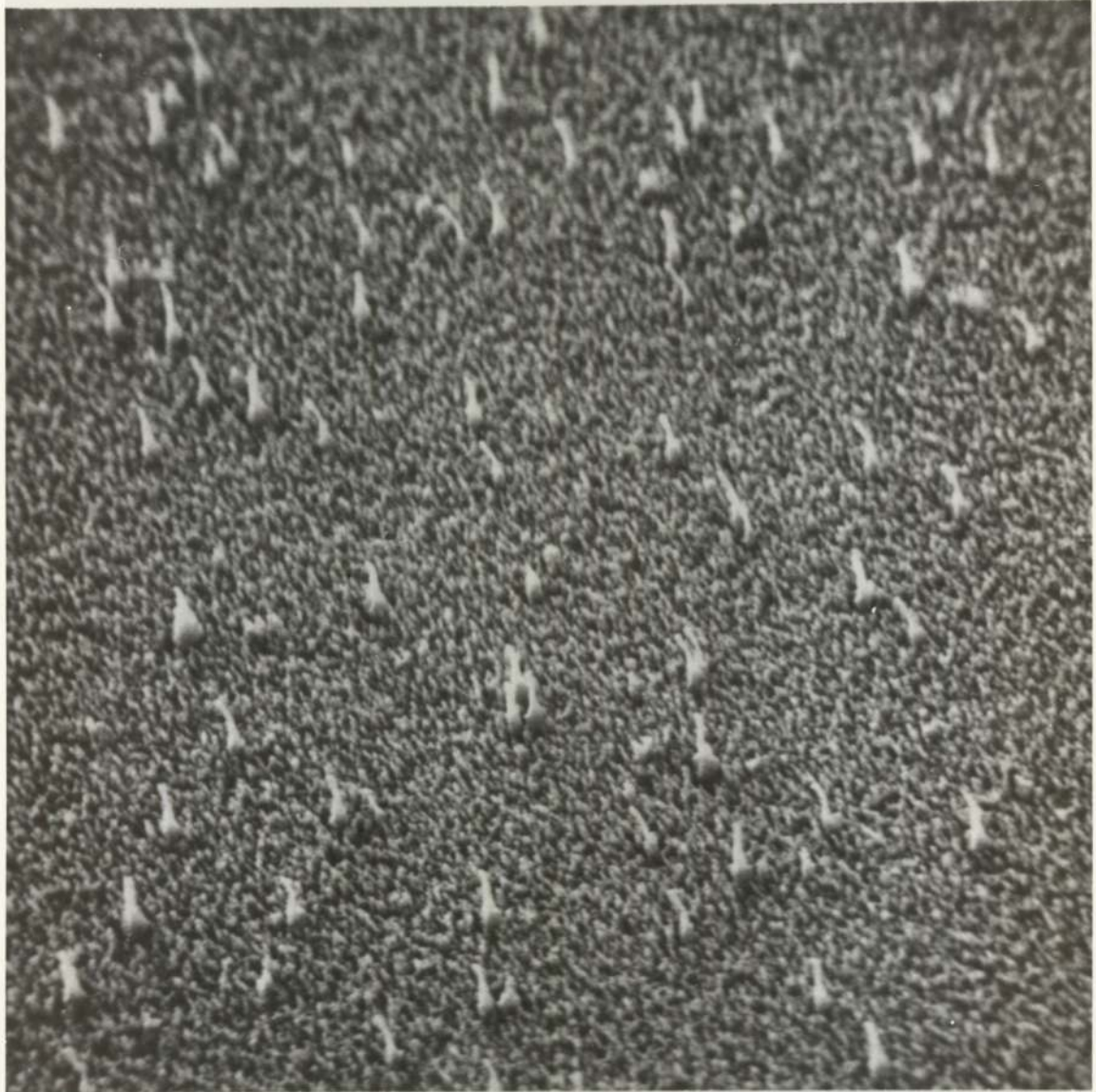
(×2k)

Fig.55. Si surface films (CCl_4/O_2).

148(b)

(×10k)

Fig.56. Si surface film (CCl$_4$/O$_2$).
148(c)
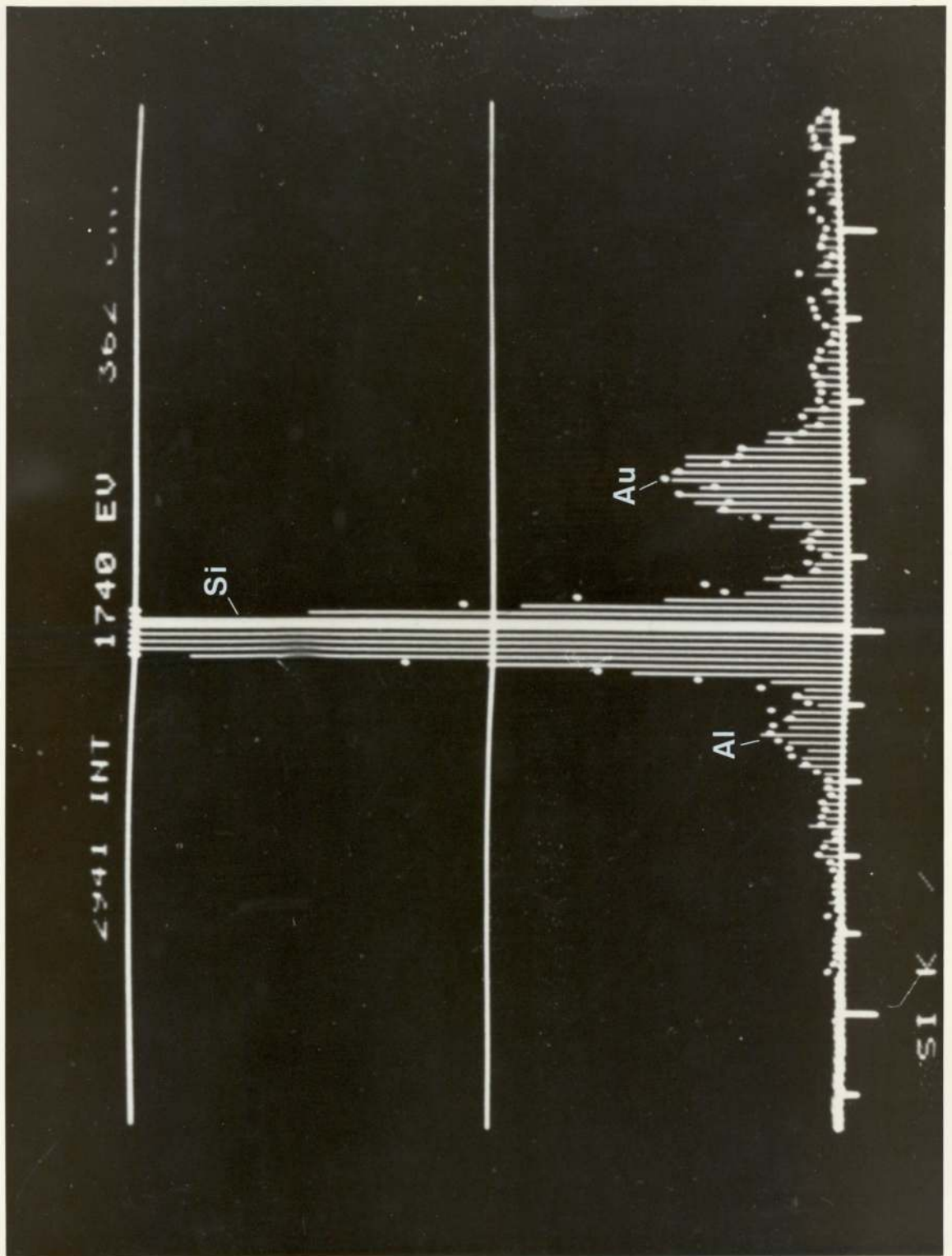
Fig.57. X-ray of surface film.
148(d)

4.9 Photoresist Stripping

After etching patterned wafers photoresist is usually removed in an oxygen plasma. Some preliminary experiments were carried out during photoresist stripping; a typical mass spectrum is shown in table:34. The intensity of the CO_2^+ ion at 44 a.m.u. was negligible. The CO^+ ion at 28 a.m.u. was most suitable for monitoring the photoresist stripping process. The results of monitoring the CO^+ ion are shown in fig:58.

There is a background CO^+ ion intensity contributing to the long tail of the curve in fig: 58. This is probably due to carbonaceous material on the inside of the reactor. Also some of the photoresist, particularly on the edges of the silicon wafer, was difficult to remove in the oxygen plasma. This material had the same properties as over-baked photoresist which is hard and brittle. There is no doubt that the wafers were warm to the touch when removed from the reactor immediately after photoresist stripping and this could have affected some of the photoresist.

Table: 34. Photoresist Stripping.

ION	MASS	O_2 GAS @ 0.25 torr	O_2 Plasma on Photoresist
C^+	12	4	27
O^+	16	150	120
H_2O^+	18	15	75
$N_2^+; CO^+$	28	30	225
O_2^+	32	1230	56
Cl^+	35	20	15
HCl^+	36	30	40
CO_2^+	44	20	60

Plasma conditions were:-

Pressure: 0.25 torr O_2 gas.

Power: 50W(F); $\sim$ 2W(R)

Flow rate: 4.55sccm (r.f. off)
            4.60sccm (r.f. on)

Electron energy: 70eV; Gain: 30;

1.5 um of photoresist AZ1350J on Silicon (not patterned)

Oxygen plasma photoresist stripping monitoring CO^+ ions.

0.25 torr O_2; 50W(F), 2W(R).

Flow rate 4.55 sccm(r.f. off), 4.58 sccm(r.f. on).

A single 2" wafer coated with 1.5 um of AZ1350J.
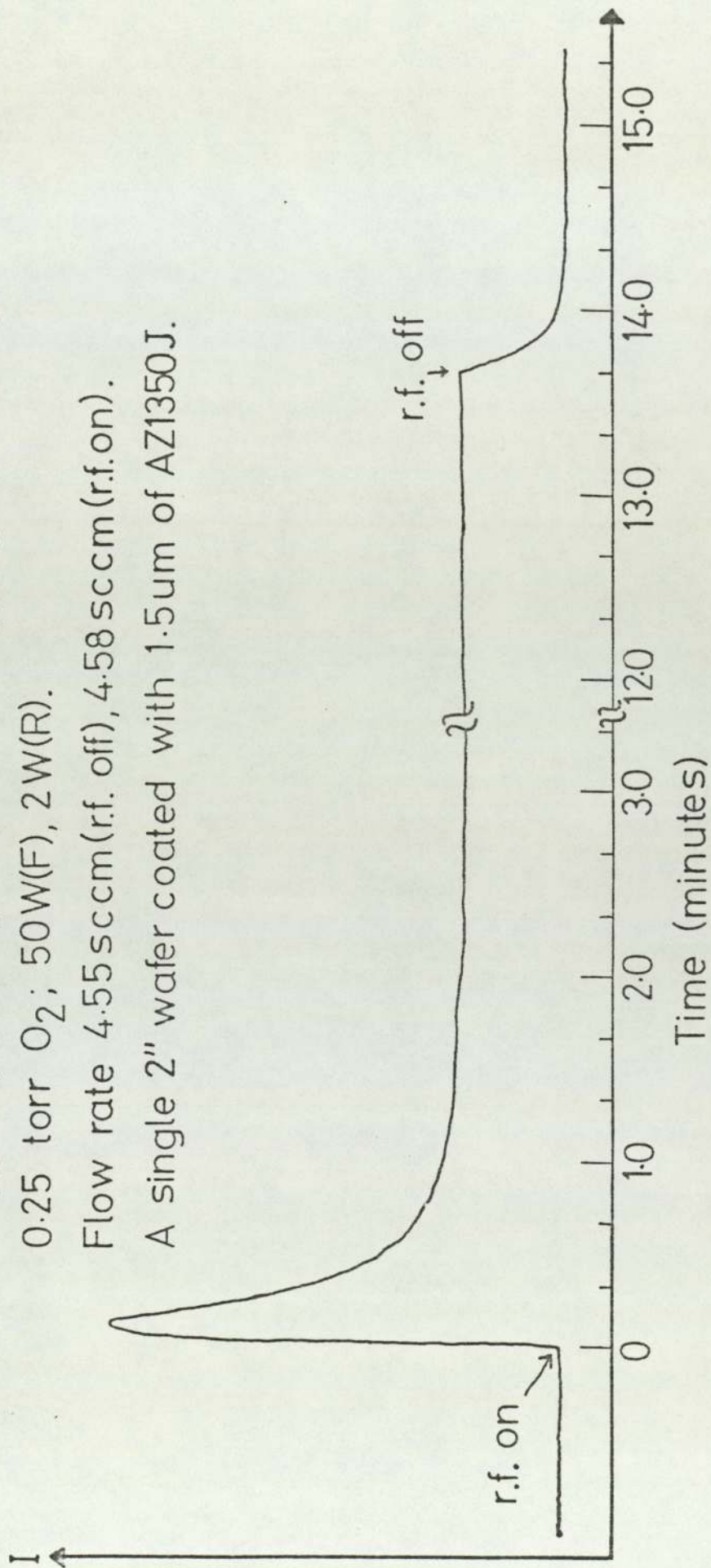
Fig.58. Photoresist stripping.

5.   DISCUSSION

5.1   Detection of Atoms and Free Radicals

As discussed in section 2.1.1. atoms and free radicals are usually identified by the method of appearance potential discrimination. That is the formation of ions with energy lower than that needed to produce the atomic or free radical ion by any fragmentation process. For this reason it is necessary to be able to record the ionisation efficiency curves of any particular species reproducibly and to operate reliably in the threshold region.

The appearance potentials of the normal fragments from CCl_4 gas were obtained with reasonable precision, table: 8. However, appearance potentials for Cl^+ ions were difficult to obtain reliably because of the large noise levels.

In the case of a discharge in CCl_4 the effects of r.f. interference on the ionisation efficiency curves made it impossible to determine appearance potentials reliably. It was therefore not possible to use the system to detect directly atoms and radicals in the discharge. Even without r.f. interference it may still be difficult to detect atoms and radicals in this sytem (219-223). It was, therefore, necessary to use indirect approaches in the interpretation of the mass spectra in order to make some deductions concerning the involvement of atoms and free radicals.

151

5.2.   Indirect Evidence for Atoms and Radicals

It is already well known that chlorine atoms are responsible for etching silicon in chlorine, Cl_2, plasmas (77 (ix), 175, 177, 178 and 212). If, in this system, gas phase recombination of chlorine atoms (with a suitable third body) is the main source of Cl_2 in the discharge the intensity of Cl_2^+ ions detected in the mass spectrometer, particularly at 20eV, could be related to the chlorine atom concentration in the plasma and hence the Si etch rate.

$$Cl^{\cdot} + Cl^{\cdot} + M \xrightarrow{\;km\;} Cl_2 + M$$
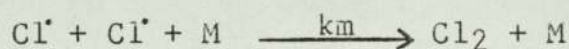
$$\frac{d\,[Cl_2]}{dt} = km\,[M]\,[Cl^{\cdot}]^2 - Rd = 0 \qquad\qquad (1)$$

where Rd is the rate of disappearence of Cl_2 and assuming Rd is proportional to the concentration of Cl_2 (ie: Rd=kd $[Cl_2]$) then:-

$$[Cl^{\cdot}] = \left(\frac{kd}{km} \; \frac{[Cl_2]}{[M]} \right)^{1/2} \qquad\qquad (2)$$

If kd is constant then km, the third body recombination constant, will depend upon the nature of the third body, M. Values for km have been determined for various molecules of differing sizes (229-231). The values of km are not widely different for the various third bodies which are similar in size to the species found in the various discharges in this work.

152

Similar arguments may be advanced for other radicals eg: CCl_3, provided suitably unambiguous ions may be found for the monitoring process. The most likely process with CCl_3 radicals is reaction (1), in table:35, leading to "hot" C_2Cl_6 which may decompose unless stabilised by collision. At 0.1 torr the collision interval is $10^{-6}s$. However, the lifetime of a hot molecule depends on the unimolecular rate constant, kd.

$$A^* \xrightarrow{\quad kd \quad} products$$

$$\frac{-d\,[A^*]}{dt} = kd\,[A^*] \tag{3}$$
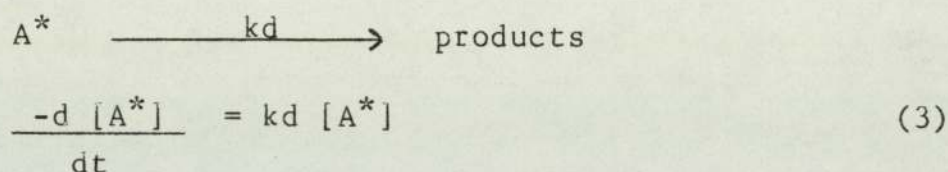
Using simple R.R.K. theory we may estimate kd:-

$$kd = \bar{v}\left(\frac{\mathcal{E}^* - \mathcal{E}_o}{\mathcal{E}^*}\right)^{s-1} = \bar{v}\left[1 - \frac{\mathcal{E}_o}{\mathcal{E}^*}\right]^{s-1} \tag{4}$$

where s is usually about half the number of vibrational modes $=(3n-6)/2$.

   $\mathcal{E}^*$ is the excess energy of the "hot" molecules.

   $\mathcal{E}_o$ is the activation energy for the decomposition.

   $\bar{v}$ may be assumed to be $\sim 10^{13}$ s-1.

For the reaction:-

$$CCl_3 + CCl_3 \longrightarrow C_2Cl_6^{*\ddagger}$$
$$C_2Cl_6^{*\ddagger} \longrightarrow C_2Cl_4 + Cl_2$$
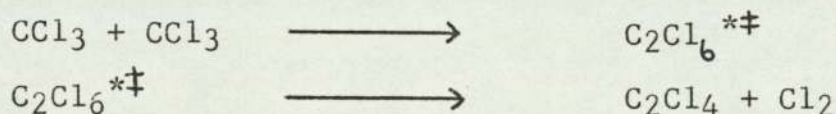
$\mathcal{E}^*$ = 300kJ mol-1 and $\mathcal{E}_o$=127 kJmol-1 (see table: 35)

s = 7-10, giving kd=10^{11}s-1 and τd=10^{-11}s.

153

Table: 35.   Enthalpies of Reaction in CCl_4 Plasmas

	REACTION	ΔH (k J mol^{-1})
(1)	$CCl_3^{\cdot} + CCl_3^{\cdot} + M \longrightarrow C_2Cl_6 + M$	-300
(2)	$:CCl_2 + :CCl_2 + M \longrightarrow C_2Cl_4 + M$	-492
(3)	$CCl_3^{\cdot} + :CCl_2 + M \longrightarrow C_2Cl_5^{\cdot} + M$	-285
(4)	$C_2Cl_5^{\cdot} \longrightarrow C_2Cl_4 + Cl^{\cdot}$	74
(5)	$C_2Cl_6 \longrightarrow C_2Cl_4 + Cl_2$	127
(6)	$CCl_3^{\cdot} + Cl^{\cdot} + M \longrightarrow CCl_4 + M$	-308
(7)	$Cl^{\cdot} + Cl^{\cdot} + M \longrightarrow Cl_2 + M$	-243
(8)	$CCl_3^{\cdot} + C_2Cl_4 \longrightarrow C_3Cl_7^{\cdot}$	-79
(9)	$Cl^{\cdot} + C_2Cl_4 + M \longrightarrow C_2Cl_5^{\cdot}$	-74
(10)	$C_2Cl_4 \longrightarrow C_2Cl_2 + Cl_2$	127 (est)
(11)	$:CCl_2 + C_2Cl_5^{\cdot} \longrightarrow C_3Cl_7^{\cdot}$	-285

154

If the lifetime of the hot molecules is very much shorter than the collision interval, as in this case, the molecule will dissociate before it is stabilised by collision with another molecule. In this case the C_2Cl_6 will dissociate into C_2Cl_4 and Cl_2 rapidly and this process could be expected to contribute large amounts of Cl_2 to the Cl_2^+ ion intensity. Some $C_2Cl_5^+$ was observed in the mass spectrometer, although of low intensity, from fragmentation of C_2Cl_6.

A similar source of Cl_2 may be from elimination of Cl_2 from "hot" C_2Cl_4 in reaction (10), table:35. If these processes ((5) and (10)) occur then the suggestion made earlier concerning the source of the high Cl_2^+ ion intensities from chlorine atoms is an oversimplification at best.

5.3 CCl₄ Plasmas

The mass spectra obtained from these discharges showed that quantities of C_2Cl_6 and C_2Cl_4 were produced, tables: 9 and 12. Large quantities of Cl_2 were also produced. On switching on a discharge in CCl_4 there is a large reduction in the intensity of CCl_3^+, CCl_2^+ and CCl^+ ions observed in the mass spectrometer, Fig:24. There is also a large increase in the intensity of $C_2Cl_x^+$, Cl_2^+ and some $C_3Cl_x^+$ ions.

The presence of C_3Cl_x species   is explained by reactions (8) and (11) in table: 35. The reduction in the ion intensities of CCl_3^+, CCl_2^+ and CCl^+ ions is thought to be due to fragmentation of the CCl_4 gas and the combination of these fragments to produce C_2Cl_6, C_2Cl_4 etc. in the discharge. The primary plasma processes being:-

$$CCl_4 + e(plasma) \longrightarrow CCl_3^+,\ CCl_2^+,\ CCl^+,\ C^+,\ Cl^+$$
$$\longrightarrow CCl_3^-,\ CCl_2^-,\ CCl^-,\ Cl^{-1},$$
$$\longrightarrow CCl_3^{\cdot},\ :CCl_2,\ CCl^{\cdot},\ C,\ Cl^{\cdot}$$
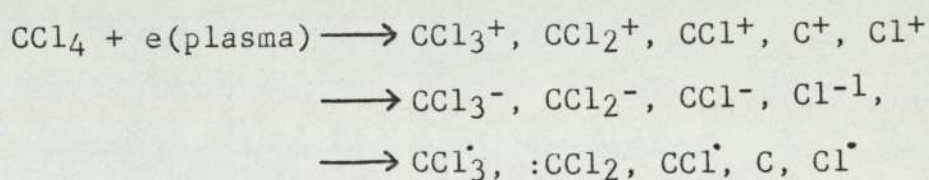
and the reactions of the radicals, which can combine, are shown in table:35. The increase in Cl_2^+ ions is probably mainly due to the elimination of Cl_2 from C_2Cl_6 and C_2Cl_4 as discussed earlier in section 5.2.

156

The complexities of the CCl_4 system are illustrated in the changes in ion intensities observed on varying the r.f. power levels, Fig: 26. The reduction in CCl_x ion intensities and the increase in the Cl_2^+ ion intensity are very pronounced at high r.f. powers. The C_2Cl_x ion intensities are also decreased at higher r.f. powers. There is a distinct change observed in the discharge at about 50-60W of forward power applied to the plasma. Below 50W(F) the discharge is a dark turquoise blue which rapidly changes to a very bright white-blue discharge above 50W(F). The change-over from one type of discharge to another is very abrupt. A detailed explanation of these changes cannot be successfully given at present.

5.4   Effect of Additives on CCl_4 Plasmas.

5.4.1.   Addition of Oxygen to CCl_4 Plasmas.

The possible additional reaction mechanism with added oxygen is shown in table: 36. The discharge in oxygen is complex but it is expected that oxygen atoms are the most important species formed in the plasma from reaction (12).

The results, in tables: 13-17, showed that addition of oxygen produced large quantities of CO, seen as CO^+ ions in the mass spectrometer. The CO_2^+ ion intensity was very small suggesting that CO_2 is not significantly formed in the plasma (reaction (33) in table:36). Large intensities for Cl_2^+ ions were observed, even at high dilutions with oxygen, which are not substantially different from the intensities in pure CCl_4 plasmas. The CCl_3^+, CCl_2^+ and CCl^+ ion intensities were reduced to a greater extent than would be expected from simply diluting the CCl_4 plasma.

Only small quantities of $COCl_2^+$ and $COCl^+$ ions were observed in the mass spectrometer. If $COCl_2$ is formed in the plasma by reactions (13), (15), (17), (21) and (26) it is not present in large quantities but quickly dissociates into CO and Cl_2 by reaction (22). This is in agreement with work done on the reaction of oxygen atoms with CCl_4 in a fast flow system (234). Standard mass spectra tables (246, 247) show that $COCl^+$ ions

158

Table: 36.   Additional Reactions with Oxygen in CCl_4 Plasmas.

REACTION		ΔH (k J mol^{-1})
(12)	O_2 + e (Plasma) $\longrightarrow$ $2O^{\bullet}$ + e	498
(13)	$O^{\bullet}$ + CCl_4 $\longrightarrow$ $COCl_2$ + Cl_2	-365
(14)	$O^{\bullet}$ + CCl_4 $\longrightarrow$ $CCl_3^{\bullet}$ + $ClO^{\bullet}$	75
(15)	$O^{\bullet}$ + $CCl_3^{\bullet}$ $\longrightarrow$ $COCl_2$ + $Cl^{\bullet}$	-430
(16)	$O^{\bullet}$ + $CCl_3^{\bullet}$ $\longrightarrow$ Cl_2 + $COCl^{\bullet}$	-393
(17)	$O^{\bullet}$ + $:CCl_2$ + M $\longrightarrow$ $COCl_2$ + M	-712
(18)	$O^{\bullet}$ + $:CCl_2$ $\longrightarrow$ CO + Cl_2	-599
(19)	$O^{\bullet}$ + $CCl^{\bullet}$ $\longrightarrow$ CO + $Cl^{\bullet}$	-636
(20)	$O^{\bullet}$ + $Cl^{\bullet}$ + M $\longrightarrow$ $ClO^{\bullet}$ + M	-232
(21)	O_2 + $CCl_3^{\bullet}$ + M $\longrightarrow$ $COCl_2$ + $ClO^{\bullet}$	-165
(22)	$COCl_2$ $\longrightarrow$ CO + Cl_2	113
(23)	$COCl_2$ $\longrightarrow$ $COCl^{\bullet}$ + $Cl^{\bullet}$	280
(24)	$COCl^{\bullet}$ $\longrightarrow$ CO + $Cl^{\bullet}$	75
(25)	$ClO^{\bullet}$ $\longrightarrow$ $Cl^{\bullet}$ + $O^{\bullet}$	233
(26)	O_2 + $:CCl_2$ $\longrightarrow$ $COCl_2$ + $O^{\bullet}$	-213
(27)	O_2 + $:CCl_2$ $\longrightarrow$ $COCl^{\bullet}$ + $ClO^{\bullet}$	-65
(28)	O_2 + $CCl_3^{\bullet}$ $\longrightarrow$ $COCl^{\bullet}$ + Cl_2O	-67
(29)	Cl_2O $\longrightarrow$ Cl_2 + $O^{\bullet}$	173
(30)	O_2 + $:CCl_2$ $\longrightarrow$ CO + Cl_2O	-273
(31)	O_2 + $CCl^{\bullet}$ $\longrightarrow$ CO + $ClO^{\bullet}$	-211
(32)	O_2 + $CCl^{\bullet}$ $\longrightarrow$ $COCl^{\bullet}$ + $O^{\bullet}$	-54
(33)	CO + $O^{\bullet}$ + M $\longrightarrow$ CO_2 + M	-532
(34)	O_2 + $Cl^{\bullet}$ + M $\longrightarrow$ ClO_2 + M	-18

159

(63a.m.u.) are the most intense fragment ions from a sample of $COCl_2$ in a mass spectrometer. The parent ion at 98 a.m.u., $COCl_2^+$, is very small compared to the intensity of $COCl^+$ ions. *Therefore, because of the very low intensities of $COCl^+$ ions* from these CCl_4/O_2 plasmas and the large CO^+ ion intensity the likely mechanism in these plasmas is by the formation of "hot" $COCl_2$ (from reactions of O_2 and O with CCl_x species; see table: 36) which then rapidly dissociates into CO and Cl_2 by reaction (22).

The addition of oxygen to CCl_4 plasmas also reduces the intensity of $C_2Cl_x^+$ ions, tables:15-17, in the mass spectrometer. This is probably due to the oxygen reacting with the CCl_x radicals before they can combine to form the C_2Cl_x species. Alternatively, though less likely, the oxygen atoms may be involved in reactions with the C_2Cl_x species, formed in the plasma, directly.

5.4.2. Addition of N_2O to CCl_4 Plasmas

The additional processes to be considered here are shown in table: 37; the reactions outlined earlier for oxygen atoms may also be significant here.

The addition of N_2O to CCl_4 plasmas produces large reductions in the intensities of CCl_x^+ ions in the mass spectra. These reductions are much greater than those seen for additions of oxygen to CCl_4 plasmas. Similarly, the $C_2Cl_x^+$ ion intensities are considerably reduced. The

160

intensity of CO^+ ions in the mass spectrometer is greatly increased and much higher compared to similar compositions of CCl_4/O_2 plasmas, tables: 13, 14 and 18. This suggests that N_2O is more efficient at oxidizing the CCl_4 fragments in the discharge. Oxygen atoms are easily produced from N_2O in the discharge from process (35). It is thought that the relative ease of formation of oxygen atoms from N_2O compared to oxygen, O_2, in process (12) table:36, and their subsequent reaction with CCl_4 fragments could account for the higher efficiency of N_2O in oxidizing the CCl_4 fragments (and hence reducing the CCl_x^+ ion intensities).

The reaction of nitrogen atoms with CCl_4 fragments is not thought to be important in these plasmas. The mechanism of reaction of CCl_4 and other chloromethanes with nitrogen atoms is discussed in greater detail by Sobering and Winkler (235).

N_2O may also react with CCl_x radicals directly as shown in reactions (41)-(48) in table: 37. These reactions would also result in large quantities of CO in the plasma.

5.4.3. Addition of Hydrogen to CCl_4 Plasmas

The results show that very large quantities of HCl^+ ions are observed in the mass spectrometer when hydrogen is added to CCl_4 plasma, table:19. The CCl_3^+ ions show a

Table: 37.   Additional Reactions with N_2O in CCl_4 Plasmas.

REACTION	$\triangle H$ (k $Jmol^{-1}$)
(35) N_2O + e(plasma) $\longrightarrow$ N_2 + $O^{\bullet}$	168
(36) N_2O + e(plasma) $\longrightarrow$ NO + N	481
(37) NO + e(plasma) $\longrightarrow$ $N^{\bullet}$ + $O^{\bullet}$	631
(38) N_2O + e(plasma) $\longrightarrow$ $2N^{\bullet}$ + $O^{\bullet}$	1113
(39) $N^{\bullet}$ + $N^{\bullet}$ + M $\longrightarrow$ N_2 + M	-945
(40) $O^{\bullet}$ + $O^{\bullet}$ + M $\longrightarrow$ O_2 + M	-498
(41) $CCl_3^{\bullet}$ + N_2O $\longrightarrow$ $COCl_2$ + N_2 + $Cl^{\bullet}$	-263
(42) $CCl_3^{\bullet}$ + N_2O $\longrightarrow$ $COCl^{\bullet}$ + N_2 + Cl_2	-225
(43) $CCl_3^{\bullet}$ + N_2O $\longrightarrow$ CO + N_2 + Cl_2 + $Cl^{\bullet}$	-150
(44) :CCl_2 + N_2O $\longrightarrow$ $COCl_2$ + N_2	-543
(45) :CCl_2 + N_2O $\longrightarrow$ $COCl^{\bullet}$ + N_2 + $Cl^{\bullet}$	-263
(46) :CCl_2 + N_2O $\longrightarrow$ CO + N_2 + Cl_2	-431
(47) $CCl^{\bullet}$ + N_2O $\longrightarrow$ $COCl^{\bullet}$ + N_2	-544
(48) $CCl^{\bullet}$ + N_2O $\longrightarrow$ CO + N_2 + $Cl^{\bullet}$	-469
(49) $Cl^{\bullet}$ + N_2O $\longrightarrow$ $ClO^{\bullet}$ + N_2	-65
(50) $CCl_3^{\bullet}$.+ NO $\longrightarrow$ $COCl_2$ + $N^{\bullet}$ + $Cl^{\bullet}$	201
(51) $CCl_3^{\bullet}$ + NO $\longrightarrow$ $COCl^{\bullet}$ + $N^{\bullet}$ + Cl_2	360

162

REACTION ΔH (k Jmol^{-1})

(52) $:CCl_2 + NO \longrightarrow COCl_2 + N^{\bullet}$ -80

(53) $:CCl_2 + NO \longrightarrow COCl^{\bullet} + N^{\bullet} + Cl^{\bullet}$ 291

(54) $:CCl_2 + NO \longrightarrow CO + N^{\bullet} + Cl_2$ 33

(55) $Cl^{\bullet} + NO \longrightarrow ClO^{\bullet} + N^{\bullet}$ 399

(56) $CCl^{\bullet} + NO \longrightarrow COCl^{\bullet} + N^{\bullet}$ -78

(57) $CCl^{\bullet} + NO \longrightarrow CO + N^{\bullet} + Cl^{\bullet}$ -5

(58) $CCl_4 + N^{\bullet} \longrightarrow CNCl + Cl_2 + Cl^{\bullet}$ -100

(59) $CCl_3^{\bullet} + N^{\bullet} \longrightarrow CNCl + Cl_2$ -408

(60) $:CCl_2 + N^{\bullet} \longrightarrow CNCl + Cl^{\bullet}$ -446

(61) $CCl^{\bullet} + N^{\bullet} \longrightarrow CN^{\bullet} + Cl^{\bullet}$ -326

(62) $CN^{\bullet} + CN^{\bullet} + M \longrightarrow (CN)_2 + M$ -538

163

decrease with the addition of hydrogen to these plasmas and an increase in the intensity of CCl^+ ions. The likely reactions are (64)-(66) in table: 38, producing HCl and consuming the CCl_x species. The hydrogen gas may also scavenge chlorine atoms in reaction (81) producing HCl.

5.4.4. Addition of Argon to CCl_4 Plasmas.

The addition of argon does not appear to alter the basic distribution of ions in the mass spectra from CCl_4 gas and plasmas. The ions are present in the same ratio as the 100% CCl_4 plasma, table: 20.

The argon metastable can provide upto 11.6eV of energy and is capable of ionising molecules with ionisation potentials less than 11.6eV (237, 238) or dissociating molecules with bond dissociation energies less than 11.6eV.

(82) $Ar + e \text{ (plasma)} \xrightarrow{11.6eV} Ar^* + e$
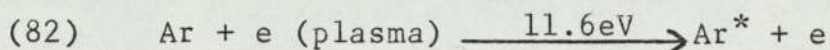
Table: 38.   Additional Reactions with Hydrogen in CCl_4 Plasmas.

REACTIONS $\qquad\qquad\qquad\qquad\qquad\qquad\qquad\qquad$ ΔH (k Jmol^{-1})

(63) $H_2 + e(plasma) \longrightarrow 2H^{\bullet}$ $\qquad\qquad$ 436

(64) $CCl_4 + H^{\bullet} \longrightarrow CCl_3^{\bullet} + HCl$ $\qquad\qquad$ -124

(65) $CCl_3^{\bullet} + H^{\bullet} \longrightarrow :CCl_2 + HCl$ $\qquad\qquad$ -151

(66) $:CCl_2 + H^{\bullet} \longrightarrow CCl^{\bullet} + HCl$ $\qquad\qquad$ -151

(67) $CCl^{\bullet} + H^{\bullet} \longrightarrow C(g) + HCl$ $\qquad\qquad$ 10

(68) $Cl^{\bullet} + H^{\bullet} + M \longrightarrow HCl + M$ $\qquad\qquad$ -432

(69) $CCl_3^{\bullet} + H^{\bullet} + M \longrightarrow CHCl_3 + M$ $\qquad\qquad$ -399

(70) $:CCl_2 + H^{\bullet} + M \longrightarrow CHCl_2^{\bullet} + M$ $\qquad\qquad$ -356

(71) $CHCl_2^{\bullet} + H^{\bullet} + M \longrightarrow CH_2Cl_2 + M$ $\qquad\qquad$ -407

(72) $CCl_3^{\bullet} + H_2 \longrightarrow CHCl_3 + H^{\bullet}$ $\qquad\qquad$ 37

(73) $CCl_3^{\bullet} + H_2 \longrightarrow :CCl_2 + HCl + H^{\bullet}$ $\qquad\qquad$ 285

(74) $CCl_3^{\bullet} + H_2 \longrightarrow CCl^{\bullet} + 2HCl$ $\qquad\qquad$ 134

(75) $:CCl_2 + H_2 \longrightarrow CHCl_2^{\bullet} + H^{\bullet}$ $\qquad\qquad$ 80

(76) $CHCl_2^{\bullet} + H_2 \longrightarrow CH_2Cl_2 + H^{\bullet}$ $\qquad\qquad$ 29

(77) $:CCl_2 + H_2 + M \longrightarrow CH_2Cl_2 + M$ $\qquad\qquad$ -327

(78) $:CCl_2 + H_2 \longrightarrow CCl^{\bullet} + HCl + H^{\bullet}$ $\qquad\qquad$ 285

(79) $CCl^{\bullet} + H_2 \longrightarrow C(g) + HCl + H^{\bullet}$ $\qquad\qquad$ 446

(80) $CHCl_2^{\bullet} + :CCl_2 \longrightarrow CHCl_2 CCl_2^{\bullet}$ $\qquad\qquad$ -317

(81) $Cl^{\bullet} + H_2 \longrightarrow HCl + H^{\bullet}$ $\qquad\qquad$ 4

165

5.5   Etching and Etch Rates

The results in table: 24, show that CCl_4 plasmas at 50W and at 0.10 and 0.15 torr etch silicon at about the same rate. At 100W and 0.15torr the etch rate of silicon in CCl_4 plasmas is about 10 times that at 50W, however undercutting, sloping edge profiles and very rough surfaces are also produced, fig: 31.

$CFCl_3$ plasmas at both 0.10 and 0.15torr give good anisotropic etching, figs: 32-34. The etch rate of silicon in $CFCl_3$ plasma at 50W is about the same as that of CCl_4. $CFCl_3$ plasmas at 0.10torr and 50W give etch rate ratios for silicon to silicon dioxide of about 2:1. This is not particularly good for selective etching of oxide over silicon but may be useful for processes where silicon, on a layer of oxide, requires etching.

At 100W and 0.15torr the etch rate ratio of CCl_4 to $CFCl_3$ plasmas etching silicon was about 2.5:1. comparing the square root of the Cl_2^+ ion intensity for CCl_4 and $CFCl_3$ plasmas gave a ratio of 1:1.3 (see section 5.2). If chlorine atoms, seen as Cl_2^+ ions in the mass spectrometer, were responsible for etching then etch rate ratios for silicon in these plasmas would have been expected to be the same ie: CCl_4: $CFCl_3$; 1:1.3 for silicon etching. However, the reverse of these etch rate ratios was observed. The only explanation for this behaviour was that some other species as well as chlorine atoms were responsible for etching the silicon.

5.6   Etching Silicon in CCl$_4$ Plasmas

It is known that chlorine atoms from Cl$_2$ plasmas are able to etch silicon (77(ix), 175, 177, 178 and 212). The mass spectrometric studies of the CCl$_4$ plasma in the presence of silicon strongly suggest that CCl$_3$ radicals are also able to etch silicon. The results in table: 25, snow that in the presence of a silicon wafer Cl$_2^+$, CCl$_3^+$, CCl$_2^+$ and CCl$^+$ ions are reduced by $\sim$50%, 13%, 16%, and 26% respectively of their intensities in CCl$_4$ plasmas without a silicon wafer. The C$_2$Cl$_5^+$, C$_2$Cl$_4^+$ and C$_2$Cl$_3^+$ ions are also reduced by about 57%, 25% and 21% respectively of their intensities in CCl$_4$ plasmas. The fact that CCl$_3^+$ ions are only reduced by 13% is probably because the main source of CCl$_3^+$ ions is from CCl$_4$ molecules in the plasma and not CCl$_3$ radicals. However, if the mechanism mentioned earlier in table: 35, is correct the large reduction in the C$_2$Cl$_x^+$ ions indicates that CCl$_3$ radicals are being consumed by some other process such as etching the silicon. The possible mechanisms for etching are shown in table: 39.

The switch-on transients of various ions were studied because of the slow rise in intensity of the SiCl$_3^+$ ion when the CCl$_4$ discharge was switched on, fig: 35. There was a strong possibility of being able to correlate this with the species which was responsible for etching silicon. Several switch-on transients were recorded, figs: 38-41, for varous ions in the mass spectrum of CCl$_4$

167

Table:39.   Etching Mechanisms in CCl_4 Plasmas.

(83) CCl_4 (g) + Si $\longrightarrow$ CCl_4 (ads)

(84) $CCl_3^{\cdot}$ (g) + Si $\longrightarrow$ $CCl_3^{\cdot}$ (ads)

(85) $:CCl_2$ (g) + Si $\longrightarrow$ $:CCl_2$ (ads)

(86) $CCl^{\cdot}$ (g) + Si $\longrightarrow$ $CCl^{\cdot}$ (ads)

(87) $Cl^{\cdot}$ (g) + Si $\longrightarrow$ $Cl^{\cdot}$ (ads)

(88) Cl_2 (g) + Si $\longrightarrow$ Cl_2 (ads)

(89) CCl_4 (ads) $\xrightarrow{\quad ions \quad}$ $CCl_3^{\cdot}$ (ads) + $SiCl^{\cdot}$ (ads)

(90) $CCl_3^{\cdot}$ (ads) $\longrightarrow$ $:CCl_2$ (ads) + $SiCl^{\cdot}$ (ads)

(91) $:CCl_2$ (ads) $\longrightarrow$ $CCl^{\cdot}$ (ads) + $SiCl^{\cdot}$ (ads)

(92) $CCl^{\cdot}$ (ads) $\longrightarrow$ C (ads) + $SiCl^{\cdot}$ (ads)

(93) $CCl_x^{\cdot}$ (ads) $\longrightarrow$ C (ads) + $SiCl_x^{\cdot}$ (ads)

(94) $CCl_x^{\cdot}$ (ads) $\longrightarrow$ $SiCCl_x^{\cdot}$ (ads)

(95) Cl_2 (ads) $\longrightarrow$ $SiCl^{\cdot}$ (ads) + $Cl^{\cdot}$ (ads)

(96) Cl_2 (ads) $\longrightarrow$ $:SiCl_2$ (ads)

(97) $SiCl_x^{\cdot}$ (ads) $\longrightarrow$ $SiCl_x^{\cdot}$ (g)

(98) $SiCCl_x^{\cdot}$ (ads) $\longrightarrow$ $SiCCl_x^{\cdot}$ (g)

(99) $SiCl_x^{\cdot}$ (g) + $Cl^{\cdot}_{(g)}$ + M $\longrightarrow$ $SiCl_{x+1}^{\cdot}$ (g) + M etc.

$\longrightarrow$ $SiCl_4$ (g).

(100) $SiCl_x^{\cdot}(g)$ + $CCl_y^{\cdot}(g)$ + M $\longrightarrow$ $SiCl_{x+1}^{\cdot}$ (g) + $CCl_{y-1}^{\cdot}(g)$ + M etc.

$\longrightarrow$ $SiCl_4$ (g)

168

plasmas etching silicon but none of these species could be correlated with the $SiCl_3^+$ or $SiCl_4^+$ switch-on transients.

There are several possible explanations of the switch-on transient studies, considering the possible mechanisms in tables: 35 and 39. The slow rise in the $SiCl_3^+$ ion intensity may be due to a surface desorption effect or surface cleaning of the silicon wafer. The $SiCl_3^+$ transient may also be related to a surface heating effect causing the desorption of species from the silicon surface at a faster rate as the temperature of the wafer rises. Alternatively the rise in temperature may give faster reaction rates causing the silicon to be etched at a faster rate. There is no doubt that the steady state $SiCl_x^+$ ion intensities in these CCl_4 plasmas is a measure of the etch rate of silicon.

If the CCl_3 radicals are responsible for etching the silicon and the mechanism of Cl_2 formation is by elimination from "hot" C_2Cl_6 (reaction (5), table: 35,) as discussed earlier then the Cl_2^+ switch-on transient might be expected to show some unusual features. For example, if the slow rise in the $SiCl_3^+$ ion intensity was due to CCl_3 radicals adsorbing onto the silicon then the Cl_2^+ ion intensity would be expected to show a maximum somewhere very close to the initial switch-on of the plasma and then a reduction in intensity as more CCl_3 radicals become involved in etching. This does not

occur, Fig: 38, and the Cl_2^+ ion intensity rises rapidly to $\sim 50\%$ of the value for the pure CCl_4 plasma. The explanation of this behaviour could be that CCl_3 radicals are rapidly adsorbed onto the silicon immediately the plasma is switched-on and hence the Cl_2 formation is much reduced to begin with. The $SiCl_x$ species simply desorb as the wafer temperature rises giving the slow transient in Fig: 35.

It is also possible that carefully loading the reactor with more silicon in steps, of say $^1/_4$ of a wafer, and observing the spectra from each successive increase in load may show a relationship between the etchant species and the area of silicon. These kind of loading effects are often reproduced for commercial reactors, although there is no reason why this should not be possible with the present system. The intensity of the ions plotted against area of silicon etched may give more information about the etching processes involved. Unfortunately it was not possible to do this in the time available.

5.6.1   Etching Silicon in CCl_4-O_2 Plasmas

The effect of adding oxygen to CCl_4 plasmas involves competition between several possible processes:-
(a) Changes in the concentration of CCl_x and Cl radicals and atoms in CCl_4 plasma as discussed earlier in section 5.4.1;

(b) Surface cleaning of the silicon wafer;

(c) SiO_2 formation on the clean silicon surfaces;

(d) Reaction of O_2 and O with $SiCl_x$ species in the gas phase.

Monitoring of $SiCl_x^+$ ion intensities is now not as straight forward as in the previous section where the steady state ion intensities were a reliable indication of the silicon etch rate. The situation is further complicated by the formation of "polymer" on the silicon surface above certain percentages of oxygen added, Fig:54.

The unusual results obtained monitoring $SiCl_3^+$ ions at 135 a.m.u. (not 133 a.m.u. because of the substantial contribution from $C_2Cl_3^+$ ions at 129 a.m.u.; see appendix E) showed that in general addition of oxygen to 0.10 torr CCl_4 plasmas reduced the intensity of these ions, fig:42. However, at 0.15torr the results appeared to show that the $SiCl_3^+$ ion intensity was enhanced up to a maximum at about 25% of oxygen added to the CCl_4 plasma. Switching off the oxygen at higher percentages (fig: 43 and 44,) and continuing to monitor the $SiCl_3^+$ ion appeared to confirm that the $SiCl_3^+$ ion intensity went through a maximum as the oxygen pumped away. There is no simple explanation for this behaviour available at present.

171

Table: 40.　　Etching Mechanisms in CCl_4-O_2 Plasmas.

(101)　O_2 (g) + Si $\longrightarrow$ O_2 (ads)

(102)　$O^{\cdot}$ (g) + Si $\longrightarrow$ $O^{\cdot}$ (ads)

(103)　$O^{\cdot}$ (ads) + CCl_4 (ads) $\longrightarrow$ $COCl_2$ (ads) + Cl_2 (ads) $\left.\right]$ etc. see

(104)　O_2 (ads) + $CCl_3^{\cdot}$ (ads) $\longrightarrow$ $COCl_2$ (ads) + $ClO^{\cdot}$ (ads) $\left.\right|$ table 36

(105)　$2O^{\cdot}$ (ads) $\longrightarrow$ SiO_2(s)

(106)　O_2 (ads) $\longrightarrow$ SiO_2 (s)

(107)　$O^{\cdot}$ (ads) + C (ads) $\longrightarrow$ CO (ads)

(108)　O_2 (ads) + C (ads) $\longrightarrow$ CO (ads) + $O^{\cdot}$ (ads)

(109)　$COCl_2$ (ads) $\longrightarrow$ CO (ads) + $2Cl^{\cdot}$ (ads)

(110)　$Cl^{\cdot}$ (ads) $\longrightarrow$ $SiCl^{\cdot}$ (ads)

(111)　CO (ads) $\longrightarrow$ CO (g)

(112)　$Cl^{\cdot}$ (ads) $\longrightarrow$ $Cl^{\cdot}$ (g)

(113)　$SiCl_x^{\cdot}$ (ads) $\longrightarrow$ $SiCl_x^{\cdot}$ (g)

(114)　$SiCl_x^{\cdot}$ (g) + O_2 $\longrightarrow$ SiO_2(s) + $XCl^{\cdot}$ (g)

(115)　$SiCl_{x(g)}^{\cdot}$ + $O^{\cdot}$ $\longrightarrow$ SiO (g) + $XCl^{\cdot}$ (g)
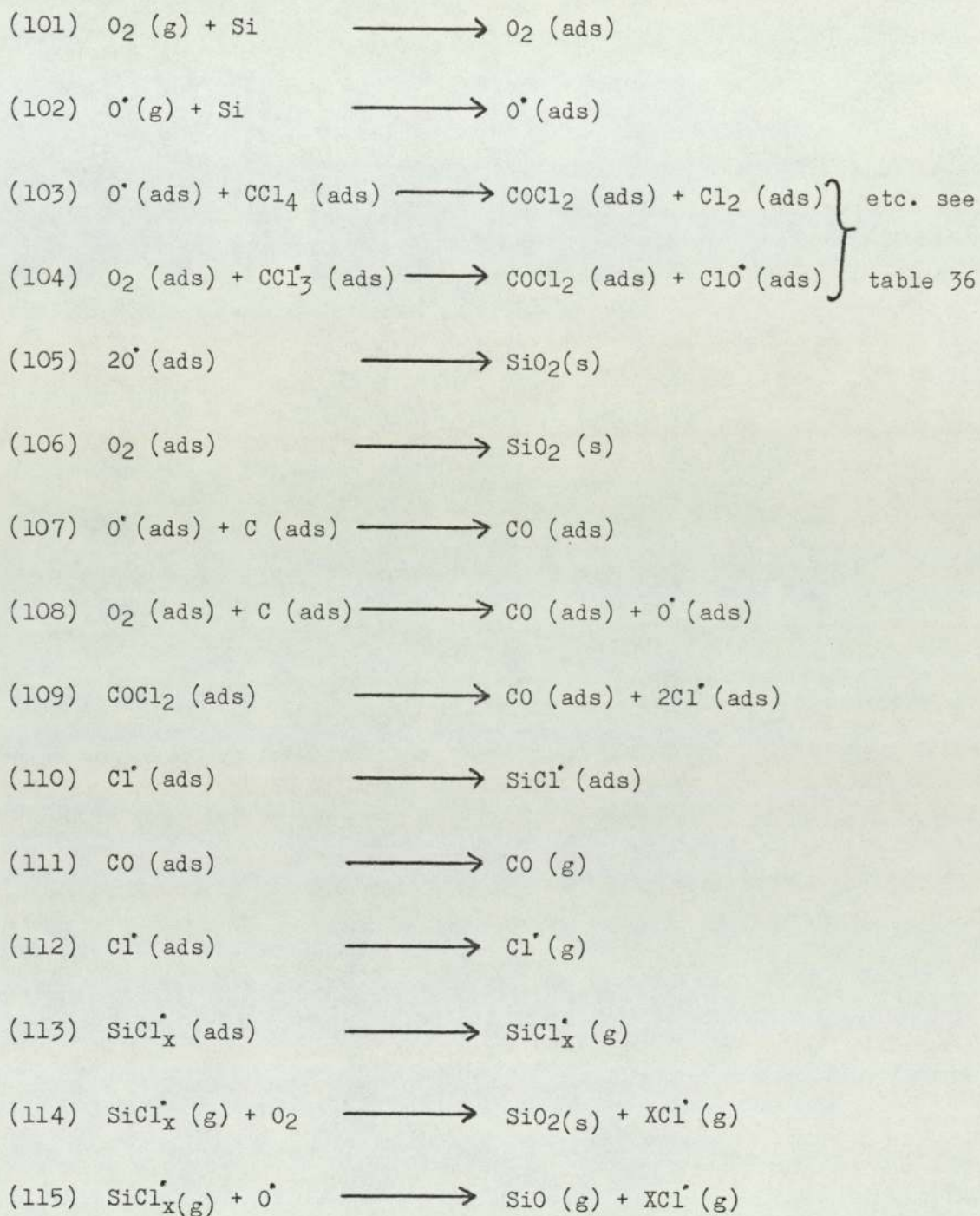
The formation of $SiO_2(s)$ may inhibit the etching process for silicon reducing the intensity of $SiCl_3^+$ ions in the mass spectrometer. However, the oxygen may also be useful for the removal of adsorbed carbon and possibly enhancing the $SiCl_3^+$ ion intensity by cleaning the silicon surface. The possible mechanisms for etching CCl_4-O_2 plasmas are shown in table: 40.

5.6.2   Etching Silicon in CCl_4-Ar Plasmas

The results of monitoring $SiCl_3^+$ ion in figs: 45, 46 and 47, show that upto 50% of argon may be added to the CCl_4 plasma enhancing the $SiCl_3^+$ ion intensity. Switching off the argon at high argon percentages and monitoring the $SiCl_3^+$ intensity showed maxima in the $SiCl_3^+$ ion intensity as the argon pumped away. Since there is no interference in the $SiCl_x$ species by reactions with the argon (c.f. oxygen) the $SiCl_x^+$ ion intensities are thought to be directly related to the etch rate of silicon.

Since addtion of argon has little effect on the ion intensities in a CCl_4 plasma (as discussed earlier in section 5.4.4.), the most likely influence on etching is the energetic argon metastable which may be able to provide additional energy to the adsorbed species on the silicon surface allowing etching reactions to occur

173

easily and quickly. Argon ions may also be involved in sputter etching tne silicon, however, this is unlikely at 0.10torr pressure because of the short mean free paths of species in the plasma resulting in relatively low ion energies.

5.7   Conclusions from CCl4 Plasma Etching

Pure CCl$_4$ plasmas have been shown to etch silicon at relatively moderate rates and the SiCl$_x^+$ ion intensities have been useful for monitoring the rate of etching. Pure CCl$_4$ plasmas have been shown to be faster etchants for silicon at higher r.f. powers. The etch rate ratio of silicon for 100W: 50W plasmas is about 10:1 at 0.15torr pressure. However, at high r.f. powers the photoresist is undercut and sloping edge profiles are produced in pure CCl$_4$ plasmas.

Addition of argon to CCl$_4$ plasmas appears to improve the etching of silicon. This suggests that these CCl$_4$/Ar plasmas are superior etchants for silicon than pure CCl$_4$ plasmas or CCl$_4$/O$_2$ plasmas.

Addition of oxygen to CCl$_4$ plasmas has a complex effect on the etching and the intensity of SiCl$_x^+$ ions is not a reliable guide to the etch rate of silicon. A number of problems were encountered with these plasmas but the main problem was the formation of "polymer" on the silicon surfaces (see section 5.8).

5.8   Polymer Formation in CCl$_4$ Plasmas.

The conditions under which "polymer" formation occurred was usually on a second run of an etching experiment on the same wafer. This was particularly bad for plasmas with oxygen added. Usually the plasma would not etch the wafer after the plasma had been switched off and the initial conditions reset and the plasma switched on for the second run on the same wafer. Cleaning the wafer in O$_2$ or Ar/O$_2$ plasmas failed to restore the normal etching behaviour previously seen on a clean silicon wafer. On several occasions polymer would form by simply adding oxygen to the plasma. Monitoring the SiCl$_3^+$ ion intensities and adding oxygen produced rapid irreversible reductions in the SiCl$_3^+$ ion intensity as shown in fig: 54. Some of these experiments were carried out for over and hour and this may have allowed the slow build up of polymer on the wafer which may have eventually prevented etching occurring.

The films deposited on the silicon from these plasmas (and CFCl$_3$ plasmas) were conductive and were shown to contain various quantities of aluminium figs: 50 and 53. the films were very dark black-blue in colour and initially this was mistaken for graphitic carbon. However, subsequent analysis showed that there was no graphitic carbon present, although carbon was present in the film, fig: 51. The films from both CCl$_4$ and CFCl$_3$ plasmas were shown to be identical and approximately

1000$\overset{\circ}{A}$ in thickness. The surface of the films was extremely rough and had "spikes" of aluminium-containing material which were somewhat different in nature to the larger part of the film surface (figs: 55 and 56). The polymer did not deposit on a glass slide placed in the discharge alongside a silicon wafer.

There are two possible mechanisms of polymer formation (a) homogeneous gas phase polymerization by radicals or (b) polymer formation from adsorbed species on the silicon surfaces.

Homogeneous gas phase polymerization mechanism:-

(116) $\quad C\overset{\bullet}{C}l_3(g) + :CCl_2(g) \quad \longrightarrow \quad C_3\overset{\bullet}{C}l_7 \ (g)$

(117) $\quad C\overset{\bullet}{C}l_3(g) + C_2Cl_4 \ (g) \quad \longrightarrow \quad C_3\overset{\bullet}{C}l_7(g)$ etc.
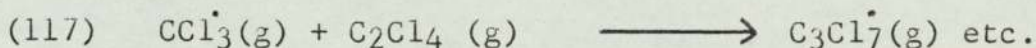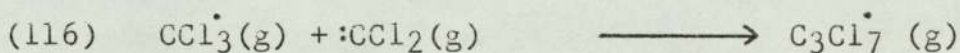
This would eventually lead to large condensable molecules which would be deposited on any surface in contact with the plasma.

Polymer formation from adsorbed species on the silicon:-

(118) $\quad C\overset{\bullet}{C}l_3 \ (ads) + :CCl_2 \ (ads) \quad \longrightarrow \quad C_2\overset{\bullet}{C}l_5(ads)$ etc.

(119) $\quad C\overset{\bullet}{C}l_3 \ (ads) + C_2Cl_4 \ (ads) \quad \longrightarrow \quad C_3 \ \overset{\bullet}{C}l_7(ads)$ etc.
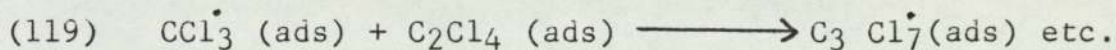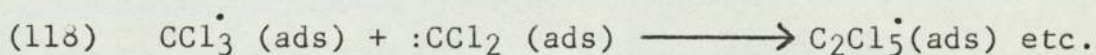
This second mechanism requires the involvement of the silicon surface which may also bond with the film to help produce involatile films.

The gas-phase mechanism probably does not occur to any appreciable extent because the same polymer material does not deposit on every surface in the plasma. The polymer was not deposited on a glass slide inserted into the plasma. A soft, light-coloured film which was deposited was completely unlike the film on the silicon wafer and was probably C_2Cl_6. The addition of oxygen and its effect on this mechanism is not clear but the oxygen would be expected to reduce the polymer formation by reacting with the CCl_x species before large molecules could be produced; see table: 36.

The mechanism involving adsorbed species on the silicon surface would account for the differences seen with the glass slide if the silicon itself was important for this type of film. For this reason this mechanism, involving adsorbed species on the silicon, is probably more plausible. The effect of addition of oxygen on this mechanism might be explained by the oxygen forming a protective layer of oxide on the silicon; table: 41. Adsorbed species would find it difficult to etch this film and consequently react with each other forming an involatile film.

Another explanation for the formation of a conductive film may be that silicon carbide, which is a semiconductor material, is formed on the silicon surface. The presence of aluminium in this film may be sufficient to act as a dopant making the silicon carbide conductive.

178

5.9   Other Gases

5.9.1.   CFCl$_3$ Plasmas

The discharges in CFCl$_3$ gave rise to a wide range of fragment ions seen in the mass spectrometer; table: 22. There were many C$_2$ and C$_3$ species formed by combination of species in the gas phase. The mechanism is expected to be similar to that for CCl$_4$ plasmas in table: 35. A possible mechanism is shown in table: 41, with the primary plasma processes being:-

$$CFCl_3 + e \text{ (plasma)} \longrightarrow CFCl_2^+, \ CFCl^+, \ CF^+, \ CCl_3^+, \ CCl_2^+,$$
$$CCl^+, \ Cl^+, \ C^+, \ F^+.$$
$$CFCl_2^-, \ CFCl^-, \ CF^-, \ CCl_3^-, \ CCl_2^-,$$
$$CCl^-, \ Cl^-, \ C^-, \ F^-$$
$$CFCl_2^{\cdot}, \ {:}CFCl, \ CF^{\cdot}, \ CCl_3^{\cdot}, \ {:}CCl_2, \ CCl^{\cdot},$$
$$Cl^{\cdot}, \ C, \ F^{\cdot}.$$
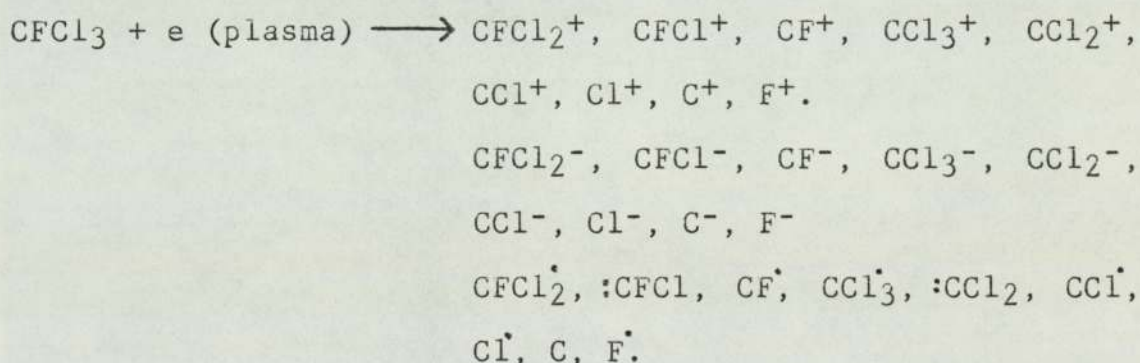
5.9.2   Addition of Oxygen to CFCl$_3$ Plasmas.

The addition of oxygen to CFCl$_3$ plasma reduces the $C_2F_xCl_y^+$ ion intensities in the mass spectrometer. The CFCl$_2^+$ and CCl$_3^+$ ion intensities are also reduced and the Cl$_2^+$ ion intensity is increased slightly with the addition of oxygen. The CO$^+$ ion intensity is increased considerably but the CO$_2^+$ ion intensity is only slightly increased and again this suggests that CO is the main product of the reaction of oxygen species with the

Table: 41.   Processes in $CFCl_3$ Plasmas.

(120) $CFCl_2^{\bullet} + CFCl_2^{\bullet} + M \longrightarrow C_2F_2Cl_4 + M$

(121) $CFCl_2^{\bullet} + CCl_3^{\bullet} + M \longrightarrow C_2FCl_5 + M$

(122) $CCl_3^{\bullet} + CCl_3^{\bullet} + M \longrightarrow C_2Cl_6 + M$

(123) $:CFCl + :CFCl + M \longrightarrow C_2F_2Cl_2 + M$

(124) $:CFCl + :CCl_2 + M \longrightarrow C_2FCl_3 + M$

(125) $:CCl_2 + :CCl_2 + M \longrightarrow C_2Cl_4 + M$

(126) $CFCl_2^{\bullet} + :CFCl + M \longrightarrow C_2F_2Cl_3^{\bullet} + M$

(127) $CFCl_2^{\bullet} + :CCl_2 + M \longrightarrow C_2FCl_4^{\bullet} + M$

(128) $CCl_3^{\bullet} + :CFCl + M \longrightarrow C_2FCl_4^{\bullet} + M$

(129) $CCl_3^{\bullet} + :CCl_2 + M \longrightarrow C_2Cl_5^{\bullet} + M$

(130) $C_2F_2Cl_3^{\bullet} \longrightarrow C_2F_2Cl_2 + Cl^{\bullet}$

(131) $C_2F_2Cl_3^{\bullet} \longrightarrow C_2FCl_3 + F^{\bullet}$

(132) $C_2FCl_4^{\bullet} \longrightarrow C_2FCl_3 + Cl^{\bullet}$

(133) $C_2FCl_4^{\bullet} \longrightarrow C_2Cl_4 + F^{\bullet}$

(134) $C_2Cl_5^{\bullet} \longrightarrow C_2Cl_4 + Cl^{\bullet}$

(135) $C_2F_2Cl_4 \longrightarrow C_2F_2Cl_2 + Cl_2$

(136) $C_2F_2Cl_4 \longrightarrow C_2FCl_3 + ClF$

(137) $C_2F_2Cl_4 \longrightarrow C_2Cl_4 + F_2$

(138) $C_2FCl_5 \longrightarrow C_2FCl_3 + Cl_2$

(139) $C_2FCl_5 \longrightarrow C_2Cl_4 + ClF$

(140) $C_2F_2Cl_2 \longrightarrow C_2F_2 + Cl_2$

Table: 41.   Continued.

(141) $C_2F_2Cl_2$ $\longrightarrow$ $C_2FCl + ClF$

(142) $C_2F_2Cl_2$ $\longrightarrow$ $C_2Cl_2 + F_2$

(143) C_2FCl_3 $\longrightarrow$ $C_2FCl + Cl_2$

(144) C_2FCl_3 $\longrightarrow$ $C_2Cl_2 + ClF$

(145) C_2Cl_4 $\longrightarrow$ $C_2Cl_2 + Cl_2$

(146) $C_2F_2Cl_3^{\bullet} + :CFCl$ $\longrightarrow$ $C_3F_3Cl_4^{\bullet}$

(147) $C_2F_2Cl_3^{\bullet} + :CCl_2$ $\longrightarrow$ $C_3F_2Cl_5^{\bullet}$

(148) $C_2F_2Cl_3^{\bullet} + F^{\bullet} + M$ $\longrightarrow$ $C_2F_3Cl_3 + M$

(149) $C_2F_2Cl_3^{\bullet} + Cl^{\bullet} + M$ $\longrightarrow$ $C_2F_2Cl_4 + M$

(150) $C_2FCl_4^{\bullet} + :CFCl$ $\longrightarrow$ $C_3F_2Cl_5^{\bullet}$

(151) $C_2FCl_4^{\bullet} + :CCl_2$ $\longrightarrow$ $C_3FCl_6^{\bullet}$

(152) $C_2FCl_4^{\bullet} + F^{\bullet} + M$ $\longrightarrow$ $C_2F_2Cl_4 + M$

(153) $C_2FCl_4^{\bullet} + Cl^{\bullet} + M$ $\longrightarrow$ $C_2FCl_5 + M$

(154) $CFCl_2^{\bullet} + F^{\bullet} + M$ $\longrightarrow$ $CF_2Cl_2 + M$

(155) $CFCl_2^{\bullet} + Cl^{\bullet} + M$ $\longrightarrow$ $CFCl_3 + M$

(156) $:CFCl + F^{\bullet} + M$ $\longrightarrow$ $CF_2Cl^{\bullet} + M$

(157) $CF_2Cl^{\bullet} + F^{\bullet} + M$ $\longrightarrow$ $CF_3Cl + M$

(158) $CFCl_3^{\bullet} + F^{\bullet}$ $\longrightarrow$ $CF_2Cl_2 + Cl^{\bullet}$

(159) $CF_2Cl_2 + F^{\bullet}$ $\longrightarrow$ $CF_3Cl + Cl^{\bullet}$

(160) $Cl^{\bullet} + F^{\bullet} + M$ $\longrightarrow$ $ClF + M$

(161) $F^{\bullet} + F^{\bullet} + M$ $\longrightarrow$ $F_2 + M$

(162) $Cl^{\bullet} + Cl^{\bullet} + M$ $\longrightarrow$ $Cl_2 + M$

181

species present in the CFCl$_3$ discharge. The basic processes with the addition of oxygen are not expected to be different from the addition of oxygen to CCl$_4$ plasmas (see table: 36.).

5.9.3   Etching Silicon in CFCl$_3$ Plasmas

The mass spectrometric results in table: 31 do not clearly show that silicon-containing species were present in the discharge. The overlap of the silicon-containing ions with the normal fragments from the CFCl$_3$ plasma made it difficult to determine whether etching was taking place.

The absence of SiCl$_4^+$ ions in the spectra suggest that either etching was not occurring (or was much reduced) or that SiCl$_4$ was not an important product of the etching process. However, by comparing the relative intensities of the ions at 85 and 87 a.m.u. (SiF$_3^+$ and CF$_2$Cl$^+$) in the CFCl$_3$ discharge with and without a silicon wafer present it was possible that some SiF$_3^+$ ions (at 85 a.m.u.) were present with a silicon wafer in the discharge. The Cl$_2^+$ ion intensity was reduced by $\sim$26% in the presence of a silicon wafer. The F$^+$ ion intensity was also reduced.

5.9.4 Etching in SiCl$_4$ Plasmas

The unusual results in figs: 48 and 49, obtained attempting to etch patterned silicon in a SiCl$_4$ discharge were thought to be due to the deposition of a silicon film on the photoresist. The chlorine from the SiCl$_x$ species might be expected to react with the carbon or hydrogen in the photoresist forming volatile materials and leaving the involatile silicon on the photoresist surface. For example:-

$$(161) \quad SiCl_x(g) + (C,H)_N \longrightarrow Si(s) + CCl_x(g); \ XHCl(g)$$
$$\text{photoresist.}$$
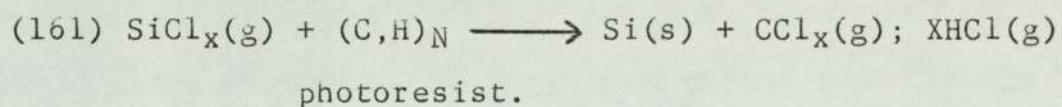
These results are in contrast to those of Sato and Nakamura (198) where SiCl$_4$ plasmas were reported to etch single crystal silicon at $\sim 15\overset{\circ}{A}$ min^{-1}, at ~ 0.06 torr pressure.

6.   Conclusions

A molecular beam mass spectrometer system has been designed, built and tested and used to study the reactive gas plasmas used in semiconductor integrated circuit manufacture. Some preliminary results have been obtained from CCl_4 and $CFCl_3$ plasmas etching silicon. These results suggest that CCl_3 radicals are probably responsible for etching silicon in CCl_4 plasmas.

"Polymer" film formation was found to be a major problem in the present reactor system, probably due to the low gas flow rates through the reactor. "Polymer" film formation was particularly marked in CCl_4-O_2 plasmas. Aluminium, etched from the r.f. electrodes, was also incorporated into these conductive films.

$CFCl_3$ plasmas, which have not been previously used to etch semiconductor materials, have been shown to be an anisotropic etchant for both silicon and silicon dioxide. The etch rate ratio for $Si:SiO_2$ in $CFCl_3$ plasmas was about 2.5:1. However, more work is needed to reveal the etching species and the major etch products from these plasmas.

A better design of reactor, capable of much higher gas flow rates, and a larger capacity pumping system is required. A throttle valve would then be required to allow a range of pressure and flow rates to be obtained in the reactor. New ways of eliminating r.f. interference should be incorporated into any new reactor design where possible.

APPENDIX A — THE EVENT PEN INTERFACE

Owing to the incompatibility of the event marker pen on the Bryans Southern 28000 chart recorder and the event driver circuitry in the Bentham Instruments SMD10S monochromator controller, the circuit in FIG:59 was designed and constructed on a small printed circuit board. The SMD10S output transistor provided insufficient short circuit to drive the event solenoid in the chart recorder. This solenoid required a short-circuit between 0 volts and -15 volts. Unfortunately, a residual resistance of 3KΩ remained on the output transistor so that the solenoid did not latch and the event pen remained motionless.

The circuit for the interface contains a dual comparator, the CA3290, (of which only half is used), a small d.i.l. reed relay, and a l.e.d. which flashes with the event pulses as the d.i.l. reed relay latches. The circuit operates by detecting a negative pulse at pin 3 (non-inverting input) with respect to pin 2 (inverting input) as the output transistor of the SMD10S switches on. This results in the output (pin 1) of the comparator going negative and allowing the l.e.d. and relay coil to pass sufficient current to latch the reed relay. If the event pen solenoid is connected to the reed relay terminals then it will be shorted, so operating the event pen and placing a calibration mark on the chart paper. When the transistor in the SMD10S switches off the 1MΩ

186
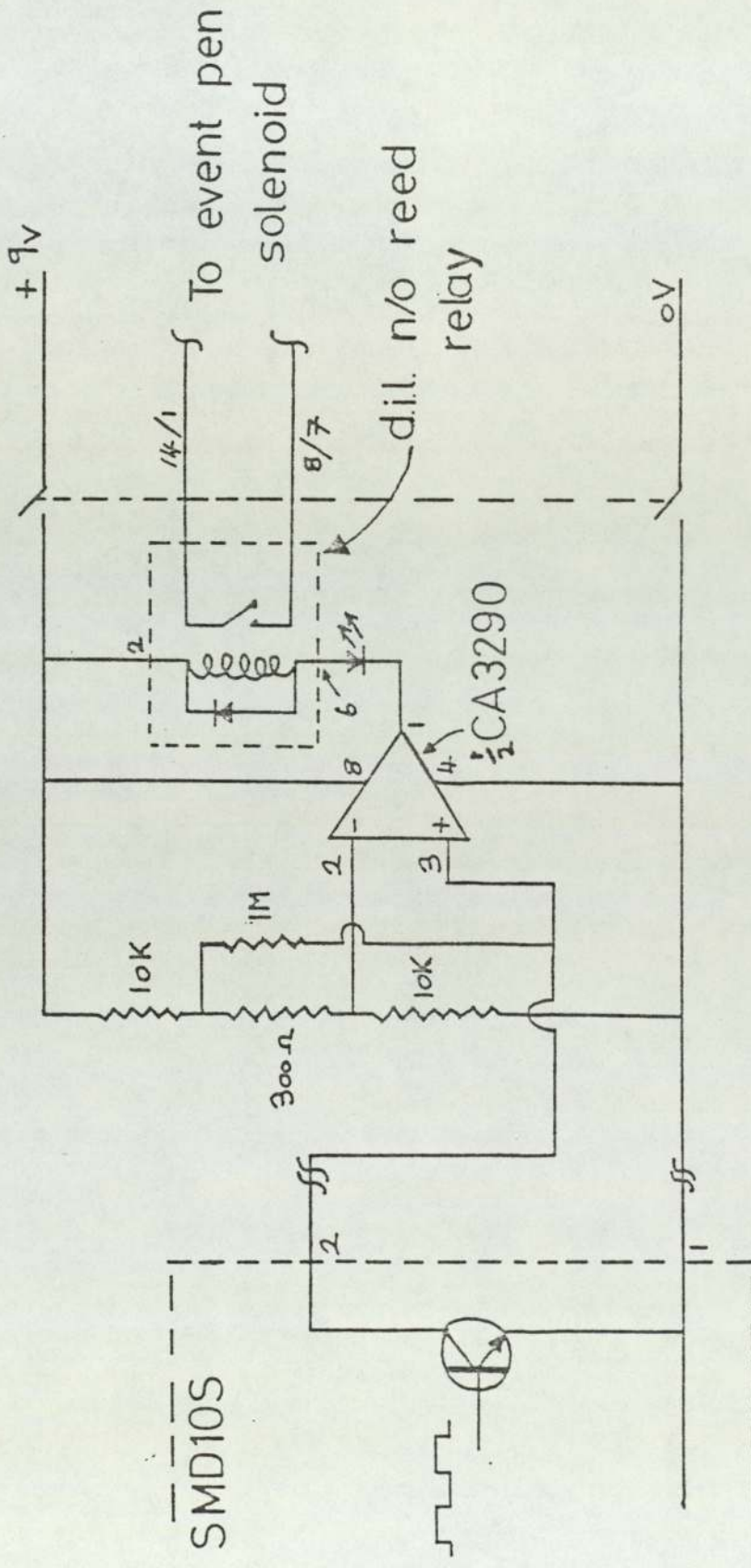
Fig:59. Event pen interface.

186(a)

resistor resets the comparator by providing a positive bias voltage to pin 3 compared to pin 2 and hence switches the l.e.d. and reed relay off as the output (pin 1) goes positive. The circuit can easily be supplied from a small 9 volt battery for six months of continuous use.

I should like to thank Mr. J.R. Cotton for his help in designing this circuit and the loan of a good quality CA3290 dual comparator.

APPENDIX B - THE X-Y PLOTTER INTERFACE

In order to display appearance potential curves in full and in detail an interface was required which could accept signals of up to -70 volts and give an output of + 2.5 volts @ 1ma for the X axis drive.

The Y axis drive only required a pulse generator for calibrating the X axis, as sufficient attenuation and amplification were available on the mass spectrometer (V.G. model QX2001) output and the X-Y plotter inputs. Also an on/off switch was fitted to the Y input to allow the mass spectrometer to scan the spectrum without interfering with the plotter.

The Bryans 21000 series X-Y plotter had sensitivities of 1,10,100 $mVcm^{-1}$ with a variable multiplication factor of 0.4 to 4 times each switched range. The X-Y plotter produced plots on sheets of A4 size paper, normally A4 size graph paper with 1,5 and 10mm scales was used for convenience.

The circuit of FIG:60 was designed using operational amplifier techniques. The circuit is a simple attenuator with switched ranges and a variable offset control arranged to be + 20 volts on each range. The ranges covered are 0 to -100, 0 to -50, 0 to -20 volts. These ranges with offset and with attenuation and zeroing on the X-Y plotter allow any part of the Appearence potential curves to be reproduced.

I should like to thank Mr. J.R. Cotton for his initial design ideas and helpful suggestions.
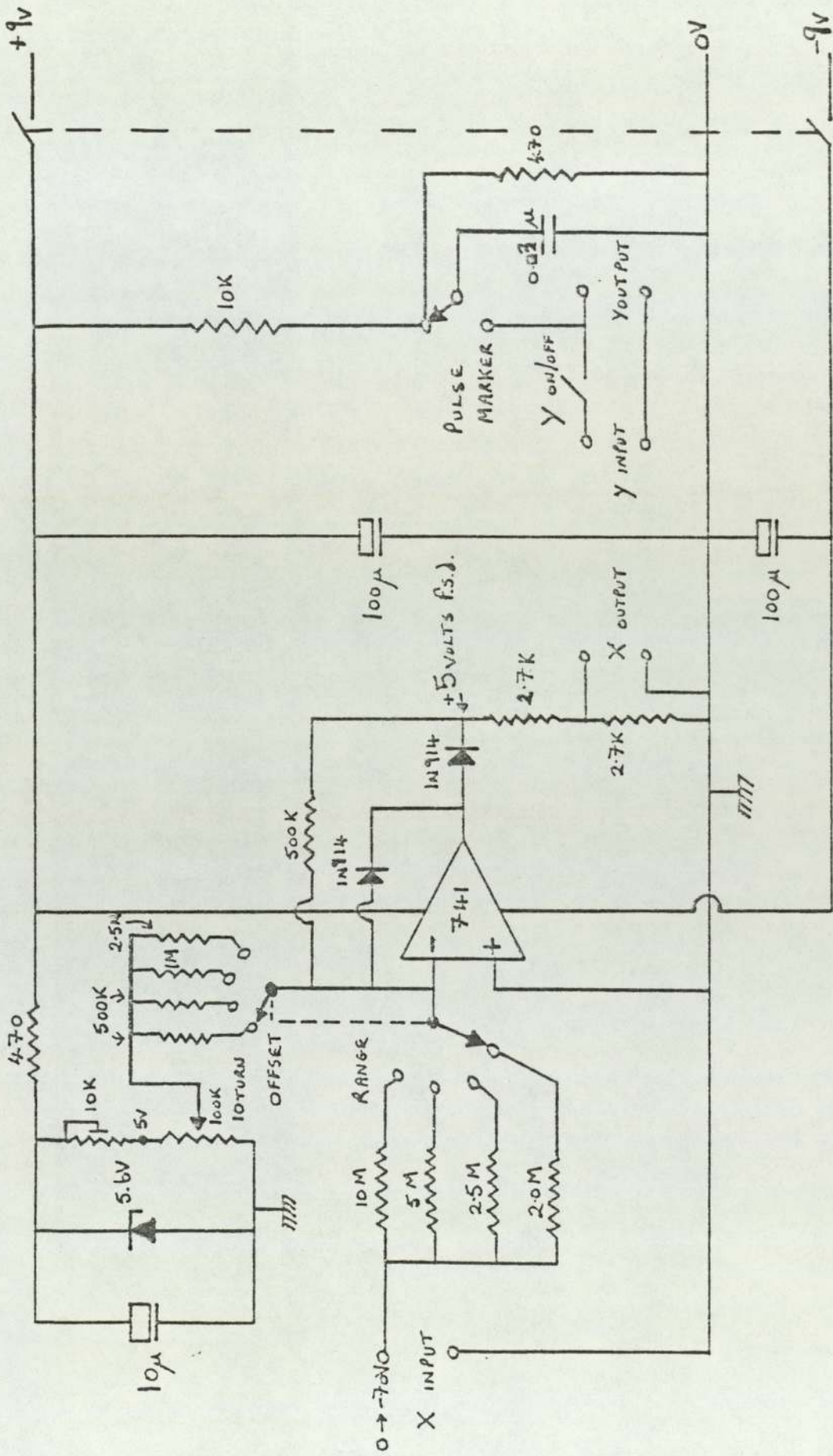
Fig.60. X~Y plotter interface

188(a)

Appendix C.   Molecular   Velocities,   Mean   free   Paths,
                Effusion   Rates,   Gas   Densities   and
                Conductances.

(i)   Gas Densities

$$\rho = \frac{n.L}{V} = \frac{L}{R.T.} \quad \frac{P}{760} \quad \text{molecules cm}^{-3} \quad \text{(if P is torr)}$$

$$\underline{\rho = 3.22 \times 10^{16} \text{ P}} \quad \text{molecules cm}^{-3} \text{ (P is in torr)}$$

where ρ = gas density in molecules cm^{-3}

   L = Avogadro's number

   R = Gas constant and is 82.053 cm^3 atm K^{-1} mol^{-1}

   T = temperature

   P = Pressure in torr

(ii)   Molecular Velocity

$$\overline{C} = \left(\frac{8 K T}{\pi m} \right)^{1/2} = \frac{2521}{m} \quad ms^{-1}$$

where m = molecular mass

   k = Boltzmann Constant

$\overline{C}$ (Ar)   = 399 ms^{-1} $\overline{C}$ (H_2) = 1782 ms^{-1}

$\overline{C}$ (CF_4) = 269 ms^{-1} $\overline{C}$ (N_2) = 476 ms^{-1}

$\overline{C}$ (CCl_4) = 203 ms^{-1} $\overline{C}$ (O_2) = 445 ms^{-1}

at 300K.

(iii)   Mean Free Path

$$\lambda = \frac{kT}{\sqrt{2}.\pi\,\sigma^2 P} = 5.69 \times 10^{-5}/P \text{ m. (P is in torr)}$$

where is σ = collision diameter $\simeq 3.5 \times 10^{-10}$ m at 300K

(note P is in torr = 1mm Hg = 133.3 Nm^{-2})

σ(Ar) = 3.96×10^{-10}m

σ(N$_2$) = 3.74×10^{-10}m

σ(O$_2$) = 3.57×10^{-10}m

σ(H$_2$) = 2.73×10^{-10}m   at   300K

(iv)   Effusion Rate

$$-\frac{dN}{dt} = R_{eff} = \frac{1}{4} . \bar{C} \text{ As } n_s \quad \text{molecules s}^{-1}$$

where $-\dfrac{dN}{dt}$ = R_{eff} = effusion rate.

N = number of molecules in the source.

As = Area of pinhole (source)

n_s = number density of molecules in the source.

(v)   Pumping Speed of Pinhole System

Let N = total number of molecules in the reactor volume, V, at pressure P, and temperature T then:-

$$N = L \frac{PV}{RT} \qquad\qquad\qquad \text{eqn. A}$$

190

Let n_s = number density of molecules in the source (reactor)

$$n_S = \frac{N}{V} = \frac{L.P}{RT} \qquad \text{eqn. B}$$

and effusion rate is (in a sealed volume):-

$$- \frac{dN}{dt} = \frac{1}{4} \bar{C} As\, n_s \qquad \text{eqn. C}$$

Therefore from equation A and B, C becomes

$$- \frac{dP}{dt} = \frac{\bar{C}As}{4V} P \qquad \text{equ. D}$$

A plot of $\frac{1}{P} \frac{dP}{dt}$ against P should be linear with slope $\frac{\bar{C}As}{4V}$

Rearrangement and integration of equation D gives.

$$\int - \frac{dP}{P} = \int \frac{\bar{C}As}{4V} \qquad \text{equ. E}$$

$$\ln \left(\frac{P^\circ}{P} \right) = \frac{cAs}{4V} t \qquad \text{equ. F}$$

A plot of $\ln (P^\circ/P)$ against t should be linear and have a slope of $\bar{c}As/4V$. However, for the pinhole system described in section 3.1.4 this plot was not linear but a curve which over short ranges was approximately linear. A polynominal was fitted to the curve using a computer package program available on Aston University's I.C.L. 1904 computer. The same program was used on the pressure against time plot and a polynominal fitted to this curve also.

191

(vi)   Conductances

It was found instructive to consult several standard texts and calculate the conductances of various parts of the apparatus (239,240). In particular the conductance for an annular space was useful.

$$\frac{1}{Fe} = \frac{3}{8} \frac{4}{V} \frac{\ell}{\pi(a_2{}^2-a_1{}^2)(a_2-a1)} \frac{1}{\sqrt{\frac{28\cdot98}{m}} \cdot \sqrt{\frac{T}{273}}} \quad cm^{-3}sec$$

that is

$$Fc = 9700 \; \pi \, (a_1-a_2)^2(a_2+a_1) \; \frac{1}{\ell} . \sqrt{\frac{T}{m}} \quad cm^3 s^{-1}$$

where

V = average molecular velocity (see $\bar{c}$, molecular velocity , (ii)) cm s^{-1}

a_1= inside radius of inner tube in cm.

a_2= inside radius of outer tube in cm.

ℓ = total length of annular space in cm.

This assumes negligible wall thickness for the inner tube compared to a_1. However, this can be corrected for by using the outer radius. There are two annular spaces in the system discussed in sections 3.1.3 and 3.1.4. The space around the top hat assembly and the reactor flow tube.

192

(a) Annular Space between the top hat and housing.

a_1 = 4.5 cm (outer dimension, radius of top hat) a_2= 5.0cm
l = 13.0 cm.   Therefore, F_c = 1.75 x 10^4 cm^3 s^{-1} for air at 298 k.

(b) Reactor Flow tube annular space, inside tube and side tubes.

   (i) annular space a_1=3.5cm, a_2=4.25cm, l=29.5cm

$$F_1 = 1.44 \times 10^4 \text{ cm}^3 \text{ s}^{-1}$$

$$\frac{1}{F_1} = 6.92 \times 10^{-5} \text{ scm}^{-3}$$

(ii) For inside tube a=3.25cm l=41.0cm l/a=12.6, K=0.176
   K is obtained from Dushman's tables. For a tube:-

$$F_2 = KF\circ \text{ where } F\circ = 36.66 \text{ } a^2 \text{ } l\text{s}^{-1}$$
$$F_2 = 6.8 \times 10^4 \text{ cm}^3 \text{ s}^{-1}$$

$$\frac{1}{F_2} = 1.47 \times 10^{-5} \text{ scm}^{-3}$$

(iii) For the side tube a=1.27cm, l=30.0 cm (to vacuum pumps)

$$l/a = 24 \quad K = 0.1 \quad F\circ = 36.66a^2 \text{ } l\text{s}^{-1}$$
$$F_3 = KF\circ$$
$$F_3 = 5.9 \times 10^3 \text{ cm}^3 \text{ s}^{-1}$$

$$\frac{1}{F_3} = 1.7 \times 10^{-4} \text{ scm}^{-3}$$

Hence,

$$\frac{1}{F_{TOTAL}} = \frac{1}{F_1} + \frac{1}{F_2} + \frac{1}{F_3}$$

$$F_{TOTAL} = 3.9 \times 10^3 \text{ cm}^3 \text{ s}^{-1}$$

$$F_{1,2} = 1.2 \times 10^4 \text{ cm}^3 \text{ s}^{-1}$$

It is clear from these conductance calculations that the connecting, 2.54cm (1") diameter, tube is the main constriction to the flow of gas through the reactor system.

APPENDIX D   MOTIONS OF ELECTRONS AND IONS IN GASES

(a)   Collision Probabilities (see ref. 202)

The probability of Collision Pc is defined as the fraction of particles seattered out of a collimated beam per centimeter path per millimeter pressure at 0°C. Similarly the "probability" of any event occurring on collision, such as excitation Px or ionisation Pi, is the fraction of particles suffering that event per centimeter path and millimeter pressures. The probability P is related to the cross section q, by:-

$$P = \frac{Lq}{760} \quad cm^{-1} \quad (mm\ Hg)^{-1}$$

where L is Loschmidt's number, or

$$P = 3.5357q$$

where q is in square Angstrom units. The mean free path ℓ is given by

$$\ell = \frac{1}{P_0} \cdot P \quad cm$$

and the mean free time T by

$$\frac{1}{T} = \frac{v}{l} = 5.93107 \times 10^7\ u^{0.5}\ p_0\ P \quad sec^{-1}$$

Here $u = mv^2/2e$ is the energy in electron volts, and $p_0 = 273.16p/T$ is the "reduced" pressure in millimeters of mercury (Torr). p_0 does not express a pressure, but a concentration

$$\frac{N}{V} = 3.5357 \times 10^{16} \, p_o \text{ molecules cm}^{-3}$$

Cross sections are sometimes given in units of $\pi a_o^2 = 0.87981 \, A^2$, and energies in Hartree units, $K^2 = V/13.605$.

If $q(\theta)$ is the differential cross section for elastic scattering into unit solid angle at an angle θ to the incident direction,

$$qc = \int q(\theta) \, 2\pi \, \sin \theta \, d\theta$$

A more important quantity is the cross section for momentum transfer.

$$qm = \int q(\theta) \, (1-\cos \theta) \, 2\pi \, \sin \theta \, d\theta$$

In general, $qm \leqslant qc$; experimental values of Pc should be "corrected" to Pm in all gas discharge applications.

(b)   Average Motions of Electrons and Ions

The drift velocity vd of a charged particle of mass m and charge e in a gas of molecules of mass M, under an electric field $\vec{E}$, is given by

$$vd = e \, \vec{E}. \, \frac{M + m}{Mm} \int \ell \, \frac{\partial f}{\partial v} \, \frac{4\pi}{3} \, v^2 \, dv$$

where f(v) is the velocity - distribution function.

196

For particles with a constant mean free time Tc this yields for all $E/_p$,

$$\vec{vd} = \frac{M + m}{Mm} \, eETc$$

If collisions are caused by a polarization force

$$Tc = \frac{1.8096 \, \varepsilon_o}{eNg} \left(\frac{Mm \, /\alpha}{M + m} \right)^{1/2}$$

where the polarizability $\alpha = (\varepsilon - \varepsilon_o)/N_g$

For particles with a constant mean free path ℓ_c (rigid spheres) there are two limiting forms:

1. Near thermal equilibrium,

$$\vec{vd} = \frac{3eE\ell_c}{8} \left(\frac{\pi}{2KT} \cdot \frac{M+m}{Mm} \right)^{\frac{1}{2}}$$

$$\alpha = \begin{cases} 0.8973 & \text{for } m \ll M \\ 0.9643 & \text{for } m = M \\ 1 & \text{for } m \gg M \end{cases}$$

The mobility μ in a mixture of gases a,b,c,.....is given by Blanc's law

$$\frac{1}{\mu} = \frac{1}{\mu_a} + \frac{1}{\mu_b} + \frac{1}{\mu_c} + \ldots\ldots$$

197

where μ_a, μ_b, μ_c,... are the mobilities in the pure gases a,b,c,... at their partial pressures p_a, p_b, p_c,... provided the mobilities are sensibly independent of field strength.

Because of charge transfer when moving in the parent gas and clustering in the presence of an attaching gas, ions may move considerably more slowly than indicated by these equations.

In the case of a constant mean free time Tc, the mobility in an a.c. electric field of circular frequency and in the presence of a magnetic field whose component perpendicular to the electric field is $B_\perp$, is given by

$$ \mu = \frac{e/2m}{V_c + j(w + wb)} + \frac{e/2m}{V_c + j(w - wb)} $$

where $wb = B_\perp e/m$ is the cyclotron frequency.

The complex conductivity of a plasma is given by

$$ \sigma = n+e\mu+ + ne\mu- + j w \varepsilon_o $$

For a completely ionised plasma

$$\sigma = \frac{1.1632m}{z \ln (q-1)} \left(\frac{4\pi\varepsilon_o}{e} \right)^2 \left(\frac{2kT}{m} \right)^{3/2}$$

$$= \frac{19,141}{z \ln (q-1)} \left(\frac{kT}{e} \right)^{3/2} \quad \text{mho m}^{-1}$$

where $q=12\pi . n . \lambda_D^3$, $\lambda_D^2 = \varepsilon_o kT/ne^2$ is the Debye length, and $n\lambda_D^2 = 3.134 \times 10^4$ T m^{-1}. Z is the charge on the ions.

If λ is the mean fraction of the energy difference which is transferred in a collision, the mean energy of an electron or ion is given by

$$\frac{1}{2} m\bar{v}^2 = \frac{3}{2} kT + eE\tau_c v_d$$

For elastic collisions

$$\lambda = \frac{2Mm}{(M+m)^2}$$

For the mean free time case

$$\frac{v_d^2}{\bar{v}^2} = \frac{M+m}{2M} \lambda \left(1 - \frac{3kT}{m\bar{v}^2} \right)$$

Mean energies are usually determined by the approximate relation

$$\frac{D}{\mu} = \frac{m (\bar{v}^2 - v_d^2)}{3e}$$

which is exact when the distribution function is Maxwellian.

The diffusion coefficient is given by

$$D = \int \frac{\ell v}{3} f 4\pi v^2 . dv$$

199

(c)   <u>Electron Loss Processes</u>   (203)

The most important loss of electrons from a discharge
is recombination of electrons and ions. Usually a gas
discharge contains molecular ions (even in the inert
gases, diatomic molecular ions exist stably), and the
reaction process is dissociative recombination.

$$e + AB^+ \xrightarrow{\quad kc \quad} A + B$$
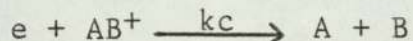
The process is strictly two-body, since the two products
can conserve energy and momentum, and the rate of
electron density loss can be described by

$$\frac{dne}{dt} = -\alpha d \, ne \, n_+$$

where αd is the dissociative recombination coefficient,
values of which are typically of the order of 10^{-7} cm^3
sec^{-1}. Since the plasma is almost electrically neutral,
the electron and ion densities are almost equal, hence

$$\frac{dne}{dt} = -\alpha d \, ne^2$$

At number densities of the order of 10^{10}cm^{-3}, the
lifetime of an electron against recombination is about a
millisecond.

It is suggested that

$$\frac{dne}{dt} = Ie - kc \, ne \, n_+ = 0$$

at stationary state conditions, where Ie is the electron current through the discharge and kc is the recombination constant. Then, if ne=n+(as above)

$$ne = \left(\frac{Ie}{kc}\right)^{1/2}$$

Values for kc may be available in the literature.

Appendix E   Natural Abundances of Chlorine

MASS	Number of chlorine atoms				
	1	2	3	4	5
A	100.0	100.0	100.0	76.9	61.5
A + 2	32.5	65.0	97.5	100.0	100.0
A + 4		10.6	31.7	48.7	65.0
A + 6			3.4	10.5	21.1
A + 8				0.9	3.4
A + 10					0.2

This table is reproduced from table: A-2 in ref: 216.

APPENDIX F   Heats of Formation

Species	Heat of formation $kJ\,mol^{-1}$
CO	-110.5
CO_2	-393.5
HCl	-92.3
CCl_4	-106.7
C_2Cl_6	-141.4
C_2Cl_4	-14.2
$COCl_2$	-223
N_2O	-81.5
$CHCl_3$	-101.3
H	218
O	249.2
Cl	121.3
CCl_3	79.5
CCl_2	239
CCl	398
C_2Cl_5	33
$COCl$	-64
ClO	138
C_3Cl_7	-13.5
ClO_2	103.3
Cl_2O	76.1
N	472.7
CN	423
$CHCl_2$	100.8
CF_2Cl	-269
$CFCl_2$	-96
$CHCl_2CCl_2$	23
NO	90.4
$CNCl$	144.3
CH_2Cl_2	-88
CH_3Cl	-82
C_2N_2	308

REFERENCES

1. "Roddy, D.; "Introduction to Microelectronics"; 1970, Pergamon press.

2. Warner, Jr, R.M. and Fordemwalt, J.N. eds, "Integrated Circuit Design and Fabrication", (Motorola Inc.) McGraw-Hill 1965.

3. Gise, P.E. and Blanchard, R.;, "Semiconductor and Integrated Circuit Fabrication Techniques" - Fairchild Corporation - 1979, Reston Publishing Company Inc.,

4. Barbe, D.F.; ed. "Very Large Scale Integration - Fundamentals and Applications"; Springer series in Electrophysics Vol. 5. 1980, Springer-Verlag.

5. Poulsen, R.G.; J. Vac. Sci. Technol., 1977, 14, 266-274.

6. Holland, L.; J.Vac. Sci. Technol., 1977, 14, 5-15.

7. Somekh, S.; IBID., 1976, 13, 1003-1007.

8. Hollahan, J.R. and Bell, A.T.; "Techniques and Applications of Plasma Chemistry". 1974, Wiley, New York.

9. Curran, J.E.; J.Vac. Sci. Technol., 1977, 14, 108-113.

10. Libby, W.F.; J.Vac. Sci. Technol., 1979, 16, 414-7.

11. Coburn, J.W. and Winters, H.F., IBID., 1979, 16, 391-403.

12. Lehmann, H.W. and Widmer, R., IBID., 1980, 17, 1177-83.

13. Bruning, J.H.; IBID., 1980, 17, 1147-1155.

14. Kramer, R.P. ed. Proceedings Int. Conf. on Microlithography, "Microcircuit Engineering 80" held in Amsterdam 30th. Sept - 2nd Oct. 1980; Delft University press 1981, Delft University of Technology.

15. Hughes, H.G. and Rand, M.J. eds., "Etching for pattern definition", 1976, Symposium publication. The Electrochem. Soc. Inc.,

16. Huff, H.R. and Sirtl, E. eds., "Semiconductor Silicon, 1977". Proc. 3RD. Int. Symp. on Silicon Materials Science and Technology. Electrochem. Soc. softbound Symp. Series, Princeton, N.J. 1977.

17. Deal, B.E. and Early, J.M., J.Electrochem. Soc., 1979, 126, 20C - 32C.

18. Bondur,J.A.; J.Vac. Sci. Technol., 1976, 13, 1023-1029.

19. Jinno, K.; Kinoshita, H. and Matsumoto,Y., J.Electrochem. Soc. 1977, 124, 1258-1262.

20. Reisman,A.; Berkenblit,M.; Chan, S.A.; Kaufman,F.B. and Green, D.C., IBID., 1979, 126, 1406-1415.

21. Veprek,S. and Venugopalan,M. eds, "Plasma Chemistry" Topics in current chemistry, 94 (Vol III), Springer - Verlag 1980.

22. Gleit, C.E.; p232 in "Chemical Reactions in Electrical Discharges" Advances in Chemistry Series 80, A.C.S., 1969, ed. Gould,R.F.

23. McTaggart,F.K., "Plasma Chemistry in Electrical Discharges." Elsevier Publishing Company. 1967.

24. Flamm, D.L., The U.T.l. Journal, 1981, 3, 1-8.

25. Bunyard, G.B. and Raby, B.A., Solid State Technol., 1977, 20 (12), 53-57.

26. Raby, B.A., J.Vac. Sci. Technol. 1978, 15, 205-208.

27. Lin, K.C. and Burden, J.D., IBID., 1978, 15 373-376.

28. Hayhurst, A.N. and Padley, P.J., Trans. Faraday Soc. 1967, 63, 1620-1630.

29. Bohme, D.K. and Goodings, J.M., J.Appl. Phys. 1966, 37, 4261-4268.

30. Kohout, F.C. and Neiswender, D.D., Int. J. Mass Spectrom. Ion Phys., 1970, 4, 21-36.

31. Vasile, M.J. and Smolinsky, G., IBID., 1973, 12, 133-146 (Part I) and 147-158 (Part II).

32. Coburn, J.W. and Kay, E., J. Appl. Phys. 1972, 43, 4965-71.

33. Purdes, A.J. et al., J.Vac. Sci. Technol. 1977, 14, 98-101.

34. Bacal, M. and Doucet, H.J., I.E.E.E. Transactions on Plasma Sciences, 1973, September, PS-1, 3, p91-99.

35. Kay, E.; Coburn, J.W. and Kruppa, G., Le Vide, 1976, No. 183, 89-95.

36. Massey, H.S.W., ed, "Negative Ions", 2nd Edition 1950, Cambridge University Press.

37. Emeleus, K.G. and Woolsey, G.A., eds, "Discharges in Electronegative Gases", Taylor and Francis Publishers.

38. Vasile, M.J. and Smolinsky, G., J.Phys. Chem. 1977, 81, 2605-9.

39. Smolinsky, G. and Vasile, M.J., J.Mass Spectrom. and Ion Phys. 1975, 16, 137-149.

40. Coburn, J.W.; Winters, H.F., and Chang, T.J., J.Appl. Phys. 1977, 48, 3532-3540.

41. Coburn, J.W. et al., J.Appl. Phys., 1974, 45, 1779-1786.

42. Coburn, J.W. and Kay,E. Appl. Phys. Lett. 1971, 19,, 350-352.

43. Coburn, J.W. and Kay, E., I.B.M. J. Res. Dev. 1979, 23, 33-41.

44. Talrose, V.L. et al., Advances in Mass Spec., 1965, 3, 993-1007.

45. Combourieu, J. and LeBras, G., C.R. Acad. Sci, Paris, 1970, t.271, 1160-1163 Series C.

46. Kwei, G.H.; "Molecular Beam Kinetics". 1967, Ph.D. thesis University of California, Berkeley.

47. Smith, K.F.; "Molecular Beams". 1955, 2nd ed, Methuen-Wiley.

48. Kaufman, M., Pure and Applied chem. 1976, 48, 155-161.

49. Kolb, C.E. and Kaufman, M., J.Phys. Chem., 1972, 76, 947-953.

50. Gutman, D.; Hay, A.J. and Belford, R.L., J.Phys. Chem. 1966, 70, 1786-1792.

51. Niki, H.; Daby, E.E. and Weinstock, B., 12th Int. Symp. on Combustion 1968. Published by the Combustion Institute (1969).

52. Biordi, J.C.; Lazzara, C.P. an Papp, J.F., Combustion and Flame, 1974, 23, 73-82.

53. IBID., 1976, 26, 57-76.

54. Watson, R.T. "The Study of some Rreactions involving halogen atoms and oxyhalide free radicals by molecular beam Mass spectrometry". 1973, PhD thesis, University of London, Queen Mary College.

55. Biordi, J.C. etal., J.Phys. Chem. 1976, 80, 1042-1048.

56. Farmer, J.B.; Henderson, H.S.; Lossing, F.P. and Marsden, D.G.H. J.Chem, Phys. 1956, 24, 348-352.

57. Foner, S.N., Adv. in Atomic and Molecular Physics, 1965, 2, 385-461.

58. Ross, J. ed, "Molecular Beams.", Adv. in Chem. Phys. 1966, Vol: X, Interscience, Publ., 1966.

59. Knuth, E.L., Appl. Mech. Rev. 1964, 17, 751-762.

60. Anderson, G.K. "Rates and Mech anisms of Borane Carbonyl and Diborane with O^3P." PhD thesis Cornell University 1975. Diss. Abs. Int., B, 36, 4503, 1976.

61. Mulcahy, M.F.R. "Gas Kinetics - Studies in Modern Chemistry", 1973, Thomas Nelson and Sons Ltd., London.

62. Anderson, J.B.; Andres, R.P. and Fenn, J.B., Adv. in Atomic and Molecular Physics, 1965, 1, 345-389.

63. Nutt, C.W.; Botterill, J.S.M.; Thorpe, G. and Penmore, G.W. Trans. Faraday soc. (pt I), 1959, 55, 1500-1515 and part II 1959, 55, 1516-1523.

64. Clyne, M.A.A. and Nip, W.S. in "Reactive Intermediates in the Gas Phase" - Generation and Monitoring edited by Setser, D.W., 1979 Academic Press.

65. Fite, W.L.; Pinnacle- J. Extranuclear Laboratories, Inc., 1974, 1, (1) p1-2.

66. McDowell, C.A. ed., "Mass Spectrometry." 1963, McGraw-Hill.

67. Williams, D.H. and Howe, I., "Principles of Organic Mass Spectrometry." 1972, McGraw-Hill.

68. Knewstubb, P.F. "Mass Spectrometry and Ion Molecular Reactions". 1969, Cambridge University Press.

69. Kiser, R.W., "Introduction to Mass Spectrometry and its Applications", 1965, Prentice-Hall Inc.

70. Warren, J.W., Nature 1950, 165, 810 - 811.

71.   Lossing, F.P.; Tickner, A.W. and Bryce, W.A., J.Chem. Phys. 1951, 19, 1254.

72.   Honig, R.E., J.Chem. Phys. 1948, 16, 105.

73.   Appleman, E.H. and Clyne, M.A.A. in "Fluorine-Containing Free Radicals - Kinetics and Dynamics of Reactions". A.C.S. Symposuim Series, No.66., ed., Root, J.W.; 1978.

74.   Clyne, M.A.A. in "Physical Chemistry of Fast Reactions." Vol. 1 Gas Phase Reactions of Small Molecules, edited by Levitt, B.P. 1975, Plenum Press.

75.   Marr, G.V. "Plasma Spectroscopy", Elsevier Publishing Co., 1968.

76.   Kaufman, F. in reference 22.

77.   "Plasma Processing". Proc. Symp on Plasma Etching and Deposition. eds., Frieser, R.G. and Mogab, C.J. Proceedings Volume 81-1, Electrochemical Soc., 1981.
       (i)   Beenakker, C.I.M.; van Dommelen, J.H.J. and Dieleman, J. p302.
       (ii)   OKano, H. and Horike, Y. P199.
       (iii)   Donnelly, V.M.; Flamm, D.L. and Mucha, J.A. p270.
       (iv)   Ven, E.P.G.T. van de; and Philips, N.V. p112.
       (v)   Eiesle, K.M. p174.
       (vi)   Sanders, F.H.M. Dommelen, J.H.J. van; Sanders, J.A.M.; Beenaker, C.I.M. and Dieleman, J. p155.
       (vii)   Nakamura, M.; Itoga, M. and Ban,Y. p225.
       (viii) Ranadive, D.K. and Losee, D.L. p236.
       (ix)   Winkler, V.; Schmidt, N. and Hoffman, N. p253.
       (x)   Schwartz, G.C. and Schaible, P.M. p133.
       (xi)   Lechaton, J.S. and Mauer, J.L. p75.
       (xii)   Bruce, R.H. p243.
       (xiii) Tsukada, T. and Ukai, K. p288.

78.   Harshbarger, W.R.; Porter, R.A.; Miller, T.A. and Norton, P. Appl. Spectros. 1977, 31, 201-207.

79.   Porter, R.A. and Harshbarger, W.R., J. Electrochem. Soc. 1979, 126, 460-464.

80.   Degengolb, E.O.; Mogab, C.J.; Goldrick, M.R. and Griffiths, J.E. Appl. Spectros. 1976, 30, 520-.

81.   Griffiths, J.E. and Degengolb, E.O. Appl. Spectros. 1977, 31, 134-137.

82.   Crooks, J.E., "The Spectrum in Chemistry." Academic Press, 1978.

83.   Derwent, R.G. and Thrush, B.A., Trans. Faraday Soc. 1971, 67, 2036.

84. Chung, P.M.; Talbot, L. and Touryan, K.J.; "Electric Probes in Stationary and Flowing Plasmas: Theory and Applications". Vol. II., 1975, Springer-Verlag.

85. Swift, J.D. and Schwar, M.J.R.; "Electrical Probes for Plasma Diagnostics". 1970, Iliffe Books Ltd.

86. Thornton, J.A.; J.Vac. Sci. Technol. 1978, 15, 188-192.

87. Clements, R.M.; IBID. 1978, 15, 193-198.

88. Eser, E. and Ogilvie, R.E.; IBID. 1978, 15, 199-202.

89. Tokiguichi, K.; Sakudo, N.; Suzuki, K. and Kanomata, I.; IBID., 1980, 17, 1247-1251.

90. Schott, L. in "Plasma diagnostics" ed. Lochte-Holtgreven, W. 1968, North-Holland Publ. Company.

91. Groh, K.H.; Walther, S.E. and Loeb, H.W. p53 of 5th Int. Conference on Gas Discharges (Liverpool, 1978) published by IEE, no: 165.

92. Burden, M. St. J. and Cross, K.B.; Vacuum. 1979, 29, 13-14.

93. Ojha, S.M.; Vacuum, 27, 65-67.

94. Vossen, J.L.; J.Electrochem Soc. 1979, 126, 319-324.

95. Tisone, T.C. and Cruzon, P.D.; J.Vac. Sci. Technol. 1975, 12, 1058-1066.

96. Yamaguchi, S.; Sawa, G. and Ieda, M.; J.Appl. Phys. 1977, 48, 2363-.

97. Westenberg, A.A.; Prog. React. Kinet. 1973, 7, 23.

98. Ambidge, P.F.; Bradley, J.N. and Whytock, D.A.; J.C.S. Faraday Trans. I. 1976, 72, 2143-2149.

99. Ashmore, P.G.; Parker, A.J. and Stearne, D.E. Trans Faraday Soc. 1971, 67, 3081-3093.

100. Bradley, J.N.; Whytock, D.A. and Zeleski, T.A.; J.C.S. Faraday Trans I, 1973, 69, 1251.

101. Tokunaga, K. and Hess, D.W.; J. Electrochem. Soc. 1980, 127, 928 - 932.

102. Kay, E. and Dilks, A.; J.Vac. Sci. Technol. 1981, 18, 1-11.

103. Kay, E.; Coburn, J.W. and Dilks, A. in reference 21.

104. Foner, S.N., and Hudson, R.L. J.Chem. Phys. 1953, 21, 1374.

105. Mason, C.; "A Spectroscopic Study of Positive Photoresist Stripping with Oxygen Plasmas." 1981, Final Year project in the Department of Chemistry, University of Aston in Birmingham, supervised by Dr. S.J. Moss.

106. Battey, J.F.; J.Electrochem. Soc., 1977, 124, 147-152.

107. Battey, J.F.; IBID., 1977, 124, 437 - 441.

108. Reichelderfer, R.F.; Weltz, J.M. and Battey, J.F.; IBID. 1977, 124, 1926-7.

109. Schwartz, G.C. and Schaible, P.M.; J.Vac. Sci. Technol.; 1979, 16, 410-413.

110. Kiesling, R.A.; Sullivan, J.J. and Santeler, D.J.; IBID., 1978, 15, 771 - 774.

111. Yamanaka, H; Wada, T.; Kudoh, O. and Sakamoto, M.; J. Electrochem. Soc. 1979, 126, 1415 - 1418.

112. Heinecke, R.A.H.; Solid State Electronics, 1975, 18, 1146 - 1147.

113. Heinecke, R.A.H.; IBID 1976, 19, 1039 - 1040.

114. Schwartz, G.C.; Zielinski, L.B. and Schopen, T. in ref. 15. p122 - 132.

115. Bersin, R.L.; Solid State Technol., May 1976, 19, 31-36.

116. Bersin, R.L.; and Reichelderfer, R.F.; IBID., 1977, 20, 78-80.

117. Lehmann, H.W. and Widmer, R.; J.Vac. Sci. Technol. 1978, 15, 319-326.

118. Matsuo, S. and Takehara, Y.; Japan. J. Appl. Phys., 1977, 16, 175-176.

119. Schwartz, G.C.; Rothman, L.B. and Schopen, T.J.; J.Electrochem. Soc., 1979, 126, 464 -469.

120. Mauer, J.L.; Logan, J.S.; Zielinski, L.B. and Schwartz, G.C.; J.Vac. Sci. Technol. 1978, 15, 1734-1738.

121. Adams, A.C. and Capio, C.D.; J.Electrochem. Soc., 1981, 128, 366-370.

122. Makino, T.; Nakamura, H. and Asano, M. IBID. 1981, 128, 103-106.

123. Matsuo, S.; J.Vac. Sci. Technol., 1980, 17, 587-594.

124. Ephrath, L.M.; J.Electrochem. Soc., 1979, 126, 1419-1421.

125. Bondur, J.A.; IBID. 1979, 126, 226 - 231.

126. Jinno, K.; Kinoshita, H. and Matsumoto, Y.; IBID., 1978, 125, 827 - 828.

127. Winters, H.F.; Coburn, J.W. and Kay, E.; J.Appl. Phys., 1977, 48, 4973 - 4983.

128. Mogab, C.J.; Adams, A.C. and Flamm, D.L.; IBID., 1978, 49, 3796 - 3803.

129. Winters, H.F.; J.Appl. Phys. 1978, 49, 5165 - 5170.

130. Smolinsky, G. and Flamm. D.L.; IBID., 1979, 50, 4982 - 4987.

131. Flamm, D.L.; Mogab, C.J. and Sklaver, E.R.; IBID., 1979, 50, 6211 - 6213.

132. Truesdale, E.A.; Smolinsky, G. and Mayer, T.M.; IBID., 1980, 51, 2909 - 2913.

133. Visser, J.; J.Vac. Sci. Technol., 1981, 19, 104-108.

134. Pitts, J.N.; Sandoval, H.J. and Atkinson, R.; Chem. Phys. Lett. 1974, 29, 31-34.

135. Atkinson, R.; Breven, G.M.; Pitts, J.N. and Sandoval, J.; J. Geophys. Res. 1976, 81, 5765 - 5770

136. Flamm, D.L.; J.Appl. Phys. 1980, 51, 5688-5692.

137. Agostino, R.D.; Cramarossa, F.; Benedictis, S.De; and Ferraro, G. IBID. 1981, 52, 1259 - 1265.

138. Coburn, J.W. and Winters, H.F.; J.Vac. Sci. Technol. 1979, 16, 391-403.

139. Rosenstock, H.M.; Drasxl, K; Steiner, B.W. and Herron, J.T.; Energeties of Gaseous Ions, J.Phys. Chem. Reference Data 1977, 6, Supplemment I.

140. Lifshitz, C. and Long, F.A.; J.Phys. Chem. 1963, 67, 2463 - 2468.

141. Waldie,B, and Farnell, G.A.; eds. Proc. 5th Int. Symp. on Plasma Chemistry. ISPC5. at Heriot-Watt University, Edinburgh, Scotland 10th-14th August 1981
(i)   Klinger, R.E. and Green, J.E. p.324.
(ii)   Agostino, R.d; Colaprico, V; and Cramarossa, F.; p25.
(iii)   Dommelen, J.H.J. van; Beenaker, C.I.M.; and Dieleman, J. p.34.
(iv)   Sanders, F.H.M. and Dieleman, J. p.29.
(v)   Donohoe, K.G. P.310.
(vi)   Curtis, B.J. and Brunner, H.R. p.318.
(vii)   Flamm, D.L.; Bruce, R.H.; Donnelly, V.M. and Collins, G.J. p.307.

142. Bosser, G.; Lebreton, J. and Rostas, J.; J. deChemie Physique 1981, 78, 787.

143. Mogab, C.J.; J. Electrochem. Soc. 1977, 124, 1262-1268.

144. Duval, M. and Theoret, A.; IBID. 1975, 122, 581-585.

145. Chapman, B.N. and Minkiewicz, V.J.; J.Vac. Sci. Technol. 1978, 15. 329-332.

146. Mauer, J.L. and Logan, J.S.; IBID., 1979, 16, 404 - 406.

147. Enomoto, T.; Solid State Technol. 1980, 4, 117-121.

148. Eisele, K.M.; J.Electrochem. Soc. 1981, 128, 123-126.

149. Agostino, R.d'.; and Flamm, D.L.; J.Appl. Phys. 1981, 52, 162-167.

150. Revell, P.J. and Goldspink, G.F. in ref. 14 p.543.

151. Goodman , J.; J.Polymer, Sci. 1960, 44, 551-

152. Matsuo, S.; Appl. Phy. Lett. 1980, 36, 768-770.

153. Flamm, D.L.; Cowan, P.L. and Golovchenko, J.A.; J.Vac. Sci. Technol. 1980, 17, 1341-1347.

154. Mogab, C.J. and Shankoff, T.A.; J.Electrochem. Soc. 1977, 124, 1766 - 1771.

155. Reinberg, A.R. in ref: 15.

156. Matsui, S.; Yamamoto, T.; Aritome, H. and Namba, S. in ref. 14. p.523.

157. Toby, S. and Toby, F.S.; J.Phys. Chem. 1981, 85, 4071-4073.

158. Hobrock, D.L. and Kiser, R.W.; IBID 1964, 68, 575-579.

159. Winborne, D.A. and Nordine, P.C.; A.I.A.A. Journal, 1976, 14, 1488-1490.

160. Nordine, P.C. J.Phys. Chem. 1974, 61, 224 - 226.

161. Nordine, P.C. and LeGrange, J.D.; A.I.A.A. Journal, 1976, 14, 644-647.

162. Foon, R. and Kaufman, M. in Progr. Reaction Kinetics, 1975, 8, 81-160. Pergamon Press, eds. Jennings, K.R. and Cundall, R.B.

163. Stokes, S. and Duncan, A.B.F.; J.A.C.S. 1958, _80_, 6177-6181.

164. Anlauf, E.G.; Charters, P.E.; Horne, D.S. etal. J.Chem, Phys. 1970, _53_, 4091-4092.

165. Lin, M.C. and Green, W.H.; IBID., 1970, _53_, 3383-3384.

166. Schafer, T.P.; Siska, P.E.; Parson, J.M.; Tulby, F.P.; Wong, Y.C. and Lee, Y.T.; IBID. 1970, _53_, 3385-3387.

167. Polanyi, J.C. and Tardy, D.C.; J.Chem. Phys. 1969, _51_, 5717-5719.

168. Jeffrey, C.L. and Sams, L.C.; J.Org. Chem. 1977, _42_, 863-865.

169. Nordine, P.C. and Rosner, D.E.; J.C.S. Faraday Trans. 1, 1976, _72_, 1526-1533.

170. Marcotte, R.E. and Hanrahan, R.J.; J.Fluorine Chem. 1972, _2_, 87-98.

171. Vasek, A.H. and Sams, L.C.; IBID. 1972, _2_, 257-262.

172. Sheinson, R.S.; Toby, F.S. and Toby, S. J.A.C.S. 1975, _97_, 6593-6595.

173. Suzuki, K.; Okudaira, S.; Sakudo, N.; and Kanomata, I.; Jap. J.Appl. Phys. 1977, _16_, 1979-1984.

174. Schaible, P.M.; Metzger; W.C. and Anderson, J.P. J.Vac. Sci. Technol. 1978, _15_, 334-337.

175. Heiman, N: Minkiewicz, V.; and Chapman, B.; J.Vac. Sci. Technol. 1980, _17_, 731-734.

176. Tokunaga, K.; Redeker, F.C. ; Danner, D.A.; and Hess, D.W.; J. Electrochem. Soc. 1981, _128_, 851-854.

177. Mogab, C.J. and Levenstein, H.J.; J.Vac. Sci. Technol. 1980, _17_, 721-730.

178. Bruce, R.H. and Reinberg, A.R. in ref. 14. p.533.

179. Yamazaki, T.; Suzuki, Y. and Nakata, H.; J.Vac Sci. Technol. 1980, _17_, 1348-1350.

180. Nakata, H.; Nishioka, K. and Abe, H.; J.Vac. Sci. Technol. 1980, _17_, 1351-1357.

181. Smolinsky, G.; Chang, R.P. and Mayer, T.M.; J.Vac. Sci. Technol. 1981, _18_, 12-16.

182. Davis, D.D.; Schmidt, J.F.; Neeley, C.M. .and Hanrahan, R.J. J.Phys. Chem. 1975, _79_, 11-17.

183. Curtis, B.J. and Brunner, H,J.; J.Electrochem. Soc. 1978, 125, 829-830.

184. Marcotte, R.E. and Hanrahan, R.J.; J.Phys. Chem. 1972, 76, 3734-

185. Steacie, E.W.R.; "Atomic and Free Radical Reactions", p.682., Reinhold, New York, 1954.

186. Sin - Shong Lin; J. Electochem. Soc. 1976, 123, 512 - 514.

187. Ayala, J.A.; Wentworth, W.E. and Chen, E.C.M.; J.Phys. Chem. 1981, 85, 3989-3994.

188. Various Papers and abstracts from Thin Solid Films. 1981, 84, 368-434.

189. Kay, E.; Coburn, J.W. and Kruppa, G.; Le Vide, 1976, No. 183, 89-95.

190. Sharma, A.K.; Millich, F. and Hellmuth, E.W.; J.Appl. Phys. 1978, 49, 5055-5059.

191. Kay, E.; Dilks, A. and Seybold, D.; J.Appl. Phys. 1980, 51, 5678-5687.

192. Morosoff, N.; Newton, W. and Yasuda, H.; J.Vac. Sci. Technol. 1978, 15, 1815-1822.

193. Kay, E. and Dilks, A.; IBID., 1979, 16, 428-430.

194. Kny, E.; J.Vac. Sci. Technol. 1980, 17, 658-660.

195. Millard, M. and Kay, E.; J.Vac. Sci. Technol. 1981, 18, 343-344.

196. "Plasma Polymerization", A.C.S. Symposium Series No:108. eds. Mitcnel Shen and A.T. Bell, 1979, based on 176th metting of A.C.S. Miami B each, Florida. Sept. 15-16th, 1978.

197. Tsuda, M; Oikawa, S.; Ohnogi, S. and Suzuki, A. in ref. 14. p.553.

198. Sato, M.and Nakamura, H.; J.Vac. Sci. Technol. 1982, 20, 186-190.

199. Chang, R.P.H.; Chang, C.C. and Darack, S. IBID., 1982, 20, 45-50.

200. Stafford, B.B. and Gorin, J.G.; Solid State Technol. 1977, Sept. 20, (9), 51-56.

201. Chapman, B. "Glow Discharge Processes- sputtering and plasma etching"; 1980, John Wiley and Sons Inc.

202. Dwight; E.D. and Gray, E. eds. American Institute of Physics Handbook; 1957, McGraw-Hill Book Company. (i)   Brown, S.C.and Allis, W.P. p.7-174.

203. Fite, W.L. in ref:22 p.10.

204. Coburn, J.W. and Winters, H.F.; J.Appl. Phys. 1979, 50, 3189-3196.

205. Bresnock, F.J. and Strumpf, Th; J.Vac. Sci. Technol. 1982, 20, 1027-1030.

206. Korman, C.S. IBID; 1982, 20, 476-479.

207. Coburn, J.W.; Knabbe, E.A.; and Kay, E. IBID, 1982, 20, 480-483.

208. Melliar-Smith, C.M. and Mogab, C.J. in "Thin Film Processes" edited by Vossen, J.L. and Kern, W. Academic Press 1978, p.527.

209. Bower, D.H.; J.Electochem. Soc. 1982, 129, 795-799.

210. Degengolb, E.O.; IBID; 1982, 129. 1150-1151.

211. Light, R.W. and See, F.C.; IBID; 1982, 129, 1152-1154.

212. Bruce, R.G. and Reinberg, A.R.; IBID; 1982, 129, 393-396.

213. Heath, B.A.; J.Electrochem. Soc. 1982, 129, 396-402.

214. Mayer, T.M. and Barker, R.A.; IBID; 1982, 129, 585-591.

215. Handbook of Chemistry and Physics 58th edition Edited by Weast, R.C. and published by CRC press, Inc. 1977-1978.

216. McLafferty, F.W. "Interpretation of Mass Spectra." 1973, W.A. Benjamin, Inc. 2nd edition.

217. Evans, S. and Thomas, J.M.; Proc. R.Soc. Lond. A; 1977, 353, 103-120.

218. Berg, S. and Anderson, L.P.; Thin Solid Films 1979, 58, 117-120.

219. Ogryzlo; E.A.; Can. J.Chem. 1961. 39, 2556-2562.

220. Herron, J.T.; J.Phys. Chem. 1963, 67, 2864-2865.

221. Westenberg, A.A. and DeHaas, N.; J.Chem. Phys. 1968, 48, 4405-4415.

222. Ashmore, P.G.; Parker, A.J. and Stearne, D.E.; Trans. Faraday, Soc. 1971, 67, 3081-3093.

223. Clyne, M.A.A. and Stedman, D.H.; IBID. 1966, <u>62</u>, 2164-2174.

224. Niki, H. AND Weinstock, B.; J.Chem. Phys.; 1967, <u>47</u>, 3249-3252.

225. Biordi, J.C.; J.Phys. Chem. 1969, <u>73</u>, 3163-3165.

226. Bradley, J.N.; Whytock, D.A. and Zaleski, T.A.; J.C.S. Faraday I, 1973, <u>69</u>, 1251-1256.

227. Bemand, B.P.; Clyne, M.A.A. and Watson, R.T.; IBID. 1973, <u>69</u>, 1356-1374.

228. Ambidge, P.F.; Bradley, J.B. and Whytock, D.A.; J.C.S. Faraday I, 1976, <u>72</u>, 2143-2149.

229. Hippler, H. and Troe, J.; Chem. Phys. Lett. 1973, <u>19</u>, 607-609.

230. Hippler, H. and Troe, J.; Int. J.Chem. Kinetics, 1976, <u>8</u>, 501-.

231. Widman, R.P. and DeGraf, B.A. J.Phys. Chem. 1973, <u>77</u>, 1325-1328.

232. Kurogi, Y. and Kamimura, K.; Jap. J.Appl. Phys.; 1982, <u>21</u>, 168-172.

233. Matsuo, S. and Adachi, Y.; IBID 1982, <u>21</u>, L4-L6.

234. Ung, A. Y-M and Schiff, H.I., Can. J.Chem. 1962, <u>40</u>, 486-494.

235. Sobering, S.E. and Winkler, C.A. IBID 1958, <u>36</u> 1223-1226.

236. Kaufman, F. and Kelso, J.R.; J.Chem. Phys. 1960, <u>32</u>, 301-302.

237. "Gas Chromatography" by Schupp III, O.E.; and edited by Perry, E.S. and Weissberger, A. p.151. 1968, Interscience Publishers.

238. Lovelock, J.E.; J.Chromatog.; 1958, <u>1</u>, 35.

239. Dushman, S.; "Scientific Foundations of Vacuum Techniques". 1949, J.Wiley and Sons, and 2nd edition, 1962.

240. Roth, A.; "Vacuum Technology", 1976, North-Holland, New York.

241. Burton, R.H. and Smolinsky, G.; J.Electrochem. Soc.; 1982, <u>129</u>, 1599-1604.

242. Kawata, H; Shibano, T; Murata, K. and Nagami, .K.; IBID, 1982, <u>129</u>, 1325-1329.

243. White, F.R.; Koburger, C.W.; Harman, D.L. and Geipel, H.J.; IBID, 1982, <u>129</u>, 1330-1335.

244. Smolinsky, G.; Truesdale, E.A.; Wang, D.N.K.; and Maydan, D.; IBID; 1982, <u>129</u>, 1036-1040.

245. Millard, M.M. and Kay, E.; J.Electrochem. Soc.; 1982, <u>129</u>, 160-165.

246. Cornu, A. and Massot, R.; Compilation of Mass Spec. Data. 2nd edition, Heyden (1975), Vol. I.

247. Stenhagen, E.; Abrahamsson, S. and McLafferty, F.W. eds. Atlas of Mass Spect. Data, Vol. I Interscience 1969.

248. "The Chemical Thermodynamics of Organic Compounds", by Stull, Westrum, and Sinke, Wiley, 1969.